



PHOTON SCIENCE 2008.

Highlights and
HASYLAB Annual Report

Accelerators | [Photon Science](#) | Particle Physics

Deutsches Elektronen-Synchrotron
A Research Centre of the Helmholtz Association





Cover

DESY photon sources – an aerial view of the curved PETRA III experiment hall (upper left), the FLASH experiment hall (bottom), and the DORIS III experiment halls (upper right). ●



PHOTON SCIENCE 2008.

Highlights and
HASYLAB Annual Report



Contents.

➤	Introduction	4
➤	News and Events	9
➤	Research Highlights	17
➤	Research Platforms and Outstations	49
➤	Lightsources	63
➤	New Technologies and Developments	81
➤	Facts and Numbers	97

The year 2008 at DESY.

Chairman's foreword

The year 2008 has been a very important one for photon science at DESY. Decisive progress was made in each of the ongoing projects and activity fields. Most impressive and most visible to everybody is the PETRA III experiment hall, which was completed on time in July 2008. Almost 300 meters long, with a one meter thick monolithic concrete slab, will it house the instruments of the world's lowest emittance and most powerful synchrotron radiation storage ring PETRA III. Installation of the instruments is under way and the user community can expect to see first photon beams of unprecedented quality in the second half of 2009. Regular user service mode is expected in 2010.

In order to prepare for the commissioning of the new storage ring, the injector chain had to be refurbished imposing a 9 month shutdown for the DORIS III facility. Nevertheless DORIS III turned on again for user operation in September 2008 without the slightest problem as if it were a simple X-ray tube, an extraordinary achievement by the staff involved. We all hope that DORIS III can continue to surprise us with unexpected discoveries such as the hidden portrait of a woman painted by van Gogh that sparked worldwide press interest.

DESY is operating the world's only soft X-ray free-electron laser FLASH and we are envied for this magnificent facility worldwide. Photons with wavelength down to 6.5 nm are produced nowadays routinely and a peak powers up to 100 μJ were achieved. FLASH even lases at higher harmonics and experiments were carried out at "high" energies approaching 900 eV. At the same time the new infrared beamline, operating at the other end of the wavelength spectrum, has started to provide the heavily demanded THz radiation. Users from all over the globe share the instruments and the results are truly exceptional. It is this scientific output that has laid the basis for important upgrade programs, such as "sFLASH" and "FLASH II". FLASH is the small brother of the European XFEL, the future flagship of European free-electron laser science. The year 2008 was also for the XFEL of utmost importance. Just recently, in December the contracts for the underground construction of the



Topping-out ceremony in the PETRA III experiment hall (November 2007)



Jochen Schneider receives the DESY medal on the occasion of the colloquium (January 2008)

tunnels and the associate buildings were awarded, the inter-governmental convention is being finalized and expected to be signed in spring 2009, thus paving the way for the foundation of the European XFEL company (GmbH). By 2014 sub-100 fs X-ray pulses each carrying more than 10^{12} photons of 1 Å wavelength will be provided to users.

The newly founded Center for Free Electron Laser Science (CFEL) has started operation under the leadership of Henry Chapman from DESY and Andrea Cavalleri as leader of a Max-Planck Research Group. Three further leading positions have been announced and interviews have started. The planning of the new CFEL building has progressed considerably and the hope is to see its completion towards the end of 2010.

Many of the ongoing projects are closely connected with the name of former photon science director Jochen R. Schneider whose retirement from his DESY duties was recognized with a colloquium during the 2008 HASYLAB Users Meeting. In October 2008 Jochen R. Schneider was honoured by the German Federal President with the Order of Merit for his contributions to light source science.

In the context of the Helmholtz Association the research strategy is being defined and reviewed every five years. The proposal for the new Helmholtz Research Programme “Research with Photons, Neutrons and Ions (PNI)” covering the years 2010-2014 will be evaluated in spring 2009. It has been formulated together with our colleagues from five other Helmholtz centres. The outstanding progress in all areas would not have been possible without the dedication of DESY staff and the support by the user community. The latter one manifested its support by a new record attendance at the last user’ meeting in which more than 350 scientists participated.

In order to adequately report about so much progress in so many areas, a new format has been developed for how we present DESY activities in photon science: For the first time the activities of the past year are covered by a Photon Science report, the one you have in front of you. We hope you will find it an interesting source of information.

As DESY is getting ready to make 2009 another year of progress in science and technology a number of changes in the directorate are taking place. Edgar Weckert, acting as interim director for photon science since January 2008, will become director for photon science, his colleague in the directorate for particle and astroparticle physics will be Joachim Mnich, taking over from Rolf-Dieter Heuer who became director general of CERN. Helmut Dosch will become the new chairman of the DESY board of directors in March 2009 when I will retire after 10 years in this position.

It is my pleasure to see DESY well prepared for the future, building on the successes of the past. I wish DESY, its staff and users many exciting scientific results in the years to come. ●

Albrecht Wagner

Albrecht Wagner
Chairman of the DESY board of directors



Photon Science at DESY.

Introduction

For photon science at DESY, 2008 was a year of changes. Most apparent is the change from the traditional “HASYLAB Jahresbericht” to the new format “Photon Science 2008” you are reading. The “Jahresbericht” carried on a long tradition and summarized the photon science activities at DESY for more than 30 years. However, covering both user experiments and facility reports it grew to more than 2500 pages in the past years making its handling on paper cumbersome. “Photon Science 2008” intends to keep you updated on the activities at DESY highlighting some of the scientific results achieved by users at our facilities as well as by in-house staff. The highlights were selected from a list of over 30 publications proposed for this issue. Users are very welcome to contact us and to nominate highlights for the next issue. All annual user experiment reports formerly covered by the “Jahresbericht” will continue to be available online.

At DORIS III, a nine months shutdown in 2008 became necessary due to the need for a refurbishment of all pre-accelerators in the frame of the PETRA III project. Although a larger number of components were exchanged, the restart of all facilities went extremely well providing reliable beam conditions as scheduled beforehand. Despite this short beamtime period about 1170 users carried out experiments at DORIS III as compared to about 2200 users in 2007. DORIS III will be operated in its present form until PETRA III is in full operation. Thereafter, the number of beamlines at DORIS III will be reduced keeping complementary techniques to the ones at PETRA III. During the second half of the next five year funding period it is planned to finally shut-down DORIS III provided the capabilities at PETRA III have been extended by those techniques available at DORIS III, that are not being realized in the first phase of the PETRA III project.

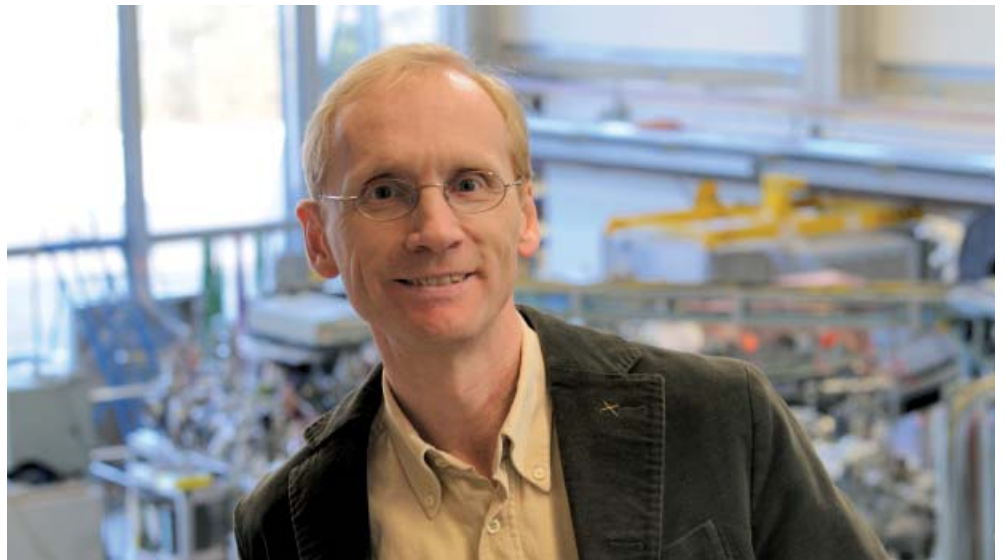
At PETRA III the most visible change is the newly erected, almost 300 m long experiment hall handed over to DESY on July 1st. Already before that date, the refurbishment of the 2 km long part of the PETRA storage ring outside the experimental hall was almost completed and the technical commissioning of the large number of components in this section is being ongoing since end of October 2008. Meanwhile, except for a few parts, the storage ring is complete and the start of the final commissioning with beam is envisaged for spring 2009. Almost all beamline front-end components are installed and most of the undulators were delivered, several of them being perfectly shimmed waiting for installation. There is also significant progress on the experimental floor. The construction of the first optics and experiment hutches is completed and instrumentation

such as monochromators, diffractometers, optical benches, and laboratory facilities is currently being installed. First beam for commissioning the beamlines is expected towards the middle of 2009 and “friendly” user groups waiting for the worldwide lowest emittance beam for first experiments are expected for the last months of 2009.

In 2008, about 220 users performed experiments at FLASH and a number of exciting results were published. Most of the applied techniques exploited the high peak power and coherence of the free-electron laser (FEL) pulses. Examples are multi-photon ionization and dissociation processes, or coherent diffractive imaging and holography. About half of the experiments make use of ultrafast pump-probe techniques combining FLASH with an optical short pulse laser. New opportunities for THz-XUV pump-probe experiments arise from the FLASH THz beamline, which transports far-infrared photon pulses, generated by an additional undulator and perfectly synchronized to the XUV pulses, to one experimental station. FLASH operation has meanwhile reached a high level of stability, facilitating experiments with sub-50 fs pulses even at the 3rd and 5th harmonic with respectively, up to about 10^{10} and 5×10^8 photons per bunch at a 13.5 nm fundamental. This is about four to five orders of magnitude more than achieved by laser slicing at synchrotrons, although at lower repetition rates. In autumn 2009, an extensive upgrade of FLASH is planned, which includes an increase of the linac energy to 1.2 GeV to reach shorter wavelengths as well as a test setup for seeding the FEL with a HHG laser in



Evolution of the HASYLAB Annual Report from 1975 to 2007



collaboration with the University of Hamburg. For the future, an extension of FLASH by a second FEL - undulator tunnel and experimental hall (FLASH II), which will also apply different FEL seeding schemes, is proposed in collaboration with the Helmholtz-Zentrum Berlin (BESSY).

Even though the administrative procedures for the foundation of the European XFEL company (GmbH) take longer than anticipated - signing of the XFEL convention by the international partners is expected for the first half of 2009 - one major project milestone, namely the contract for the construction of the underground buildings, was placed in December 2008. Activities on the construction site have started and official groundbreaking is scheduled for spring 2009. In addition, there is also considerable progress in forming the consortium headed by DESY for the production of the superconducting LINAC and in the preparatory and design effort of many other work packages.

Therefore, we are quite confident to see the first of these extremely intense, 100 fs hard X-ray laser pulses in 2014/15 at the European XFEL.

Experiments at FEL sources are in many aspects different from those at synchrotron radiation sources. New techniques, sample environments, and methods have to be developed in order to exploit the unique potential of these sources. To cope with these challenges on one hand and for the scientific exploitation of FEL sources on the other hand, Max Planck Society, University of Hamburg, and DESY have established the Centre for Free Electron Laser Science at Hamburg (CFEL). The first two group leaders (H. Chapman and A. Cavalleri) have taken up their work in 2008 and the recruiting procedure for further three group heads is in progress. The planning for the new CFEL building accommodating almost 300 people, which is financed by the City of Hamburg, is nearly complete and the preparation of the construction ground close to the PETRA III experimental hall has started.

DESY has a long tradition of hosting outstations of external institutions using the photon sources on site for their research and user programs. At present, outstations of EMBL, Max-Planck-Society and the Universities of Hamburg and Lübeck in structural biology, of GKSS research centre (Geesthacht) for engineering

materials science, and of GFZ (Helmholtz Centre Potsdam) for geo-science are very successfully active. In addition, about ten institutions - almost all universities, Leibniz and Helmholtz institutes working in the field of structural biology and located in the northern German area and EMBL - propose a common "Centre for Structural System Biology" (CSSB) to be built next to the PETRA III hall. Discussions with various funding bodies are ongoing and, if successful, this center would significantly enrich the scientific environment on campus.

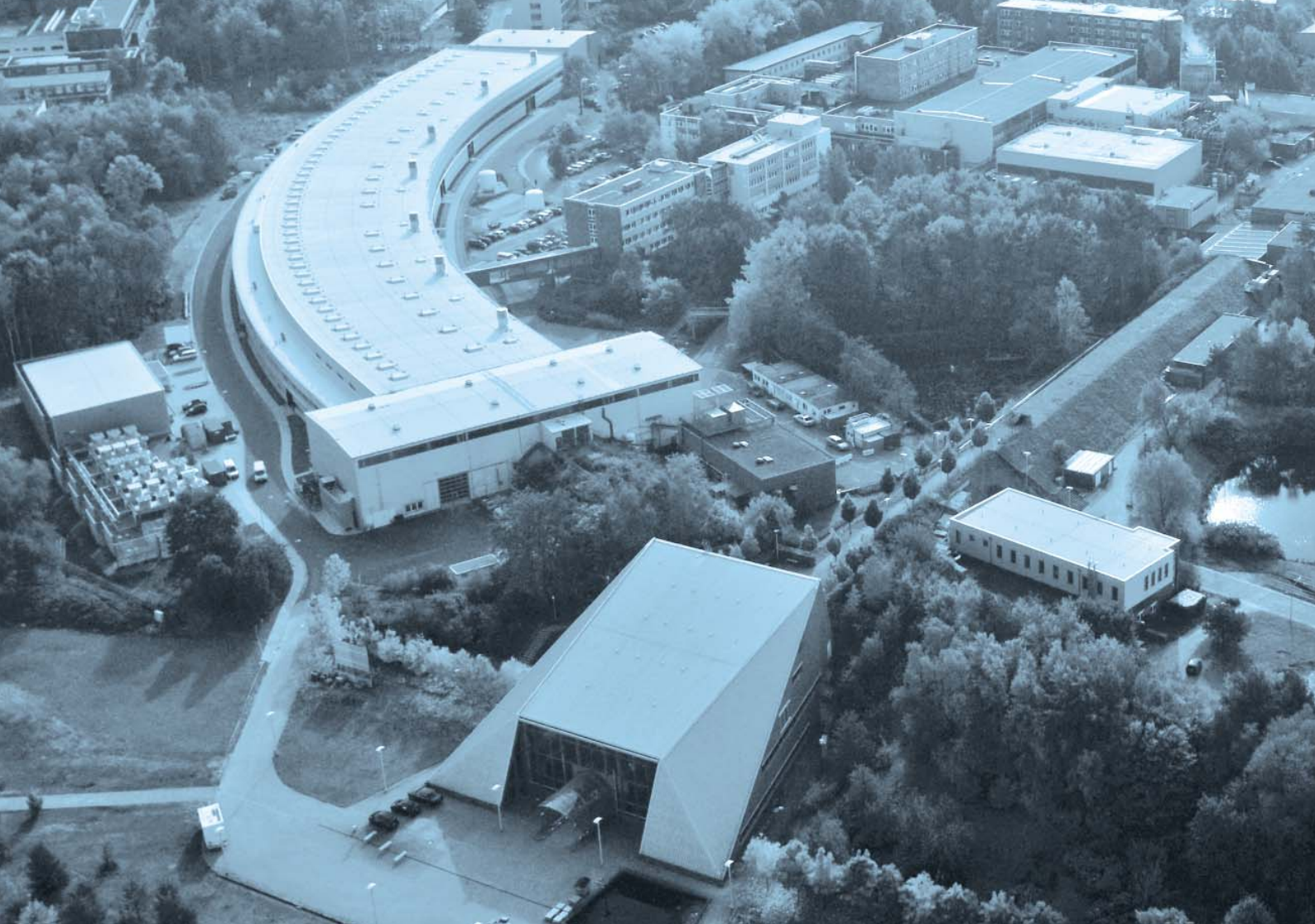
Being part of the HGF program „Research with Photons, Neutrons and Ions“ (PNI) in the research field "Structure of Matter", DESY photon science was heavily involved in preparing the strategic program for the next five years period (2010-2014) to be evaluated in spring 2009. In this period, the most important strategic tasks and projects for photon science will be the DESY contribution to the European XFEL, the proposed FLASH II, an extension of PETRA III allowing for a shutdown of DORIS III, and strengthening of photon science in-house research at DESY including the realization of CFEL and a development program for novel 2D photon detectors.

Another change took place with the beginning of 2008, Jochen R. Schneider retired from his DESY duties taking over new responsibilities at SLAC (Stanford). We are very grateful to him for his contributions to photon science, which were honored with the Order of Merit by the President of Germany, and we wish him all the best for the future.

All these activities and scientific results would not have been possible without our dedicated user community and motivated staff. Also, the generous support by the national funding agencies and the EU is gratefully acknowledged. As the new DESY director for photon science I would like to thank everyone for the combined efforts making Hamburg such an exciting place for multi-disciplinary research and I'm looking forward to a brilliant future for photon science at DESY. ●

A handwritten signature in black ink, appearing to read 'E. Weckert'.

Edgar Weckert
Director Photon Science



News and Events.

News and Events.

A busy year
2008

January

January 23–25:

Record attendance at the HASYLAB and XFEL users' meetings 2008

Record attendance at the three day event: about 380 scientists came to DESY in the last week of January, 2008. On January 23–24, 2008, the European XFEL Users' Meeting took place, which brought together the future users of the European X-ray laser facility. On the next day the 2008 HASYLAB Users' Meeting, accompanied by a poster session with 160 posters, attracted the many participants. Information on the status of the



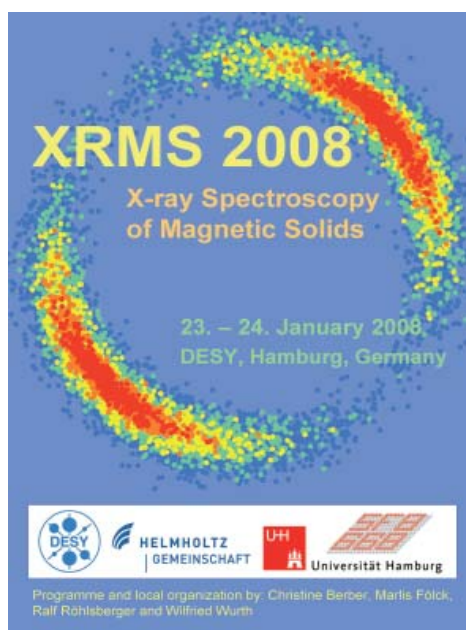
HASYLAB users' meeting 2008

operating photon sources FLASH and DORIS III and different current projects was provided. Four science talks complemented the program. Koen Janssens from the University of Antwerp, the Netherlands presented the first results concerning an investigation of a painting by Vincent van Gogh. The applied technique allows pictures, which were later painted over, to be revealed once more. Together with Joris Dik from TU Delft, Belgium and other colleagues, a 'colour photo' of the concealed portrait could be revealed. The publication of these results in July 2008 caused a sensation and was announced in hundreds of newspapers and other media worldwide.

January 23–24:

For the magnetic moments in life – XRMS 2008 workshop at DESY

On January 23–24, 2008, DESY provided a forum for more than 75 scientists from 12 countries to discuss recent developments in the investigation of magnetic solids with synchrotron radiation. The context for this meeting was the International Workshop for X-ray Spectroscopy of Magnetic Solids (XRMS 2008) which is held annually in conjunction with a user meeting of a synchrotron radiation facility in Europe. Invited and contributed talks were distributed over five sessions during the 1 ½ day workshop. The first session was devoted to the exploitation of X-ray coherence to reveal structure and dynamics of magnetic domains in thin films. In a keynote talk, Eric Isaacs (Argonne National Laboratory) showed how to apply X-ray photon correlation spectroscopy (XPCS) to study the slow dynamics of antiferromagnetic domains in thin films. In the same session, Simone Streit-Nierobisch (DESY) presented first results of magnetic small-angle scattering that were obtained at FLASH. These data actually inspired the design of the conference poster. The final session was organized together with the 2nd XFEL Users' meeting at DESY that ran parallel to the XRMS workshop. The central theme of this session was the time-resolved study of magnetization dynamics that will gain substantially by application of femtosecond pulses delivered by the European XFEL.



January 24:

Colloquium honoring Jochen R. Schneider

The colloquium for Jochen R. Schneider, who retired from his position as director for photon science at DESY at the end of 2007, took place on January 24. Science talks and greetings from many colleagues and friends from photon science facilities around the world, i.e. SLAC, ESRF, SLS, BESSY, ANKA and from institutions like the Federal Ministry of Education and Research BMBF and committees like the Committee Research



Colloquium honoring Jochen R. Schneider

with Synchrotron Radiation KFS, alternated in the afternoon. And so did the titles, going from “the early years” (Andreas Freund) to “long nights at DESY” (Helmut Dosch), and ranging from “the quest for higher resolution in space and in time” (Philip Coppens), to “imaging at FLASH and beyond” (Henry Chapman). About 300 colleagues, friends and Jochen Schneider’s family attended the colloquium and enjoyed the witty and inspiring presentations.

March

March 10–11:

Workshop on data acquisition and control for XFEL photon beamline systems

The XFEL work package for data acquisition (DAQ) and control, WP76, was established at the beginning of the year. A kick-off “DAQ and control for photon beamline systems workshop” was held on 10 - 11th March, at DESY. The workshop was attended by 50 DAQ readout and control experts from 3rd and 4th generation light sources, high energy physics laboratories, and universities. The workshop’s aim was to review all aspects of DAQ and control anticipated at the European XFEL, to meet other groups and exchange ideas, to identify regions of common interest and possible in-kind contributions, and to understand what other facilities were planning. Three key items were identified during the workshop as being of particular importance: 1) the readout architecture, capable of handling the high data rates expected at XFEL, must be defined, 2) a common DAQ and control backend solution for the 2D pixel detectors, as requested by the XFEL review board, needs developing, and 3) concepts for managing, archiving, and analyzing the large amounts of data to be produced at XFEL are required, and should be detailed in a computing technical design report (TDR). Other items, such as control system software, beam line instrumentation, photon diagnostics development, etc., could be addressed later. In this respect the further development of systems in use or proposed for FLASH are an attractive option. The importance of developing online and offline data rejection and reduction methods to reduce the data volumes produced at XFEL will be critical. As scientific input, including simulations of detector response, has only recently started, this topic will be readdressed later.

March 17–20:

404th Wilhelm and Else Heraeus seminar “Matter in Coherent Light”

The 404th WE Heraeus Seminar “Matter in Coherent Light”, held at the ‘Physikzentrum’ in Bad Honnef from March 17 to 20, informed the interested user community on the coherence properties of the novel, accelerator based light sources – storage rings and free-electron lasers (FELs). New, coherence based methods were presented and their application to open questions in biology and physics were discussed. A total of 25 speakers shared their views with an audience of more than 80 participants. The necessity for wave-front preserving optics and fast 2D detectors was illustrated. The latest results ob-

tained with Coherent Diffraction Imaging (CDI), Fourier Transform Holography (FTH) and X-ray Photon Correlation Spectroscopy (XPCS) were reported. The response of the audience was very positive culminating in the wish to repeat a similar seminar in 2-3 years time.

April

April 9–11: IRUVX-PP – A kick-off for a European FEL research infrastructure

The IRUVX-PP is an EU-project funded under the Seventh Framework programme for Research (FP7) by the European Commission to prepare the foundation of the 'EuroFEL' Consortium, which is one of the 35 ESFRI roadmap 2006 European research infrastructure projects. The aim of this preparatory project (PP) is to facilitate novel and wide-ranging studies of matter for a large science community by creating a distributed research infrastructure, based on the existing (FLASH) and planned FELs in Europe. 92 scientists and experts from the five partner and four potential partner institutions met at DESY in April formally starting the IRUVX-PP project and defining the first steps within the eight work packages. Following a general welcome, the participants were introduced to the key aims of the ESFRI roadmap and the preparatory project. A panel discussion illuminated the various legal, financial and administrative challenges of setting up a pan-European consortium and gave an overview on science cases for free electron lasers. On the following 1 ½ days the experts worked out the first detailed work plans in each work package.

May

May 16: Brainstorming meeting on computational materials science

With the increasing complexity of new materials there is a growing need for computational methods to understand and control their properties. The Bremen Center for Computational Materials Science (BCCMS), headed by Thomas Frauenheim, has established substantial resources in this field. A common workshop between the BCCMS and DESY, held on May 16, 2008 at DESY, was organized to identify common areas of cooperation, particularly with respect to upcoming experimental possibilities at the photon sources at DESY. About 20 participants discussed experimental, theoretical and computational approaches that could guide research efforts in the following fields: Dynamics of friction and lubrication, structure evolution in metallic glasses and amorphous materials, structure and dynamics in H₂-storage materials, dynamics of dissociation and isomerization processes in photochemically sensitive molecules, nonperturbative interactions of ultra-short laser pulses with nanostructures, and the development of methods for XFEL-based experiments.

July

July 1: PETRA III experimental hall – construction site handed over to DESY

Exactly one year after the official PETRA III construction began, the experimental hall, including the outside facilities, was handed over to DESY. The 10 metre high experimental hall has been finished in accordance with the schedule, in spite of its complex construction. As of 2009, the foundation, consisting of 99 deep piles and the world's largest single-slab concrete plate, will ensure a vibration-free experimental environment.



Main entrance

July 9–11: BMBF Verbundforschungstreffen for projects at FLASH and PETRA III

In July 2008 the "BMBF Verbundforschungstreffen" gathered all projects related to FLASH and PETRA III and supported by the Federal Ministry of Education and Research (BMBF). The success of the „BMBF Verbundforschung“ is based on the interaction of excellent research groups which are mainly from universities with the experimental facilities at DESY for research with photons. As a result, the usability of our facilities has clearly



Attendees at the "BMBF Verbundforschungstreffen"

been improved. The unique research possibilities at FLASH and PETRA III have attracted a large number of research projects. In total the „BMBF Verbundforschung“ supports current projects at FLASH and PETRA III with 27.5 million Euro in the 2007-2010 funding period. The programme of the three day meeting gave a broad overview over the scientific goals and methods which are pursued by these projects. The meeting started with an introductory session including welcome addresses from the BMBF (Rainer Koepke) and the president of the Hamburg University (Monika Auweter-Kurtz). This was followed by four sessions devoted to PETRA III projects ranging from materials characterisation using hard X-rays to soft X-ray scattering. An overview talk on the current status of the LCLS project (Jochen Schneider) served as a smooth transition to the four sessions on FLASH projects where the reports on current project activities could be spiced with recent research highlights. In addition to the 30 talks during the oral sessions, a poster session allowed for further discussion of the planned projects as well as the anticipated instrumentation. More than 125 participants (2/3 coming from universities) contributed to a very lively meeting. For the local DESY attendants the meeting provided first-hand information on the needs of the users. In summary, one can expect that this meeting will certainly have an impact on the future success of the “BMBF Verbundforschung” projects at FLASH and PETRA III.

July 23–September 16: International DESY summer student program at HASYLAB

Out of 54 applicants, 21 undergraduate students (7 female and 14 male) from Germany, Russia, Thailand, Great Britain, Poland, Spain, Austria, and Brazil were selected to join the international DESY summer student program at HASYLAB in 2008. During their eight week stay starting on July 23 the students participated in the work of various research groups at HASYLAB, MPG, or EMBL where they worked on their own small projects. Additionally, they attended a series of lectures covering DESY topics in general and topics especially related to research with synchrotron radiation. Most of the relevant experimental techniques used with synchrotron radiation were introduced in 17 talks given by experts in the corresponding fields. Usually, the students would also have a dedicated exercise week to practice experiments at selected DORIS III beamlines.



Summer students at HASYLAB

However, in 2008 the summer students stay coincided with the extended shutdown of the storage ring and therefore this event could not be arranged. The students appreciated the stimulating atmosphere at DESY, the international spirit, the engagement of the staff to make their stay a great experience, and the lectures that covered topics usually not presented in such a comprehensive manner in university courses.

September

September 8-10: 4th FLASH user workshop

The fourth FLASH user workshop, held over three days with 101 participants, which made it the largest so far at DESY, was split in two parts. The first part dealt with the planned upgrades (e.g. increased electron beam energy to reach wavelengths near the carbon K-edge) during the 2009 FLASH shutdown. The users were informed about new developments and expected improvements regarding FLASH performance, and the scientific infrastructure in the experimental hall. This included talks on the performance and upgrades of the accelerator and of the photon diagnostics, the beamlines, and the pump probe laser facility. The opportunity to comment on the planned activities was welcomed by the user community and led to a number of fruitful and lively discussions. The second part of the workshop was dedicated to the recently completed and currently commissioned terahertz radiation (THz) beamline at FLASH. Speakers presented ideas for future pump-probe experiments utilizing the new beamline with the aim to direct the remaining commissioning time towards the requirements of these initial experiments. Experts from Germany, the US, England, Italy and the Netherlands held a series of lectures or presented posters. The first oral session aimed to put the beamline at FLASH into perspective with respect to other accelerator based THz sources. G.P. Williams (Jefferson Lab) gave a brief history and a look forward on research with THz synchrotron radiation from linac and storage ring based sources, and W. Seidel (FZ Dresden/Rossendorf) presented the status and performance of Germany's first working THz FEL, “FELBE”. This was followed by a session to define and discuss areas of research at FLASH that would benefit most from the availability of naturally synchronized THz pulses as either pump or probe. This session was opened by M. Drescher (University of Hamburg), who presented the results of the first pilot THz pump XUV probe experiment performed at the beamline, and outlined the potential of applying techniques for THz field assisted XUV photoionization in atomic and molecular physics. J. Marangos (Imperial College London) discussed the possibility to utilize the THz pulses for molecular alignment, and M. Vrakking (FOM/Amsterdam) presented ideas to utilize the THz beamline for field ionization. The session ended with a lecture by A. Cavalleri (MPGSD/CFEL), who presented the fascinating prospects for studying ultra fast vibrational control of electronic phases in complex condensed matter systems. Several potential future users used the opportunity to present and discuss their experimental ideas in oral and poster sessions.

**September 26:
X-ray scattering and rheology – Perspectives at DORIS III and
PETRA III**

The aim of the workshop on the combination of X-ray scattering and rheology was to bring together experts of the rheology community at HASYLAB to initiate a future 'Rheo/Saxs' project and also to learn about ideas and demands of possible future user groups. Nine speakers were invited to report on their actual research and future perspectives. The participants came from Germany, the Netherlands, Belgium, France and Switzerland. The topics discussed ranged from polymer science to colloids, food rheology, and theoretical approaches to the interplay of mechanical deformation and microstructure formation. Furthermore, the new approach to the combination of X-ray scattering and rheology recently developed at HASYLAB was discussed in detail. Several participants expressed strong interest in that technique and its ability to be further developed for the use at PETRA III in combination with techniques such as XPCS to gain first detailed information about dynamics in complex fluids in non-equilibrium states. A multi purpose rheometer will be available for users at the DORIS III beamline BW1 in 2009.

October

**October 6:
The Order of Merit for the former DESY research director Jochen
R. Schneider**



The German Federal President Horst Köhler awarded Jochen R. Schneider with the Order of Merit of the Federal Republic of Germany (right: Horst Köhler and his wife Eva Luise Köhler)

The German Federal President Horst Köhler awarded long-time DESY research director Jochen R. Schneider with the Order of Merit of the Federal Republic of Germany (Bundesverdienstkreuz 1. Klasse) on October 6, 2008. He was honoured for his prominent contributions in making DESY one of the world-leading centres for research with photons. Starting in 1993, Jochen R. Schneider was the head of HASYLAB and from 2000 to 2007 he was the director of the photon science division at DESY. During this period, the unique free-electron laser FLASH had come into operation and the course has been set for the future projects, PETRA III and the European XFEL. Currently, Jochen R. Schneider is the director of the Experimental Facilities Division at SLAC in Stanford.

**October 6–7:
International collaboration meeting on peak brightness
experiments at FLASH**

The Peak Brightness Experiments at FLASH collaboration formed in 2002 on the occasion of the first call for proposals for this facility. The scientific topic of this international collaboration, led by R.W. Lee (Livermore/Berkeley) and D. Riley (Belfast), is the investigation of dense matter under extreme conditions. Investigated systems include for example, solids exposed by focussed FEL radiation or plasmas generated by a high energy optical laser. Approximately fifty scientists from more than ten countries met at DESY to review the results of recent experiments at FLASH, to discuss ideas for next experiments and possibilities of future collaboration, and to gather information about upcoming activities at future FEL facilities. The recent success of the FLASH experiments, e.g. the intensity dependent transmission of aluminium, created excitement in the audience and led to many fruitful discussions.

**October 8–10:
Interaction of FEL radiation with matter - recent experimental
achievements and challenges for theory**

This workshop was devoted to recent experimental and theoretical achievements obtained from studies on the interaction of intense VUV and soft X-ray FEL radiation with matter. The aim was to present experimental results that could stimulate novel theoretical research, identify problems important for planning future experiments where theoretical input would be required, and initiate collaborations between experimental and theoretical groups. The workshop attracted well-known speakers covering both theoretical and experimental developments. They gave 38 talks in total; among them were review talks and talks on recent experimental highlights. The broad overview of this novel research field was summarized within the twelve sessions of the workshop: status and perspectives for FLASH and XFELs, research on atoms and molecules, non-linear processes, modelling the dynamics of irradiated samples, clusters and bio-molecules, solids and surfaces, plasma and warm dense matter research, radiation damage to optical elements, and coherent diffraction imaging with

FELs. The poster session attracted 54 very interesting poster presentations. In total 200 participants from all over the world registered for the workshop. The participants found that the meeting was important for strengthening the community interested in FEL research and suggested to continue with these kinds of workshops in the future.

**October 16–17:
Joint workshop on detector development for future particle physics and photon science experiments**

As a satellite meeting to the 2008 IEEE Nuclear Science Symposium - Medical Imaging Conference (NSS-MIC) meeting in Dresden, a 1 ½ day Joint Workshop on Detector Development for Future Particle Physics and Photon Science Experiments was held at DESY; it attracted more than 70 participants. Eleven invited speakers from the high energy physics (HEP) and photon science (PS, synchrotron and free-electron laser X-ray sources) communities reviewed present and future trends in detectors, electronics, novel interconnection technologies and data acquisition architectures. Opening the meeting, Rolf-Dieter Heuer (DESY/CERN) stressed the workshop goal of bringing together both communities to foster joint developments. In order to collaborate, the communities also have to understand their differences. Veljko Radeka (BNL) pointed out the “cultural” challenge involved: while HEP involves teams of hundreds of scientists and engineers developing one complex detector over many years, PS experiments involve generally a few scientists performing an experiments in hours or days, and they mostly use commercially available detectors. Various examples of existing synergies were also presented. Michael Campbell (CERN) gave an example of positive synergy in pixel detector developments within the Medipix Consortium: this

work saw its genesis within HEP, found applications in PS, and the case of the new Timepix detector is seeing a “spin back” of benefit to HEP applications. The meeting left several clear messages: both communities face the same challenges in exploiting the exciting possibilities offered by deep sub-micron CMOS and 3D-integration techniques, and DAQ processing and GRID needs are broadly similar. It was, however, encouraging to see that over the recent years the number of collaborative efforts between the two fields has rapidly increased, and an increasing number of bridges have already been built. All participants were convinced that this process should and will continue.



Joint workshop on detector development

November

**November 5:
Industry forum 2008**

On November 5th 2008, the HASYLAB Service Group Industry together with GKSS organized the 2008 industry forum “New Materials in the Light of the Future”. The one day workshop comprised of a selection of talks about materials science research and applications. An opening speech by A. Wagner (DESY) was followed by the presentation of the photon science facilities at DESY. The facilities for materials science at GKSS and its outstation at HASYLAB were presented by W. Kaysser and A. Schreyer (both GKSS). The second session of the forum was devoted to applications of synchrotron radiation in materials science, such as tomography and the determination of residual stresses. In the afternoon, the construction site of the new synchrotron radiation laboratory PETRA III, including the components that had already been installed in the accelerator tunnel, could be visited. Of special interest in the experimental facilities at the storage ring DORIS III were the stations for small angle scattering and materials diffraction imaging at HASYLAB and the new diffractometer at the GKSS outstation. After the tour, the programme continued with presentations of tomography at the AUDI laboratories and materials research performed at the Helmholtz-Zentrum Berlin (HZB). One topic of the ensuing discussion was where analyses with synchrotron radiation can go beyond tomography. The participants found the forum very useful; a first request for beamtime came just one week after the industry forum. ●

Joint Workshop on Detector Development
for Future Particle Physics and Photon Science Experiments

Satellite workshop of the 2008 IEEE NSS/MIC Symposium

Joint Workshop on Detector Development
for Future Particle Physics and Photon Science Experiments

Workshop to highlight differences and synergy between photon science and particle physics experiments.

- Educational talks
- Overview talks about the future of both fields
- Sessions:
 - active elements
 - front-end electronics and related issues
 - back-end (DAQ, data flow and storage)
- Round table discussions

**16-17 October 2008,
DESY Hamburg, Germany**

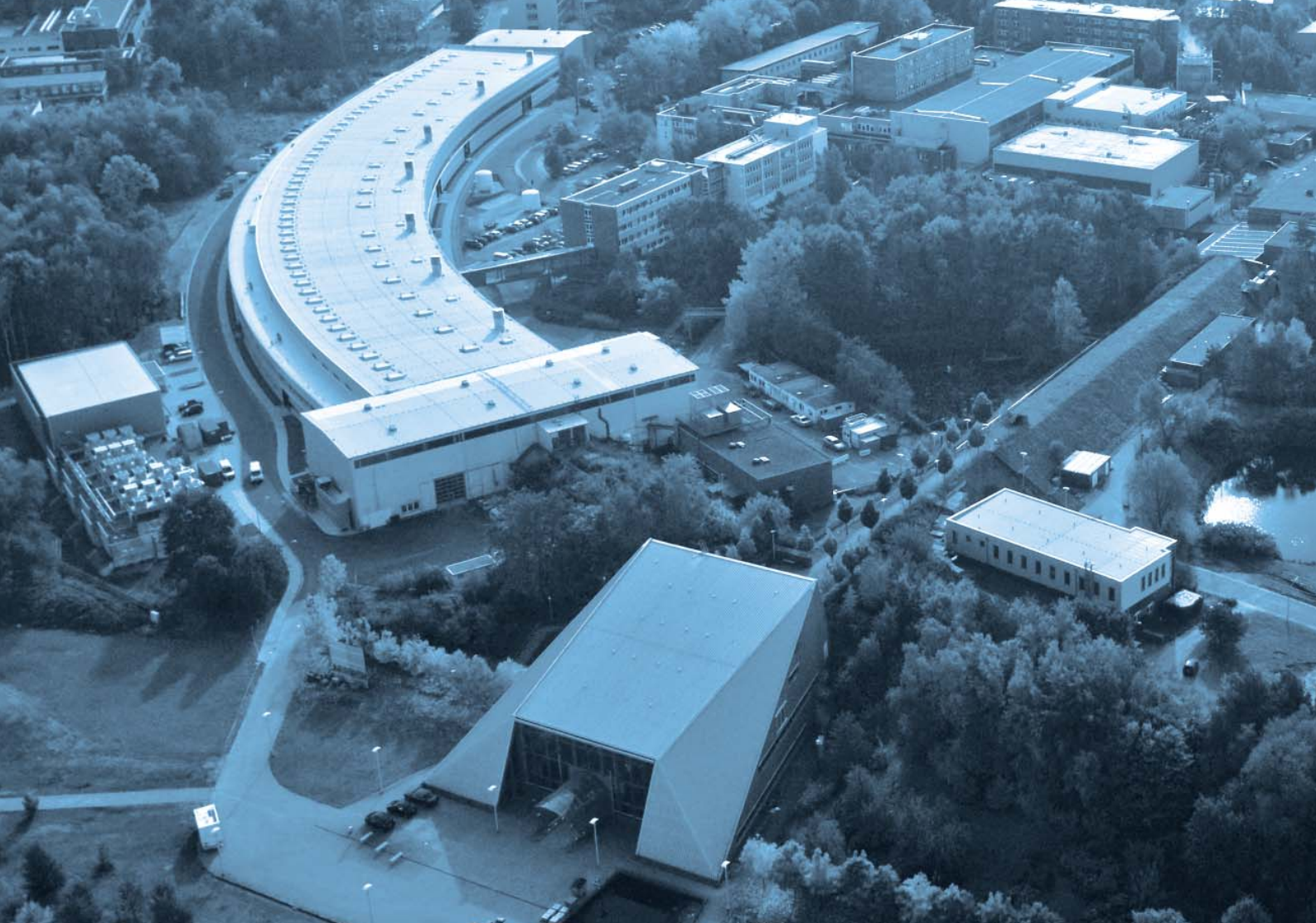
Erik Holme, CERN, Switzerland
Christophe De La Taille, LAL, France
Heinz Graesslin, DESY, Germany
Ingrid Maria Greger, DESY, Germany
Sol Gruner, Cornell, USA
Rolf-Dieter Heuer, DESY, Germany
Roland Hortsberger, PSI, Switzerland

John Morse, ESRF, France
Felix Sefkow, DESY, Germany
Paul Seller, RAL, UK
Toshio Takeda, Sinsu Univ., Japan
Niels van Bakel, SLAC, USA
Norbert Wimmer, Univ. Bonn, Germany
* organization committee

More information: SatWorkshop2008@desy.de • Contact: SatWorkshop2008@desy.de

NUCLEAR & PLASMA SCIENCES SOCIETY
2008 NSS-MIC Dresden
IEEE

Joint workshop on detector development for future particle physics and photon science experiments' poster.



Research Highlights.

- **A femtosecond X-ray / optical cross-correlator** 18
- **Ultrafast movies of nanoscale dynamics** 20
- **Massively parallel X-ray holography** 22
- **Clusters in super intense FLASH pulses** 24
- **A chemically driven insulator-metal transition** 26
- **Tough silk** 28
- **Insight into the reactivity** 30
- **The many faces of molecular assemblies in electronic devices** 32
- **Cooperative or self-centred** 34
- **Visualizing a lost painting by Vincent van Gogh** 36
- **Metal contaminations in small water fleas** 38
- **Small-angle X-ray scattering complements crystallography** 40
- **Mapping the protein world** 42
- **How metallic iron eats its own native oxide** 44
- **Hard X-ray holographic diffraction imaging** 46

A femtosecond X-ray / optical cross-correlator.

FLASH X-ray pulses induce transient changes in optical reflectivity

For scientists, a longstanding dream has been to record a molecular movie, where both the atomic trajectories and the chemical state of every atom in matter is followed in real time. X-ray free-electron lasers (FEL) are about to enable this research as they deliver brilliant femtosecond X-ray pulses for time resolved spectroscopy, imaging and diffraction. To utilize the method of two-colour pump/probe spectroscopy, the temporal and spatial overlap of an optical and the X-ray laser pulses – called cross-correlation – need to be monitored for various experimental environments in a simple and efficient way. Since FLASH pulses are sufficiently brilliant to modify the optical properties of a solid material, the rapid X-ray pulse induced transient change of optical reflectivity on a GaAs surface can be used for such cross-correlation.

The principle of X-ray induced transient changes of the optical reflectivity is depicted in Fig. 1. The temporal changes of the optical reflectivity following the absorption of a femtosecond X-ray pulse on a GaAs(100) surface was determined. Pulse energies of an optical laser synchronized to FLASH [1] were detected in a reference path and after reflection with two fast photodiodes, allowing for reflectivity measurements pulse by pulse. The visible laser operates at twice the repetition rate (1 MHz) of FLASH (500 kHz) within each pulse train of 30 radiation bursts. This results in alternating measurements of the reflectivity with the X-ray pump pulse and without it as a reference.

In Fig. 2, the time scales of the transient reflectivity changes $\Delta R/R$ are presented. The intense X-ray excitation leads to an ultra-fast drop in optical reflectivity, which recovers within a few picoseconds – and depends in detail on X-ray fluence and probe wavelength. We focus on the femtosecond time scale of $\Delta R/R$, which is relevant for cross-correlation measurements, Fig. 2 b+c. The rapid drop in reflectivity occurs independently of the optical probe wavelength. A fit with an exponentially decaying response function convoluted with a Gaussian, yields a FWHM of 160 ± 44 fs. Thus, the intrinsic time constant is small compared to the cross-correlation width making it suitable for such measurements. In practice, we have employed this method to detect the temporal variations within FLASH bunch trains and performed in a time-to-space mapping geometry single-shot timing measurements [2].

The physical mechanism of X-ray pulse induced transient reflectivity changes starts with the absorption of the FEL radiation, governed by the atomic photoionization cross sections [3] leading preferentially to Ga 3d vacancies. Within 10 nm of the GaAs sample 10% of the incident photons are absorbed, staying below the damage threshold of the GaAs surface [4]. At an excitation fluence of 10 mJ/cm^2 , within the 10 nm thick surface layer a Ga 3d excitation density of approx. $1.6 \cdot 10^{20} \text{ cm}^{-3}$ is created. Within a few femtoseconds, Auger decay and auto-ionization convert the initial inner shell excitation [5] into twice

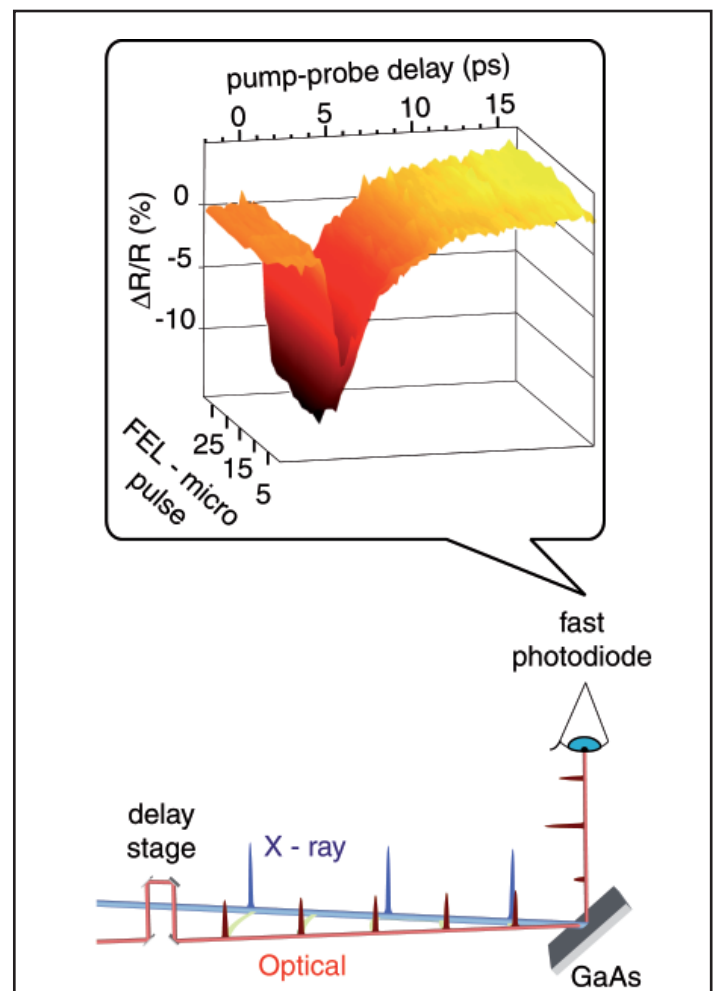


Figure 1

Transient X-ray induced optical reflectivity ($\Delta R/R$) measurement - schematic overview: Extreme ultraviolet FEL pulses (39.5 eV , $< 50 \text{ fs}$, $< 16 \mu\text{J}$) impinge onto a crystalline GaAs (100) surface and generate photoexcited carriers. The transient changes of the dielectric function are probed by visible laser pulses (800 nm or 400 nm , 120 fs , $< 10 \text{ nJ}$) reflected from the GaAs surface at 53° as a function of their temporal delay relative to the FEL radiation pulse. Experimental reflectivity data for a bunchtrain of 30 microbunches is shown.

the number of valence excitations and finally, equilibration to the mean energy of electron-hole pair creation in GaAs [6] produces an electron-hole pair density of $1.5 \cdot 10^{21} \text{ cm}^{-3}$. With optical laser excitation at and above the optical damage-threshold photo-generated free carriers exceeding 10^{20} cm^{-3} lead to similar $\Delta R/R$ transients as we find for X-ray excitation below the damage threshold. There, the free carrier absorption changes the dielectric function as described by the Drude model. Beyond that, screening of ionic potentials and electron many-body effects are important as they modify the band structure [7]. A full theoretical model of the X-ray pulse induced optical transient reflectivity needs to consider the response of the dielectric function to the distortion of the valence electronic structure through photoionization and Auger decay, electronic screening, electron-electron scattering and phonons in the crystal lattice. Based on this physical mechanism, we expect X-ray induced transient optical reflectivity to be applicable to the energy range of present and future FEL sources. As the photoabsorption decreases less than inversely with photon energy, the reduced absorption probability is compensated by the higher photon energy, as the density of the excited carrier distribution responsible for the changes in reflectivity also depends on the absorbed energy. In summary, the technique of X-ray induced transient optical reflectivity on a GaAs surface has been established as a powerful tool for cross-correlation between femtosecond optical and X-ray pulses, spanning the energy range of present and future X-ray free-electron laser sources. Furthermore, X-ray induced non-equilibrium dynamics opens a new field of time resolved studies of matter which is highly relevant for X-ray induced chemistry in biological systems, solids and interfaces e.g. present in atmospheric and interstellar dust. Thus, our findings pave the way towards time resolved structural dynamics in chemistry, biology and materials science. ●

Contact: Alexander Föhlisch, Alexander.Foehlich@desy.de

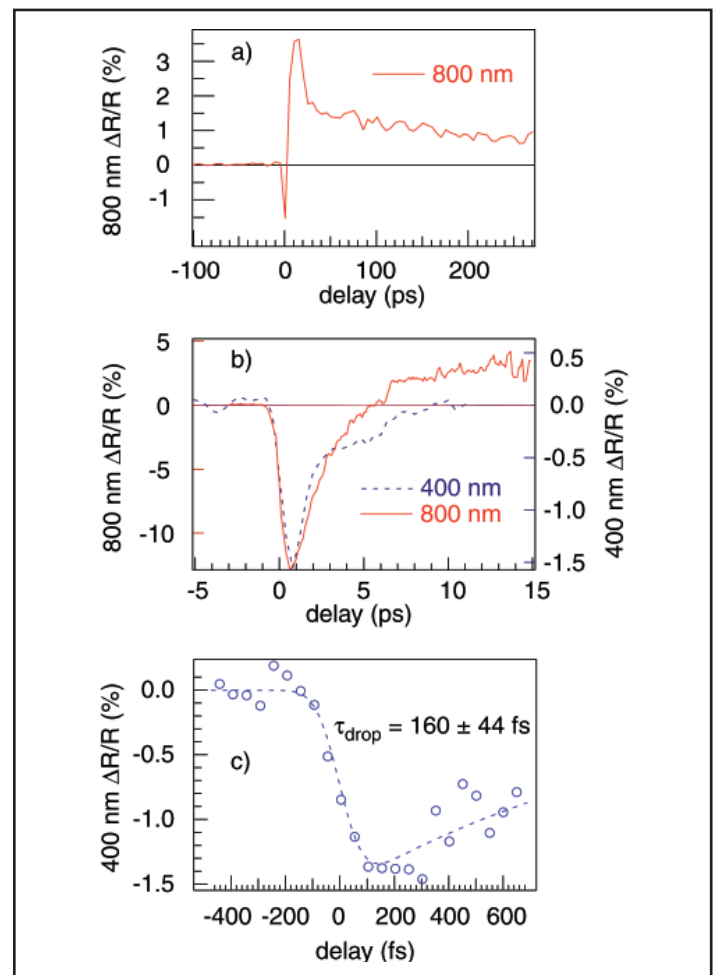


Figure 2

Transient X-ray induced optical reflectivity ($\Delta R/R$) – temporal characteristics: a) X-ray pulse induced dynamics: A rapid initial electronic response is followed by slower lattice dynamics on a picosecond timescale b) Ultra fast electronic response after X-ray pump: The rapid drop of $\Delta R/R$ observed for 400 nm and 800 nm probe wavelength is followed by a recovery which depends on the GaAs band structure and the time scale of electronic relaxation. c) The width of the initial drop in optical reflectivity as determined fitting an exponentially decaying response function convoluted with a Gaussian (full width at half maximum of 160 ± 44 fs) is limited by the pulse length of the optical laser pulse (120 – 150 fs). To eliminate temporal jitter from the accelerator the delay is corrected for the electron bunch arrival determined with electro optical sampling (EOS) [8].

Authors

C. Gahl^{1,3}, A. Azima⁵, M. Beye², M. Deppe², K. Döbrich¹, U. Hasslinger², F. Hennies^{2,4}, A. Melnikov¹, M. Nagasono², A. Pietzsch², M. Wolf¹, W. Wurth², A. Föhlisch²

1. Fachbereich Physik, Freie Universität Berlin, Arnimallee 14, 14195 Berlin, Germany
2. Institut für Experimentalphysik, Universität Hamburg, Luruper Chaussee 149, 22761 Hamburg, Germany
3. Max-Born-Institut für nichtlineare Optik und Kurzzeitphysik, Max-Born-Str. 2A, 12489 Berlin, Germany
4. MAX-lab, Lund Universitet, Ole Römers väg 1, Box 118, 221 00 Lund, Sweden
5. HASYLAB/DESY, Notkestr. 85, 22607 Hamburg, Germany

References

1. P. Radcliffe et al., “Single-shot characterization of independent femto-second extreme ultraviolet free electron and infrared laser pulses”, *Appl. Phys. Lett.* **90**, 131108(1-3) (2007).
2. T. Maltezopoulos, S. Cunovic, M. Wieland, M. Beye, A. Azima, H. Redlin, M. Krikunova, R. Kalms, U. Frühling, F. Budzyn, W. Wurth, A. Föhlisch, M. Drescher, “Single-shot timing measurement of extreme-ultraviolet free-electron laser pulses”, *New Journal of Physics* **10**, 033026 (2008).
3. J.-J. Yeh and I. Lindau, “Atomic Subshell Photo ionization Cross Sections and Asymmetry Parameters: $1 < Z < 103$ ”, *At. Data Nucl. Data Tables* **32**, 1 (1985).

J.-J. Yeh, “Atomic Calculations of Photo ionization Cross Sections and Asymmetry Parameters”, Gordon and Breach, Langhorne, PA (1993).

4. A. Cavalleri, et al., “Ultra fast x-ray measurement of laser heating in semi-conductors: Parameters determining the melting threshold”, *Phys. Rev. B* **63**, 193306(1-4) (2001).
5. M. O. Krause and J. H. Oliver, “Natural widths of atomic K and L levels, K alpha X-ray lines and several KLL Auger lines”, *J. Phys. Chem. Ref. Data* **8**, 329-338 (1979).
6. M. Krumrey, E. Tegeler, J. Barth, M. Krisch, F. Schäfers, and R. Wolf, “Schottky type photodiodes as detectors in the VUV and soft X-ray range”, *Applied Optics* **27**, 4336-4341 (1988).
7. L. Huang, J. P. Callan, E. N. Glezer and E. Mazur, “GaAs under intense ultra fast excitation: Response of the dielectric function”, *Phys. Rev. Lett.* **80**, 185-188 (1998).
8. A. L. Cavalleri et al., “Clocking Femtosecond X-Rays”, *Phys. Rev. Lett.* **94**, 114801(1-4) (2005).

Original publication

“A femtosecond X-ray/optical cross-correlator”, *Nature Photonics* **2**, 165 (2008).

Ultrafast movies of nanoscale dynamics

Diffraction and destroy

Combining an optical laser with FEL pulses from FLASH in a pump-probe set-up enables imaging with high temporal and spectral resolution. A nanostructure is ablated by an optical laser and this process is followed with lensless coherent diffractive imaging using FLASH pulses. A spatial resolution of better than 50 nm is achieved. By taking pictures of a succession of exploding targets, a movie can be made following the dynamics of the solid material on a 10 ps timescale. With short-wavelength X-ray FEL sources this method will enable higher spatial resolution imaging and could be used to measure the dynamics of highly correlated systems at nanometer length scales.

The FLASH FEL provides soft X-ray pulses with pulse durations down to a few tens of femtoseconds. This pulse duration provides the shutter speed to produce a movie of a nanostructure that is ablated by an optical laser. The ablating optical laser pulses are synchronized to FLASH and the relative delay was incremented with 10 ps steps with an optical delay line to observe the time evolution. We achieved a spatial resolution better than 50 nm, using 13.5 nm wavelength FLASH pulses, and the lensless imaging technique of coherent diffractive imaging [1]. This ultrafast high-resolution imaging opens up the study of condensed phase dynamics, such as crack formation, phase separation and nucleation, and rapid fluctuations in liquids or biologically relevant environments [2].

To demonstrate ultrafast single-shot imaging we fabricated many identical nanostructured samples in a 20 nm thick silicon nitride membrane coated with a 100 nm thick iridium film, using a focused-ion beam (FIB) to mill out a 2.5 μm wide structure similar to the logo of a Canadian Hockey team of renown (to some of the authors). A 130 nm diameter pinhole was also milled into the membrane, 6 μm from the structure. The entire fabricated structure served as a reference in which to observe dynamics on a wide range of length scales. The ablation process was initiated with the FLASH facility's 12.5 ps duration Nd:YLF laser operating at 532 nm wavelength and focused onto the sample with a peak intensity of about $2.2 \times 10^{11} \text{ W cm}^{-2}$. The movie was recorded with FEL pulses of 20 μJ mean energy that were focused onto the sample. Since each FEL pulse completely destroyed the object, we recorded each frame with a separate identical structure. As previously seen from studies of spherical test objects at FLASH [3] the FEL pulse duration is shorter than the radiation damage processes caused by the rapid photoionization and heating that occurs upon irradiation. Thus the destruction initiated by the FEL probe pulse does not influence the laser-induced dynamics under observation. Frames of the ultrafast movie are shown in Fig. 1. These are coherent diffraction patterns acquired for different delay times after the laser pulse. The disintegration of the structured

sample is evident as a loss of information at high scattering angles. At the same time, additional structure is induced in the foil by the ablation pulse, which shows up as fine speckles at scattering angles corresponding to structures smaller than 100 nm. Additionally, a pair of strong diffraction peaks is observed after about 140 ps due to a light-induced periodic structure in the foil [4]. We can quantify the changes in the structure by correlating the time-dependent patterns with the undamaged pattern. We use a correlation analysis similar to that used in X-ray photon correlation spectroscopy [5]. These correlation functions, averaged over shells of constant momentum transfer q , are shown in Fig. 2. A unity value of the normalized correlation function corresponds to an unchanged structure. We see the drop in correlation occurs at smaller q values (longer length scales) as time progresses, propagating at 5000–6000 ms^{-1} during the first 20 ps, consistent with the sound speed in the heated membrane. The explosion slows to 1000–2000 ms^{-1} by 140 ps as the resultant plasma expands and cools.

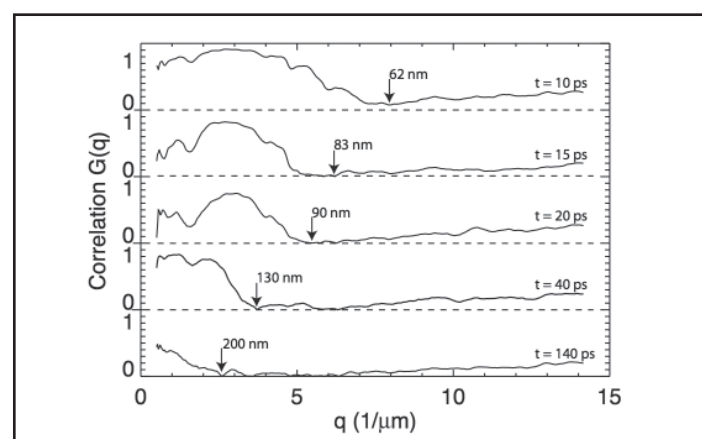


Figure 2

Cross-correlation functions of the time-dependent diffraction intensities with the diffraction of the unablated sample. Arrows point to the largest feature size at which the correlation function approaches zero, indicating the length scale of destruction in the sample.

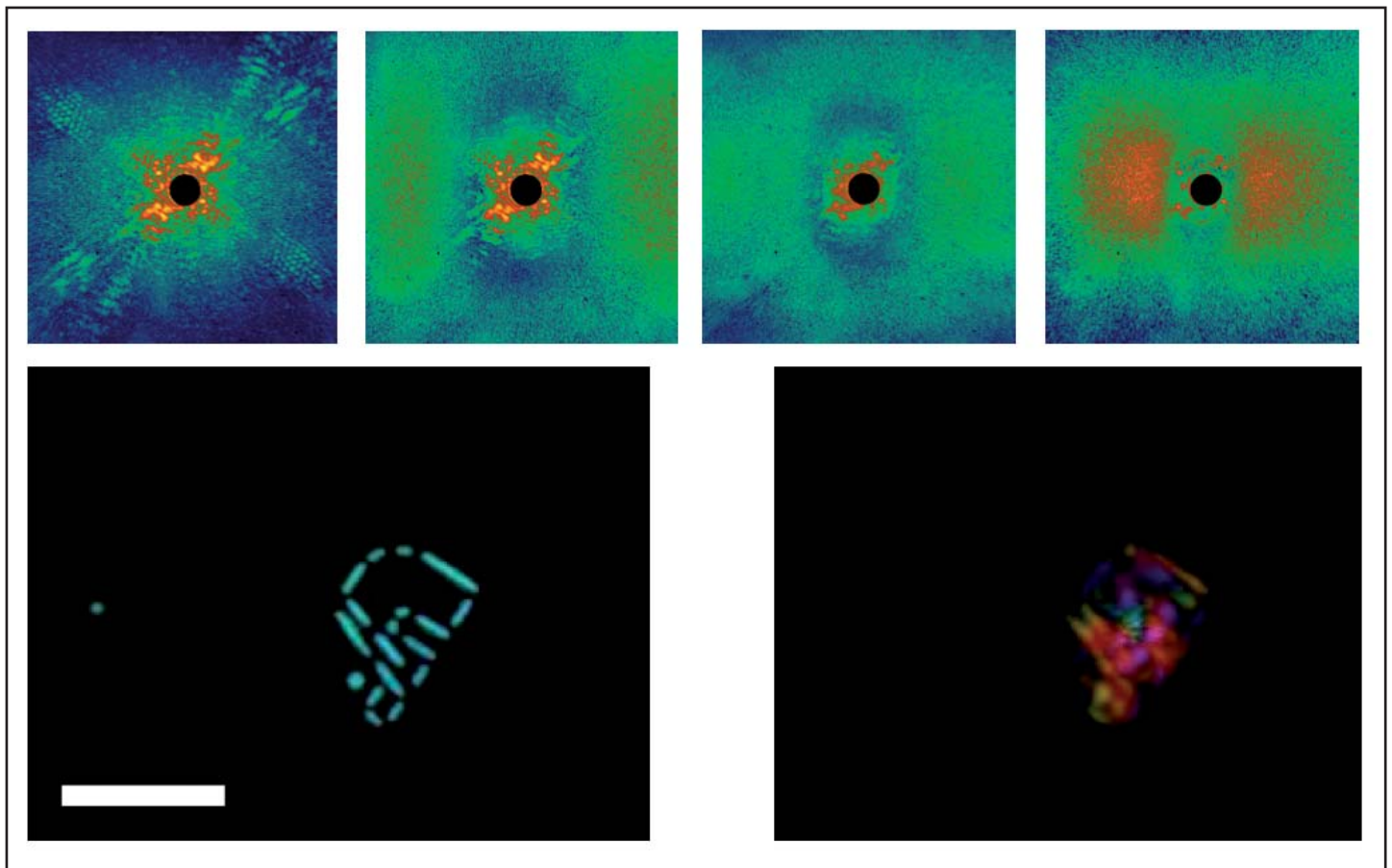


Figure 1

Coherent diffraction patterns recorded for delays of -5, 10, 15, and 40 ps after the optical laser ablation pulse. Degradation of the nanofabricated sample appears as a loss of high spatial frequency information. Additional structure that causes speckles at around 100 nm spatial period, and a periodic structure, grows with time. Phase retrieval reconstructions of the undamaged sample (left) and at a 15 ps delay (right) are also shown, with a 2 μm scale bar.

We have also reconstructed images of the ablating structures, by iterative phase retrieval (see Fig. 1). At short time delays the 130 nm reference dot provides a reference wave that aids reconstruction. However, after 10 ps this dot is half its initial size and it is no longer visible after 15 ps.

The method of ultrafast diffractive imaging will be further developed to achieve higher spatial resolution at future short-

wavelength X-ray FELs. In particular we aim to measure the dynamics of highly correlated systems at nanometer length scales. Such methods are only possible with the unique characteristics of FEL sources: high peak brightness, short wavelength, and full coherence. ●

Contact: Henry N. Chapman, henry.chapman@desy.de

Authors

Anton Barty^{1,7}, Sebastien Boutet^{2,3}, Michael J. Bogan¹, Stefan P. Hau-Riege¹, Stefano Marchesini¹, Klaus Sokolowski-Tinten⁴, Nikola Stojanovic⁴, Ra'anan Tobey⁵, Henri Ehrke⁵, Andrea Cavalleri^{5,9}, Stefan Düsterer⁶, Matthias Frank¹, Saša Bajt^{1,8}, Bruce W. Woods¹, M. Marvin Seibert³, Janos Hajdu³, Rolf Treusch⁶, and Henry N. Chapman^{1,7,8}

1. Lawrence Livermore National Laboratory, 7000 East Avenue, Livermore, California 94550, USA
2. SSRL, Stanford Linear Accelerator Center, 2575 Sand Hill Road, Menlo Park, California 94025, USA
3. Laboratory of Molecular Biophysics, Department of Cell and Molecular Biology, Uppsala University, Husargatan 3, Box 596, SE-75124 Uppsala, Sweden
4. Institut für Experimentelle Physik, Universität Duisburg-Essen, Lotharstraße 1, 47048 Duisburg, Germany
5. Department of Physics, Clarendon Laboratory, University of Oxford, Parks Road, Oxford OX1 3PU, UK
6. HASYLAB at DESY, Notkestraße 85, D-22607 Hamburg, Germany
7. Center for Biophotonics Science and Technology, University of California, Davis, 2700 Stockton Boulevard, Ste 1400, Sacramento, California 95817, USA
8. CFEL, Universität Hamburg at DESY, Notkestraße 85, 22607 Hamburg, Germany
9. Max Planck Research Group for Structural Dynamics, CFEL, Universität Hamburg at DESY, Notkestraße 85, 22607 Hamburg, Germany

References

1. H.N. Chapman et al. "Femtosecond diffractive imaging with a soft-X-ray free-electron laser", *Nature Physics* 2, 839 – 843 (2006).
2. K. Sokolowski-Tinten, J. Bialkowski, A. Cavalleri, D. von der Linde, A. Oparin, J. Meyer-ter Vehn, and S. I. Anisimov, "Transient states of matter during short pulse laser ablation", *Phys. Rev. Lett.*, 81, 224–227 (1998).
3. H.N. Chapman et al., "Femtosecond time-delay x-ray holography", *Nature* 448, 676–679 (2007).
4. J. F. Young, J. S. Preston, H. M. van Driel, and J. E. Sipe, "Laser-induced periodic surface structure. II. Experiments on Ge, Si, Al, and brass", *Phys. Rev. B* 27, 1155–1172 (1983).
5. G. Grübel, G. B. Stephenson, C. Gutt, H. Sinn and T. Tschentscher, "XPCS at the European X-ray free electron laser facility", *Nucl. Instrum. Meth. B* 267, 357–367 (2007).

Original publication

"Ultrafast single-shot diffraction imaging of nanoscale dynamics", *Nature Photonics* 2, 415–419 (2008).

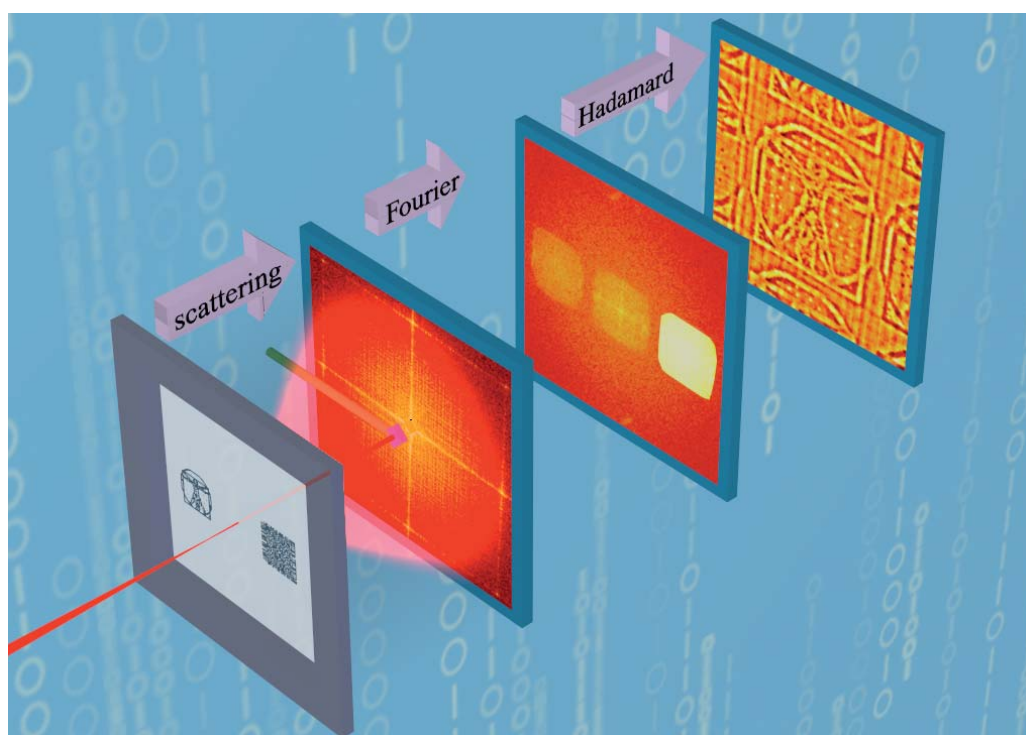
Massively parallel X-ray holography.

Taking a leaf from astronomy to reach the nanoscale

The ultrafast pulses from short-wavelength free-electron lasers (FELs), such as FLASH, give us the possibility for imaging processes on the timescale of atomic motions. The upcoming X-ray FELs such as Linac Coherent Light Source and European XFEL will additionally allow us to probe dynamic processes approaching inter-atomic length scales. For many such experiments it is necessary to extract spatially-resolved information from a single pulse since sample damage may prevent stroboscopic methods. We have developed an extremely photon-efficient method to form a real-space image of the object. Borrowing concepts from X-ray astronomy, our method of “Massively Parallel Holography” utilizes a special kind of coded pattern called a uniformly redundant array to form a hologram of the object. We showed that the pattern amplified the holographic signal of a bacterial cell by three orders of magnitude. This coherent imaging process also has the advantage of providing absorption, refraction, and depth information of a hologram.

Figure 1

The steps to obtaining an image using massively parallel X-ray holography. The sample consists of an object with a URA next to it. The coherent diffraction pattern is recorded on a CCD and Fourier transformed (with an Hadamard transformation) in the computer. The holographic term is isolated and further transformed to recover the image.



Recording single-shot high-resolution ultrafast images with a FEL offers several challenges. Since generally the object is destroyed by the FEL interaction (unless much less intense pulses are used to stroboscopically image repeatable processes) there is no second chance to improve the image, for example if it was out of focus. High-resolution X-ray lenses might not survive the damaging pulses either. Lensless methods overcome these problems, and furthermore provide a path to reach near-atomic resolution with future sources. We have successfully developed single-shot coherent diffractive imaging [1], in which the far-field coherent diffraction pattern of the object is recorded. Using

phase-retrieval methods, the diffraction pattern may be inverted to give the complex-valued image. Such retrieval methods require a minimum scattered signal to obtain the highest resolution. Adding a reference structure that is located close to the object of interest can essentially amplify the measured signal [2-4]. This is, in fact, the method of Fourier transform holography (FTH) [5,6] which also has the huge benefit of encoding the phases in the diffraction pattern. We extend the method of FTH by using a specially designed reference pattern called a uniformly redundant array (URA) that boosts signal by three orders compared with a single reference source, without sacrificing resolution.

A Fourier transform hologram is the interference between the light scattered from the reference structure (usually a small pinhole) and from the object. A simple Fourier transform of this pattern produces an image of the specimen convolved with the pinhole. As in a pinhole camera, the image is weak and the signal to noise ratio (SNR) of the image increases as the pinhole increases in size at the expense of image resolution. We may deconvolve the effect of the pinhole (using phase retrieval) but the Fourier spectrum of a pinhole has regions of zero intensity which actually mask out the object signal we are trying to enhance. We overcame this by using a URA, which has the interesting property that all inter-pinhole distances are equally represented [7]. As such, it has a flat power spectrum without zero intensity regions. Importantly, the gain in flux compared with a single pinhole is given by the number of open elements in the URA, equal to 162 in our FLASH experiments. (We have subsequently produced arrays with over 9000 active elements.) The image may be retrieved directly by convolving with the dual of the URA, to the resolution of the URA pitch, which we extend to the limit of our detector by phase retrieval. The steps to obtaining an image using massively parallel X-ray holography are shown in Fig. 1.

In our experiments at FLASH, we focused a 13.5 nm wavelength pulse with 10^{12} photons onto a sample consisting of a helical *Spiroplasma melliferum* bacterium next to a 162-element URA that was milled into the silicon nitride membrane using a focused ion beam. The reconstructed image, shown in Fig. 2, demonstrates the feasibility of imaging micrometer-sized biological objects with a FEL pulse. The resolution of the retrieved image was 75 nm. We are planning to use this method at FLASH to achieve the highest possible imaging resolution of non-repeatable dynamic processes [8]. ●

Contact: Henry N. Chapman, henry.chapman@desy.de

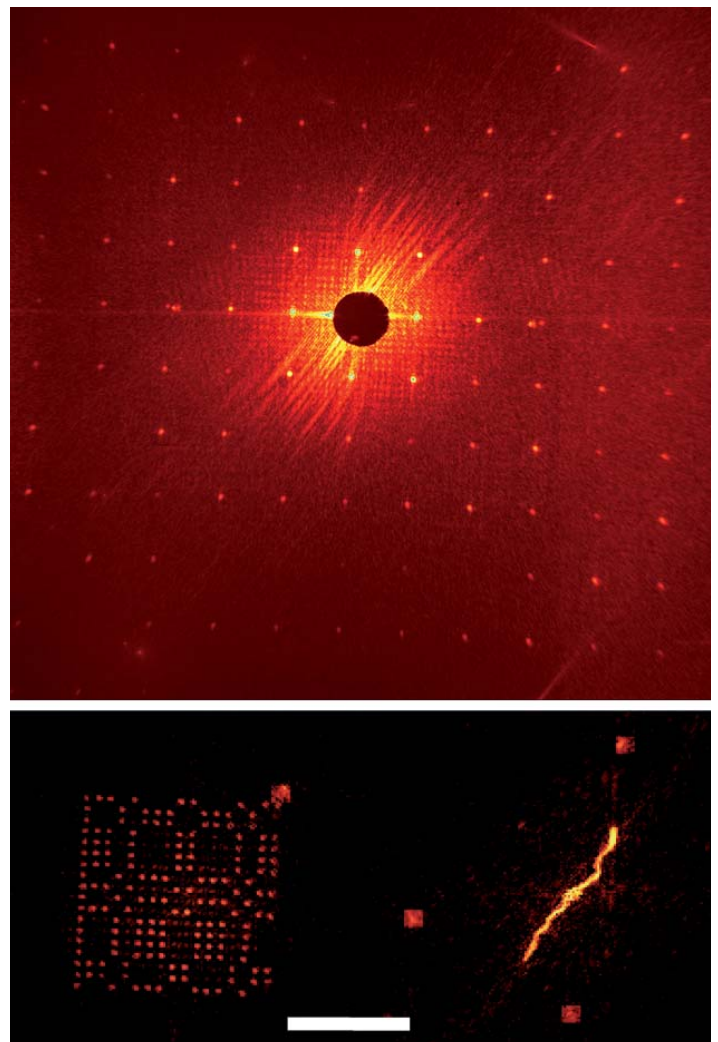


Figure 2
(top) A URA hologram of a *Spiroplasma melliferum* bacterium cell, recorded with a single FLASH pulse at 13.5 nm wavelength. (bottom) The reconstruction of the image after decoding the hologram and applying further phase retrieval to achieve resolution beyond the 150 nm resolution of the URA pattern. The final resolution was 75 nm. The scalebar is 4 μm .

Authors

Stefano Marchesini^{1,2}, Sebastien Boutet^{3,4}, Anne E. Sakdinawat⁵, Michael J. Bogan¹, Saša Bajt^{1,6}, Anton Barty¹, Henry N. Chapman^{1,10}, Matthias Frank¹, Stefan P. Hau-Riege¹, Abraham Szöke¹, Congwu Cui², David A. Shapiro², Malcolm R. Howells², John C. H. Spence⁷, Joshua W. Shaevitz⁸, Joanna Y. Lee⁹, Janos Hajdu^{3,4}, Marvin M. Seibert⁴

1. Lawrence Livermore National Laboratory, 7000 East Avenue, Livermore, California 94550, USA
2. Advanced Light Source, Lawrence Berkeley National Laboratory, Berkeley, California 94720, USA
3. SSRL, Stanford Linear Accelerator Center, 2575 Sand Hill Road, Menlo Park, California 94025, USA
4. Laboratory of Molecular Biophysics, Department of Cell and Molecular Biology, Uppsala University, Husargatan 3, Box 596, SE-75124 Uppsala, Sweden
5. Centre for X-ray Optics, Lawrence Berkeley National Laboratory, Berkeley, California 94720, USA
6. DESY, Notkestraße 85, D-22607 Hamburg, Germany
7. Department of Physics and Astronomy, Arizona State University, Tempe, Arizona 85287-1504, USA
8. Department of Physics and Lewis-Sigler Institute, 150 Carl Icahn Laboratory, Princeton, New Jersey 08544, USA
9. Department of Plant and Microbial Biology, University of California, Berkeley, 648 Stanley Hall #3220, Berkeley, California 94720, USA
10. CFEL, Universität Hamburg at DESY, Notkestraße 85, 22607 Hamburg, Germany

Original publication

“Massively parallel X-ray holography,” *Nature Photonics* 2, 560–563 (2008).

References

1. H.N. Chapman et al. “Femtosecond diffractive imaging with a soft-X-ray free-electron laser”, *Nature Physics* 2, 839 – 843 (2006).
2. W. F. Schlotter, J. Lüning, R. Rick, K. Chen, A. Scherz, S. Eisebitt, C. M. Günther, W. Eberhardt, O. Hellwig, and J. Stöhr, “Extended field of view soft X-ray fourier transform holography: toward imaging ultrafast evolution in a single shot”, *Opt. Lett.* 32, 3110–3112 (2007).
3. S. Boutet, M. J. Bogan, A. Barty, M. Frank, W. H. Benner, S. Marchesini, M. M. Seibert, J. Hajdu, and H. N. Chapman, “Ultrafast soft x-ray scattering and reference-enhanced diffractive imaging of weakly scattering nanoparticles”, *J. Elect. Spect. Rel. Phenom.*, 166, 65–73 (2008).
4. T. Shintake, “Possibility of single biomolecule imaging with coherent amplification of weak scattering X-ray photons”, *Phys. Rev. E* 78, 041906 (2008).
5. G. W. Stroke, “An Introduction to Coherent Optics and Holography”, Academic, New York (1969).
6. I. McNulty, J. Kirz, C. Jacobsen, E. H. Anderson, M. R. Howells, and D. P. Kern, “High-Resolution Imaging by Fourier Transform X-ray Holography”, *Science* 256, 1009–1012 (1992).
7. E.E. Fenimore and T.M. Cannon, “Coded aperture imaging with uniformly redundant arrays”, *Appl. Opt.* 17, 337–347 (1978).
8. A. Barty et al. “Ultrafast single-shot diffraction imaging of nanoscale dynamics”, *Nature Photonics* 2, 415–419 (2008).

Clusters in super intense FLASH pulses.

Frustrated multistep ionization

The soft X-ray free electron laser FLASH allows for the first time to probe the super intense light pulse – matter interaction at short wavelength, providing the basis for a large variety of studies with femtosecond X-ray pulses. We have performed a photoelectron spectroscopy study complemented with Monte Carlo simulations about the ionization dynamics of atomic clusters at FLASH at power densities exceeding 10^{13} W/cm². We find that the cluster ionization process is a sequence of direct electron emission events in a developing Coulomb field. In contrast to earlier studies in the infrared and vacuum ultraviolet regime, there are no indications for efficient plasma heating processes. The current findings have large implications for the ionization and dissociation dynamics of nanometer scale objects illuminated by intense short wavelength pulses.

Understanding the interaction of light with matter has been a central theme of physics for the past century. The invention of the laser and the continuing advance in laser technologies has made it possible to explore non-linear light – matter interaction leading to novel laser based concepts from particle accelerators to nuclear fusion [1]. Currently, we are witnessing the advent of intense free electron lasers in the soft X-ray regime such as FLASH and in the near future also in the hard X-ray regime. One of the most exciting prospects of research with X-ray lasers is direct imaging of nonperiodic nanoscale objects, such as biomolecules, nanocrystals, living cells and viruses [2]. Even though it is crucial for the success of the imaging experiments, understanding the interaction of intense X-ray pulses with atomic systems and the underlying dynamics is still in its infancy [3]. In this context it is of fundamental importance to study how the absorption and ionization properties of extended systems develop in the short-wavelength strong-field domain. For such investigations, atomic clusters are ideal targets as hidden energy dissipation into surrounding media is virtually absent.

To gain insight into the ionization dynamics of clusters in intense soft X-ray laser pulses, we have performed photoelectron spectroscopy (PES) at the 20 μ m focus beamline BL2 of the FLASH facility on Ar_N with $\langle N \rangle = 100$ at $h\nu = 38$ eV and power densities up to 5×10^{13} W/cm², complemented by Monte Carlo simulations. PES is an ideal tool for investigating the light – matter interaction because the photoelectron energy distribution provides insight into the coupling between the photon field and the cluster. In the top panel of Fig. 1 single-shot electron time-of-flight spectra for Ar clusters and atoms are shown. While the atomic spectrum displays only one peak at 57 ns flight times from the Ar 3p level, the cluster spectrum exhibits additional peaks towards longer flight times, indicating a series of subsequent ionization events. The increasing flight times, i.e., decreasing electron kinetic energies reflect the developing Coulomb potential of the cluster. The differences between the atomic and cluster spectra become even more apparent in the

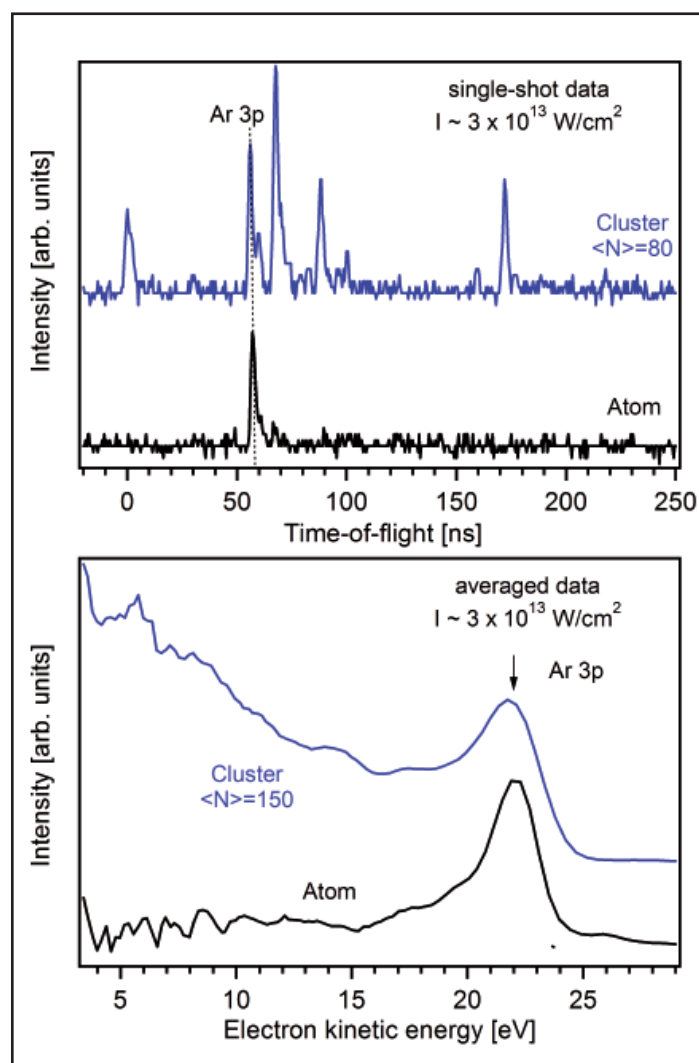


Figure 1 Single-shot time-of-flight (top) and averaged photoelectron (bottom) spectra from Ar atoms and clusters. In the averaged spectra, the clusters show continuous electron intensity towards low kinetic energies due to multistep ionization in the developing cluster Coulomb field.

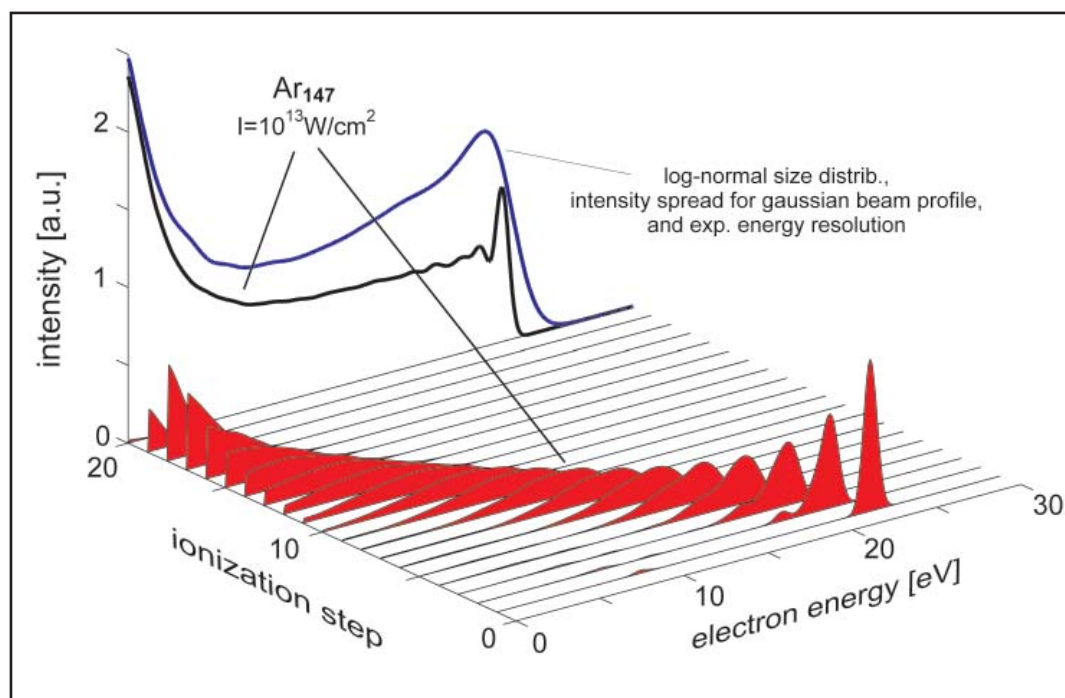


Figure 2

Monte Carlo simulations of the electron emission from an Ar_{147} cluster. In the front each ionization step is shown individually. For comparison with the data the average spectrum and the spectrum considering all relevant broadening effects are displayed in the back as a solid black line.

averaged spectra on a kinetic energy scale shown in the lower panel of Fig. 1. The cluster spectrum displays a continuous electron signal below the Ar 3p level. Except for the Ar 3p main line, all other peaks observable in the single-shot data completely average out suggesting a statistical photoemission process from the cluster. For comparison, photoelectron spectra are simulated with a Monte-Carlo approach assuming a statistical ionization of the cluster constituents with their atomic cross sections. In the model, the escape of the electrons is described as an instantaneous process. For calculating the final electron kinetic energies the effective cluster Coulomb potential is considered for each ionization process. In Fig. 2 the modeled spectrum averaged over about 10^4 simulations are shown for both, each individual ionization step and the overall spectrum. The spectrum of the first ionization step represents the photoemission spectrum of a cluster in the single photon regime. However, already for the second ionization step the spectrum becomes significantly broader and shifts towards lower kinetic energies. This trend continues until about the 19th ionization step, where the developing Coulomb field leads to total frustration of direct ionization for this cluster size. The sum over all single ionization spectra is shown as a solid black line. When further effects such as the Gaussian beam profile and the cluster size distribution are considered, the modeled spectrum

shows a remarkable similarity to the experimental data in Fig. 1. In particular, the prominent Ar 3p peak and the continuous spectral intensity at lower kinetic energies are well reproduced. The observed cluster ionization at short wavelength as a multistep process of direct electron emission after single photon absorption stands in contrast to the processes in the optical and vacuum ultraviolet spectral regime. At longer wavelength, the intense laser field can efficiently couple to the transient nanoplasma through plasma absorption and collective effects. This results in extremely high absorption and electron kinetic energies clearly exceeding the incoming photon energies. The present experiments at FLASH show that for shorter wavelength the plasma absorption processes are of no significant effect. The transition from plasma type absorption at long wavelength towards the multistep ionization process has significant implications on the explosion dynamics of the clusters. The highly non-thermal nanoplasma created with soft X-ray laser pulses decay by explosion of the surface layers followed by hydrodynamic expansion and recombination of the nanoplasma core [4] because only a fraction of the photoelectrons can leave the cluster Coulomb potential. ●

Contact: Christoph Bostedt,
christoph.bostedt@physik.tu-berlin.de

Authors

C. Bostedt¹, T. Fennel², H. Thomas¹, M. Hoener¹, E. Eremina¹, H. Wabnitz³, M. Kuhlmann³, E. Plönjes³, K. Tiedtke³, R. Treusch³, F. Feldhaus³, K.-H. Meiwes-Broer², A.R.B. de Castro⁴, T. Möller¹

1. Institut für Optik und Atomare Physik, Technische Universität Berlin, Hardenbergstrasse 36, 10623 Berlin, Germany
2. Institut für Physik, Universität Rostock, 18051 Rostock, Germany
3. HASYLAB at DESY, 22603 Hamburg, Germany
4. Laboratorio Nacional de Luz Sincrotron, 13084-971 Campinas, Brazil

Original publication

“Multistep Ionization of Argon Clusters in Intense Femtosecond Extreme Ultraviolet Pulses”, *Physical Review Letters* 100, 133401 (2008).

References

1. H.C. Kapteyn and T. Ditmire, “Ultraviolet upset”, *Nature* 420, 467 (2002).
2. R. Neutze, R. Wouts, D. van der Spoel, E. Weckert, and J. Hajdu, “Potential for biomolecular imaging with femtosecond x-ray pulses”, *Nature* 406, 752 (2000).
3. H. Wabnitz, L. Bittner, A.R.B. de Castro, et al., “Multiple ionization of atom clusters by intense soft X-rays from a free electron laser”, *Nature* 420, 482 (2002).
4. M. Hoener, C. Bostedt, H. Thomas, et al., “Charge recombination in soft X-ray laser produced nanoplasmas”, *J. Phys. B: At. Mol. Opt. Phys.* 41, 131001 FTC (2008).

A chemically driven insulator-metal transition.

Amorphous and non-stoichiometric main group oxide goes metallic

Insulator–metal transitions are well known in transition metal oxides, but inducing an insulator–metal transition in the oxide of a main group element is a major challenge. We succeeded in demonstrating that highly non-stoichiometric, amorphous gallium oxide shows an insulator–metal transition, with a conductivity jump of seven orders of magnitude at a temperature around 670 K. Through experimental studies and density-functional-theory calculations we confirmed that the conductivity jump takes place at a critical gallium concentration and is induced by crystallization of stoichiometric Ga_2O_3 . This novel mechanism – an insulator-metal transition driven by a heterogeneous solid state reaction within an amorphous matrix – opens up a new route to achieve metallic behaviour in oxides that are expected to exist only as classic insulators.

Insulator–metal transitions belong to the most fascinating phenomena in condensed-matter physics [1]. The transition can be caused by strong electron–electron interactions (Mott transition) [2] or by structural disorder (Anderson transition) [3]. As shown by Anderson [3] and Mott [4], in any non-crystalline material the lowest states in the conduction band are localized. Only for energies above the mobility edge do states become non-localized or extended. If the Fermi energy is below the mobility edge, the material is an electronic insulator, but if the number of electrons increases and the Fermi energy rises above the mobility edge, the material becomes metallic. Most examples of insulator–metal transitions concern transition metal compounds [4,5] as transition metals change their valence state easily. However, this does not exclude the possibility of inducing an insulator–metal transition in a simple binary oxide of a main group element, even without doping. Instead, large deviations from the ideal stoichiometry, i.e. high defect concentrations, provide a high concentration of electronic defects (self-doping). And if, in addition, the oxide is amorphous, there are two phenomena, strong chemical and strong structural disorder, which could result in an insulator–metal transition. We made thin films of highly non-stoichiometric, amorphous gallium oxide with approximate compositions of $\text{GaO}_{1.2}$ using pulsed laser deposition under reducing conditions and Ga_2O_3 as starting material. The films are insulating but, on heating, they show a sudden jump in conductivity of around seven orders of magnitude at ~ 670 K (Figure 1a). As the temperature increases towards the insulator–metal transition, $\beta\text{-Ga}_2\text{O}_3$ nuclei crystallize, requiring more oxygen than gallium. Hence, the surrounding amorphous region becomes even more non-stoichiometric. The material becomes conducting when the gallium concentration in the amorphous region reaches a critical level. Then, the conducting material consists of nuclei of crystalline and stoichiometric $\beta\text{-Ga}_2\text{O}_3$ surrounded by amorphous and highly non-stoichiometric gallium oxide (Figure 1b). One key to the success of this new insulator–metal transition can be attributed to the formation of extremely non-stoichiometric

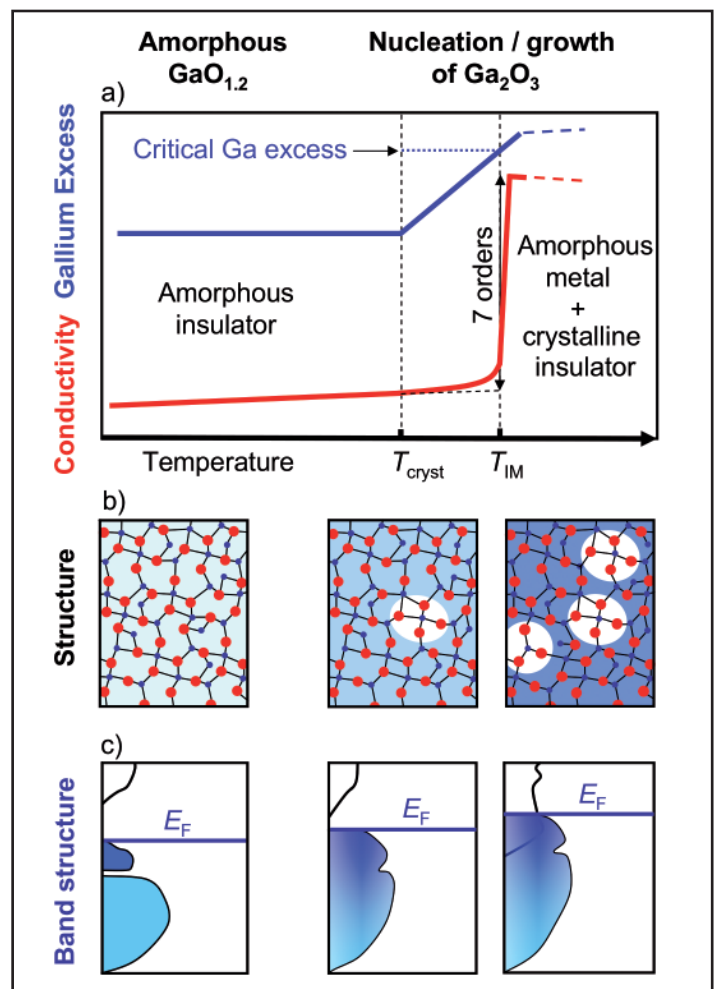


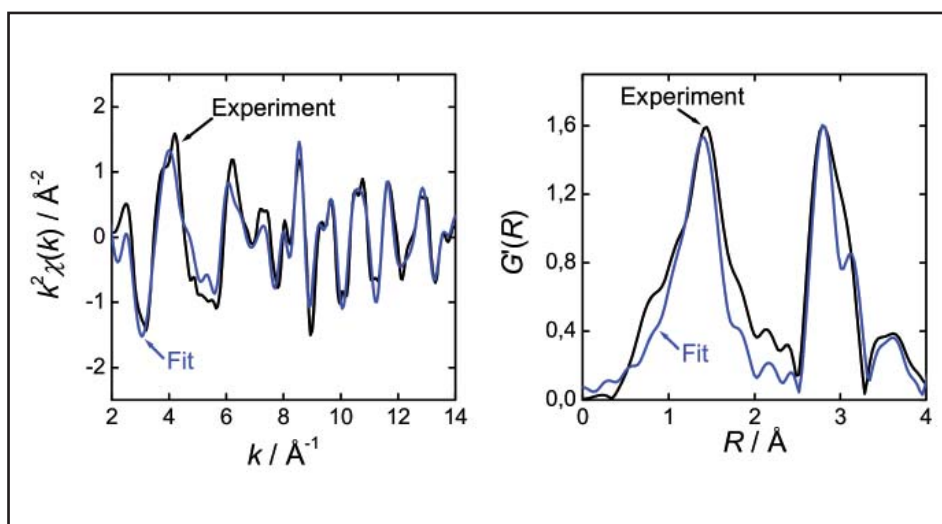
Figure 1

Schematic description of the correlation between electrical conductivity and gallium excess (a), geometrical structure (b), and band structure (c) of highly non-stoichiometric and amorphous gallium oxide as a function of temperature. As the temperature increases, $\beta\text{-Ga}_2\text{O}_3$ nuclei start to crystallize at T_{cryst} and both the gallium excess and the related Fermi energy, E_F , in the amorphous oxide increase. Once the gallium excess reaches its critical value, the bandgap is closed and the insulator-metal transition occurs at the temperature T_{IM} .

Figure 2

The local structure of amorphous and non-stoichiometric gallium oxide films, $\text{GaO}_{1.2}$, was investigated by X-ray absorption spectroscopy at the Ga K-edge.

(a) EXAFS, $k^2 \cdot \chi(k)$, of an as-prepared, amorphous gallium oxide film. (b) Modified radial distribution function $G'(R)$ (Fourier transform of the EXAFS in (a)). The experimental data (black lines) were fitted with a linear combination of theoretical spectra for gallium atoms with tetrahedral oxygen surrounding, Ga_{tet} , and octahedral surrounding, Ga_{oct} . The fit (blue lines) yields a distribution $\text{Ga}_{\text{tet}}:\text{Ga}_{\text{oct}} = (57 \pm 3):(43 \pm 3)$, i.e. a significantly higher occupation of tetrahedral sites compared to $\beta\text{-Ga}_2\text{O}_3$ having identical occupation numbers.



and amorphous GaO_x as starting material. To obtain insights into its local structure, X-ray absorption spectroscopy at the Ga K-edge was performed at the beamlines of HASYLAB at DESY in Hamburg (Figure 2). Modelling of the extended X-ray absorption fine structure (EXAFS) with FEFF8 [6] indicates that the local structure around the gallium atoms can be described reasonably well by the same oxygen coordination polyhedra as in crystalline $\beta\text{-Ga}_2\text{O}_3$, i.e. strongly distorted oxygen octahedra and tetrahedra. However, in contrast to $\beta\text{-Ga}_2\text{O}_3$, which has equal amounts of gallium atoms with octahedral and tetrahedral oxygen coordination, the amorphous and highly non-stoichiometric gallium oxide $\text{GaO}_{1.2}$ contains a significantly higher fraction of gallium atoms with tetrahedral oxygen coordination, $\text{Ga}_{\text{tet}}:\text{Ga}_{\text{oct}} \approx 57:43$. The EXAFS results show that the concept of point defects, which is strictly speaking only valid for crystalline structures, should be applicable to amorphous gallium oxide as well. In this sense, the gallium excess of $\text{GaO}_{1.2}$ can be due to gallium interstitials and/or oxygen vacancies. Theoretical calculations of the electronic structure of highly non-stoichiometric gallium oxide by means of density functional theory DFT [7] show, however, that the amorphous phase may be considered more appropriately as containing gallium interstitials (donor states close to the conduction band) rather than oxygen vacancies (donor states close to the valence

band). By increasing the Ga-excess the number of states in the original optical band gap increases and the energy gap between the highest occupied states and the lowest conduction states decreases (Figure 1c) until the gap is closed at a critical gallium excess – resulting in the observed insulator-metal transition. The results of these investigations have been published in the May issue of Nature Materials. In this context the question arises whether this new mechanism for an insulator-metal transition may have an immediate impact on applications such as electronic devices and permanent data storage. For the latter, the high stability of the material is a key requirement. One drawback at present, however, is that the transition from a metastable to a stable state is only one-way. If a reversible transition was achieved, this would surely have great implications for applications such as multiple read/write storage devices. If the principle is applied to other main group oxide systems, it may be possible to tune the thermal stability of the crystalline regions and realize reversible transitions. ●

Contact: Manfred Martin, martin@rwth-aachen.de

Authors

Lakshmi Nagarajan¹, Roger A. De Souza¹, Dominik Samuelis^{1,5}, Iliia Valov², Alexander Börger³, Jürgen Janek², Klaus-Dieter Becker³, Peter C. Schmidt⁴ and Manfred Martin¹

1. Institute of Physical Chemistry, RWTH Aachen University, 52056 Aachen, Germany
2. Institute of Physical Chemistry, Justus Liebig University, 35392 Giessen, Germany
3. Institute of Physical and Theoretical Chemistry, Technical University of Braunschweig, 38106 Braunschweig, Germany
4. Institute of Physical Chemistry, Technical University of Darmstadt, 64287 Darmstadt, Germany
5. Present address: Max Planck Institute for Solid State Research, Heisenbergstr. 1, 70569 Stuttgart, Germany

Original publication

“A chemically driven insulator-metal transition in non-stoichiometric and amorphous gallium oxide”, *Nature Materials* Vol. 7, 391-398 (2008)

References

1. Kotliar, G., “Driving the Electron over the Edge”, *Science* 302, 67-68 (2003).
2. Mott, N. F., “Metal-Insulator Transition” (Taylor & Francis, London, 1974).
3. Anderson, P. W., “Absence of Diffusion in Certain Random Lattices”, *Phys. Rev.* 109, 1492-1505 (1958).
4. Mott, N. F., “Electrons in disordered structures”, *Adv. Phys.* 16, 49-144 (1967).
5. Gebhard, F., “The Mott Metal-Insulator Transition” (Springer, Berlin, 1997).
6. Ankudinov, A. L., Ravel, B., Rehr, J. J. and Conradson, S. D., “Real-space multiple-scattering calculation and interpretation of x-ray-absorption near-edge structure”, *Phys. Rev. B* 58, 7565-7576 (1998).
7. Kresse, G. & Furthmüller, J., VASP the guide, <http://cms.mpi.univie.ac.at/vasp/vasp/vasp.html> (2007)

Tough silk.

Interplay of deformation on macroscopic and molecular length scales

Using an *in situ* combination of tensile tests and X-ray diffraction, we have determined the mechanical properties of both the crystalline and the disordered phase of the biological nanocomposite silk by adapting a model from linear viscoelastic theory to the semicrystalline morphology of silk. We observe a strong interplay between morphology and mechanical properties. Silk's high extensibility results principally from the disordered phase; however, the crystals are also elastically deformed.

Silkworm silk is a natural composite material produced by silkworms (*Bombyx mori*) and has been in use by human for several thousands of years, mainly for textiles with a silky shine and with excellent thermal insulation properties. Similar to spider silk, silkworm silk has a tensile strength comparable to that of steel. But, unlike steel, it is also extremely stretchable allowing for extreme elongation before breaking and possessing a high degree of toughness with the specific fracture energy much larger than of a high-tensile steel. It would be highly desirable to mimic nature's spinning process to produce artificial fibres with optimized mechanical performance either from silkworm or recombinant spider silk spinning dope.

The response of silk to an external force has a very dynamic nature and shows a rich spectrum of relaxation times from the fractions of a second through many hours up to days. This non-static nature of the response together with the very specific morphology of silk is the key to its extraordinary mechanical property. Morphologically, spider and silkworm silk are hierarchically structured nanocomposite materials consisting of fibres containing ordered regions (β -sheet protein nanocrystals) embedded in a softer matrix of disordered material. Tensile deformation of silk fibres involves a strong contribution of viscoelastic material, presumably in the disordered regions. We carried out two kind of complementary experiments to establish a model for silk incorporating the macroscopic mechanical behaviour, in particular, viscoelasticity, on the basis of its semicrystalline morphology. To this end, we combined high-resolution cyclic stress-strain measurements of single silkworm silk fibres with *in situ* tensile tests during synchrotron radiation X-ray diffraction experiments, the latter probing directly the deformation of the nanocrystals.

Silkworm silk was investigated at ambient humidity content in all experiments. The stretching measurements on single fibres were carried out with a piezo stretching device equipped with a force sensor. Force and distance were sampled with 1000 s^{-1} . The triangular strain excitation signal is a stepwise realization

of a constant rate of strain change $0.1 \text{ \%}/\text{s}$. The stress-response function was measured for increasing and decreasing strain on a previously unstretched fibre (2.0 mm initial length) and then again in a second cycle for the same, thus, pre-stretched sample. X-ray diffraction experiments were carried out *in situ* during a stretching experiment on fibre bundles of silkworm silk required for a good signal-to-noise ratio. Synchrotron radiation X-rays were used at Beamline A2, HASYLAB. Fibre diffraction patterns were recorded on a two-dimensional CCD detector. The lattice strain of the β -sheet fibroin crystals in the direction of the tensile stress was determined from the shift of the radial position of the 002 reflection (Fig. 1).

Unlike the unstretched fiber, the pre-stretched sample can be considered to be in a metastable state, because at the time scale of our experiments (which is of the order of seconds to

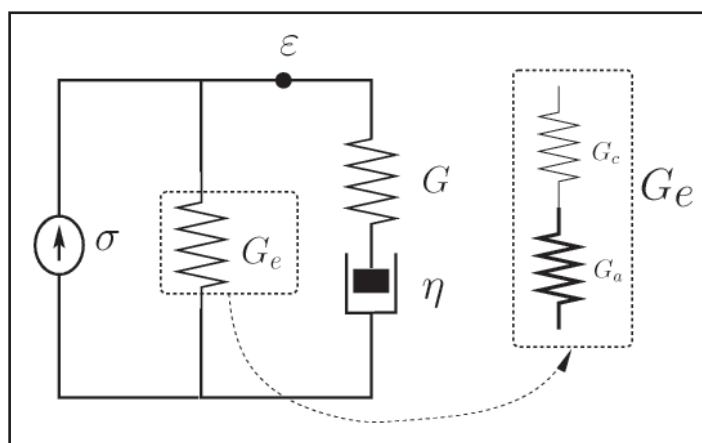
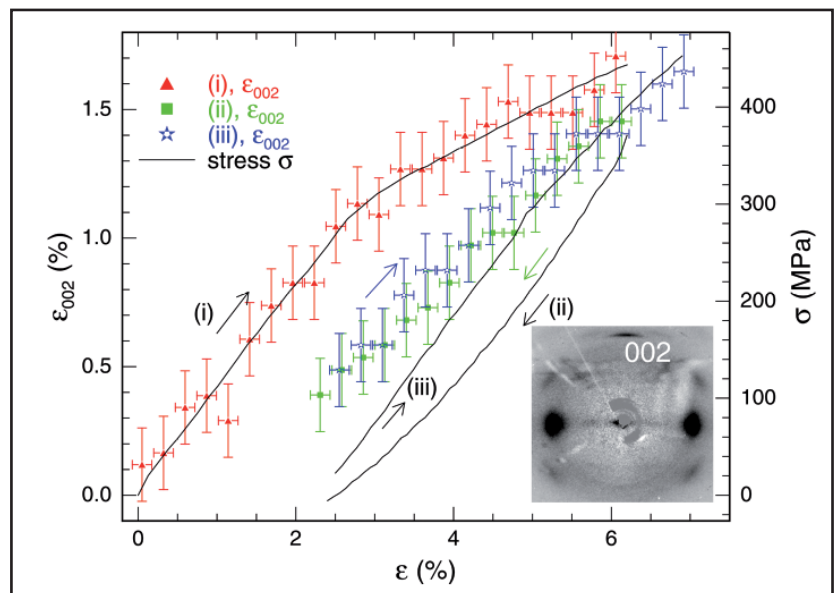


Figure 2

Dashpot-spring representation of the standard three-parameter Maxwell model of a solid. The purely elastic contribution (modulus G_e) may be split up in amorphous and crystalline contribution in serial arrangement (constant stress; G_a and G_c , respectively). The viscoelastic contribution (G and viscosity η) is from the amorphous regions only. All parameters could be determined quantitatively in the *in situ* X-ray diffraction experiment.

Figure 1

Stress-strain curves of a bundle of silkworm silk fibres (solid lines, right-hand scale). (i) is the initial stretching of a previously unstretched fibres whereas (ii) and (iii) correspond to the same fibres but pre-stretched (decreasing and increasing strain, respectively). The symbols give the strain of the fibroin crystals (ϵ_{002} , left-hand scale) as determined from the 002 reflections of the fibre diffraction diagram (inset) measured at HASYLAB Beamline A2. The crystals are deformed by about 25 % of the macroscopic fibre strain, under the assumption of a constant-stress scenario (see also Fig. 2).



minutes) no changes are observed. However, it returns to the unstretched state after a few days, recovering its initial length and stress-strain behaviour. Most surprisingly, the pre-stretched sample shows a behaviour which allows a very simple phenomenological description in the context of linear viscoelastic theory. The measured data can be well described with the simplest rheological model, the standard three-parameter Maxwell model of a solid (Fig. 2).

The model parameters are independent of the sample shape and of the time-dependence of the strain excitation. They have to be interpreted as average macroscopic material properties. Known model parameters give us access to values such as elastic modulus, relaxation time, viscosity of the material as whole. However, the model does not allow separating the characteristics of the crystalline phase from those of the amorphous one. In situ X-ray diffraction provides unique access to such individual quantitative information on the crystalline phase as it probes the lattice deformation of the fibroin crystals under tensile load. This delivers a value for the elastic modulus of the crystalline phase and thus allows us to calculate the respective parameter of the amorphous part.

In conclusion, we clearly separated the mechanical properties of the crystalline and the amorphous phase, as well as their interplay, of silk. A link between the macroscopic viscoelastic behaviour and the mechanisms at the molecular length scale has been established. The β -sheet crystals do not only act as nodes in a disordered molecular network [1], but they are elastically deformed themselves and thus contribute to the extensibility of silk. Our new model is purely rheological and does not require any geometrical information (or assumptions) on the distribution of crystalline and amorphous phases, which an analysis in the framework of composite mechanics would do [2]. The model fully accounts for the semicrystalline morphology of silk and is also able to explain the mechanical properties of pre-stretched spider dragline silk, as we confirmed in a fit of data in [3]. ●

Contact: Martin Müller, martin.mueller@gkss.de

Authors

Igor Krasnov¹, Imke Diddens^{1,4}, Nadine Hauptmann¹, Gesa Helms¹, Malte Ogurreck¹, Tilo Seydel², Sérgio S. Funari³, Martin Müller^{1,5}

1. Institut für Experimentelle und Angewandte Physik, Christian-Albrechts-Universität zu Kiel, 24098 Kiel, Germany
2. Institut Laue-Langevin, BP 156, 38042 Grenoble Cedex 9, France
3. HASYLAB at DESY, Notkestr. 85, 22607 Hamburg, Germany
4. Present address: Oxford Silk Group, Department of Zoology, Oxford University, Oxford, OX1 3PS, UK
5. Present address: GKSS Forschungszentrum Geesthacht GmbH, Max-Planck-Straße 1, 21502 Geesthacht, Germany

References

1. Y. Termonia, *Macromolecules* **27**, 7378, "Molecular modeling of spider silk elasticity", (1994).
2. J. Pérez-Riguero, C. Viney, J. Llorca, and M. Elices, *Polymer* **41**, 8433, "Mechanical properties of silkworm silk in liquid media", (2000).
3. D. Porter, F. Vollrath, and Z. Shao, *Eur. Phys. J. E* **16**, 199, "Predicting the mechanical properties of spider silk as a model nanostructured polymer", (2005).

Original publication

"Mechanical Properties of Silk: Interplay of Deformation on Macroscopic and Molecular Length Scales", *Phys. Rev. Lett.* **100**, 048104, (2008).

Insight into the reactivity.

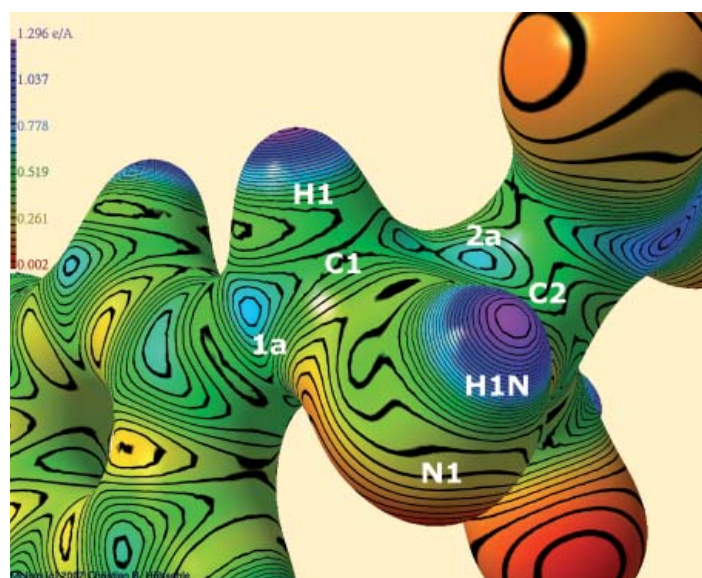
Study of biologically active molecules from ground-state electron densities

In order to contribute to a rational drug design with ground-state electron densities, it is important to evaluate the deduced functions and properties that provide information on reactivity. Electrostatic potentials mapped on molecular surfaces and Zero-Laplacian iso-surfaces can be referred to as reactive surfaces because they show centres of nucleophilicity or electrophilicity. Derived from experimental densities, these surfaces are directly dependent on intermolecular interaction patterns within the crystal environment. Therefore, the information deduced from experimental electron densities are generally a better approximation for biological enzyme-ligand interactions than gas phase calculations or properties derived from the liquid phase. Within this study, we have determined the electron densities of three protease inhibitor model compounds: acceptor substituted aziridine, oxirane and olefin.

Single crystals of aziridine I and olefin III (see Figure 1) were measured at beamline D3 of HASYLAB at 9K. For aziridine I, 163095 reflections were collected of which 18527 were unique with a completeness of 84.5% to a resolution of 1.02 Å⁻¹. For olefin III, 104810 reflections were collected of which 9203 were unique with a completeness of 90.2% to a resolution of 1.02 Å⁻¹. A single crystal of oxirane II was measured at beamline F1 of HASYLAB at 100 K. 126224 reflections were collected of which 14724 were unique with a completeness of 84.2% to a resolution of 1.19 Å⁻¹. All compounds crystallized in the space group P $\bar{1}$. For integration, the program XDS [1] was used and oblique incidence correction [2] was applied. The electron-density distribution obtained from multipole refinement [3] with XDLSM of the XD2006 suite of programs [4] was analyzed with XDPROP and Mollso [5].

To correlate the biological activity with the electrostatic potential (esp), it has become common practise to scrutinize the electrostatic potential on a molecular surface of 0.001 a.u. (=0.0067 e Å⁻³) [6]. To quantify the effects of the esp on this surface, the average deviation Π from the mean surface potential can be used. It is a measure of the internal charge separation or local polarity which is present even in molecules having zero dipole moment. For compounds I to III the values of Π are: $\Pi(\text{cpd. I}) = 0.089 \text{ e \AA}^{-1}$, $\Pi(\text{cpd. II}) = 0.035 \text{ e \AA}^{-1}$ and $\Pi(\text{cpd. III}) = 0.079 \text{ e \AA}^{-1}$. These differences in the overall polarization are caused by the different intermolecular interactions and the structural differences in the reactive regions. The intermolecular bonding network for aziridine I is stronger than for the other compounds and is therefore responsible for the greater overall polarization. These findings may contribute to an explanation for the greater reactivity of aziridine I in biochemical model reactions compared to oxirane II or olefin III.

To obtain information about the location of possible electrophilic centres that can be target of a nucleophilic attack followed by



the formation of a covalent bond (ring-opening reaction), an electrostatic potential mapped on a density surface that is much closer to the nuclei should be examined. Figure 2 (left) shows the electrostatic potential of aziridine I mapped on the density isosurface of 0.5 e Å⁻³. Several maxima (green/blue colour) in the reactive region can be found on the isosurface (most important ones labeled 1a and 2a in Figure 2). The maximum labeled 1a seems to be the sterically most favorable reaction site because there is no bulky sidechain and no negatively polarized carbonyl oxygen atom nearby as it is in the case of the maxima around C2. This finding is confirmed by biochemical model reactions: Carbon atom C1 is attacked regioselectively. All the other maxima at C1 cannot be reached from the direction of the flat aryl plane but only from the side of the aryl group where hydrogen or nitrogen atoms hinder the attack. Moreover, the maximum 1a has the highest esp value compared to all

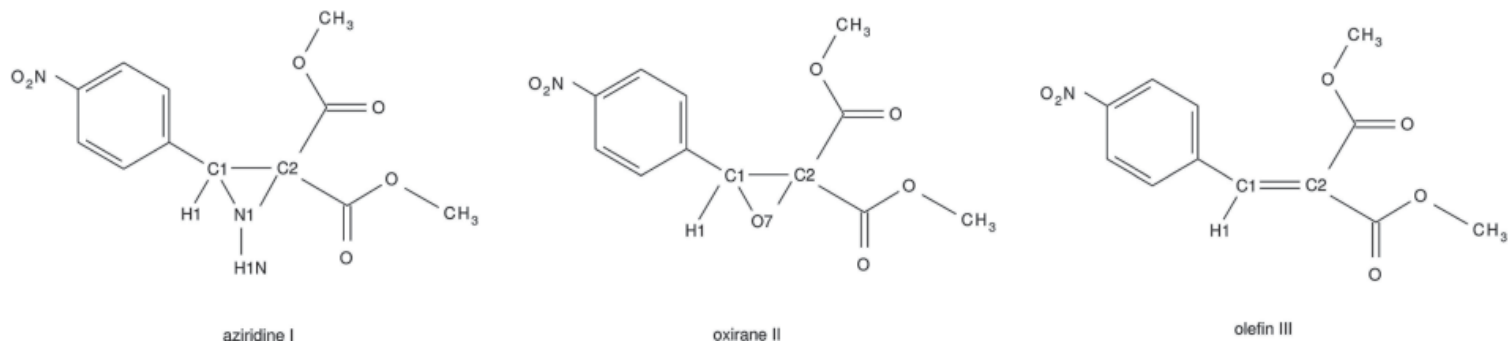


Figure 1

Molecular structures with atom numbering scheme in the reactive region of aziridine I, oxirane II and olefin III.

the maxima around C1 ($\text{esp}(1a)=0.73 \text{ e } \text{\AA}^{-1}$). So even stereoselectivity of the ring-opening reaction can be predicted. The Zero-Laplacian iso-surface (defined by $\vec{\nabla}^2\rho=0$) shows the location of electrophilic centres by means of reduced valence shell charge concentrations (reduced VSCCs) which appear as holes in the surface. Figure 2 (right) shows the isosurface of aziridine I. There are larger reduced VSCCs at carbon atom C1 (four large holes at C1, two large and one small hole at C2) so that the experimentally found regioselectivity of the ring-opening reaction can again be confirmed. Another important

information from the Zero-Laplacian iso-surface are the positions of the reduced VSCCs around the atoms: Although their number and the number of the maxima in the esp do not agree, the agreement of the positions is quite high. Exactly on the position where the maximum in the esp labeled 1a was found, a reduced VSCC can be found in Figure 2 (right), too. This is a further hint that this sterically most favorable position is also electronically preferred. ●

Contact: Peter Luger, luger@chemie.fu-berlin.de

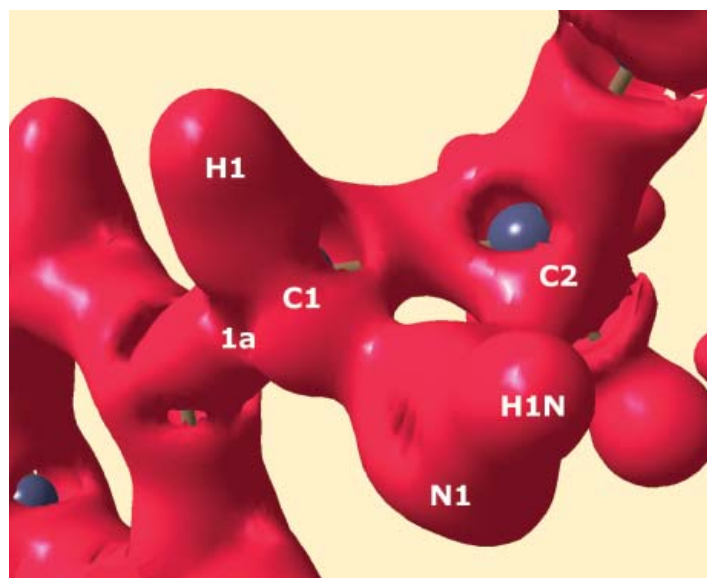


Figure 2

Left: Electrostatic potential in $\text{e } \text{\AA}^{-1}$ of the reactive region of aziridine I, mapped on an isosurface of the electron density at $0.5 \text{ e } \text{\AA}^{-3}$.

Right: Zero-Laplacian iso-surface of the reactive region of aziridine I. Positions of atoms under the surface and maxima of the electrostatic potential or reduced valence shell charge concentrations in the Zero-Laplacian at C1 and C2 are plotted.

Authors

Simon Grabowsky¹, Thomas Pfeuffer², Wolfgang Morgenroth^{3,4,5}, Carsten Paulmann^{3,6}, Tanja Schirmeister², Peter Luger¹

1. Freie Universität Berlin, Institut für Chemie und Biochemie / Kristallographie, Fabeckstr. 36a, 14195 Berlin, Germany
2. Universität Würzburg, Institut für Pharmazie und Lebensmittelchemie, Am Hubland, 97074 Würzburg, Germany
3. c/o DESY/HASYLAB, Notkestr. 85, 22607 Hamburg, Germany
4. Georg-August-Universität, Institut für Anorganische Chemie, Tammannstr. 4, 37077 Göttingen, Germany
5. Aarhus University, Department of Chemistry, Langelandsgade 140, 8000 Aarhus C, Denmark
6. Universität Hamburg, Mineralogisch-Petrographisches Institut, Grindelallee 48, 20146 Hamburg, Germany

Original publication

“A Comparative Study on the Experimentally Derived Electron Densities of three Protease Inhibitor Model Compounds”, *Org. Biomol. Chem.* **6**, 2295-2307 (2008).

References

1. W. Kabsch, XDS (version 08/2006) in: a) W. Kabsch, *J. Appl. Crystallogr.* **21**, 916-924 (1988); b) W. Kabsch, *J. Appl. Crystallogr.* **26**, 795-800 (1993).
2. S. K. J. Johnas, E. Weckert, “A Program for Oblique Incidence Correction”, S. K. J. Johnas, W. Morgenroth, E. Weckert, *HASYLAB Annual Report*, 325-328 (2006).
3. N. K. Hansen, P. Coppens, *Acta Cryst.* **A34**, 909-921 (1978).
4. A. Volkov, P. Macchi, L. J. Farrugia, C. Gatti, P. Mallinson, T. Richter, T. Koritsanszky, XD2006, “A Computer Program for Multipole Refinement, Topological Analysis of Charge Densities and Evaluation of Intermolecular Energies from Experimental or Theoretical Structure Factors”, (version 5.34) (2006).
5. C. B. Hübschle, P. Luger, *J. Appl. Cryst.* **39**, 901-904 (2006).
6. a) J. S. Murray, P. Lane, P. Politzer, *J. Am. Chem. Soc.* **85**, 1-8 (1995); b) P. Politzer, J. S. Murray, Z. Peralta-Inga, *Int. J. Quant. Chem.* **85**, 676-684 (2001).

The many faces of molecular assemblies in electronic devices.

Orientation-dependent ionization potentials

Organic molecules provide fascinating possibilities for fabricating inexpensive novel electronic devices, organic light-emitting diodes, and flexible environmentally-friendly low-cost solar cells [1]. The efficiency of organic solar cells depends on the chemistry of the materials employed and critically on the electronic properties and nanomorphology of the molecules in the active layer [2]. We have used synchrotron light at HASYLAB to investigate how the orientation of the organic molecules in thin films affects the electronic structure [3].

The work function of a metal is defined as the energy difference between the Fermi level (EF) and the vacuum level (Vvac) and depends on the crystallographic orientation of the surface. For van der Waals crystals of non-dipolar molecules, surface dipoles and work-function anisotropy have yet to be investigated systematically. In the past variations in the ionization potential (IP; the molecular equivalent of the work function) with molecular orientation were interpreted in terms of variable photo-hole screening [4], but could never be quantified satisfactorily. Here, we propose a novel explanation of the intriguing observation that one and the same molecule can have different, yet still well-defined, ionization potentials if it forms part of an ordered supramolecular structure.

We performed photoelectron spectroscopy investigations on α,ω -dihexyl-sexithiophene (DH6T) and α -sexithiophene (6T), deposited on Ag(111) substrates at the FLIPPER II beamline. The ionization potentials of the molecules change by up to 0.6 eV, depending on whether they are lying flat on the substrate, or standing upright. We explain these observations in terms of the collective electrostatic effect of the highly anisotropic intra-molecular charge distribution based on density-functional theory (DFT) calculations and electrostatic modeling. Supplementary studies on different substrates and molecules underline the universality of the observed effects and their explanation. We stress that the general concept is also valid for single crystals and ordered polymers.

The valence band spectra for DH6T on Ag(111) in the monolayer (L for „lying“) and multilayer (S for „standing“) regimes are shown in Figure 1a, and the corresponding simulated spectra from density functional theory (DFT) are shown in Figure 1b. Three low binding energy (BE) peaks can be clearly distinguished with maxima at 1.6 eV, 2.3 eV, and 2.9 eV in the L-regime, and at 1.0 eV, 1.7 eV, and 2.3 eV in the S-regime. These peaks are derived from the highest occupied molecular orbital (HOMO).

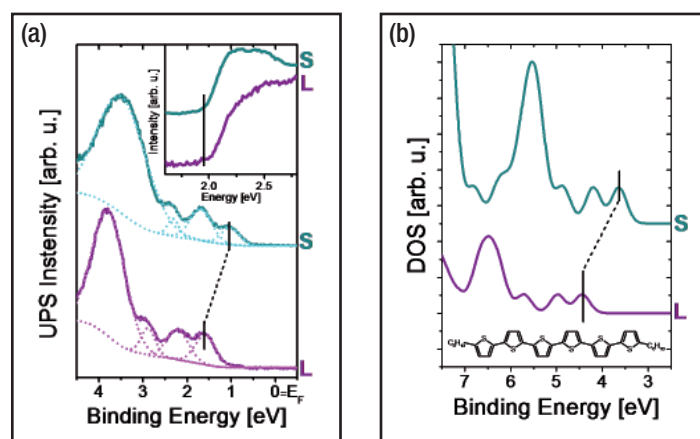


Figure 1

(a) Experimental valence band spectra for 4 Å of DH6T (wine), and 40 Å of DH6T (olive) on Ag(111), corresponding to a lying monolayer (L) and a second standing layer (S). The dotted lines indicate the least-squares fit to determine the peak positions. The inset shows the secondary electron cut-offs used to determine the work function of the respective sample. (b) DFT calculated density-of-states (DOS) of a single layer of lying (wine) and standing (olive) DH6T molecules; the zero of the energy scale is the vacuum level.

All peaks are at 0.6 eV lower BE for the (standing) multilayer (S) compared to the (lying) monolayer (L). The change in the intensity ratio of the first two peaks arises from the different orientations of the molecular axes. The -0.6 eV binding energy shift of the molecular levels directly translates into a reduction of the molecular IP (i.e., the energy difference between HOMO and Vvac).

While DFT calculations permit a quantitative analysis (Fig. 1b), an even simpler, purely electrostatic model can be used to provide a more intuitive picture. We approximate the charge distribution corresponding to one 6T molecule (the conjugated core of DH6T; Figure 2a) by a number of point-charges (Fig-

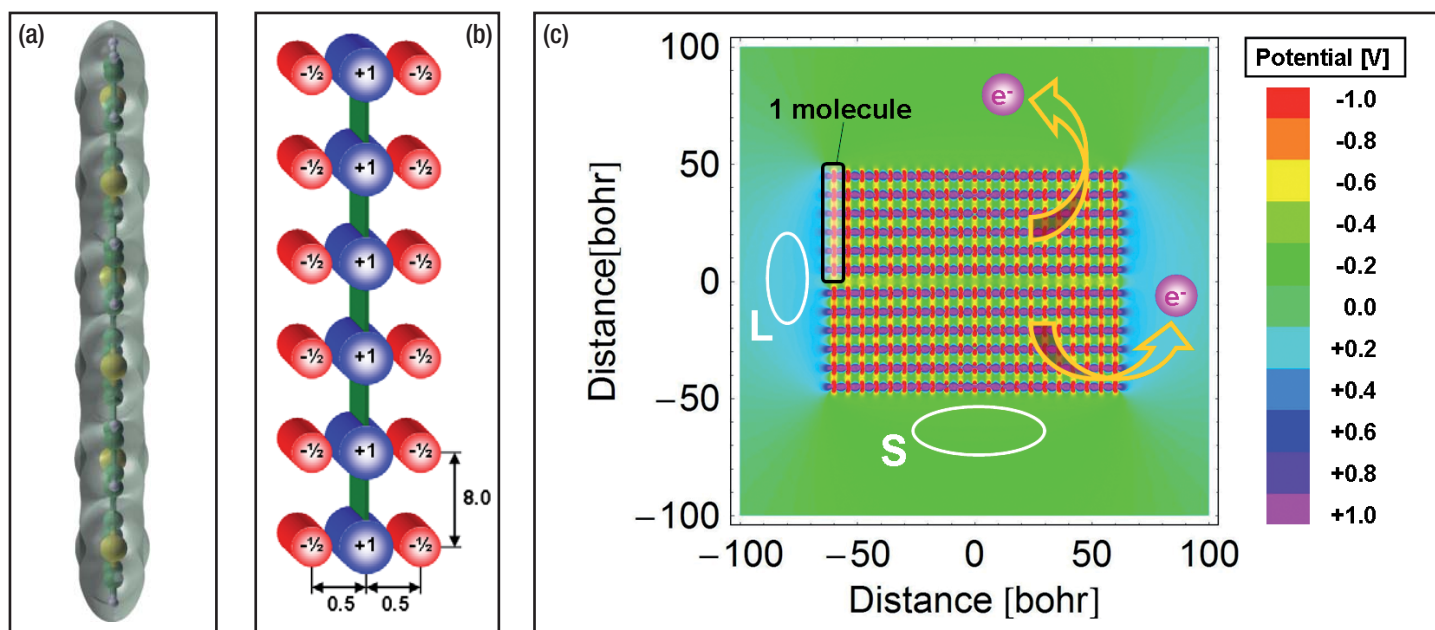


Figure 2
 Electrostatic modeling of the orientation-dependent ionization potential. The electron density of a single 6T molecule (a), is approximated by a model molecule consisting of a series of point charges (b) (distances and charges are given in atomic units). (c) Electrostatic potential in and around a model molecular crystal consisting of two layers of 21 model-molecules.

ure 2b): The π -electron system above and below each ring is clearly negatively charged; this is represented by negative point charges of $-0.5 e$ (elementary charge) placed 0.5 bohr above and below the molecular plane. These negative charges are compensated by a $+1.0 e$ point charge in the plane of the molecule. This pattern is repeated six times (one for each ring) along the long molecular axis with a spacing of 8 bohr (\approx distance between individual thiophene rings). Next a 2D molecular crystal is built using this model molecule (Figure 2c), consisting of 21 standing model-molecules in one layer with a distance of 6 bohr between the long molecular axes with a second layer placed under the first layer with a 10 bohr gap.

This model-crystal has two distinctly different crystal faces: the top and bottom are terminated by the point-charge pattern $-0.5|+1.0|-0.5|-0.5|+1.0|-0.5|...$ given by the hydrogen-terminated ends of the 6T molecules exposed in a standing layer; the left and right faces are terminated by negatively charged sheets that represent the π -electron cloud exposed in a lying layer. The electrostatic potentials of all point charges are summed to yield the potential within and around the model-crystal (shown

in color in Figure 2c). In analogy to the results from the DFT calculations, we find an extended region of lower electrostatic potential (green) over the hydrogen-terminated ends of the molecules, relevant for the standing layer (S). Above the π -system, there is an extended region of higher electrostatic potential (cyan), relevant for the lying layer (L). As a consequence, the work required to promote an electron from any energy level within the crystal into the region above the hydrogen-terminated ends (S) is less than that for promoting an electron into the region above the π -electron clouds (L). This difference can be measured provided the lateral extent of the supramolecular structure is large compared to a single molecule.

We have shown that pre-patterning of a metal surface with an appropriate molecular species is a promising tool for controlling the orientation of subsequently deposited molecules. Since the charge-carrier mobility and photoluminescence depend on the orientation of the intrinsically anisotropic molecules our findings will lead to improved organic electronic devices. ●

Contact: Norbert Koch, norbert.koch@physik.hu-berlin.de

Authors

Steffen Duhm¹, Georg Heimel¹, Ingo Salzmann¹, Hendrik Glowatzki¹, Robert L. Johnson², Antje Vollmer³, Jürgen P. Rabe¹, and Norbert Koch¹

1. Institut für Physik, Humboldt-Universität zu Berlin
Newtonstr. 15, D-12489 Berlin, Germany
2. Institut für Experimentalphysik, Universität Hamburg
D-22761 Hamburg, Germany
3. Berliner Elektronenspeicherring-Gesellschaft für Synchrotronstrahlung m.b.H.
D-12489 Berlin, Germany

Original publication

“Orientation-dependent ionization energies and interface dipoles in ordered molecular assemblies”, *Nature Materials* 7, 326 (2008).

References

1. S. R. Forrest, M. E. Thompson, „Introduction: Organic electronics and optoelectronics“, *Chemical Reviews* 107, 923 (2007).
2. N. Koch, „Organic electronic devices and their functional interfaces“, *ChemPhysChem* 8, 1438 (2007).
3. S. Duhm, G. Heimel, I. Salzmann, H. Glowatzki, R. L. Johnson, A. Vollmer, J. P. Rabe, N. Koch, „Orientation-dependent ionization energies and interface dipoles in ordered molecular assemblies“, *Nat. Mater.* 7, 326 (2008).
4. H. Fukagawa, H. Yamane, T. Kataoka, S. Kera, M. Nakamura, K. Kudo, N. Ueno, „Origin of the highest occupied band position in pentacene films from ultraviolet photoelectron spectroscopy: Hole stabilization versus band dispersion“, *Phys. Rev. B* 73, 245310 (2006).

Cooperative or self-centred.

Can an electron make the choice?

Nitrogen molecules were irradiated with soft X-rays over a wide energy range. Because of this irradiation electrons are emitted from the molecule with a kinetic energy that depends on the choice of photon energy. This means slow or fast, where the velocity determines the resolving power of the electron for its environment. The researchers succeeded in demonstrating that there is a transition between a cooperative and self-centred behaviour of the electron and that this behaviour depends on its kinetic energy during intramolecular scattering. Beyond a critical energy the scattered electron no longer superposes with its phase-coupled neighbouring electron, but with itself, thereby generating an image of its environment. This demonstrates that the electron's cooperative and resolving powers are complementary properties, which do not coexist alongside each other.

A situation analogous to the famous double slit experiment with single electrons [1] arises when an electron is emitted from a homonuclear diatomic molecule due to the absorption of a highly energetic photon because the two atoms are mirror symmetric and indistinguishable [2]. Due to these two fundamental properties, the electrons can tunnel between the two atoms with an “overlap-specific” tunneling frequency. As a result, the electron is unable to distinguish from which atom it was originally emitted and instead shows properties of a coherent superposition of two waves which have been “simultaneously” emitted from both sides [3]. These superpositions may be distinguished with respect to sign, showing sum or difference properties. However, they reflect no specific properties of the corresponding individual waves. This coherent non-self-centred behaviour is even preserved upon scattering of the emitted electron by its neighbouring atom. The scattered electron is furthermore superimposed with the electron wave emitted from the neighbouring atom, but not with its own non-scattered wave. The corresponding superposition is, however, destructive due to the phase shift of π caused by the scattering process. In this way the amplitude of the original wave changes but its coherent character is, however, basically preserved. The electrons remain part of a coherent, non-self-centred environment. Is this principle of coherence conservation valid for all electrons, the scattered and the non-scattered ones, independent of their corresponding energies?

For this purpose they irradiated nitrogen molecules over a wide photon energy range with monochromatic soft X-ray radiation from beamlines of HASYLAB at DESY in Hamburg and BESSY in Berlin. This gave rise to emission of photoelectrons with correspondingly different kinetic energies. The intensity of these electrons should oscillate with kinetic energy in a way expected for a coherent superposition of two waves emitted from two spatially separated positions. This should be the case

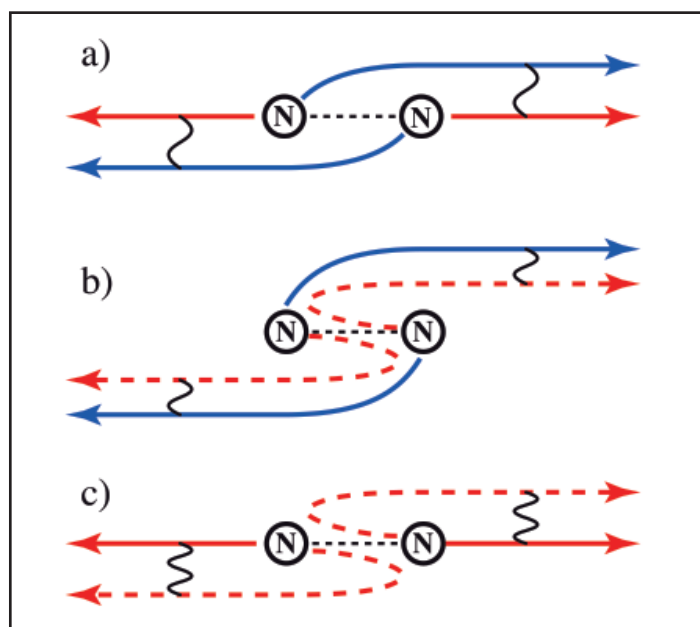


Figure 1

Electrons between cooperative (coherent) and egocentric behavior: If an electron is catapulted out of a nitrogen molecule at relatively low speed, it behaves cooperatively. The waves are sent out like a pseudo pair from both atoms and are superimposed coherently (a). This also remains the case so if one of these electron waves is scattered off the atom (b). On the other hand, an electron behaves egocentrically or like an individual if it leaves the molecule quickly (c). If the electron now hits the adjacent atom and is scattered by it, it recognizes from which atom it started and superimposes itself on its non-scattered wave.

for both the unscattered as well as the scattered electrons. Unexpectedly, the coherent behaviour appears for the latter one only for kinetic energies corresponding to a matter (de Broglie) wavelength larger than the distance between the two emitter atoms. For matter wavelengths smaller than this distance the coherence between the two emitter positions is lost and the scattered wave is superimposed with its own unscattered wave in a self-centred way. The results of these investigations have been published in the August issue of Nature Physics. In this context the question arises to why this dramatic change from cooperative coherent to self-centred explorative behaviour appears? The answer is the spatial resolution capability. As long as the scattered wave is unable to resolve the distance between the two emitter centres, the original coherence is preserved even in case of scattering. However, as soon as the matter wavelength becomes shorter than the emitter distance between the two atoms of the molecule, and is hence able to resolve this distance spatially in the sense of a Heisenberg microscope [4], this coherence is lost. This position-resolving electron becomes re-scattered independently of the phase of the neighbouring atom and subsequently superimposes with its own un-scattered wave. This process, which modulates the absorption spectrum, has been known for many decades as “Extended X-ray Fine Structure”, abbreviated as EXAFS [5]. The EXAFS analysis of the energy-dependent oscillating photoabsorption intensities forms the basis of one of the most successful methods for the structural analysis of condensed matter, because the self-centred behaviour of the scattered photoelectron yields detailed information on its environment. In our case it is sensitive to its spatially local environment because it has lost its original non-local coherent character and could collect information on its environment. In this way the German-American collaboration succeeded for the first time to demonstrate the transition from cooperative coherent to self-centred explorative behaviour of interacting particles, in this case of electrons, experimentally and theoretically. ●

Contact: Uwe Becker, becker_u@fhi-berlin.mpg.de

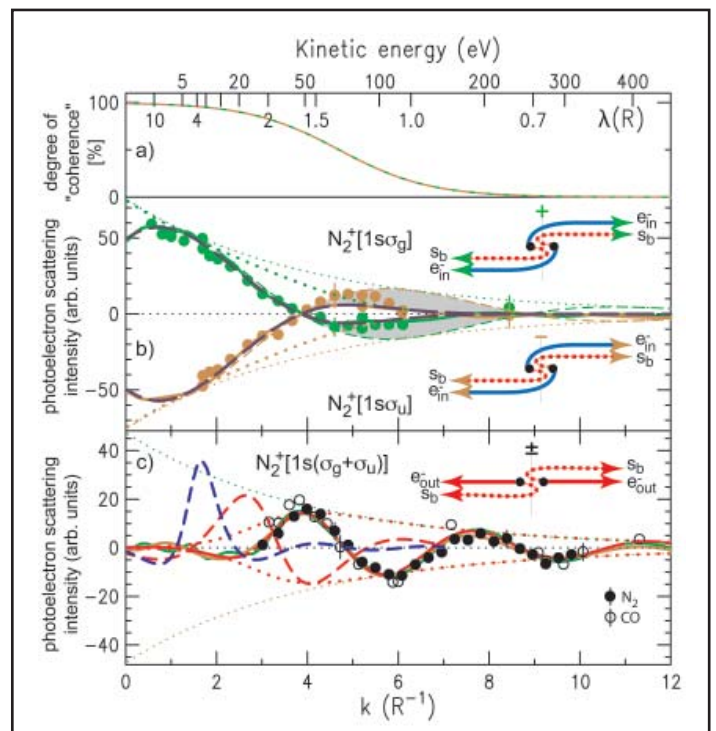


Figure 2

The transition from coherent to non-coherent individual behavior is given by the “decoherence” curve [6] shown in part a) of this figure. This curve shows the nearly complete degradation of coherent behavior upon scattering for a de Broglie wavelength matching the bond length R of the nitrogen molecule. Part b) of this figure shows the strength of the coherent superposition between the scattered and unscattered electron wave in the coherent two-centre scattering regime. It clearly shows how this regime dies out above the critical de Broglie wavelength $\lambda = R$. In place of this process, the individual self-interference of the scattered electron with its own unscattered wave becomes the dominant process. This process resolves its environment and hence provides structural information on it.

Authors

Björn Zimmermann^{1,5}, Daniel Rolles^{2,6}, Burkhard Langer^{3,6}, Rainer Hertges², Markus Braune², Slobodan Cvejanovic^{2,8}, Oliver Geßner^{2,9}, Franz Heiser^{2,10}, Sanja Korica², Toralf Lischke^{2,11}, Axel Reinköster², Jens Viehhaus^{2,12}, Reinhard Dörner⁴, Vincent McCoy¹, Uwe Becker²

1. California Institute of Technology, Pasadena, CA 91125, USA
2. Fritz-Haber-Institut der Max-Planck-Gesellschaft, 14195 Berlin, Germany
3. Max-Born-Institut für Nichtlineare Optik und Kurzzeitspektroskopie, 12489 Berlin, Germany
4. Institut für Kernphysik, Universität Frankfurt, 60486 Frankfurt, Germany
5. Present address: Department of Physics, Tulane University, New Orleans, LA 70118, USA
6. Present address: Physikalische und Theoretische Chemie, Institut für Chemie, Freie Universität Berlin, 14195 Berlin, Germany
7. Present address: University of Western Michigan, Kalamazoo, MI 49008, USA
8. Present address: Medical Faculty, Physics Department, University of Rijeka, 51000 Rijeka, Croatia
9. Present address: Chemical Sciences Division, Lawrence Berkeley National Laboratory, Berkeley CA 94720, USA
10. Present address: Ericsson AB, Torshamnsgatan 39 A, 16493 Kista, Sweden
11. Present address: Max-Planck-Institut für Plasmaphysik, 85748 Garching, Germany
12. Present address: Deutsches Elektronen-Synchrotron DESY, 22603 Hamburg, Germany

References

1. Jönsson, C., “Elektroneninterferenzen an mehreren künstlich hergestellten Feinspalten”, *Z. Phys.* **161**, 454–474 (1961).
2. Rolles, D. et al., “Isotope-induced partial localization of core electrons in the homonuclear molecule N_2 ”, *Nature* **437**, 711–715 (2005).
3. Cohen, H. D. & Fano, U., “Interference in the Photo-Ionization of Molecules”, *Phys. Rev.* **150**, 30–33(1966).
4. Heisenberg, W., “Über den anschaulichen Inhalt der quantentheoretischen Kinematik und Mechanik”, *Z. Phys.* **43**, 172–198 (1927).
5. Sayers, D.E, Stern, E.A., and Lytle, F.W., “New Technique for Investigating Noncrystalline Structures: Fourier Analysis of the Extended X-Ray-Absorption Fine Structure”, *Phys. Rev. Lett.* **27**, 1204–1207 (1971).
6. Hacker Müller, L., Hornberger, K., Brezger, B., Zeilinger, A. & Arndt, “M. Decoherence of matter waves by thermal emission of radiation”. *Nature* **427**, 711–714 (2004).

Original publication

Localization and loss of coherence in molecular double-slit experiments
Nature Physics Vol.4, 649–655, 2008

Visualizing a lost painting by Vincent van Gogh.

Application of X-ray fluorescence imaging

Many paintings by Vincent van Gogh cover a previous composition, because the artist frequently re-used the canvas of abandoned paintings. Using synchrotron induced X-ray fluorescence mapping we visualized a woman's head hidden under the work Patch of Grass. The resulting elemental distributions and additional X-ray absorption spectroscopy on selected points on the painting enabled an approximate colour reconstruction of the hidden face. This proved to be the missing link in comparing the head with Van Gogh's known oeuvre.

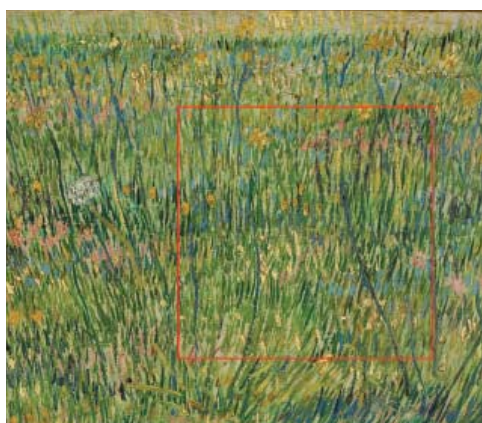


Figure 1
Vincent van Gogh, "Patch of Grass", Paris, summer 1887, Kröller-Müller Museum, Otterlo. The red frame indicates the field of view in images figure 2,5.

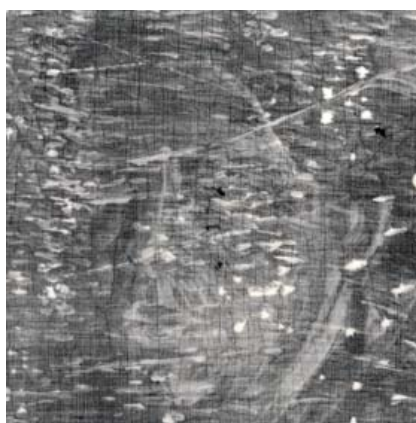


Figure 2
X-ray radiation transmission radiograph (XRR).

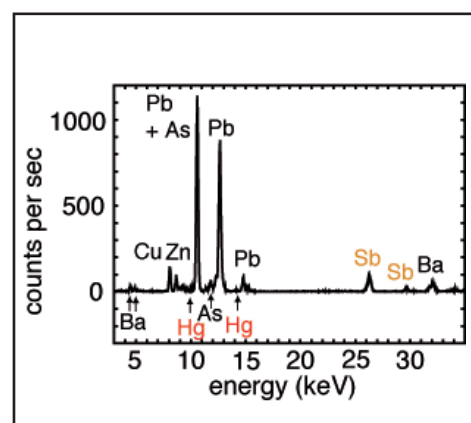


Figure 3
X-ray fluorescence spectrum of 1 sec exposure time from one location on the painting, showing the presence of Sb and Hg.

Vincent van Gogh (1853-1890), one of the founding fathers of modern painting, is best known for his vivid colours, his vibrant painting style and his short, but highly productive career. The artist would often re-use the canvas of an abandoned painting and paint a new composition on top (Fig. 1) [1]. These hidden paintings offer a unique and intimate insight into the genesis of his works.

Van Gogh's painting palette contains a range of colours with an equally diverse chemical composition. Ranging from organometallic compounds, transition metals to heavy metals, van Gogh's pigments virtually cover the entire periodic table of elements.

For the visualization of hidden paint layers, museums usually resort to tube-based X-ray transmission radiography (XRR, Fig. 2). In these images, the absorption contrast is mostly caused by strong concentrations of heavy metal pigments,

such as lead white. Other compounds, notably low concentrated or low Z pigments are obscured. Earlier examinations with XRR of the painting by Van Gogh from his 1886-87 Paris period, Patch of Grass (Kröller-Müller Museum, Otterlo, the Netherlands) vaguely revealed a head under the surface painting. The facial characteristics could not be clearly read, making the person portrayed far from identifiable.

Visualizing hidden paint layers, therefore, requires an elementally resolved view on the paint substructure. In order to obtain such elemental distribution images, we decided to scan Patch of Grass with X-ray fluorescence microanalysis (XRF, Fig. 3). In case that the detected element could not be assigned to a colour, in addition, X-ray absorption near edge spectroscopy (XANES, Fig. 4) was performed on selected points on the painting and on reference colours. Use was made of a pencil beam of high-energy, high-intensity synchrotron radiation so

as to penetrate all paint layers. The experiments were performed at the DORIS III beamline L (XRF) and C (XANES). Three elements were found to overlap with the hidden face: Hg, Sb and Zn. Mercury is associated with the red pigment cinnabar and Zn with zinc white. Sb was found in the lighted parts of the face and XANES measurements revealed Sb to be present as Naples yellow. Based on these results, a tri-tonal reconstruction of the hidden head could be made. This approximate colour reconstruction presents a clear and detailed image of the hidden composition, including physiognomic details, as eyes, nose, mouth and chin (Fig. 5). Our reconstruction proved to be the missing link in comparing the hidden face with the artist's

known oeuvre. The hidden painting dovetails with an extensive series of heads from the artist's period in Nuenen (the Netherlands) in the winter of 1884/85. More specifically, the present head must belong to a smaller group of studies that Vincent gave to his brother Theo in Paris (Fig. 6), as mentioned in his letters [2]. Two and a half years later Vincent went to join Theo in Paris and may very well have found the woman's head hopelessly old-fashioned by then. This can explain the presence of a colourful, Parisian style floral painting on top of a dark and sombre head of a provincial Dutch woman. ●

Contact: Joris Dik, j.dik@tudelft.nl

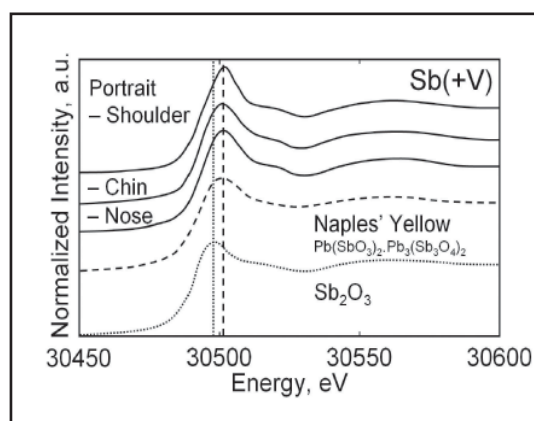


Figure 4
Comparison of Sb-K edge XANES spectra from three positions on the painting with reference XANES spectra of Naples yellow ($Pb(SbO_3)_2$, $Pb_3(Sb_3O_4)_2$) and antimony white (Sb_2O_3). All spectra recorded in fluorescent mode.

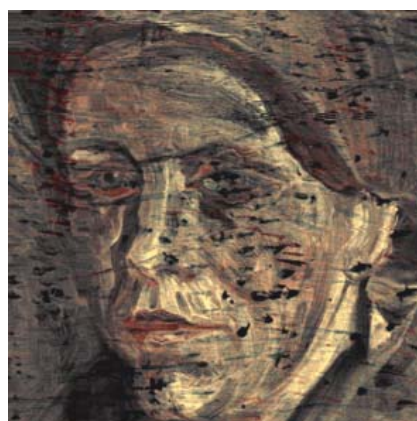


Figure 5
Colour reconstruction of Sb (pale yellow) and Hg (red) representing the flesh colour of the hidden face.



Figure 6
Detail from Vincent van Gogh, "Head of a Woman", Nuenen, winter 1884-85, Van Gogh Museum, Amsterdam.

Authors

Joris Dik¹, Koen Janssens², Geert van der Snickt², Luuk van der Loeff³ and Karen Rickers⁴, Marine Cotte^{5,6}

1. Department of Materials Science, Delft University of Technology, the Netherlands
2. Centre for Micro- and Trace Analysis, Department of Chemistry, Universiteit Antwerpen, Belgium
3. Kröller-Müller Museum, Otterlo, the Netherlands
4. Deutsches Elektronen-Synchrotron (DESY), Hamburg, Germany
5. Centre of Research and Restoration of the French, Museums, UMR-171 – CNRS, Palais du Louvre, Paris, France
6. European Synchrotron Radiation Facility (ESRF), Grenoble, France

Copyrights:

Figure 1: Kröller- Müller Museum, Otterlo, the Netherlands
Figure 6: Van Gogh Museum, Amsterdam, the Netherlands

References

1. S. van Heugten, "Radiographic images of Vincent van Gogh's painting in the Kröller-Müller Museum, Otterlo, and the Van Gogh Museum Amsterdam", *Van Gogh Museum Journal* (1995)
2. V. van Gogh, "Letter to Theo van Gogh". Written mid-March and April 1st, 1885 in Nuenen. Translated by J. van Gogh-Bonger, edited by R. Harrison, published in *The Complete Letters of Vincent van Gogh*, Publisher: Bulfinch, 39 (1991)

Original publication

"Visualization of a lost painting from Vincent van Gogh using synchrotron-radiation based X-ray fluorescence elemental mapping"
Anal. Chem., 80, 16, 6436 - 6442, 2008, doi:10.1021/ac800965g

Metal contaminations in small water fleas.

A combination of X-ray imaging experiments

What is the effect of transition metals on the health of freshwater invertebrates? One problem is to determine the concentration of trace-level distributions within the organs of the animal, which is the size of a few mm in the case of a typical model system – the water flea *Daphnia magna*. The combination of 2D/3D fluorescence micro-probe and X-ray absorption tomography allows creating a detailed map of metal concentrations within the invertebrate. This non-destructive method allows a qualitative determination of metal-distribution within the different organs of the invertebrate, which can be used for scientifically based environmental regulations.

One problem in environmental toxicology is to define scientifically relevant environmental regulations, which are based on accurate biotic ligand models. These models are used to predict the toxicity of pollutants in surface water on living organisms like pelagic and benthic invertebrates. In order to develop these biotic ligand models [1,2], toxicological effects and accumulation of pollutants in various organs of the organism have to be measured. The freshwater crustacean *Daphnia magna* is one model organism to study the effect of transition metals like Fe, Ni, Cu, and Zn on various organs. The size of daphnids is rather small with a length of 1-4 mm, which makes it difficult to use conventional methods like dissection and acid digestion of various organs, which remains are then studied with atomic absorption spectrometry. Other methods cannot distinguish between whole-body accumulation and accumulation within specific organs, which is important to determine the organ-specific accumulation and toxicity.

Micro X-ray fluorescence techniques, such as fast 2D mapping, 2D computed tomography and 3D confocal imaging are ideal non-destructive tools to study trace-level distributions of metals in small biological samples. The high intensity of synchrotron radiation allows measuring fluorescence maps with resolution of 5-20 μm within a few hours. Despite the high flux, radiation damage of the organism is negligible. We combined data of 2D/CT high-resolution fluorescence maps with X-ray absorption computed tomography rendered volumes, in order to compare the metal concentrations in *Daphnia magna* which were kept in aquatic environments with normal and elevated Zn concentrations. These comparisons show enrichment of Zn in specific organs (e.g. gill and eggs), which give important information about ingestion and accumulation of Zn in *Daphnia magna*. Figure 1 illustrates two-dimensional scanning micro-XRF results showing the elemental distributions within two *Daphnia magna* samples corresponding to different levels of aquatic Zn exposure. These scans were performed at Beamline L of the DORIS III storage ring. The elemental maps correspond to the Ca, Fe and Zn distribution within an unexposed sample (left), and within a sample which was exposed to $120 \mu\text{g L}^{-1}$ Zn for

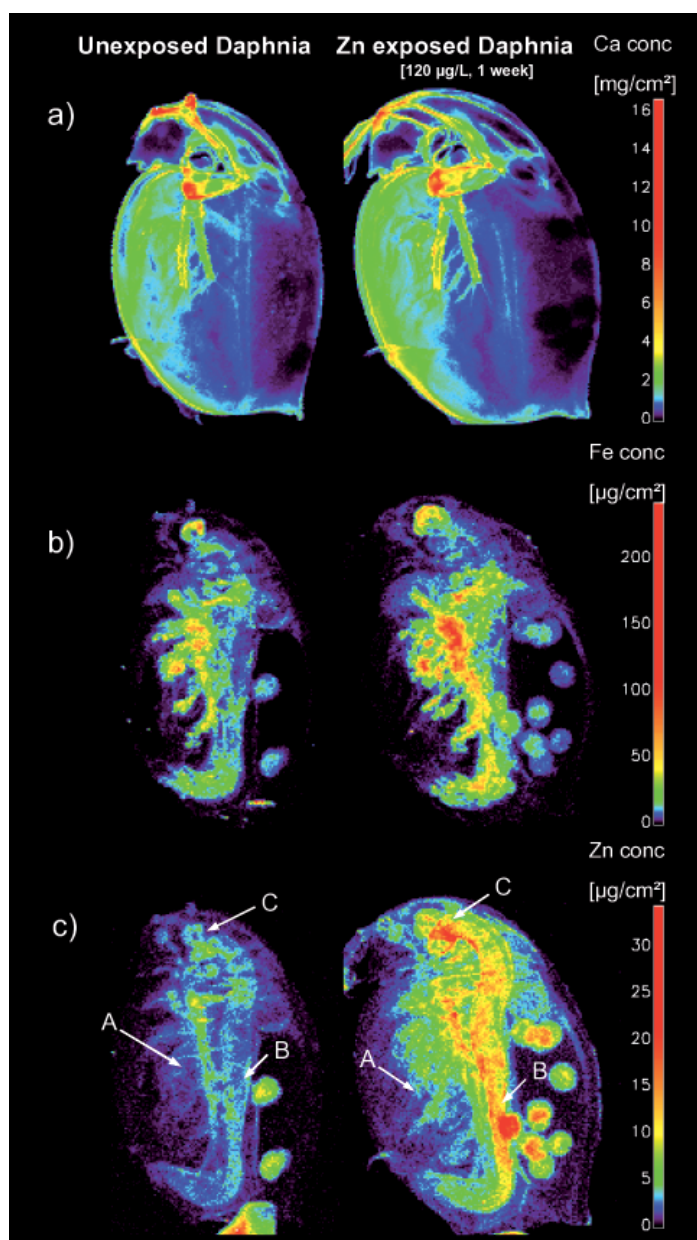
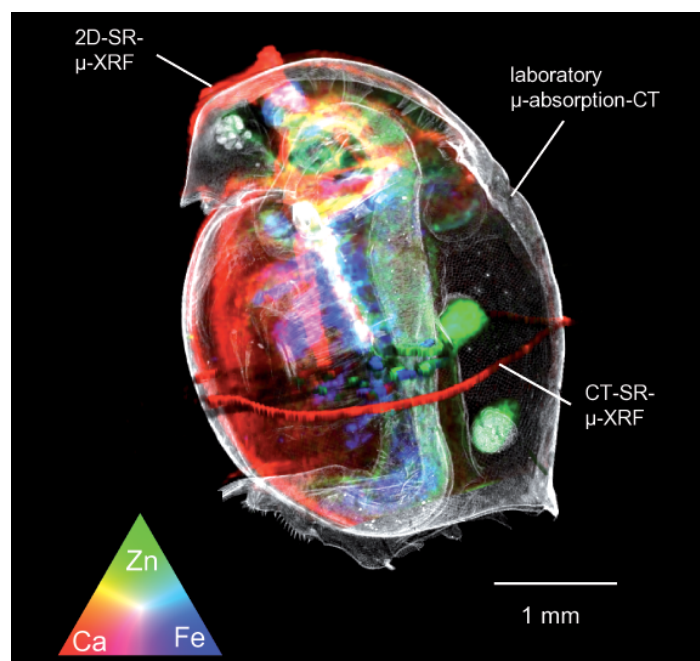


Figure 1
2D μ -XRF element maps (Ca, Fe and Zn) for the unexposed and exposed *D. magna*.

Figure 2
3D rendered image of the unexposed *D. magna*, combining laboratory micro absorption CT and synchrotron 2D/CT μ -XRF data



1 week (right). Since metals can only influence physiological processes where they are effectively present, insight into the tissue-specific distribution of elements contributes to an increased understanding of possible consequences of an exposure [3]. The accumulation of Zn in the different tissues is clearly visible. A color bar, which gives the areal Zn concentration in micrograms per square centimeter for both samples, is given on the right. A distinct enrichment of Zn can be observed in (A) the gill-like osmoregulatory tissue, and in the digestive system, i.e., (B) the gut and (C) the digestive gland. The accumulation in gills may suggest that zinc accumulation may interfere with osmoregulation (as in fish). The accumulation in the digestive system may suggest that nutrient assimilation from food is a possible Zn toxicity target.

Figure 2 shows the result of the “cross-fertilization” between laboratory X-ray absorption microtomography and SR micro-XRF techniques (2D dynamic scanning and XRF computed tomography). The measurements were complemented by absorption CT measurements at the UGCT micro/nano-CT set-up at Ghent University. The reconstructed 3D image allows a thorough investigation of the tissue structures and their corre-

sponding elemental contents. The colors red, green, and blue are the scaled Ca, Zn, and Fe intensities, proportional to the elemental concentration. A color triangle at the left bottom of the image renders the colors which indicate the correlating or complementary behaviour of the elements in question. The very distinct accumulation of Ca in the exoskeleton, Fe in the gill-like tissue, and Zn in the gut and eggs can be clearly observed. The illustrated research demonstrates the potential of combining ecotoxicological experiments with X-ray techniques which can both visualize the elemental composition and structure of biological samples on the microscopic scale. With respect to biological imaging, shifting from the microscopic tissue scales towards a subcellular field of view is expected at PETRA III. Using nanobeams of X-rays coupled with state-of-the-art scanning systems and multi-element detectors, a detailed 3D structure of the elemental distributions within individual cells will be detectable, which is likely to provide new insights into the role of metals in cell biology. ●

Contact: B. De Samber, Bjorn.Desamber@UGent.be
L. Vincze, Laszlo.Vincze@UGent.be

Authors

B. De Samber¹, R. Evens², K. De Schampelaere², G. Silversmit¹, B. Masschaele³, T. Schoonjans¹, B. Vekemans¹, C. Janssen², L. Van Hoorebeke³, I. Szaloki⁴, L. Balcaen¹, F. Vanhaecke¹, G. Falkenberg⁵ and L. Vincze¹

1. Department of Analytical Chemistry, Ghent University, Krijgslaan 281-S12, B-9000 Ghent, Belgium
2. Laboratory of Environmental Toxicology and Aquatic Ecology, Ghent University, Jozef Plateaustraat 22, B-9000 Ghent, Belgium
3. Centre for X-Ray Tomography, Department of Subatomic and Radiation Physics, Proeftuinstraat 86, Ghent University, B-9000 Ghent, Belgium
4. Institute of Experimental Physics, University of Debrecen, 4026 Debrecen, Bem tér 18/a, Hungary
5. Hamburger Synchrotronstrahlungslabor at DESY, Notkestr. 85, D-22603 Hamburg, Germany

References

1. P. Paquin, J. Gorsuch, S. Apte, G. Batley, K. Bowles, P. Campbell, C. Delos, D. Di Toro, R. Dwyer, F. Galvez, R. Gensemer, G. Goss, C. Hogstrand, C. Janssen, J. MCGeert, R. Naddy, R. Playle, R. Santore, U. Schneider, W. Stubblefield, C. Wood and K. Wu, *Comp. Biochem. Physiol. C. “Pharmacol. Toxicol.”*, **133**, 3-35 (2002).
2. D. Heijerick, K. De Schampelaere and C. Janssen, *Environ. Toxicol. Chem.*, **21**, 1309-1315 (2002).
3. K. De Schampelaere, M. Canli, V. Van Lierde, I. Forrez, F. Vanhaecke, C. Janssen, *Aquat Toxicol.*, **70**, 233-244 (2004)

Original publications

- “Combining Synchrotron and Laboratory X-Ray Techniques for Studying Tissue-Specific Trace Level Metal Distributions in *Daphnia Magna*”, *J Anal At Spectrom.*, **23**, 829-839 (2008)
- “Three Dimensional Elemental imaging by means of synchrotron radiation micro-XRF: developments and applications in environmental chemistry”, *Anal Bioanal Chem.*, **390**, 267-271 (2008)

Small-angle X-ray scattering complements crystallography.

Structural basis of recognition and activation of mRNA decapping complex

Small-angle X-ray scattering (SAXS) is rapidly becoming a streamline tool in structural molecular biology providing unique information about overall structure and conformational changes of native macromolecules in solution. Of particular interest is the joint use of SAXS with the high resolution methods like crystallography to study functional complexes. For a Dcp1p-Dcp2n protein complex playing a major role in the process of messenger RNA degradation, crystallographic analysis combined with SAXS and functional studies revealed that Dcp2p exists in open and closed conformations, the latter being the catalytically more active form. This suggests a decapping mechanism controlled by a conformational change between the open and closed complexes.

Tremendous progress has recently been achieved in structure determination of individual proteins due to large-scale initiatives in macromolecular X-ray crystallography (MX) [1]. Although high resolution information on isolated proteins is extremely valuable, it is also limited, as the most important cellular functions are accomplished by macromolecular complexes. The focus of modern structural biology is shifting towards the functional complexes [2], which are often of transient and flexible nature, hampering the growth of well-diffracting crystals. Even if the high resolution structure is solved, it represents a snapshot of the static structure in the crystal, which may be influenced by the crystallographic packing forces. Moreover, structural changes initiated by ligand binding or by alterations in external physical and chemical conditions are difficult to study in the crystal. Synchrotron small-angle X-ray scattering (SAXS) is a rapid technique to study overall structure of native macromolecules in solution. Recent progress in instrumentation and data analysis [3] significantly enhanced resolution and reliability of structural models provided by the technique. In the absence of other data, SAXS provides low resolution macromolecular shapes *ab initio*, but very important are its applications together with MX. Most notably, quaternary structure of complexes can be analyzed by rigid body refinement using high resolution models of the subunits [3].

At the EMBL beamline X33 (DORIS III ring at DESY), SAXS is employed to validate and complement structural models provided by MX in numerous user projects. One of the examples is the study of a functional protein complex involved in messenger RNA (mRNA) degradation, an important cellular process controlling gene expression and the elimination of aberrant mRNAs [4]. A critical step in mRNA degradation is the removal of its 5' cap terminal structure, which is catalysed by a decapping complex consisting of the two proteins, Dcp1p and Dcp2p, where the latter is a catalytic subunit recognizing and cleaving the capped mRNA substrate. Their individual crystal structures have recently been solved [5,6].

A recent publication in February 2008 issue of *Molecular Cell*

presents a joint MX, SAXS and biochemical study providing insight into how Dcp1p interacts with and influences Dcp2p activity. The crystal structure of a complex of *Schizosaccharomyces pombe* Dcp1p with Dcp2n (a truncated version of Dcp2p) was solved at 2.8 Å resolution. Surprisingly, the asymmetric crystallographic unit contained two types of complexes, one with open, the other with closed conformation of Dcp2n (Figure 1). Moreover, an ATP molecule used as a crystallization additive was located in the catalytic centre of closed Dcp2n form but not in the open form. The closed conformation could correspond to the catalytically active enzyme, where the ATP

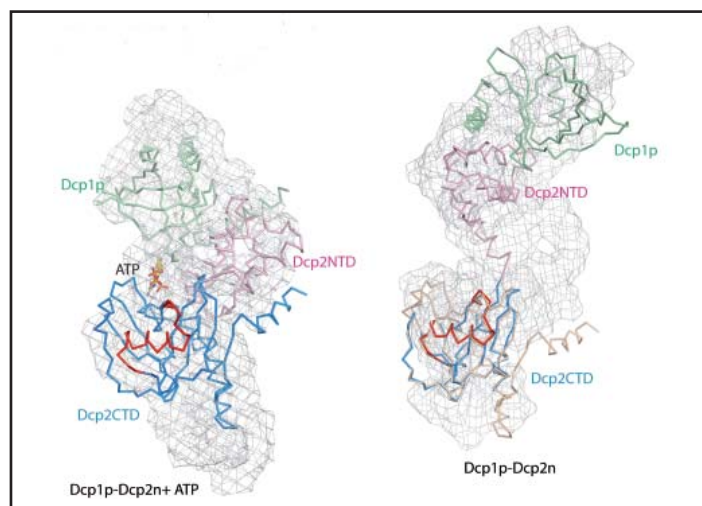


Figure 1

Structural models of Dcp1p-Dcp2n complex. The backbones of the crystal structures are superimposed onto the *ab initio* shapes generated from SAXS (shown as mesh). Left panel, closed crystallographic complex and SAXS model for the ATP-containing solution, right panel, open crystallographic complex and SAXS model for the ATP-free solution. Dcp1p is colored green, the N- and C-termini of Dcp2n are displayed in pink (Dcp2CTN) and blue (Dcp2CTD), respectively, and the so-called "Nudix" motif is in red. In the left panel, ATP molecule is shown as sticks, and in the right panel, Dcp2CTD from the closed Dcp1p-Dcp2n complex is superimposed onto the open Dcp1p-Dcp2n backbone and colored in wheat.

molecule may be mimicking the interaction of the RNA substrate with Dcp2p. The observed effect could however also be an artifact generated by the crystal packing. Also, the open structure was incomplete with numerous missing loops in the C-terminus of Dcp2n.

SAXS was employed to study the solution structure of the Dcp1p-Dcp2n complex in the absence and presence of ATP (Figure 2). The radius of gyration R_g and the maximum size D_{max} of the complex without ATP agree well with those of the open crystal form. Addition of ATP decreases the R_g by 5 Å and D_{max} by about 10 Å making the parameters compatible with those of the closed crystal form. The low resolution shapes of the complex with and without ATP reconstructed ab initio from the scattering patterns agree well with the closed and open crystal structures, respectively (Figure 1). Moreover, the experimental data in the presence of ATP is neatly matched by the scattering pattern computed from the closed model but not from the open model (Figure 2). In contrast, the measured scattering from the ATP-free complex agrees better with the pattern computed from the open form (after addition of the missing loops using the coordinates of the Dcp2n C-terminus in the closed form) but displays some deviations suggesting that the structure in solution may be flexible.

For the Dcp2n alone (Figure 2), addition of ATP did not prompt a change in the SAXS scattering pattern. The overall shape of free Dcp2n agrees well with the extended Dcp2n conformation as in the open crystallographic model of the complex, but not with the compact structure of free Dcp2n in the crystal [6]. This indicates that Dcp2n exists in an extended conformation in solution and also that the closure of Dcp2n requires its complex with Dcp1p.

These structural results were further corroborated by biochemical assays and mutagenesis demonstrating the higher catalytic activity of the close form. One may therefore conclude that Dcp1p activates Dcp2p by stabilizing a closed conformation of the complex and that a conformational change between these open and closed complexes might control the mRNA decapping mechanism. Overall, the study underlines the power of the joint use of MX and SAXS in the study of functional macromolecular complexes. ●

Contact: Dmitri Svergun, svergun@embl-hamburg.de

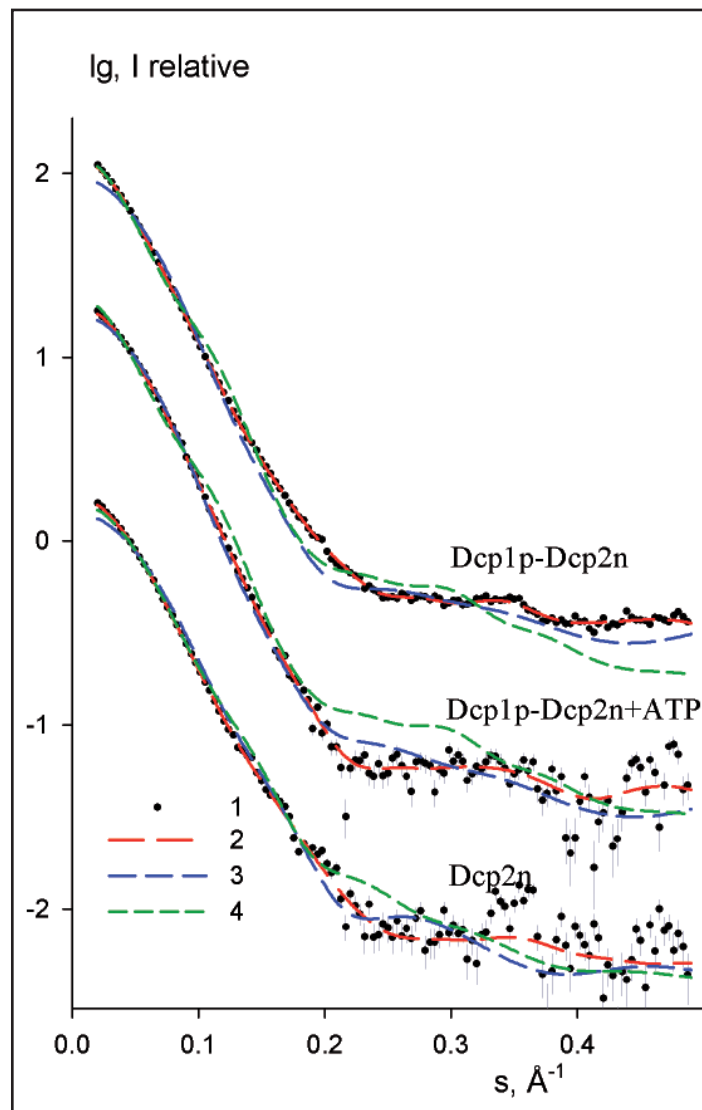


Figure 2

Experimental and computed SAXS data. From top to bottom: Dcp1p-Dcp2n complex without and with ATP, and free Dcp2n without ATP (addition of ATP to Dcp2n yields the curve coinciding within the errors). The logarithm of the scattering intensity is plotted against the momentum transfer $s = 4\pi \sin\theta/\lambda$, where 2θ is the scattering angle and $\lambda = 1.5 \text{ \AA}$ is the X-ray wavelength. The plots are displaced along the ordinate for better visualization. Dots with error bars: experimental scattering; dashed lines: scattering from the models. Red: ab initio GASBOR models; green: open crystal complex, blue closed crystal complex (for Dcp2n, green and blue are extended Dcp2n as in the open crystal complex and compact free Dcp2n in the crystal, respectively).

Authors

Meipei She¹, Carolyn J. Decker², Dmitri I. Svergun³, Adam Round^{3, 4}, Nan Chen¹, Denise Muhlrad², Roy Parker² and Haiwei Song^{1,5}

- Laboratory of Macromolecular Structure, Institute of Molecular and Cell Biology, Agency for Science, Technology and Research, 61 Biopolis Drive, Proteos, 138673 Singapore
- Department of Molecular and Cellular Biology, Howard Hughes Medical Institute, University of Arizona, Tucson, AZ 85721, USA
- Hamburg Outstation, European Molecular Biology Laboratory, Hamburg 22603, Germany
- Institute of Crystallography, Russian Academy of Sciences, Leninsky pr. 59, 117333 Moscow, Russia
- Department of Biological Sciences, National University of Singapore, 14 Science Drive, 117543 Singapore

Original publication

Structural basis of Dcp2 recognition and activation by Dcp1
Mol. Cell 29, 337-349 (2008)

References

- Levitt, M. "Growth of novel protein structural data", *Proc Natl Acad Sci U S A*, 104, 3183-3188 (2007).
- Aloy, P. and Russell, R.B. "Structural systems biology: modelling protein interactions", *Nat Rev Mol Cell Biol*, 7, 188-197 (2006).
- Petoukhov, M.V. and Svergun, D. I. "Analysis of X-ray and neutron scattering from biomacromolecular solutions", *Curr Opin Struct Biol*, 17, 562-571 (2007).
- Parker, R., and Song, H. "The enzymes and control of eukaryotic mRNA turnover", *Nat. Struct. Mol. Biol.* 11, 121-127 (2004).
- She, M., Decker, C.J., Sundramurthy, K., Liu, Y., Chen, N., Parker, R. and Song, H., "Crystal structure of Dcp1p and its functional implications in mRNA decapping", *Nat. Struct. Mol. Biol.* 11, 249-256 (2004).
- She, M., Decker, C.J., Chen, N., Tumati, S., Parker, R., and Song, H. "Crystal structure and functional analysis of Dcp2p from *Schizosaccharomyces pombe*", *Nat. Struct. Mol. Biol.* 13, 63-70 (2006).

Mapping the protein world.

Advanced software assists to expose the hidden world of biological molecules

ARP/wARP is a software suite to build macromolecular models in X-ray crystallographic electron density maps. Structural genomics initiatives and the study of complex macromolecular assemblies and membrane proteins rely on advanced methods for 3D structure determination. ARP/wARP 7.0 meets these needs by providing the automated tools for: iterative protein model building including a high-level decision-making control module; fast construction of the secondary structure of a protein; building flexible loops in alternate conformations; placement of ligands, including a choice of the best-fitting ligand from a 'cocktail'; and finding ordered water molecules. All protocols are easy to handle by a non-expert user and the time required is typically a few minutes, although iterative model building may take a few hours. ARP/wARP is a continuous collaborative project between two groups at the EMBL in Hamburg and the NKI in Amsterdam.

Structural genomics initiatives and medically oriented high-throughput structure determination projects emphasise the need for advanced methods for structure determination [1]. In X-ray macromolecular crystallography, availability of comprehensive software packages has had a major impact on structural biology research. Crystallographic model building has been traditionally done by expert users, with the aid of specialised interactive graphics software. The automation of this process and linking model building and refinement together into a unified process, first exemplified in the ARP/wARP package [2], was followed promptly by significant developments worldwide. ARP/wARP has been used extensively for thousands of structure determinations. Examples include a three-protein complex that is crucial in chromosome segregation (hereafter please refer to the original publication for the complete list of cited literature); complexes in spindle assembly checkpoint formation; ubiquitin conjugation; transcriptional regulation of mRNA; cargo transport along microtubules; studies of bioluminescence; the structural dissection of an enzyme involved in the synthesis of inflammatory mediators; ligand recognition by lipoprotein receptors; investigation of membrane-binding proteins in signal transduction in photo-response, the plant aquaporin mechanism and the functional characterisation of a prokaryotic Ca^{2+} -gated K^+ channel. Moreover, ARP/wARP is often used as a benchmark to evaluate the quality of electron density produced by new methods [3] and has been integrated in many crystallographic software pipelines as the default model-building engine [4]. Successful automated building of a considerable part of models is now possible at a resolution as low as 2.7 Å [5] and a wide spectrum of ARP/wARP functionalities is outlined below.

Free atoms and hybrid models. Firstly ARP/wARP condenses the map information to a set of identical free atoms that represent the electron density. As model building iteratively proceeds, some free atoms are recognised as part of a protein chain and gain chemical identity. This mixture is an ARP/wARP hybrid model

that incorporates chemical knowledge from the partially built protein model, whereas its free atoms continue to interpret the electron density in areas where no model is yet available.

Main chain tracing in ARP/wARP uses all atoms of the hybrid model as potential $\text{C}\alpha$ atoms. Peptide units are recognised by matching the surrounding electron density to that precomputed from known structures. The recognised peptides are assembled into linear chain fragments with partial 'guessed' side chains using a limited depth-first graph-search algorithm.

Side chains are subsequently docked in protein sequence and built in the best rotamer configuration.

Loop building. Using the sequence docking and a distribution of penta-peptide fragments derived from known structures, several loop conformations are constructed and the one fitting best the density is chosen. This helps model building in low-density areas.

Secondary structure recognition. At a resolution where electron density maps lack atomic features sparse map grid points with 1 Å spacing are selected as potential $\text{C}\alpha$ atoms. After succes-



Figure 2

Remote execution of ARP/wARP protein model building directly through the web link <http://cluster.embl-hamburg.de/ARPwARP/remote-http.html>.

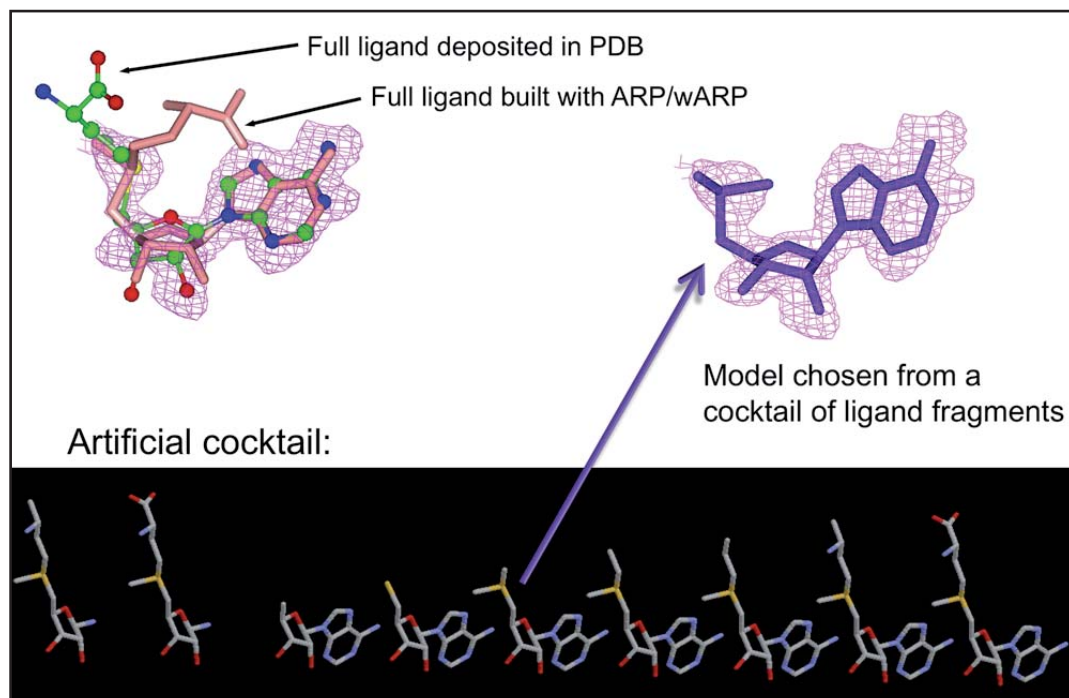


Figure 1

Building partially ordered ligands. Top left: the difference density map in the area of the ligand; Adenosylmethionine as in the PDB model (1v2x); full ligand built with ARP/wARP – none of the two models fit the density well. Bottom: an artificial cocktail of ligand fragments. Top right: a partial ligand built with ARP/wARP, matching the density.

sive filtering steps trace assemblies of helical or stranded fragments are generated and averaged. Peptide backbone and $C\beta$ atoms are added and the most likely chain direction is selected. The procedure is applicable to a resolution as low as 4.5 Å. **Ligand building.** When the protein structure is completed, bound ligands or cofactors can be built in the difference electron density map. First, regions of density that have the same volume as the ligand are identified. Then we use numeric features of the density region and its sparse representation to produce an ensemble of putative ligand structures. The single best model is chosen after refinement of the whole ensemble [6].

Cocktail screening. The comparison of the shapes of electron density blobs with the shape of the search ligand is used to distinguish compounds from a list (cocktail) of candidates. The ligand that fits best is selected for its further construction. An application of the cocktail screening for building a partially ordered ligand is exemplified in Figure 1.

Solvent building. After the protein part of the model is complete, a solvent structure can be constructed in the electron density map.

Availability and use of the software. ARP/wARP is freely available to all users and free of charge for academic usage, <http://www.arp-warp.org>. Software installation is user friendly and a User Guide can be referred to for additional information. There are no software dependencies other than the CCP4 package and particularly the program REFMAC6. ARP/wARP model building can be used after experimental phasing or molecular replacement. ARP/wARP can run through the CCP4i interface or be launched from the command line. A protein model-building task can be submitted to a 64-processor Linux cluster at the EMBL Hamburg; the results can be viewed through a web browser, <http://cluster.embl-hamburg.de/ARPwARP/remote-http.html>, Figure 2. Typically, the secondary structure tracing and ligand building run within a few minutes. Model building for a 500-residue protein takes about an hour and the time needed scales about linear with the size of the structure. ●

Contact: Victor Lamzin, victor@embl-hamburg.de
Anastassis Perrakis, a.perrakis@nki.nl

Authors

Gerrit G. Langer¹, Guillaume X. Evrard¹, Venkataraman Parthasarathy¹ und Victor S. Lamzin¹, Serge X. Cohen², Krista Joosten² und Anastassis Perrakis²

1. European Molecular Biology Laboratory, c/o DESY, Notkestrasse 85, Hamburg 22607, Germany
2. Department of Molecular Carcinogenesis, Netherlands Cancer Institute, Plesmanlaan 121, Amsterdam 1066CX, the Netherlands

Original publication

Langer, G., Cohen, S.X., Lamzin, V.S. and Perrakis, A., "Automated macromolecular model building for X-ray crystallography using ARP/wARP version 7", *Nature Protocols* 3, 1171-1179. PMID: 18600222 (2008).

References

1. Stevens, R.C., Yokoyama, S. and Wilson, I.A., "Global efforts in structural genomics", *Science* 294, 89-92 (2001).
2. Perrakis, A., Morris, R. & Lamzin, V.S., "Automated protein model building combined with iterative structure refinement", *Nat. Struct. Biol.* 6, 458-463 (1999).
3. Qian, B., Raman, S., Das, R., Bradley, P., McCoy, A.J., Read, R.J. and Baker, D., "High-resolution structure prediction and the crystallographic phase problem", *Nature* 450, 259-267 (2007).
4. Ness, S.R., de Graaff, R.A., Abrahams, J.P. & Pannu, N.S., "CRANK: new methods for automated macromolecular crystal structure solution", *Structure* 12, 1753-1761 (2004).
5. Colf, L.A., Juo, Z.S. & Garcia, K.C., "Structure of the measles virus hemagglutinin", *Nat. Struct. Biol.* 14, 1227-1228 (2007).
6. Murshudov, G.N., Vagin, A.A. and Dodson, E.J., "Refinement of macromolecular structures by the maximum-likelihood method", *Acta Crystallogr. D Biol. Crystallogr.* 53, 240-255 (1997).

How metallic iron eats its own native oxide.

An in-situ surface study using XAFS
(in-house research performed at DORIS III)

What happens to an ultrathin film of iron oxide when metallic iron is deposited on top of it? We have investigated this question by X-ray absorption spectroscopy performed in-situ during the deposition process. Typically, the native oxide is a non-stoichiometric mixture of different Fe oxide phases, containing even some Fe atoms in a metallic-like state. Deposition of metallic Fe on such an oxide leads to a reduction of the higher-valent oxides, leaving only iron atoms in a FeO-like phase. This approach allows one to prepare nanometer thin films of single-phase FeO. Further studies show that the Néel temperature of such FeO films is significantly enhanced compared to bulk FeO, and that its magnetic properties lead to remarkable coupling effects between two adjacent metallic Fe layers.

The oxidation of iron surfaces has been extensively studied in the past [1] due to the wide use of iron in technologically relevant systems. It was recently shown that nanometer thick native-oxide layers (produced by exposure of metallic Fe to oxygen) can be used as building blocks in new magnetic structures [2]. For example in multilayers consisting of alternating Fe and Fe-oxide layers, the magnetic moments of the Fe layers are arranged in a non-collinear fashion [3]. Understanding these remarkable magnetic properties requires a precise knowledge of the structure and composition of the oxide layer formed in the oxidation process. This is particularly important because there exist different crystallographic sites for the Fe atoms in the oxide phases, resulting in strongly structure dependent magnetic properties. One method to study the oxidation state and the local symmetry of atoms in solids is X-ray absorption spectroscopy. The near-edge structure (XANES) depends directly on the oxidation state, and the extended fine structure (EXAFS) includes information on the local symmetry. To understand the change in structure and chemistry at every step of the growth, the analysis was carried out under well controlled conditions in a dedicated UHV chamber [4].

The experiment was performed at the A1 beamline of the DORIS III storage ring. Extreme sensitivity, down to the mono-layer regime, was achieved using a total electron yield detector. First, a thin layer of iron (0.8 nm) is sputter deposited on a silicon substrate (capped with a Pd buffer-layer). The Fe K-edge absorption spectrum shows a clean metallic iron surface (Fig. 1a). Then, the layer is oxidized by controlled introduction of molecular oxygen into the vacuum chamber. The absorption edge shifts towards higher energy, indicating the progressive oxidation of

the layer. Above an exposure of 1300 Langmuir ($1\text{L} = 1 \times 10^{-6} \text{ Torr} \cdot \text{s}$) only little changes are still visible in the XANES spectra, indicating that the saturation regime is reached. The oxide growth virtually stops. Quantitative analysis using different oxide reference spectra shows that all types of oxides are growing at the same time during the oxidation process. In saturation, a complex mixture of Fe^{2+} and Fe^{3+} is observed (Fig. 1c). At this stage, it is quite surprising that some of the Fe atoms remain in a metallic state, even in the saturated oxide.

When only 0.2 nm of Fe (this corresponds to one atomic layer) is deposited on top of such an oxide layer, the metal immediately oxidizes and literally eats the excess of oxygen present in the layer. The result is the formation of a pure FeO layer composed of Fe^{2+} sites only, the lowest oxidation state of Fe in an oxide phase. The analysis of the extended fine structure (EXAFS) part of the absorption signal, which is sensitive to the local symmetry of the absorbing atom, supports that finding but indicates that the FeO layer formed has a poor crystallinity compared to the bulk FeO phase.

These experiments show a rather elegant and easy way to produce nanometer thick FeO layers. This is quite remarkable because pure FeO is rather unstable under ambient conditions, so that other types of iron oxide dominate. The experimental method developed here can be applied to the oxidation process of metals and, in general, to the study of interface formation between reactive compounds. This opens interesting perspectives for in-situ studies using X-ray absorption spectroscopy at modern synchrotron radiation sources. ●

Contact: Ralf Röhlberger, ralf.roehlsberger@desy.de

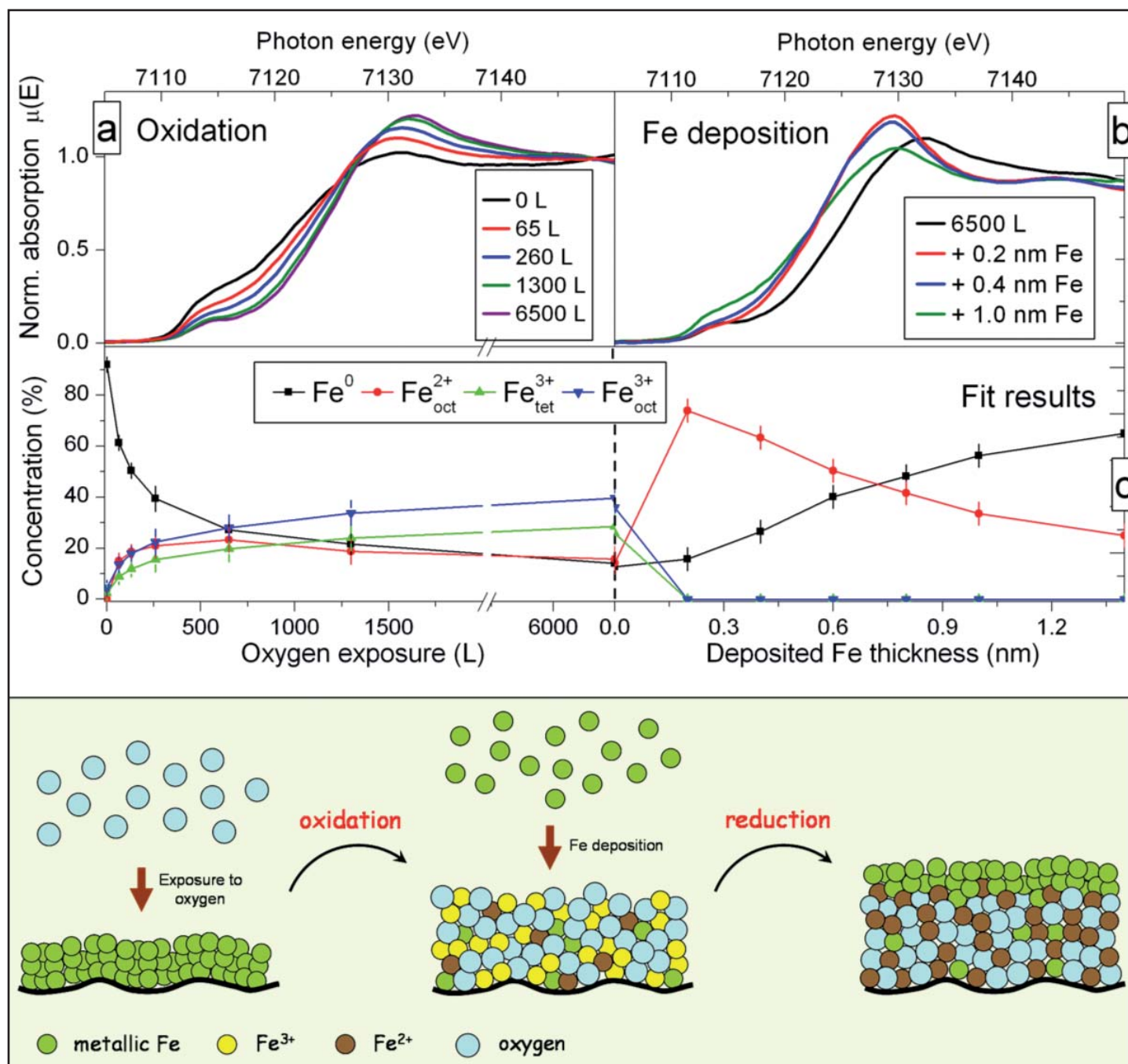


Figure 1
 (a) Evolution of the near edge spectra (XANES) of a thin (0.8nm) Fe layer exposed to an increasing amount of oxygen. The progressive shift towards higher energy indicates an increase of the oxidation state of the Fe atoms. (b) Upon deposition of Fe the spectra changes dramatically and adopt a shape never observed during the oxidation procedure. (c) Quantitative analysis shows that, in saturation, the oxide is a mixture of different Fe sites. After deposition of Fe, the layer reduces to a pure FeO-like phase. The lower panel summarizes the oxidation and reduction processes.

Authors

S. Couet¹, K. Schlage¹, K. Saks², R. Röhlberger¹

- Hamburger Synchrotronstrahlungslabor at Deutsches Elektronensynchrotron DESY, 22603 Hamburg, Germany
- Institute of Materials Research, Slovak Academy of Sciences, 04353 Kosice, Slovak Republic

Original publication

“How Metallic Fe Controls the Composition of its Native Oxide”, *Phys. Rev. Lett.* 101 056101 (2008)

References

- S.J. Roosendaal, A.M. Vredenberg and F.H.P.M. Habraken, *Phys. Rev. Lett.* 84, 3366 (2000)
- G.S.D. Beach, F.T. Parker, D.J. Smith, P.A. Crozier and A.E. Berkowitz, *Phys. Rev. Lett.* 91, 267201 (2003)
- Th. Diederich, S. Couet and R. Röhlberger, *Phys. Rev. B* 76, 054401 (2007)
- S. Couet, Th. Diederich, K. Schlage and R. Röhlberger, *Rev. Sci. Instrum.* 79, 093908 (2008)

Hard X-Ray holographic diffraction imaging.

Lensless imaging for determining electron density profiles on the nanoscale (in-house research performed at the ESRF)

Nanoscience mandates the ability to characterise the structure of objects on the nanoscale. For several reasons, hard X-rays are very attractive for that purpose: a wavelength in the order of $\approx 1 \text{ \AA}$ allows for excellent spatial resolution; the high penetration into matter permits to study thick samples or even buried structures in an easy-to-realise experimental setup; and with the upcoming hard X-ray free-electron lasers the achievable time resolution will be pushed down to the femtosecond (fs) regime. Here, we demonstrate how coherent hard X-rays can be used for a determination of the absolute electron density of a lithographically tailored gold nanostructure (the letter P) from a single diffraction experiment, yielding both the shape and the height of the sample. We combine Fourier transform holography (FTH) [1], which – by a single Fourier transform – gives an unambiguous image of the sample structure, with iterative phase retrieval procedures known in the field of coherent diffraction imaging (CDI) [2]. The latter enable us to push the spatial resolution toward the diffraction limit, which is determined by the maximum photon momentum transfer.

In FTH phase retrieval becomes particularly simple, since in a typical setup the object and a spatially nearby reference are coherently illuminated and a single Fourier transform of the recorded hologram yields the convolution of the object and reference amplitudes, where the spatial resolution achievable is comparable to the reference source size [1,3]. Provided the sampling of the diffraction pattern is sufficiently high [4], the FTH result can be used as starting point for further iterative phase retrieval in order to increase the resolution. In the present case 5 gold dots with about 175 nm diameter were placed on a circle of 2.5 μm radius around the gold nanostructure, each acting as reference source in the scattering process.

The corresponding hologram, which is shown in Fig. 1, was recorded at the ESRF beamline ID10C using coherent 8 keV photons. The hologram is the sum of 200 single pictures each exposed 3s. That is the hologram has been recorded with 10^{10} photons. A single Fourier transform of the measured intensities gives the spatial autocorrelation of the overall object, including the cross-correlation between the object and the dots, which directly yields the object shape and its complex conjugate (a 180°-rotated copy) for each dot, as can be seen in Fig. 1. The letter P is clearly recognizable, its shape is, however, slightly distorted and the contrast is reduced by the wavy background. This image degradation stems from the pixels blocked by the beamstop. In addition the big reference source size causes a blurring of the P structure in the FTH reconstruction. For further progress the individual images are averaged for improving statistics and the result – already comprising a qualitative image of the object – is fed into iterative CDI algorithms [2]. Carrying out such phase retrieval runs yielded an image of the sample's

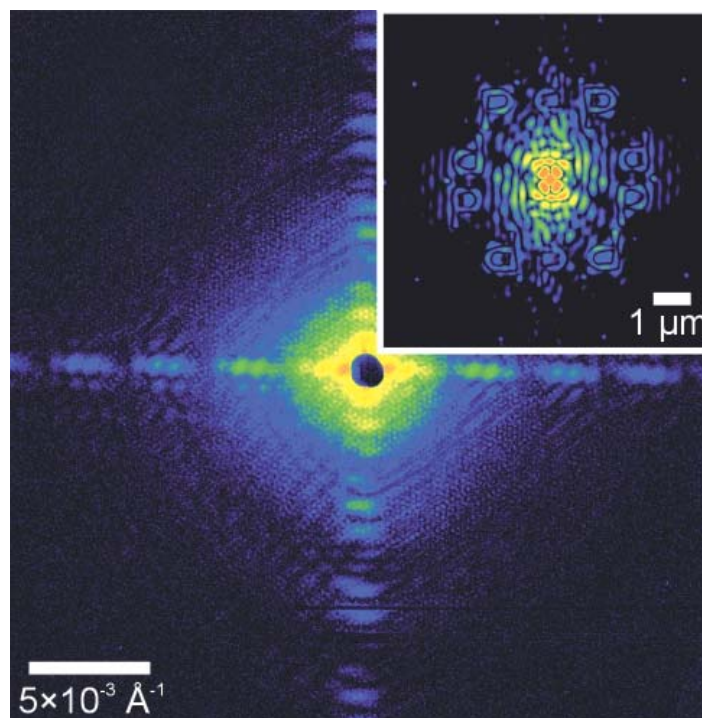


Figure 1

Recorded hologram of a gold nanostructure – the capital letter P – surrounded by 5 reference scatterers. The inset shows the central part of the modulus of the Fourier transform of the recorded diffraction intensities, imaging the object and its rotated copy 5 times each. Logarithmic pseudocolour scale each.

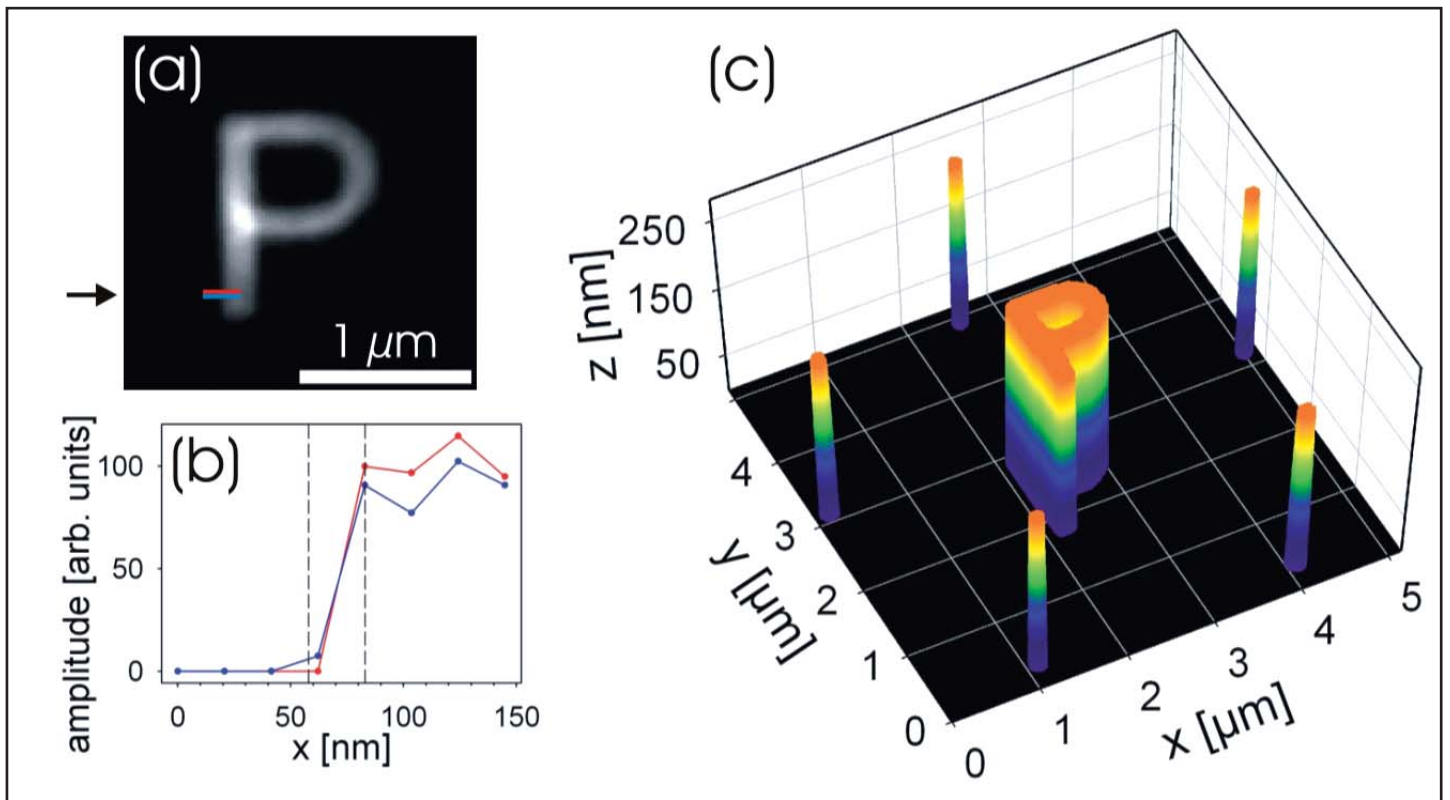


Figure 2
Results from the FTH-based phase retrieval runs. (a) Average amplitude of 100 phase retrieval runs. (b) Slices through an individual run demonstrating a resolution of 25 nm. (c) The overall object geometry.

electron density projected along the beam direction with ≈ 25 nm resolution (see Fig. 2b). Knowing that the sample under investigation was made of gold and exploiting the fact that the scattering process can be described as Thomson scattering, it is straight forward to derive a mean sample height, which would be the correct height if the sample were flat. Actually, in the present case we can, in fact, tell how well the assumption of a flat sample topography is, since this information is encoded in the phases of the hologram's Fourier transform. This allowed us to obtain the phase profile of the sample and by taking Fresnel diffraction effects [5] into account we could deduce the corresponding height profile. For our sample we find a homogeneous height of approximately 235 nm. The final reconstruction yielded the overall object geometry and height as shown in Fig. 2.

In conclusion, we have shown that hard X-ray holographic diffraction imaging is an excellent technique for determining

electron density profiles on the nanoscale. Using the FTH result as input facilitates the following iterative phase retrieval dramatically and the spatial resolution can be pushed toward the diffraction limit. By virtue of this concept we determined the absolute electron density and derived both shape and height of a lithographic gold nanostructure. The presented approach with coherent hard X-rays is ideally suited for applications in materials science, where samples can be thick, may consist of buried structures, or have to be measured under extreme conditions such as high pressure. Finally, we envision experiments of similar type to be carried out at future hard X-ray free-electron laser sources, where diffraction patterns can be collected within a single shot at the time scale of ≈ 10 fs, opening fascinating possibilities for imaging fast dynamic processes. ●

Contact: Christian Gutt, christian.gutt@desy.de

Authors

L.-M. Stadler¹, C. Gutt¹, T. Autenrieth¹, O. Leupold¹, S. Rehbein², Y. Chushkin³, G. Grübel¹

- HASYLAB at DESY, 22607 Hamburg, Germany
- BESSY, 12489 Berlin, Germany
- ESRF, 38043 Grenoble, France

References

- S. Eisebitt, J. Lüning, W.F. Schlotter, M. Lörger, O. Hellwig, W. Eberhardt, and J. Stöhr, "Lensless imaging of magnetic nanostructures by X-ray spectro-holography", *Nature (London)* 432, 885 (2004).
- H.N. Chapman, A. Barty, S. Marchesini, A. Noy, S.P. Hau-Riege, C. Cui, M.R. Howells, R. Rosen, H. He, J.C.H. Spence et al., "High-resolution ab initio three-dimensional x-ray diffraction microscopy", *J. Opt. Soc. Am. A* 23, 1179 (2006).

- W.F. Schlotter, R. Rick, K. Chen, A. Scherz, J. Stöhr, J. Lüning, S. Eisebitt, C. Günther, W. Eberhardt and O. Hellwig et al., "Multiple reference Fourier transform holography with soft X-rays", *Appl.Phys.Lett.* 89, 163112 (2006)
- J. Miao, P. Charalambous, J. Kirz, and D. Sayre, "Extending the methodology of X-ray crystallography to allow imaging of micrometre-sized non-crystalline specimens", *Nature (London)* 400, 342 (1999)
- S.K. Sinha, M. Tolan, A. Gibaud, "Effects of partial coherence on the scattering of x rays by matter", *Phys. Rev. B* 57, 2740 (1998)

Original publication

"Hard X-Ray Holographic Diffraction Imaging", *Phys. Rev. Lett.* 100, 245503 (2008)



Research Platforms and Outstations.

- **Centre for Free-Electron Laser Science CFEL** 50
- **EMBL – Hamburg Unit** 52
- **Max-Planck Unit for Structural Molecular Biology** 56
- **GKSS Research Centre Geesthacht – Outstation at DESY** 58
- **GFZ Helmholtz Centre Potsdam – Outstation at DESY** 60
- **University of Hamburg on the DESY site** 61

Centre for Free-Electron Laser Science CFEL.

Exploring the limits of X-ray science and applications

Preparations are underway for the construction of a new laboratory and office building at DESY that will house the Centre for Free-Electron Laser Science (CFEL). The CFEL is a new common effort between the University of Hamburg, DESY and the Max Planck Society to advance science with next generation light sources. Groundbreaking for the building will take place early in 2009, at a site just north of the new PETRA III experimental hall. When completed, the building will add to the vibrant new photon science research campus that is currently taking shape on the DESY campus (Figure 1). Funded by the State of Hamburg and the Federal Government, and designed by the architectural firm of Hammeskrause, this modern building has been defined according to the requirements and wishes of the groups within the CFEL. Beyond purely practical needs, however, it will breathe the spirit of a new enterprise, collaborative between the different institutions involved, across the classical scientific disciplines, synergetic towards new science, a place of creative and, simultaneously, of hard and concentrated work. Thus, the office layouts encourage communication and discussion, and the distribution of laboratories emphasizes current and future collaborations, for example in the development of detectors, biology and biochemistry, and use of laser facilities.

The CFEL will consist of five core groups, two of which have already begun: the Max Planck Research Group for Structural Dynamics, headed by Andrea Cavalleri, and the DESY Research Group for Coherent X-Ray Imaging, led by Henry Chapman. A search is currently underway for directors of another Max Planck experimental group, a DESY experimental group, and a DESY theory department. In addition the CFEL accommodates an Advanced Study Group (ASG) from the Max Planck Society, and another ASG from the University of Hamburg. The spokespersons for the Max Planck and University Advanced Study Groups are Joachim Ullrich and Wilfried Wurth, respectively. In addition, DESY supports a detector group led by Heinz Graafsma.

The CFEL groups have been busy establishing laboratories at DESY and growing their experimental programs. The first Department of the Max Planck Research Group for Structural Dynamics works in the area of Condensed Matter Physics. The goal is to use ultrafast THz, visible and X-ray pulses (and possibly also electrons) from tabletop sources, Synchrotron sources and Free Electron Lasers to measure the microscop-

ic dynamics of atomic, electronic, magnetic and orbital structures in matter. Beyond conventional tabletop techniques the group is currently using THz radiation from FLASH and the ELBE FEL in Rossendorf to control the quantum phase of complex solids with coherent light. They have also used 640 eV radiation from the 5th harmonic of FLASH to measure the ordered orbital pattern in manganese oxides, opening the way to new studies of orbital and spin dynamics in the time domain. The Coherent X-ray Imaging Group has advanced the field of ultrafast imaging with FEL sources. At FLASH, in collaboration with the Structural Dynamics Group and scientists from Lawrence Livermore National Laboratory, the University of Duisburg, and SLAC, the group carried out ultrafast holography and diffraction experiments on materials under extreme conditions. The combination of coherent X-ray diffractive imaging with the ultrafast X-ray pulses from FLASH has enabled time-resolved imaging to be performed at both high spatial and temporal resolution, by synchronizing the FLASH diffraction patterns with an optical laser pump. They are now applying this technology towards the goal of single-particle imaging, and in particular to the investigation of the control and alignment of particles that are shot across the FEL beam. This capability

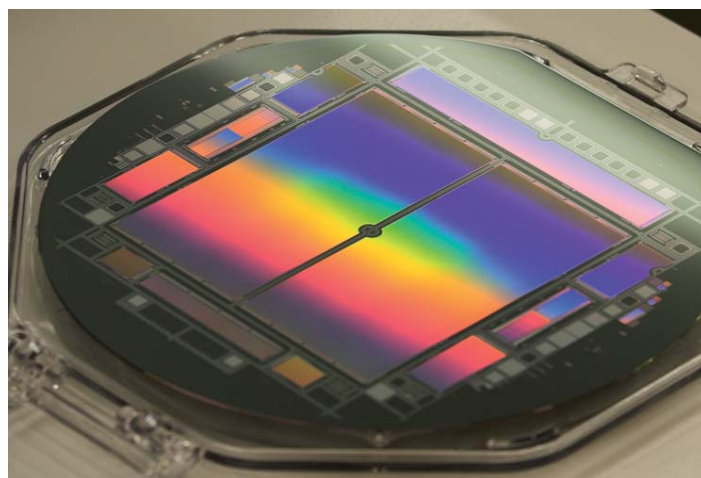


Figure 2

The Max Planck ASG pnCCD photon detector. Four individual chips will be combined to two large detector set-ups for measuring coherent X-ray diffraction patterns and fluorescence spectra at FEL sources. The installation of the detector and its commissioning is pursued in collaboration with the DESY detector group.

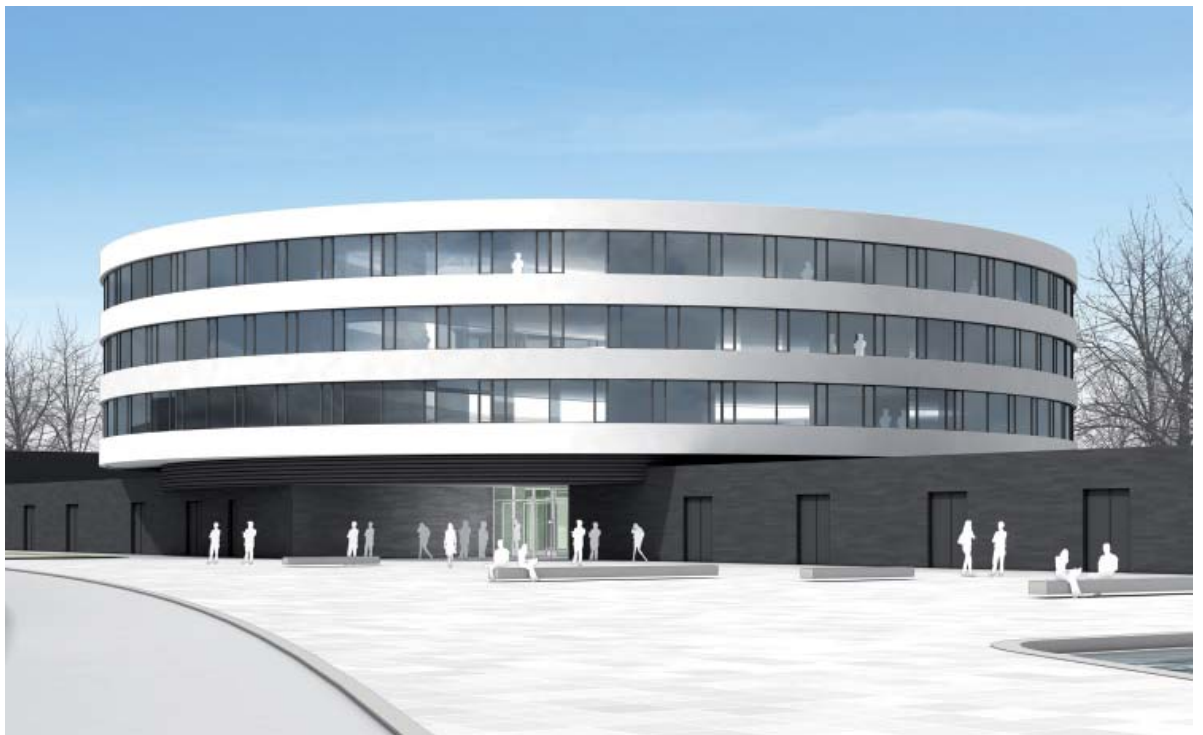


Figure 1

The architects' conception of the CFEL building, close to the PETRA III experimental hall (Courtesy: hammeskrause architekten).

will allow them to build up high-resolution three-dimensional diffraction patterns from many weakly scattering but identical objects. They are also developing unique dynamic holographic methods for time-resolved imaging to recover the change in structure induced by the laser.

In collaboration with the Max Planck ASG, Uppsala University, and others, the Coherent X-ray Imaging Group is investigating the high-resolution imaging of biological objects. The goal is to use ultrafast X-ray pulses to outrun radiation damage processes and achieve higher resolution than could be obtained by steady-state imaging. After the upgrade of FLASH in 2009 it will be possible to record images in the "water window" where the carbon of organic matter provides strong contrast against oxygen-rich water. Along with the shorter wavelength, this will vastly improve the spatial resolution of single-shot images of cells. By collecting coherent diffraction patterns to extremely high angles, with higher intensity by focusing the FLASH beam to a tighter focus, it will be possible to obtain images of biological cells beyond the current limits of X-ray microscopy.

The Max Planck ASG supports experiments from groups from different Max Planck Institutes to conduct experiments at FELs. Presently, seven MPIs are involved pursuing a broad experimental and theoretical research program. Topics include exploring the basic mechanisms of light-matter interactions in this new regime of ultra-intense FEL radiation, photolysis of molecular or cluster ions that are of importance for the physics and chemistry of upper planetary atmospheres and of interstellar clouds, or the tracing in time of molecular reactions in the gas-phase, as well as in solution, exploiting the ultra-fast timing feature of FELs. One of the major efforts within the ASG is the development of the world's largest (58 cm²) and fastest X-ray pixel detectors (pnCCD), as depicted in Figure 2, and the design of

the CFEL ASG Multi-Purpose (CAMP) chamber. With a frame rate of 200 Hz, single photon counting abilities at a resolution of 50 eV at 0.8 keV and 80 eV at 2 keV, a high quantum efficiency, and a 10⁴ dynamic range, this detector provides unprecedented features that are of decisive importance for coherent imaging, cluster, or fluorescence detection experiments.

The ASG of the University Hamburg currently comprises groups that explore fundamental laser-matter interaction with the focus on manipulation of nanoparticles and (bio-) molecules in light fields, work on ultrafast science to study electron, nuclear and spin dynamics in molecules, at surfaces, and in functional materials, and develop innovative concepts for accelerator-based X-ray lasers and new fast imaging X-ray detectors.

A large proportion of the CFEL activities involve preparing for experiments at Linac Coherent Light Source (LCLS) at SLAC. For example, the CAMP chamber has become the common platform of seven proposals submitted by large international collaborations to the LCLS management in October 2008.

Some of these experiments will be carried out at a new soft-X-ray beamline currently under design at the LCLS to deliver FEL pulses to a photon energy of 2 keV. The beamline is being built and supported by a consortium consisting of the LCLS, LBNL, the University of Hamburg, CFEL, and BESSY. When it comes on line at the end of 2009 the CFEL will be among those to use the beamline to investigate the behavior of atomic, molecular, and condensed matter systems under the intense X-ray pulses, push coherent imaging to the highest spatial and temporal resolutions, directly probe the dynamics of highly correlated electronic systems, and study the new realm of nonlinear X-ray optics. ●

Contact: Henry N. Chapman, henry.chapman@desy.de

EMBL Hamburg Unit.

Structural Biology with Synchrotron Radiation

The EMBL-Hamburg Unit belongs to the European Molecular Biology Laboratory with its headquarters in Heidelberg, and further units in Grenoble (France), Monterotondo/Rome (Italy) and Hinxton/Cambridge (UK). The Hamburg Unit presently hosts six research groups (C. Hermes, V. Lamzin, T. Schneider, D. Svergun, P. Tucker, M. Wilmanns) and four research teams (S. Fiedler, W. Meyer-Klaucke, J. Müller-Dieckmann, M. Weiss). The overall number of staff and fellows is close to 100, of which more than 50% are supported by external funds. While most of the present staff is hosted in EMBL's Building 25A, the crystallization facility is presently situated in Building 3, close to the DESY main entrance. The unit's major activities are in the provision of synchrotron experiment stations, a high-throughput facility for crystallization and several software packages that are available either via remote services or for downloading; advanced training, and research. The two major directions of the present research portfolio are in methods and technology development, associated with the locally available research service facilities, and in a number of challenging biology projects. Several of the latter address areas that are associated with infectious diseases, either of viral origin (Tucker group) or drug targets from *M. tuberculosis* (Wilmanns, Weiss, Müller-Dieckmann).

The extended DORIS III shutdown during most of the year 2008 offered EMBL a special opportunity to focus on its most pivotal project 'EMBL@PETRA3', in particular the preparation of the construction of the three future EMBL beamlines with applications in protein crystallography and small angle X-ray scattering of biological material. 2008 was the first complete working year for the new EMBL team for Petra III under the leadership of Thomas Schneider (project co-ordination), Stefan Fiedler (instrumentation) and three beamline scientists Gleb Bourenkov, Michele Cianci and Manfred Roessele.

For each of the three beamlines, updated designs were presented to the EMBL Scientific Advisory Board of the EMBL@PETRA III-project and the DESY Photon Science Committee. Both committees approved the design and made suggestions for improvements, which were taken into account in the final optical design of the beamlines (Figure 1). For the main components of the beamlines the technical specifications have been worked out and negotiations with suppliers are underway. To date, several orders have been placed, including three double

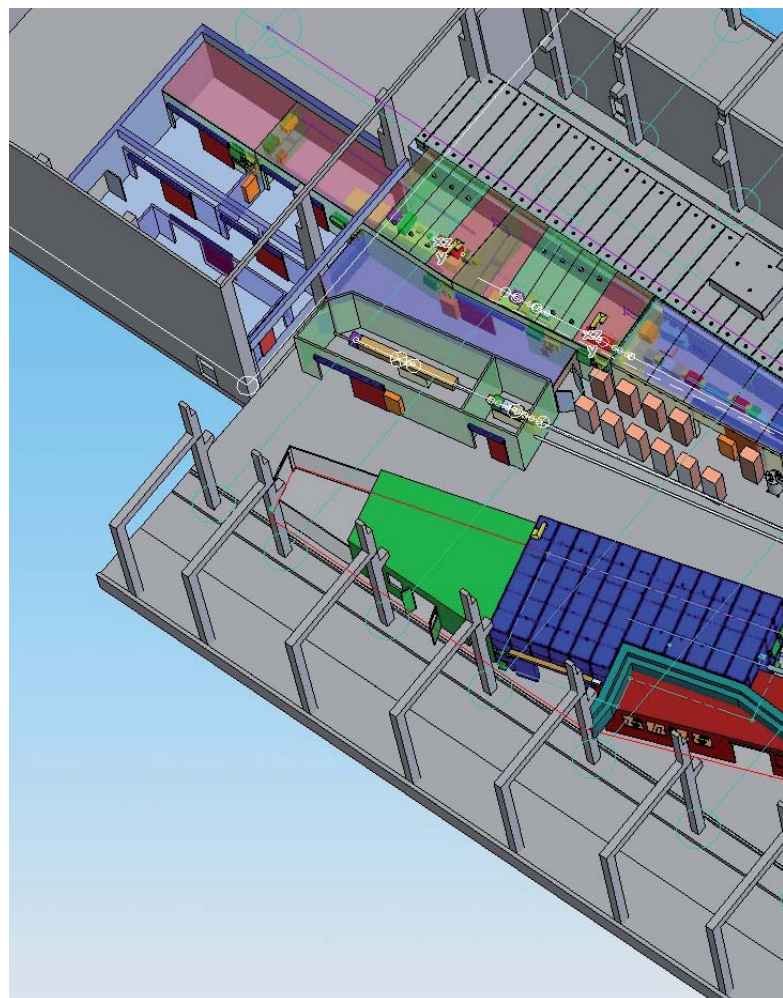


Figure 1

Layout of the EMBL beamlines (BioSAXS, MX1, MX2) in the last two sectors (8 and 9) of the PETRA III experimental hall.

crystal monochromators (designed in collaboration between HASYLAB and FMB Oxford) and a first MD2 micro-diffractometer for crystallographic experiments (designed by EMBL Grenoble and ESRF and manufactured by ACCEL). Several modules and concepts to be employed on the future beamlines are being prototyped on the BW7 wiggler beamlines on DORIS. Notably, on BW7A, the control of the majority of the beamline elements including a multilayer monochromator (Figure 2), is now implemented using industry-standard control

Figure 2

Interior of the focusing double multilayer monochromator at beamline BW7A.



electronics (Beckhoff) integrated into the TINE control system. The excellent performance of this combination in the prototype makes us confident in using this system on the future EMBL beamlines on PETRA-III.

At DORIS III, EMBL has reduced its open beamlines from seven to four, to release needed working power for the work on the EMBL@PETRA III project. The three protein crystallography beamlines at fan K (X11, X12, X13) and the SAXS beamline X33

at fan D remained in operation, whereas the EXAFS beamline was closed by the beginning of 2008. The two wiggler beamlines BW7A and BW7B have become test beamlines for the EMBL@PETRA3 project, with the option to allow temporary access to external users.

The level of collaboration with our colleagues from EMBL-Grenoble in synchrotron instrumentation kept increasing. In 2008, EMBL-Hamburg hosted the 5th bilateral meeting of the respective activities in the two units, with the general objective to update and synchronize the activities and developments. Topics of the meeting covered the automation of protein crystallization and synchrotron beamlines, including sample handling, detection and centering. One session was dedicated to software developments in the areas of sample tracking and data collection. Collaborative projects have been set up on the evaluation of X-ray detectors, the framework for beamline control systems and the development of LIMS. Finally, in a trilateral project by scientists from the ESRF, EMBL-Grenoble and EMBL-Hamburg, a prototype sample changer from EMBL's present SAXS beamline is presently remodeled into a more advanced system, to meet the state-of-the-art standards of 3rd generation SAXS beamlines at the ESRF and PETRA III.

Due to the limited space in the PETRA III hall, EMBL in collaboration with HASYLAB/DESY has designed an Annex Building (48E), which will host state-of-the-art sample preparation facilities, the EMBL high-throughput crystallization unit, facilities for on-site automated data interpretation and additional office space. Construction of this unit was approved in October 2008. We expect building construction to be finished during autumn 2009.

Last not least, EMBL is participating and pushing the planning for a new Center in Structural and Systems Biology (CSSB) on DESY campus, under coordination of the Helmholtz Centre for Infection Biology, Braunschweig. Present plans focus on themes from Infection Biology, reflecting the high level of research by several institutes from Northern Germany in the field. The approval process is well underway and we hope that in 2009 this center will become reality. The CSSB could become a landmark, to complement world-leading synchrotron and laser infrastructures at DESY with a complementary research center in biomedical sciences.



Figure 3
Group photograph of the final BIOXHIT meeting, April 2008.



Figure 4
Teachers explore the structures of life – ELLS in Hamburg.

EMBL with its three structural biology-oriented units in Grenoble, Heidelberg and Hamburg actively participates in the ESFRI project INSTRUCT, which aims for a concerted plan for coordinated infrastructures in structural biology across Europe. Scientists from EMBL have been active in many INSTRUCT committees and meetings. One of the open INSTRUCT meetings, a tandem workshop from two working groups (Intrinsically Unfolded Proteins and Complementary Methods) in September 2008 in Hamburg, was coordinated by EMBL-Hamburg and the Weizmann Institute, Israel.

One of the largest projects with external funds, coordinated by EMBL-Hamburg, BIOXHIT, came to an end in 2008. The project's coordinators Victor Lamzin and Manfred Weiss organized the final meeting of the project in April 2008 at the premises of EMBL/DESY (Figure 3). Highlights of the project were coupling crystallization with X-ray data collection, a high precision kappa-goniometer with a fully motorized goniometer head, automated centering and tomography of crystalline samples, sophisticated and robust algorithms for modeling statistical results of data collection, remote data collection, multi-option structure determination pipeline, molecular replacement as a structural genomics tool as well as Europe-wide train-



Figure 5

EMBL booth at the 21st International Union of Crystallography (IUCr) Congress and General Assembly in Osaka, Japan.

ing, implementation and dissemination of the project's results. Other large-scale projects (3D REPERTOIRE, SPINE-COMPLEXES, SAXIER, VIZIER) with the EMBL participation will continue in 2009. Several new applications, mostly to the European Commission, are currently pending.

In 2008, EMBL-Hamburg has recruited a dedicated training officer, Rosemary Wilson (email: r.wilson@embl-hamburg.de), to improve the promotion and coordination of EMBL's programme in advanced training. Two major training courses were organized in 2008, "EMBO Practical course on Protein Expression, Purification and Crystallisation (PEPC6)" and "EMBO Practical Course on Solution Scattering from Biological Macromolecules". The first EMBO world lecture course, "Recent developments in macromolecular crystallography", was organized by Manfred Weiss in Pune, India, in November 2008. EMBL-Hamburg also hosted its first European LearningLAB for the Life Sciences (ELLS) teachers' workshop on 24-26 April. Seventeen teachers from Germany, Austria, Belgium and Sweden came for the course, entitled 'Strukturbiologie – ein Blick auf die Chemie des Lebens' ('Structural Biology-Deciphering the Chemistry of Life') (Figure 4). Finally, EMBL was present with institutional stands at two major in-

ternational meetings, the 21st International Union of Crystallography (IUCr) Congress and General Assembly in Osaka, Japan, and the 2008 Meeting of the International Structural Genomics Organization in Oxford, UK (Figure 5).

Scientific highlights from EMBL-Hamburg, in part in collaboration with groups from its user community, are summarized elsewhere. ●

Contact: Matthias Wilmanns,
matthias.wilmanns@embl-hamburg.de

Max-Planck Unit for Structural Molecular Biology

Biological structure and function
in order and disorder

Knowledge of the structure of biomolecules is an essential prerequisite for understanding biological processes on a molecular and cellular level, with applications in biotechnology, medicine, and pharmacology. Because of the high intensity and variable wavelength of the synchrotron light generated at DESY it is possible to carry out X-ray structure investigations of biomolecules rapidly and accurately. This allows one to meet the rising demand of structure determinations and to offer the most modern methods and equipment to an international community of scientific users.

The “Protein Dynamics” group (H. D. Bartunik) of the Max-Planck Unit for Structural Molecular Biology is interested in the reaction mechanisms of enzymes and in the rapid changes in conformation which determine their biological functions and form the basis of many biotechnological applications. The activities include the development and operation of a variable wavelength synchrotron beamline, optimization of data acquisition and processing strategies, handling of samples (protein expression, crystallization, cryoprotection), and interpretation and visualization of biological structures.

The “Cytoskeleton” group (E. Mandelkow) focuses on the structure, self-assembly, and dynamics of protein fibers in cells which are responsible for cell movement, cell division, differentiation and intracellular transport, in particular on microtubules, their motor proteins, and their associated proteins. Some of these are important for neurodegenerative diseases, such as Alzheimer’s disease, where transport in nerve cells is blocked and proteins form insoluble aggregates.

Structural analysis of a nicking endonuclease and its catalytic associate

Prokaryotic organisms use restriction-modification (RM) systems to protect their genomes against foreign invading DNA, in particular to resist infections by destroying viral DNA. Each RM system contains a set of methyltransferases and restriction endonucleases that recognize a defined nucleotide sequence.

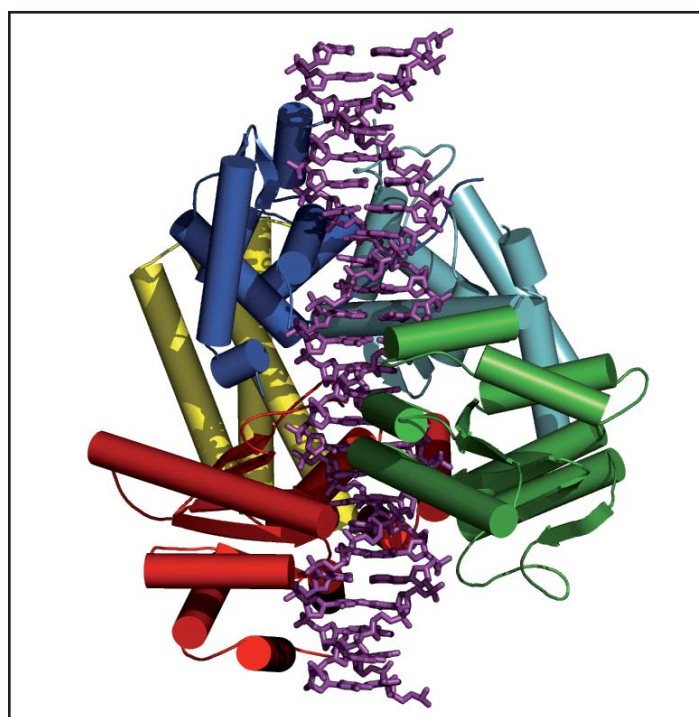


Figure 1

Structural model of Nt.BspD6I in complex with ss.BspD6I (green) and cognate DNA (magenta). Nt.BspD6I contains a recognition domain (blue) with two subdomains, a cleavage domain (red) and a rigid linker domain (yellow) that adjusts the distance between the recognition and cleavage sites.

The number and organization of the functional units vary with the Type (I-IV) of the RM system. The modification enzyme methylates DNA of the host at the recognition site, thus preventing attack by the corresponding restriction endonuclease (RE). Type II REs recognize unmethylated DNA sequences and cleave at constant positions at or outside the recognition sequence. Their high specificity makes them important tools in recombinant DNA technologies.

Most Type II REs act as homo- or heterodimers, whereby both

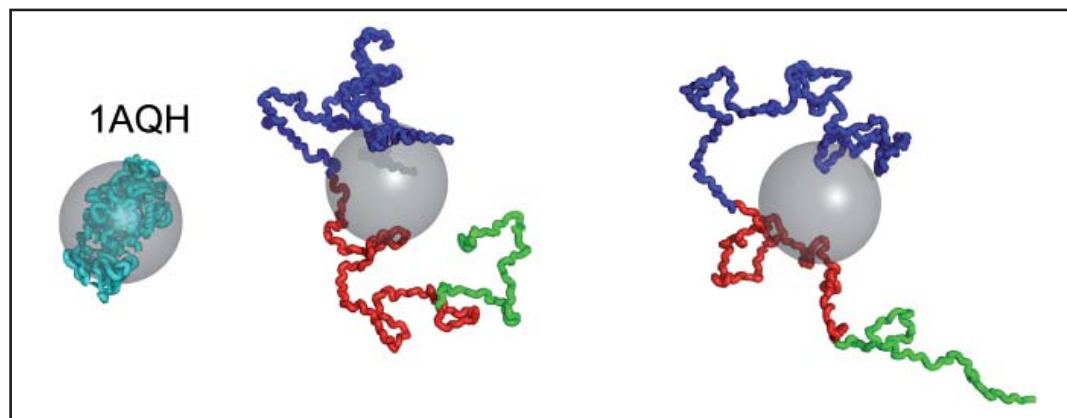


Figure 2

Two representative structures of human tau. N-terminus (residues 1-243) in blue, repeat domain (residues 244-368) in red, and C-terminus (369-441) in green. For comparison, the structure of a folded protein with a similar number of residues (beta-amylose, 1AQH) is shown in cyan. Grey spheres with a radius of gyration (2.4 nm) corresponding to that of the folded protein are positioned at the mass centre of each model.

subunits recognize and cleave duplex DNA. The heterodimeric endonuclease R.BspD6I from *Bacillus* species D6, however, functions in a substantially different way. The large subunit (Nt.BspD6I) alone acts as a Type IIS monomeric nicking endonuclease (nickase) that recognizes an asymmetric sequence and cuts one DNA strand outside the recognition site. The isolated small subunit (ss.BspD6I), which lacks a recognition domain, is inactive but exhibits cleavage activity when complexed to the large subunit. In a collaboration between the Max-Planck Unit for Structural Molecular Biology and institutes of the Russian Academy of Sciences, the three-dimensional structures of both subunits were determined using synchrotron radiation [1]. The crystal structure of the large subunits represents the first structure of a monomeric nickase. A model of the ternary complex suggests interactions between both subunits that may control the cleavage activity of the small subunit. Further studies combining mutational and structural analysis are in progress. The results may provide a basis for possible engineering of novel nicking enzymes with new specificities.

Contact: H.D. Bartunik, bartunik@mpghdb.desy.de

Tau protein: Structure in solution and aggregation in Alzheimer Disease

Tau is a microtubule-associated protein that is essential for the stability and the dynamics of microtubules. It regulates the microtubule-based intracellular transport, especially the outward-directed movement of proteins and organelles that is effected by the family of kinesin motor proteins. Altered binding properties of tau cause transport problems that can result in cellular malfunction which is accompanied by the formation of insoluble tau aggregates. Tau is a natively unfolded protein and it remains mostly unstructured even when bound to microtubules. The conformation of tau in solution was now characterized by small angle X-ray scattering (SAXS) [2] using ensemble optimization (EOM), a recently developed method which takes the flexibility of tau into account by allowing for the coexistence of multiple conformations in solution (in collaboration with EMBL) [3]. Short tau constructs containing the microtubule-binding repeat domain are more extended than expected for a random coil. Longer constructs are comparable in size with random coils, indicating that contacts between N- and C-terminal regions compensating for the extension of the repeat domain [4]. The absence of major differences between aggregation-promoting mutants and wild-type constructs suggests that the formation of pathological tau aggregates requires the pre-existence of aggregation cores. ●

Contact: E. Mandelkow, mandelkow@mpasmb.desy.de

References

1. Kachalova G. S., Rogulin E. A., Yunusova A. K., Artyukh R. I., Perevyazova T. A., Matvienko N. I., Zheleznaya L. A. and Bartunik H. D., "Structural analysis of the heterodimeric Type IIS restriction endonuclease R.BspD6I acting as a complex between a monomeric site-specific nickase and a catalytic subunit", *J. Mol. Biol.* 384, 489-502 (2008).
2. Mylonas E., Hascher A., Bernado P., Blackledge M., Mandelkow E. and Svergun D. I., "Domain conformation of tau protein studied by solution small-angle X-ray scattering", *Biochemistry* 47, 10345-53 (2008).
3. Bernado P., Mylonas E., Petoukhov M. V., Blackledge M. and Svergun D. I., "Structural characterization of flexible proteins using small-angle X-ray scattering", *J. Am. Chem. Soc.* 129, 5656-64 (2007).
4. Jeganathan, S., von Bergen, M., Mandelkow, E.-M., Mandelkow, E., "The natively unfolded character of Tau and its aggregation to Alzheimer-like paired helical filaments", *Biochemistry* 47, 10526-10539 (2008).

GKSS Research Centre Geesthacht Outstation at DESY.

Material science research
with high-energy X-rays

The outstation of the GKSS Research Centre Geesthacht at DESY provides instrumentation for investigating engineering materials and biomaterials with imaging and diffraction techniques. Until 2010, it will develop into the German Engineering Materials Science Centre for Research with Photons (GEMS-P). Together with the complementary GEMS-N for Research with Neutrons, GEMS will be the major point of access within the Helmholtz Association for users in scientific and applied engineering materials research with photons and neutrons.

The current GKSS Outstation (and thus the future GEMS-P) comprises a suite of instruments at the DESY storage rings with an emphasis on the use of the new and most brilliant synchrotron radiation source PETRA III. Two high-energy beamlines (HARWI II at DORIS III, HEMS at PETRA III) and a beamline optimized for micro- and nano-tomography (IBL at PETRA III) address the requirements of research in materials science over a wide range of X-ray energies and of spatial resolution. These facilities have been funded by major investment grants from the HGF. The BioSAXS beamline at PETRA III (in collaboration with EMBL) is optimized for time-resolved soft matter structure research.

HARWI II was constructed in 2004 – 2006 at the site of DESY's first beamline for high-energy radiation HARWI (Hard Radiation Wiggler), making use of a new wiggler providing a broad beam up to $7 \times 1 \text{ cm}^2$ for the investigation of large strongly absorbing samples. The beamline is optimized for research with monochromatic and white beam, large view and moderate resolution, using high-energy X-rays (20-250 keV). HARWI II is in full user operation, highly overbooked and very well accepted in the materials science community with experiments in the fields of texture, residual stress and structure analysis, absorption micro-tomography, and high-energy small-angle scattering. In 2008, a new materials science diffractometer for heavy loads up to 600 kg has been commissioned (see Fig. 1). It can be equipped with a Eulerian cradle for flexible orientation of small samples and with various sample environments (from temperature control to stress rigs). The set-up has been completed by a new large-area two-dimensional detector. The spacious experimental hutch of HARWI II allows for the installation of novel *in situ* experiments. The most prominent example is the *in situ* friction stir welding apparatus FlexiStir with very successful diffraction and

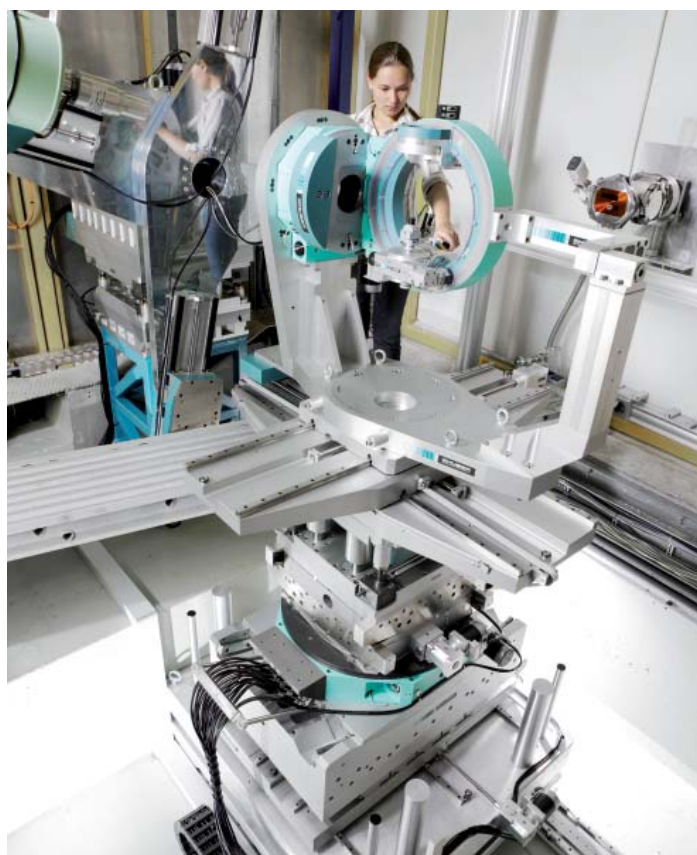


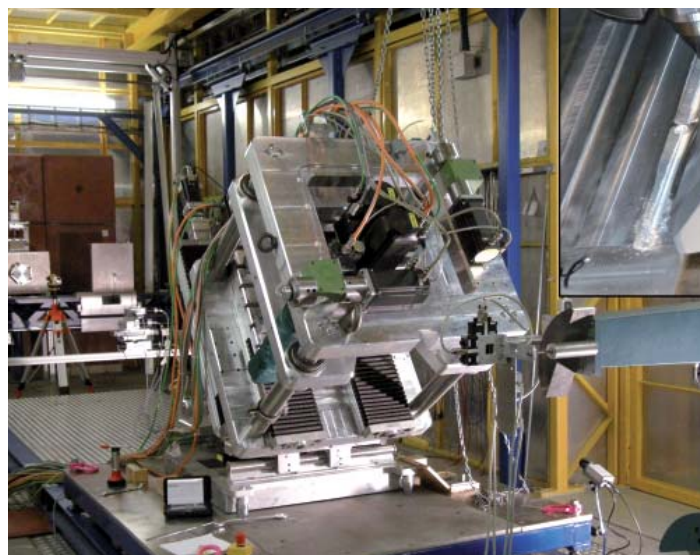
Figure 1

On account of its size, the new HARWI II diffractometer is installed in a pit 1.5 m in depth. In the configuration shown, the specimen is placed in a Eulerian cradle, which is mounted in a special frame so as to permit the use of both horizontal and vertical diffraction.

small-angle scattering experiments in 2008 (Fig. 2). The encouraging results trigger plans for the adaptation of other joining techniques (such as laser welding) to *in situ* investigations. At the wiggler beamline BW2 at DORIS III about a third of the beamtime is made available by DESY for tomography experiments operated by the GKSS Outstation **tomography** team, providing large field of view experiments extending the photon energy range below that available at HARWI II to 7-24 keV for lower absorbing samples. A portable tomography camera

Figure 2

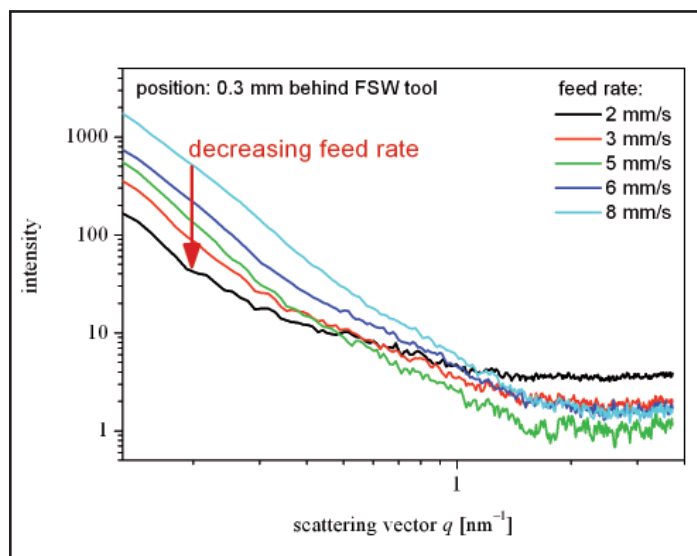
(Top) *In situ* friction-stir welding (FSW) machine machine FlexiStir at the HARWI II beamline. The inset shows details of the welded joint. (Bottom) Small-angle scattering intensity (photon energy 70 keV) as measured 0.3 mm behind the FSW tool as a function of the tool's feed rate. The measurements were done *in situ* during welding. A reduction of the SAXS intensity by one order of magnitude at small scattering vectors q was observed with decreasing feed rate.



can be flexibly used at the two beamlines. The construction of new tomography cameras is currently under way. In the beginning of 2009, the new instrumentation of the HARWI II tomography setup will be completed including the implementation of a phase contrast measurement method. This tomography setup is optimized for the automated investigation of a large number of samples.

The projects of beamlines at PETRA III have made great progress in 2008. The High Energy Materials Science (**HEMS**) beamline for research with high resolution, monochromatic, high-energy X-rays (50-250 keV) from a 5 m in-vacuum undulator will encompass fundamental research in the fields of metallurgy, physics and chemistry and applied research for manufacturing process optimization and smart material development. HEMS targets the materials science and engineering community allowing measurements of large structural components up to 1 t, 3DXRD investigations down to the single grain level, micro-tomography (see also below) and texture determination with beam sizes in the mm² to 50 μm² range. The HEMS hutches and control cabins in the PETRA III hall have been finished. Most of the instrumentation has already been delivered (1 t heavy load hexapod; heavy load tables; surface/interfaces diffractometer) or are in the design/manufacturing phase (detector portals; monochromators). The HEMS commissioning phase will start as soon as synchrotron radiation is provided by the PETRA III storage ring in 2009.

The Imaging Beamline (**IBL**) is optimized for micro- and nano-tomography with highest spatial and density resolution. Highly coherent hard X-rays (photon energy 5-50 keV) will be generated by a 2 m undulator. The IBL micro-tomography will be optimised for the automated investigation of large numbers of samples and will answer questions from materials science (e.g. imaging and quantitative analysis of pores, cracks, precipitations, phase transitions) and solve problems in the area of biomaterials (e.g. structures of cells, tissues, bones and implants). A second identical tomographic setup located at the HEMS beamline will extend the energy range to higher energies from 50-150 keV for the investigation of highly absorbing materials. In a second experimental station at IBL, new focussing possibilities will extend the spatial resolution below 100 nm for μm-sized samples for nano-tomography and imaging experiments. The micro-



tomography instruments are in the manufacturing phase and is expected to be delivered in early 2009. The IBL commissioning phase will start midyear 2009.

For the EMBL **BioSAXS** instrument GKSS contributes the detector tube and detector platform in a flexible design to allow rapid sample-detector distance changes over a range of 0.5-5 m with an additional option for vertical lift (off-set mode for anisotropic scattering). A special temperature-controlled sample environment will also be provided by GKSS. With the BioSAXS instrument GKSS will provide time-resolved measurements for the soft matter and life sciences user community, which has so far complementarily used the SANS facilities at FRG-1 and FRM II. Additionally, it will significantly contribute to the in-house research dealing with biomaterials and polymers. The design of components is in the final stage in order to finalise the GKSS contribution in 2009.

With the new beamlines, the GKSS outstation at DESY will cover a large range of synchrotron radiation applications in materials science by using X-ray beams of various sizes from wiggler and undulator sources. ●

Contact: Martin Müller, martin.mueller@gkss.de
Andreas Schreyer, andreas.schreyer@gkss.de

GFZ Helmholtz Centre Potsdam Outstation at DESY.

Opening a high-pressure, high-temperature window
into the earth

Twenty years ago geo-scientists from all over the world launched in-situ X-ray diffraction experiments under extreme pressure and temperature conditions at synchrotron beamlines. One of the first apparatus was installed at HASYLAB, MAX80, a single-stage multi-anvil system. MAX80 allows in-situ diffraction studies in conjunction with the simultaneous measurement of elastic properties up to 120 000 bar and 1600°C. This very successful experiment, unique in Europe, is operated by GFZ Potsdam and is used by more than twenty groups from different countries every year.

Experiments for both, applied and basic research are conducted, ranging from life-sciences, chemistry, physics, over material sciences to geo-sciences. Today new materials and the use of high brilliant synchrotron sources allow to construct double-stage multi-anvil systems for X-ray diffraction to reach much higher pressures. The newly designed high-flux hard X-ray wiggler beamline HARWI II is an ideal X-ray source for this kind of experiments.

As only the uppermost few kilometres of the Earth (less than 0.1% of its radius) are accessible for direct observations (e.g. deep drilling), sophisticated techniques are required to observe and to understand the processes in the deep interior of our planet. In-situ studies are an excellent tool to investigate ongoing geodynamic processes within the laboratory. One of the fundamental regions to study geodynamic processes is the so-called transition zone, the boundary between upper and lower earth's mantle between ≈ 410 and ≈ 670 km depth. Mineral reactions, phase transitions, as well as fluid rock interaction in this area might have the potential to strongly influence and control the dynamic motions within our whole planet. Around 250 kbar and 2 000 K are required to simulate these processes in the laboratory. The new MAX200x is an excellent tool for these ambitious experiments. ●

Contact: Jörn Lauterjung, lau@gfz-potsdam.de
Frank Schilling, frank.schilling@gfz-potsdam.de
Christian Lathe, lathe@gfz-potsdam.de



Figure 1

The MAX200x instrument in its experiment hutch in the HARWI II hall. This press can generate a pressure of 1750 tons and itself weighs 30 tons. It is movable in z- and x-direction to align the sample relative to the X-ray beam.

University of Hamburg on the DESY site.

Close links to DESY Photon Science

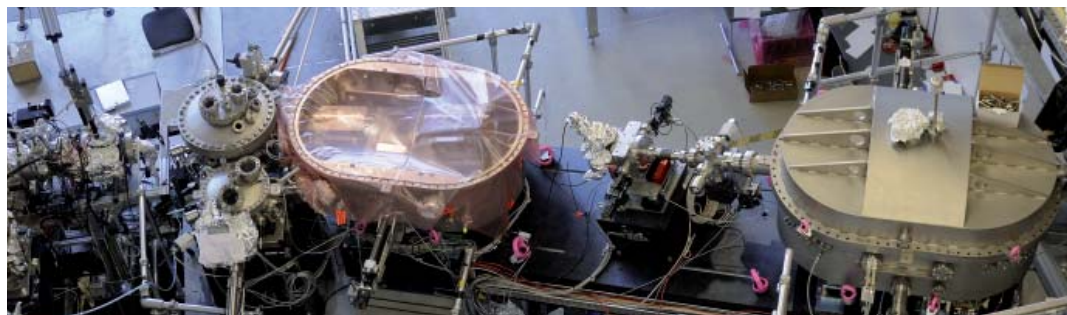


Figure 1

VUV Raman spectrometer
at FLASH beamline PG1
(group of M. Rübhausen,
University of Hamburg)

Research with synchrotron radiation and the collaboration with HASYLAB have a long tradition at the University of Hamburg. From the very beginning members of the Institute of Experimental Physics have been actively pursuing research programs using light sources at DESY. These activities have grown continuously and today many groups from the faculty of mathematics, informatics and natural sciences are active users of the DESY photon science facilities. Even more importantly, groups of the University have been and still are developing and running beamlines and instruments in the framework of the BMBF Verbundforschung and hence help shaping the future of HASYLAB.

At DORIS III, spectroscopy in the VUV and XUV spectral range has been one of the focal points of research. The SUPERLUMI beamline for VUV luminescence spectroscopy was built and operated by the institute for many years (Georg Zimmerer) before it was taken over by HASYLAB recently. Further instruments developed and operated by University groups are the angle-resolved photoemission endstation at FLIPPER 2 (Robert Johnson) and the Kappa diffractometer for single-crystal X-ray diffraction at beamline F1 (Ulrich Bismayer, department of geosciences).

Apart from the research at DORIS III, groups from the University are actively involved in building endstations at PETRA III: a low temperature cryostat with integrated high-field magnet for X-ray absorption spectroscopy is being developed at the variable polarization XUV beamline P04 (Wilfried Wurth), they are partners (Michael Martins) in the PIPE consortium which build an ion-storage ring for ion spectroscopy at PETRA III and are involved in the hard X-ray photoemission project (Robert Johnson). The effort in structural biology started at DORIS III and will now move to PETRA III (Christoph Betzel, Institute for Biochemistry and Molecular Biology). To foster these activities, the University of Hamburg and the University of Lübeck (Rolf Hilgenfeld) founded a joint Laboratory for Structural Biology of Infection and Inflammation on the DESY site in 2007.

The biggest efforts are, however, related to research projects in connection with FLASH. Here, groups of the University are

major partners in the BMBF Research Centre (Forschungsschwerpunkt) “FLASH: Matter in the light of ultrashort and extremely intense X-ray pulses” coordinated by Wilfried Wurth. Aim of this priority program which is funded by more than 15 M€ over a three year period and comprises 17 projects from 10 different universities is to develop and perform pioneering experiments at FLASH. Projects from the University of Hamburg include the instrumental efforts at the plane-grating monochromator beamline (Wilfried Wurth), the new VUV Raman spectrometer (Fig. 1) (Michael Rübhausen), the seeding experiment “sFLASH” (Markus Drescher, Shaukat Khan (now in Dortmund), and Jörg Roßbach), as well as strong research activities in the field of small quantum systems, nano materials and ultrafast science.

Most prominently, the University of Hamburg has recently founded the Centre for Free-Electron Laser Science (CFEL) together with DESY and the Max-Planck Society to foster interdisciplinary science with free-electron laser sources, as outlined in detail in the CFEL chapter.

At the same time, academic education is pursued in collaboration between HASYLAB and the Department of Physics of the University. An example for the multidisciplinary approach is the new university graduate training programme (Graduiertenkolleg) GRK 1355 “Physics with new advanced coherent radiation sources”, dedicated to the development, characterization and application of modern sources for light and matter waves. It combines the expertise of scientists from the fields of laser physics, quantum optics, X-ray physics, ultra-short pulse physics and accelerator physics in order to study the joint and complementary aspects of systems like fibre lasers, crystalline waveguide lasers, fs-lasers, XUV free-electron lasers, synchrotron radiation and atom lasers.

In summary, photon science using the light sources at DESY is and will be a major research focus in natural sciences at the University of Hamburg. ●

Contact: Wilfried Wurth (University of Hamburg),
wilfried.wurth@desy.de



Lightsources.

>	DORIS III	64
>	FLASH	66
>	PETRA III	70
>	European XFEL Project	76

After a productive year with very reliable user operation, DORIS III was „put to sleep“ for almost nine months in 2008. This was inevitable in order to access the pre-accelerator systems and other machine related infrastructure such as cooling water and control systems which had to be refurbished in preparation for the PETRA III start-up. DORIS III is benefiting from these measures because the refurbished systems are expected to further the same pre-accelerator increase its reliability of operation since both machines share the same pre-accelerator chain. The shutdown was also used for maintenance at the storage ring such as the replacement of parts of the dipole magnet coil supports and the exchange of magnet power supplies for the storage ring and the transfer line. During the last weeks of the shutdown period all DORIS III units were powered up again and re-calibrated where necessary and the machine start-up on August 25 was on schedule. Unfortunately, a cooling water leak occurred on one of the vacuum chambers due to the initial thermal stress requiring its complete removal for repair. This did not, however, compromise the start of the machine and beamline commissioning one week before the regular user operation which began as scheduled on September 22. During the operation period until December 22, user beamtime was scheduled for 80% of the time (Fig. 1) yielding 1874 h for user experiments which is about 1/3 of what is usually provided per year (Fig. 2). The machine was performing again nicely with an user beam availability during user beamtime of 97.2% and a mean time between failure (MTBF) of 75 h which are excellent

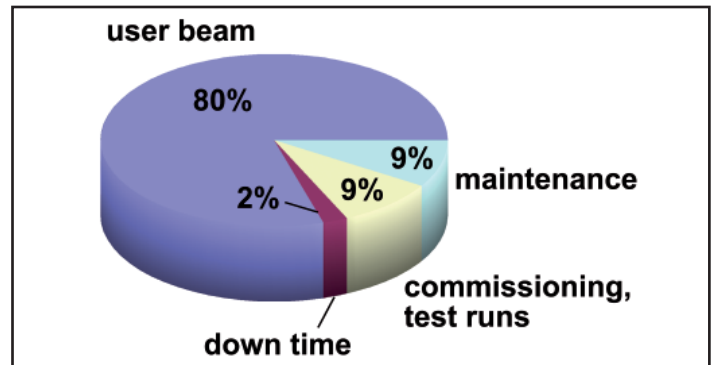


Figure 1

Distribution of times within the operation period from September 15 to December 22, 2008. The preceding machine startup procedures are not included.

conditions in view of the long shutdown. The beam lifetimes during 5-bunch operation were 20 h after a filling of 140 mA increasing to 30 h towards run end at around 100 mA. Occasional breaks were mainly caused by beamline interlock triggers and initial problems in the refurbished pre-accelerator chain. Otherwise, the operation was very reliable with stable beam conditions and scheduled three 8h runs per day (Fig. 3). As usual, a small fraction of the beamtime was reserved for time-resolving experiments needing a 2-bunch mode of operation (see Fig. 2).

The extended shutdown was used as well to upgrade and refurbish a few DORIS III beamlines and instruments. Beamline

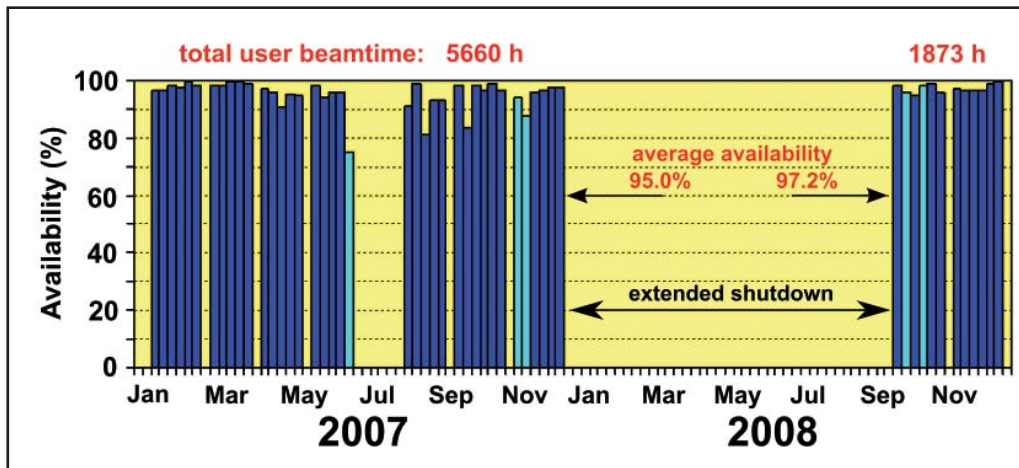


Figure 2

DORIS III user beamtime statistics for 2007 and 2008. The dark blue colored dates mark 5-bunch mode of operation, the light blue stand for 2-bunch mode.



Figure 5
Scanning the van Gogh painting „Patch of Grass“ at micro-fluorescence beamline L.

A1 for X-ray absorption spectroscopy (XAS) is being upgraded substantially. It is now equipped with a new double-crystal monochromator of the „CEMO type“ (Fig. 4), which is a fast-scanning UHV-compatible device designed and built by HASYLAB already operating successfully at XAS beamline C. The monochromator was relocated further upstream and is currently being complemented by a pair of new X-ray mirrors downstream for focusing and harmonics rejection. The refurbished beamline is expected to be commissioned in early Spring 2009 and then be available for user XAS experiments in the energy range from 2.4 to 8 keV, finally replacing beamline E4 which will be closed down. The same type of new X-ray monochromator is also currently being installed at powder diffraction beamline B2, which will also be re-commissioned in Spring 2009.

At the materials science beamline HARWI II, which is operated by the GKSS research centre in collaboration with DESY and GFZ, a new heavy-load diffractometer for high-energy X-ray diffraction experiments on engineering materials was installed and is available for users since September 2008.

The EMBL-Hamburg Outstation has reduced its open beamlines at DORIS III from seven to four in order to free resources for the work on the EMBL@PETRA3 project. While the three protein crystallography beamlines at fan K and the SAXS beamline at fan D remain in full user operation, the bio-EXAFS beamline D2 was closed down and the wiggler beamlines BW7A and BW7B will primarily be used as test beamlines.

Because of the extended shutdown, there was only one call for

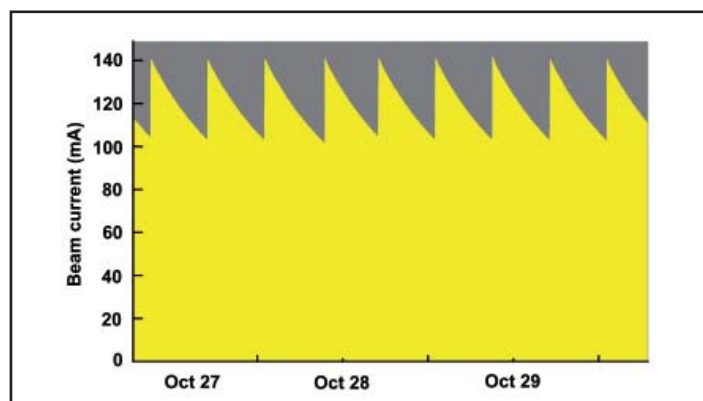


Figure 3
A run period without any interruption.



Figure 4
New UHV-compatible double-crystal monochromator of the „CEMO type“ at X-ray absorption beamline A1.

proposals in 2007, whereas in 2008 the call procedure was as usual with separate calls in the Spring and Fall. In total, 208 new research proposals for experiments at DORIS III were accepted by HASYLAB, 150 in category I (1 year term) and 58 in category II (3 years term). As in previous years, the number of proposals by international research groups is high (44%), however, the share of proposals from EU countries has decreased (38%) noticeably compared to previous years (~47%) which may be attributed to the additional availability of the new sources Diamond (Great Britain) and Soleil (France). Interestingly, the total number of proposals remained constant (for comparison: 209 in 2006) which implies an increased share of German user groups. The numbers above do not include proposals for the EMBL and MPG beamlines for structural biology research. DORIS III, which is the last 2nd generation light source in Europe, will continue to operate in its present configuration until PETRA III is reliably operating and the beamlines are fully commissioned. Then, the number of beamlines at DORIS III will be reduced in order to focus on techniques being complementary to those provided at PETRA III in its initial phase. In the longer run, the most important of these techniques will also be made available at PETRA III by adding suitable beamlines so that DORIS III can finally be shut down to free resources. ●

Contact: Wolfgang Drube (DESY-HASYLAB),
wolfgang.drube@desy.de

Frank Brinker (DESY-MDO), frank.brinker@desy.de

Soft X-ray free-electron laser user facility thriving and prospering



View into the FLASH experiment hall

FLASH is worldwide the only operational free-electron laser (FEL) facility for vacuum-ultraviolet and soft X-ray radiation. It delivers 10-50 fs pulses with high repetition rate and pulse energies of 10-100 μJ in a wavelength range tunable from ~ 50 nm down to 6.5 nm in the first harmonic. In 2008, 3636 hours of beamtime (41,6 % of 8736 hours) were allocated to user experiments (Fig. 1). 3696 hours (42,3 %) in total were scheduled for work on the accelerator, the FEL, the photon beamlines and photon diagnostics in order to steadily improve the performance of the facility and to prepare the user runs. 1404 hours (16,1 %) were scheduled for maintenance (5 weeks plus 12 hours every week). This time included also a 3-week shutdown in May required for PETRA III installation work, which was used for small upgrades at FLASH and for preparatory work for the sFLASH project (see below).

During scheduled operation, FLASH reached a record availability of 94 %. The change of a 10 MW klystron in January and many small improvements related to the RF stations (klystrons and modulators) contributed significantly to reducing the total downtime due to component failures from 9 % in 2007 to 6 % in 2008. During scheduled user runs 75 % of the time was actually available for user experiments, 17 % was required for tuning, more than half of which was spent with changing wavelength (Fig. 2). Although experiments are scheduled such that the number of beam parameter changes is minimized, the FEL wavelength was changed 89 times between 20 different values in a range from 27 nm to 7 nm. A wavelength change takes about 2 hours on average. Some experiments require special tuning of the FEL by experts, for example to optimize the

intensity of the 3rd or 5th harmonic of the FEL, or to set the wavelength precisely to an atomic resonance in the sample, or to minimize the FEL bandwidth. In addition, the experiments required various bunch patterns with intra-train repetition rates of 100, 200, 250, 500 and 1000 kHz and 1, 10, 20, 30, 50, or 100 bunches/train (with 5 pulse trains per second). Most experiments used 1 bunch or 30 bunches at 1 MHz.

The experimental program run at FLASH during 23 weeks (plus 2 days) of beamtime in 2008 included almost all of the 32 approved proposals and covered a wide range of applications, including atomic and molecular physics, precision spectroscopy of highly charged ions, the study of clusters and warm dense matter, dynamic processes at surfaces and in solids, the characterization of the FEL pulses and the development of new experimental methods. Meanwhile, 50 % of the experiments combine the optical femtosecond laser system with the FEL

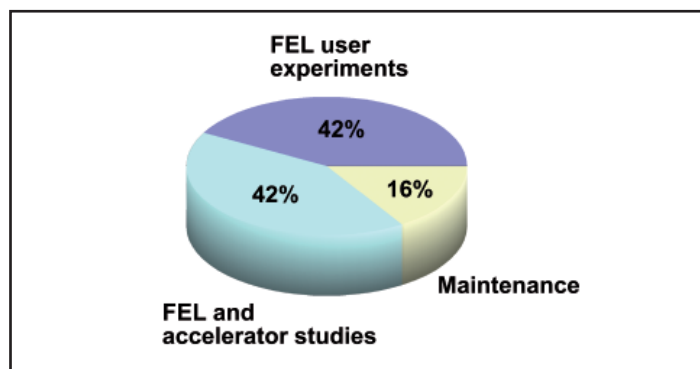


Figure 1

Scheduled beam time distribution in 2008

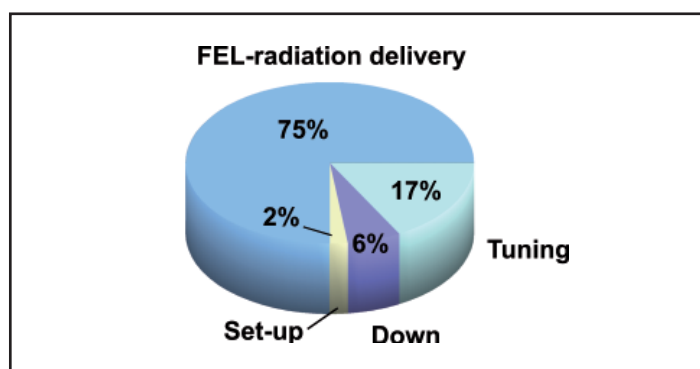


Figure 2

Distribution of beam time in 2008 during user runs

beam in order to exploit the short FEL pulses for investigating fast dynamics. Several results are described in detail in the highlights section of this report. Only two examples are briefly presented at this point:

For the first time, researchers from the FOM-Institute for Atomic and Molecular Physics (AMOLF), Amsterdam, investigated aligned molecules at FLASH. They used a strong optical femto-second laser pulse to give CO₂ molecules a rotational kick, and probed the molecules by ionizing them with an FEL pulse after some picoseconds when the molecules had realigned, so that no optical laser field was present that would disturb the ionization process. Typical velocity distributions of O⁺ ions from CO₂ before and during alignment are shown in Fig. 3. It is the aim of this development to use the aligned molecules for studies of ultra-fast dissociation dynamics by observing photo electron diffraction in the molecular frame.

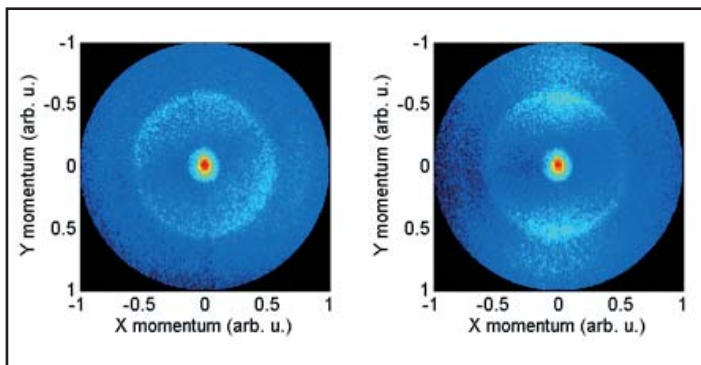


Figure 3 Velocity map image of O⁺ ions from dissociating CO₂ molecules, taken before (left) and during (right) alignment of the molecules (courtesy P. Johansson, AMOLF, Amsterdam)

Scientists from Max-Planck-Institute for Nuclear Physics, Heidelberg, studied ultra-cold lithium atoms in the intense FLASH beam. In their experiments a cloud of lithium atoms was cooled down to a temperature of ≈ 1 mK in a magneto-optical laser trap and prepared in specific quantum states. The emission patterns of the emerging electrons and ions were recorded by a multi-particle imaging spectrometer, giving detailed insight into the photoionization mechanisms involved. An exemplary Li⁺ ion momentum distribution is shown in Fig. 4. Since FLASH started operation in 2005, approximately half the time has been regularly scheduled for accelerator and FEL re-

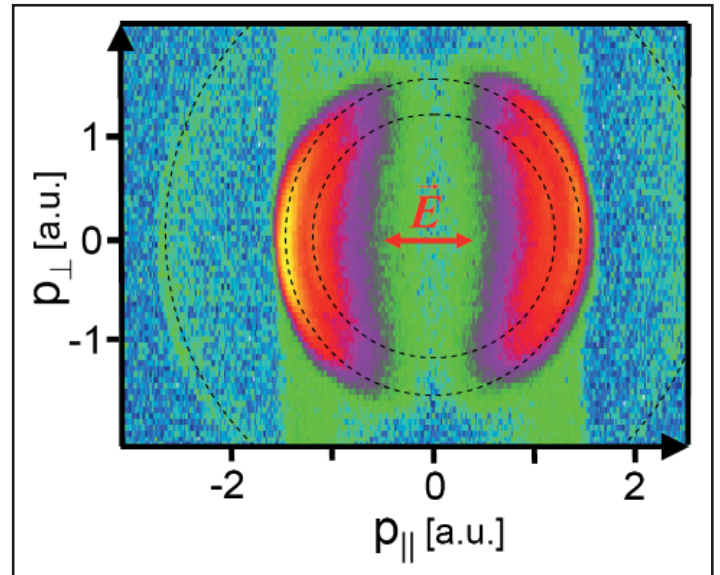


Figure 4 Experimental lithium ion momentum spectrum. The arrow indicates the direction of the FEL polarization (courtesy A. Dorn, MPI Heidelberg)

lated studies in order to constantly improve the performance of the facility and thus to provide better conditions for user experiments. The major activities in 2008 included the commissioning of and first experiments with the FIR-undulator, tests of the optical replica synthesizer and a new beam arrival time feedback system, many studies to improve the low-level RF system, a high bunch current experiment, and beam dynamics studies. One highlight was the successful generation of a bunch train with a current of 3 mA (Fig. 5). This is especially important for the European XFEL, where the design asks for 5 mA current in a train. High currents are especially demanding for the low-level RF, where a substantial beam loading needs to be compensated. Also, experience with running superconducting modules at their performance limit is gained. For high-resolution pump-probe experiments it is essential to provide a highly stable synchronization system for all components along the facility and to reduce the arrival time jitter of the FEL pulses which is mainly generated in the magnetic chicane bunch compressors due to energy fluctuations of the electron bunches. Even with a record stability of the accelerating gradient of 0.014 %, the jitter is still in the order of 200 fs rms. Promising results have now been obtained with the new synchronization system based on special pick-up monitors installed

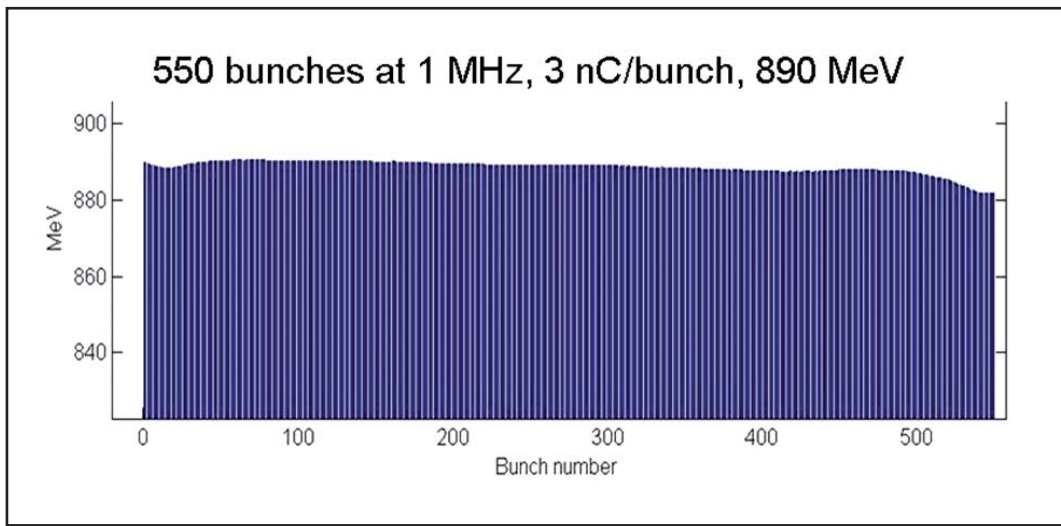


Figure 5
Bunch train with an average current of 3 mA and a length of 550 μ s.

in the electron beam line. The signal picked up from the electron bunches is compared with a stabilized fiber laser and a correction signal derived acting on the gradient of the first accelerating module. Using this system, the arrival time could be stabilized to ~ 40 fs rms after ~ 50 bunches in a bunch train (Fig. 6). A new, state-of-the-art RF master oscillator has been installed in the maintenance weeks in May. Together with higher stability, the new system includes various diagnostic features and promises an improved overall reliability and a reduced sensitivity to external noise sources. It also includes a backup system to be installed soon.

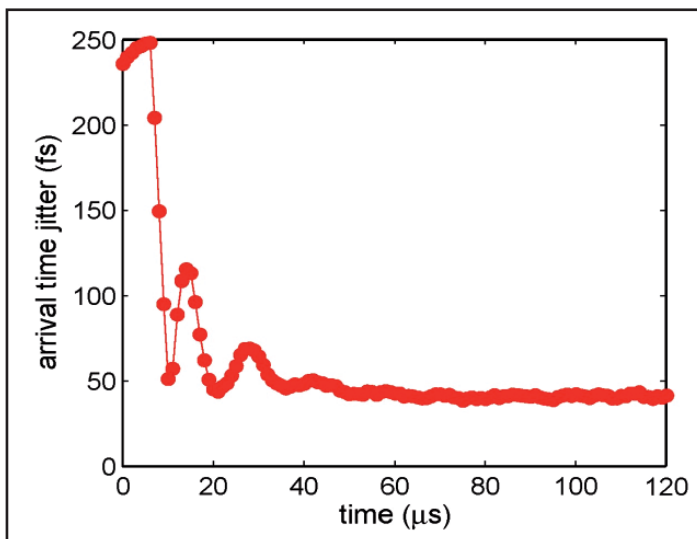


Figure 6
Arrival time jitter from bunch to bunch in a bunch train. The feedback reduces the jitter from initially more than 200 fs rms to ~ 40 fs rms after ~ 50 bunches.

The development of advanced diagnostic techniques for measuring the properties of both, the electron bunches and the FEL photon pulses has been a major part of the studies program at FLASH. One of the most difficult tasks is the measurement of the longitudinal electron bunch properties with high resolution, i.e. the density, the emittance and the energy spread of the electrons in an individual bunch at a resolution better than the

coherence length of the FEL (typically some 100 FEL wavelengths). These parameters are called “slice emittance” and “slice energy spread”, respectively, and their control is of crucial importance for the FEL process. The optical replica synthesizer promises to deliver these parameters in a non-destructive way and, in particular, at high electron energies where deflecting cavities become impractical. The technique uses an external laser to produce fs pulses which interact with the electrons in a modulator undulator creating energy modulation which is transformed into density modulation in the following chicane. The radiator undulator located downstream radiates coherently and the emitted light pulse has the same longitudinal profile as the electron beam, hence the name Optical Replica Synthesizer. The replica pulse is then extracted and analyzed by a FROG (frequency resolved optical gating) device, called GRENOUILLE. A complete optical replica synthesizer experiment was installed at FLASH during the shutdown in 2007 and has now succeeded in producing first traces showing a glimpse of the longitudinal bunch shape (Fig. 7) [G. Angelova et al., Proc. EPAC08, Genoa, Italy, p. 1332].

Currently FLASH operates in the SASE (self-amplified spontaneous emission) mode and produces extremely short pulses of ~ 10 fs duration. Due to the start-up from noise, the SASE radiation consists of a number of uncorrelated modes resulting in reduced longitudinal coherence and shot-to-shot fluctuations (of the order 20 % rms) of the output pulse energy. Other drawbacks of this mode of operation are strong space charge effects which are difficult to control, and relatively large timing jitter compared to the pulse duration as discussed above. Seeding can significantly reduce most of these drawbacks. The sFLASH project, funded by BMBF since July 2007, is currently preparing all the components required for directly seeding the electron beam at FLASH with high-order harmonics of an optical laser generated in a gas target (HHG). The installation is planned during the next shutdown of FLASH starting in September 2009. It is expected that the output pulses will be ~ 20 fs FWHM long with a smooth longitudinal profile and GW peak power. In particular, the seeded FEL pulses will be strictly synchronous with the seed laser pulses making

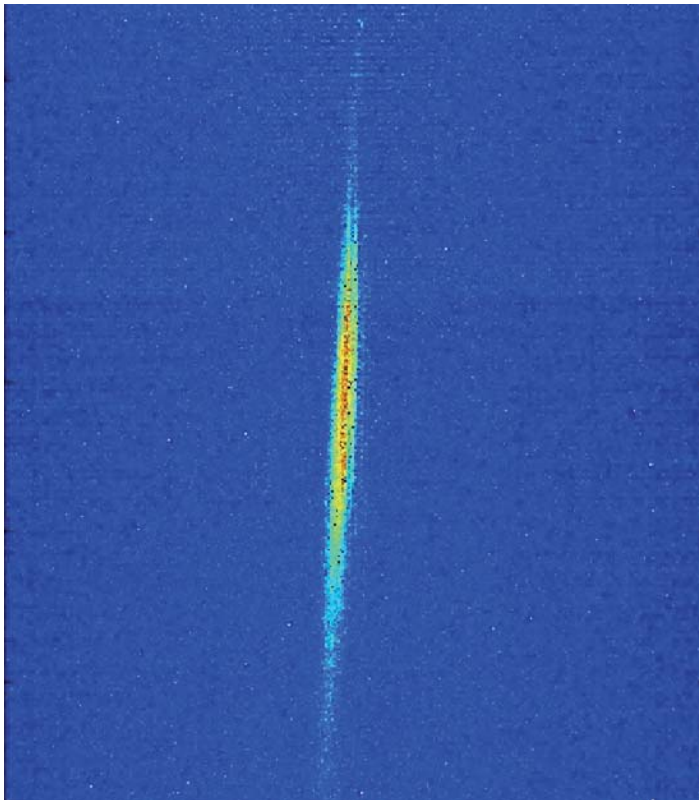


Figure 7
 One of the first qualitative FROG traces from the optical replica synthesizer experiment at FLASH. The horizontal axis is time, the vertical wavelength. From this image the amplitude and the phase of the coherent light pulse can be reconstructed and the slice properties of the electron bunch determined.

pump-probe experiments possible whose resolution is only limited by the duration of the FEL and the laser pulses. A first demonstration of HHG seeding at 160 nm wavelength has recently been performed by a French-Japanese collaboration at the SPring-8 Compact SASE Source [G. Lambert et al., Nature Physics 4, 296 - 300 (2008)]. The aim of the sFLASH project is to study the technical feasibility of HHG seeding at shorter wavelengths (at 30 nm and 13.5 nm) and to determine the technology required for reliable and stable user operation. The results of this project will be vital for the realisation of a second FEL undulator beamline at FLASH (FLASH II) which has just been proposed for funding.

The schematic layout of sFLASH is shown in Fig. 8. It will be installed at the end of the linac, upstream of the existing fixed-gap SASE-undulators. The HHG seed pulses are produced in a laser hutch adjacent to the accelerator tunnel and coupled into the 10 m long, variable-gap sFLASH undulator through the collimator section, making use of the existing electron beam offset. After amplification, the output radiation is separated from the electrons using a set of plane Si mirrors coated with amorphous carbon and mounted in a small magnetic chicane behind the undulator. The light can be switched either to a grazing incidence spectrometer in the tunnel to measure the spectral profile of individual pulses, or to the experimental area outside the FLASH tunnel. Here, the seeded FEL pulses are combined with part of the naturally synchronized optical seed laser pulses in order to perform pilot pump-probe experiments with a resolution of the order of 30 fs. ●

Contact: Josef Feldhaus (DESY-HASYLAB),
 josef.feldhaus@desy.de
 Siegfried Schreiber (DESY-MIN), siegfried.schreiber@desy.de

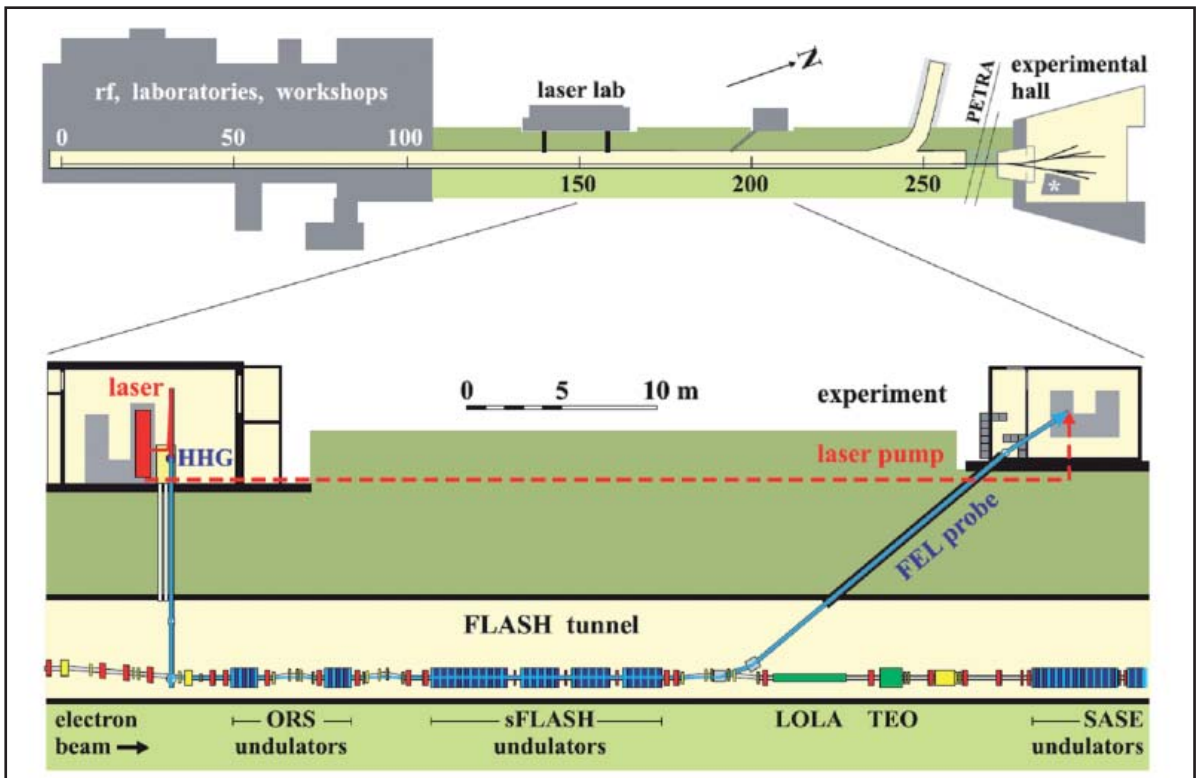


Figure 8
 Schematic layout of the seeding experiment „sFLASH“.

PETRA III.

Brilliant light on the horizon

The PETRA accelerator on the DESY site in Hamburg is currently in its final stage of being converted into the most brilliant storage ring based X-ray source worldwide.

Exactly one year after the official PETRA III construction start, the experimental hall including the outside facilities, was handed over to DESY on July 1, 2008. Figure 1 shows an aerial view of the almost 300 m long experimental hall that runs along one octant of the 2304 m long PETRA storage ring on the DESY site. The end of its construction phase was celebrated by handing over the key for the experimental hall on the same day (Fig. 2). This day marks the completion of several challenging tasks during the construction process, including the fabrication of the world's longest single-slab concrete plate and the production of 99 sleeved concrete piles that reach 20 m deep into the earth to carry the outer shell of the experimental hall. These measures will ensure a nearly vibration free experi-

mental environment on the 7000 m² large experimental floor that provides space for 14 beam-lines and up to 30 experimental stations. Here, some of the most brilliant beams of hard X-rays worldwide will be available with a brilliance exceeding 10^{21} ph/(s mm² mrad² 0.1% BW).

The PETRA III project is the third reincarnation for the PETRA storage ring, which was built as an electron-positron collider in the 1980s and later became a pre-accelerator for the proton-electron collider HERA. The overall budget of the PETRA III project is €225 million, shared between the German Federal Government (90%) and the City of Hamburg (10%).

The particle energy of the storage ring will be 6 GeV which is a compromise between achieving a small horizontal emittance and providing high photon flux in the energy range of 50–150 keV. The beam current will initially be limited to 100 mA, however, all components handling heat load or dealing with radiation



Figure 1
Aerial view of the almost 300 m long PETRA III experimental hall in October 2008. (Photo: Ed. Züblin AG)



Figure 2

Delegates from the general contractor Ed. Züblin and DESY right after the handover ceremony of the PETRA III experimental hall on July 1, 2008.

safety have been designed for a current of at least 200 mA in order to leave room for further upgrades.

The conversion of the PETRA machine into PETRA III comprises the complete rebuilding of one octant of the 2304 m long storage ring and the modernisation and refurbishment of the remaining seven octants. In this process all the accelerator components of the storage ring had to be removed from the tunnel, an operation that was achieved in only three months. Within one year more than 600 dipole, quadrupole and sextupole magnets were refurbished, most of them received new coils and were magnetically characterized. They were then re-installed together with a new accelerator vacuum system, the last dipole having been back in place in May 2008.

PETRA III will operate in top-up mode, i.e. the storage ring current will be kept constant to within 1% via frequent injections of particles. Since the time between top-up injections can be as short as 70 s for a 40 bunch filling pattern, a very high availability of the injector and pre-accelerator systems is mandatory which required significant refurbishments of these systems. The new light source will have a horizontal emittance of 1 nm rad being 3 – 4 times smaller than that of other high-energy (above 6 GeV) storage rings world-wide. This will be achieved by installing 20 damping wigglers, 4 m long each, in two of the long straight sections of the ring (West and North). The radiative power loss of the beam in these wigglers damps the horizontal motion of the stored particles and thus reduces the horizontal momentum spread of the photon beams. The vertical beam parameters are close to the diffraction limit and hence

are very similar to other high-energy 3rd generation sources. The major improvement provided by PETRA III therefore concerns the horizontal emittance. Figure 3 shows one of the straight sections in the tunnel that is equipped with damping wigglers which were developed and produced by the Budker Institute in Novosibirsk, Russia.

Except for the additional damping wigglers, the magnetic lattice, i.e. the arrangement of quadrupole and dipole magnets, in the original seven octants will remain unchanged. In the new octant, however, the magnets are arranged in a so-called Chasman-Green lattice which is optimized for synchrotron radiation sources. In this section, the magnet structures are mounted on separate girders and have been precisely pre-aligned before installation in the tunnel.

The magnetic structure in the arc of the new experimental hall comprises nine straight sections allowing the installation of either one 5 m or two 2 m long insertion devices (ID). In order to split the beam of two 2 m IDs into independent beamlines, they are inclined relative to each other by 5 mrad. In the present layout, five straight sections will accommodate two 2m long undulators and three a 5 m long undulator resulting in 13 independent beamlines. The ninth straight section is considerably longer and allows the installation of an ID up to a length of 20 m. Initially a 10 m long undulator is planned for this section. Similar to the ESRF there will be the option to choose between a low or a high value of the β -function in a straight section of the new octant. Changing the β -function in a straight section will be possible in a short shut down time of the machine.



Figure 3
One of the two damping wiggler sections in the PETRA III storage ring.

The beamline frontends, i.e. the beamline components located in the ring tunnel, serve to condition the photon beam for the downstream experiments. Here the beam cross section is defined by high-power slit systems capable of withstanding the considerable heatload of the direct undulator beams. Moreover, the frontend comprises elements like collimators and primary beamshutters to fulfill radiation safety requirements. All frontend devices were designed to be accommodated in a very compact arrangement on granite girders (Fig. 4). The arrangement of the beamlines and hutches on the experimental floor is schematically shown in Fig. 5. Due to the relatively large bending radius of the storage ring, the angular separation of the beams is small and hence the space between neighbouring beamlines is rather confined leaving only narrow aisles between hutches. As a consequence, there is no space for additional bending magnet beamlines inbetween. The space limitation is even more stringent for the two beams coming from a pair of canted undulators. In these cases, one of the beamlines is either designed as a “side station” or a larger geometric separation is achieved by specially developed large offset monochromators.

First installations on the experimental floor began right after it was officially handed over to DESY in April 2008, starting with the placement of the concrete shielding blocks for the ring tunnel, followed by the installation of optics enclosures for the beamlines in mid-July and setting up of the first lead hutches for end stations in August 2008.

The beamlines are organized in nine sectors which correspond to the straight sections in the new octant of the storage ring. Beamlines in sectors 3, 5, 7 receive radiation from a 5 m long

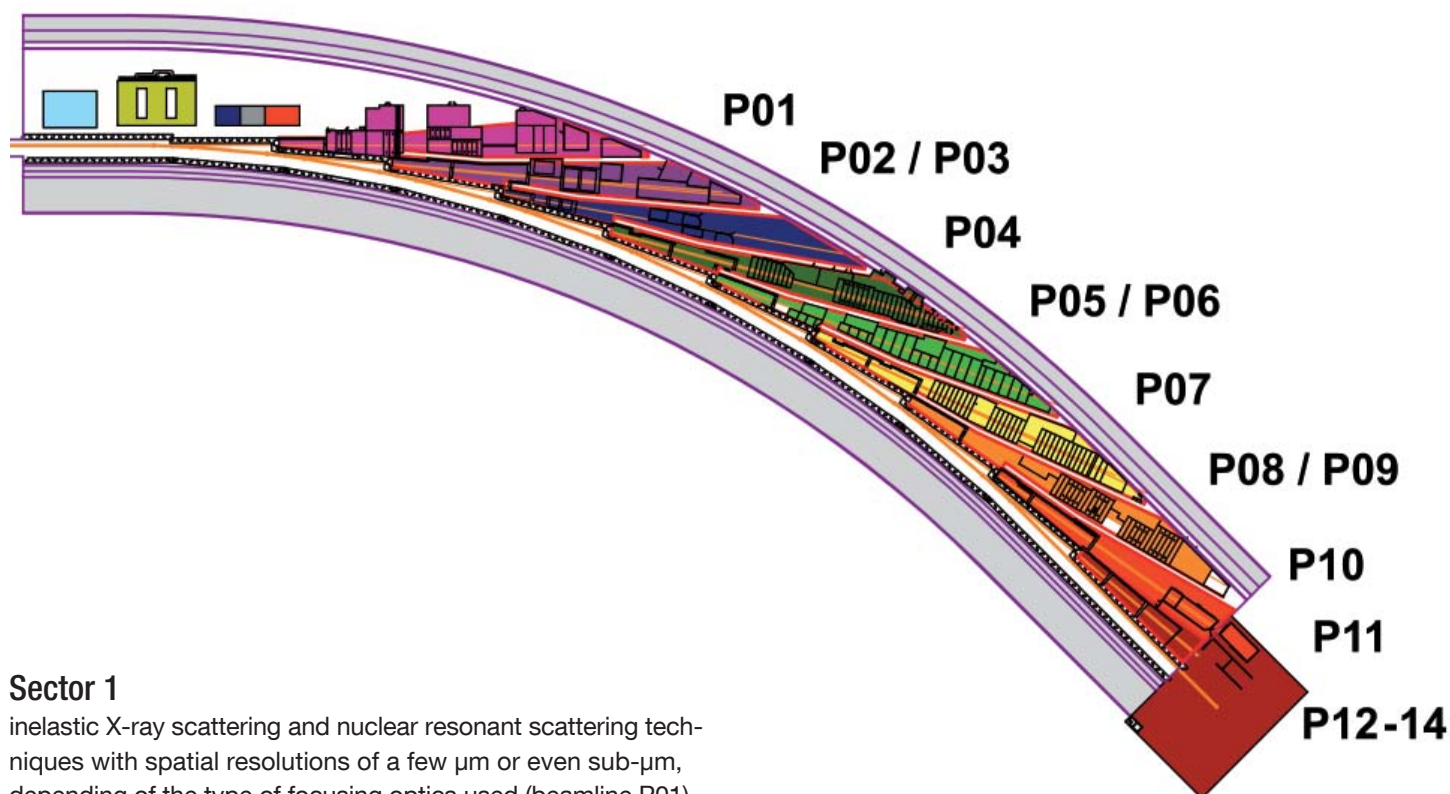
undulator (10 m device for sector 1), the other sectors host two independent beamlines each attached to a 2 m long section of a canted undulator. The techniques and instruments were selected by an international advisory board based on proposals as part of the technical design report and make specifically use of the high brilliance of the PETRA III beam:



Figure 4
A view into the ring tunnel within the PETRA III experimental hall, showing a machine girder that carries quadrupole magnets (left). The undulator of this straight section will be mounted in the foreground. Behind it (right part of the picture) some of the granite girders for the beamline frontend components are seen.

Figure 5

Schematic layout of the installations on the PETRA III experimental floor including the ring tunnel, the optics and experiment hutches as well as control cabins.



Sector 1

inelastic X-ray scattering and nuclear resonant scattering techniques with spatial resolutions of a few μm or even sub- μm , depending of the type of focusing optics used (beamline P01).

Sector 2

shared by a hard X-ray beamline (P02), with one fixed energy end-station for powder diffraction and one for extreme conditions experiments, and a beamline for micro and nano small-angle X-ray scattering applications (P03).

Sector 3

variable polarization soft X-ray beamline (P04) using an Apple-II type undulator, different specialized end-stations.

Sector 4

imaging applications comprising a beamline for tomography (P05, operated by the GKSS Research Centre, Geesthacht) and a hard X-ray nano-probe beamline (P06) including spatially-resolved absorption spectroscopy and fluorescence analysis.

Sector 5

a beamline optimized for very hard X-rays (>50 keV) dedicated mainly to applications in materials science (P07), jointly operated by GKSS and DESY.

Sector 6

diffraction experiments with very high-resolution (P08) and a beamline for resonant scattering and diffraction experiments (P09) with two different instruments in separate hutches. In

addition, there is a dedicated end station for hard X-ray photo-electron spectroscopy.

Sector 7

experiments utilizing the large coherent flux of the brilliant PETRA III source. This beamline (P10) will focus on X-ray photon correlation spectroscopy and coherent imaging experiments.

Sectors 8 and 9

dedicated to life science applications. One beamline (P11) is jointly operated by DESY, the Max Planck society and the Helmholtz Centre for Infection Research. The remaining three beamlines belong to the European Molecular Biology Laboratory (EMBL) and provide small-angle scattering, macro-molecular crystallography and bio-imaging endstations (P12 – P14). These instruments are being combined with several laboratories in a special annex to the experimental hall to form an integrated center for life science applications, run by EMBL.

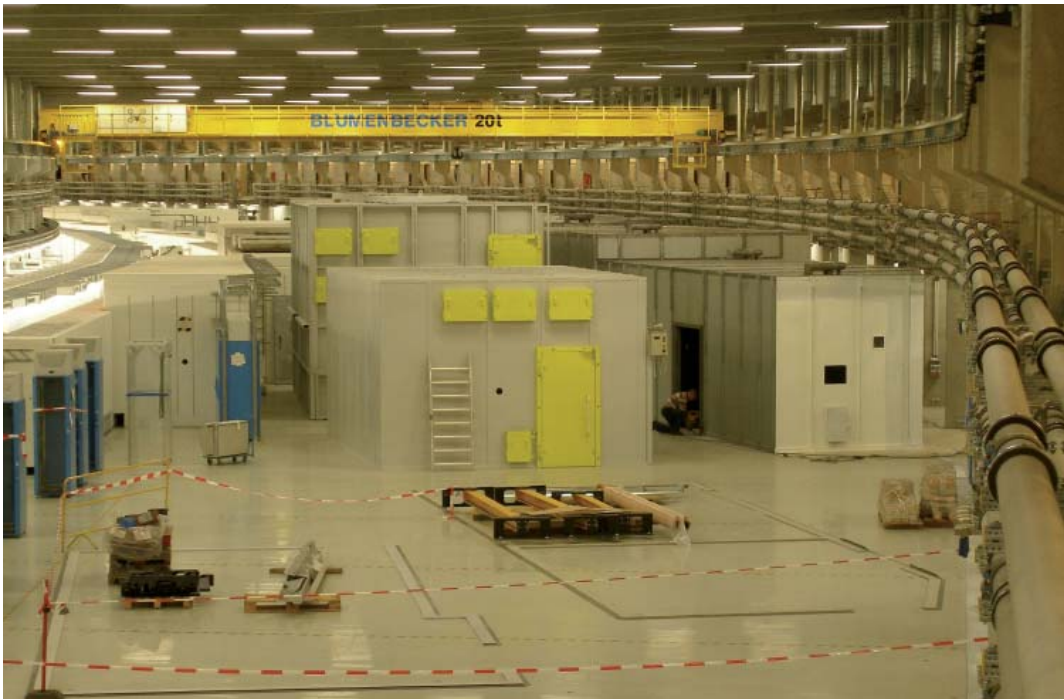


Figure 6

View into the experimental hall with first experiment hutches of beamlines P07, P08 and P09.

Many of the beamlines will host additional instrumentation which is provided by German university groups within the frame of the “Verbundforschung”, funded by the BMBF (German ministry for education and research) from 2007 - 2010. These instruments are summarized in the table of beamlines at PETRA III (in the last section of this report).

Figure 6 shows a view into the experimental hall in November 2008, with some of the plain experimental hutches of beamlines P07, P08 and P09, just having been set up on the floor. Many of the large instruments for the different end stations have been ordered and some were already delivered, such as a diffractometer for high-resolution diffraction installed in the experiment hutche of beamline P08 (Fig. 7). This hutche is resting on a large monolithic block of concrete on top of its canted counterpart

beamline P09. The monochromatic beam for this elevated station is delivered by the combination of a cryogenically cooled high heat-load double crystal monochromator and a special large offset monochromator raising the beam by 1.25 m to gain a sufficiently large separation from the neighboring beam of P09. This device was developed in-house and is currently under construction (details may be found elsewhere in this report). Another large offset monochromator combines cryogenic cooling of the crystals together with a negative offset by 50 cm and is currently being developed for beamline P03.

Apart from these special large-offset monochromators, most of the high heat-load monochromators for the PETRA III beamlines are of a generic type and will be produced in series with minor modifications for special requirements at some beam-

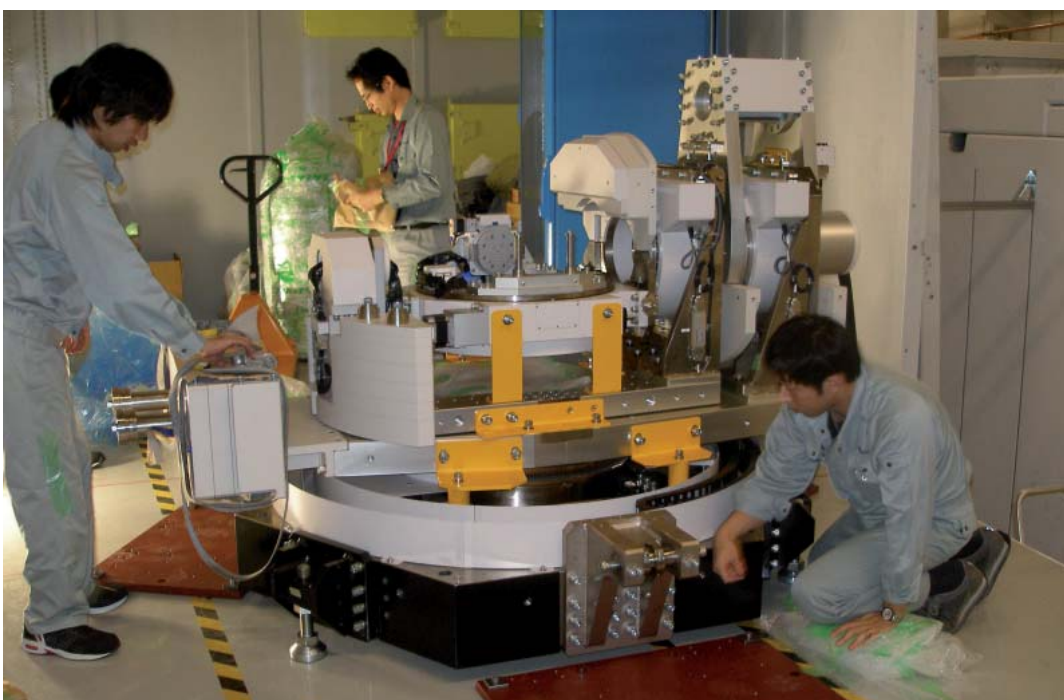


Figure 7

Installation of a diffractometer for high-resolution diffraction at beamline P08.

Figure 8
View into the (still open)
PETRA III ring tunnel.



lines. Two prototypes were already delivered earlier this year and underwent intensive testing procedures, both on site at DESY (for mechanical tests and further development of a beam position feedback system) and at ESRF where it was installed at beamline ID06 to measure its performance under realistic beam conditions, which are similar to those expected at PETRA III. In fact, the results of these initial tests gave valuable input for technical improvements and modifications for the series production, thus saving time and resources upon commissioning at PETRA III. In particular, the monochromator installation at ID06 served as a good training ground for technicians and engineers from DESY to gain practical experience with this device. In this context, the support of the ESRF management and the ID06 beamline staff is highly appreciated and acknowledged.

The technical commissioning of the original seven octants of the storage ring has started in November 2008, the entire storage ring will be ready for commissioning by the end of January 2009. First beam into the optics hutches is expected for April 2009 (Fig. 8). During the commissioning of the first beamlines, starting in late spring / early summer 2009, DESY will invite “friendly” users to participate in first experiments at this exciting new facility (Fig. 9). ●

Contact: Hermann Franz (DESY-HASYLAB),
hermann.franz@desy.de

Ralf Röhlsberger (DESY-HASYLAB), ralf.roehlsberger@desy.de
Klaus Balewski (DESY-MPE), klaus.balewski@desy.de

Figure 9
Rear view of the PETRA III hall
showing the bridge to the
HASyLAB office building.



European XFEL project.

Getting ready to take off

The European XFEL project achieved in 2008 major milestones towards its realization: The international negotiations preceding foundation of the European XFEL company (GmbH) have been completed. Agreements on contributions in-kind are ready for signature. The distribution of tasks between the European XFEL GmbH and its main collaborating institute, DESY, was defined and the contracts for the underground civil construction were awarded.

The European XFEL will consist out of a 1.7 km long superconducting electron accelerator delivering low emittance electron bunches at 17.5 GeV to three X-ray free-electron laser (FEL) undulators, which are up to 256 m long (Fig. 1). Two undulators for the hard X-ray regime and one for soft X-ray operate in the self-amplified spontaneous emission (SASE) mode and produce FEL radiation which is guided through beam transport sections

to the experiment stations. The initially six experiment stations will enable a wide range of scientific applications and experimental techniques. The use of femtosecond time-resolution, highly coherent X-rays, high peak intensities and the combination of these properties will distinguish the European XFEL from other X-ray sources. Furthermore, the superconducting linear accelerator will deliver up to 30 000 electron bunches per second thus allowing a large flexibility in beam distribution and FEL pulse patterns. Compared to other X-ray FEL facilities the average brightness will therefore be much higher and the operation conditions will be very flexible allowing for quasi-parallel operation of several experiment stations and additional options for a stabilization of the electron and X-ray beam delivery.

The European XFEL is an international project for which govern-

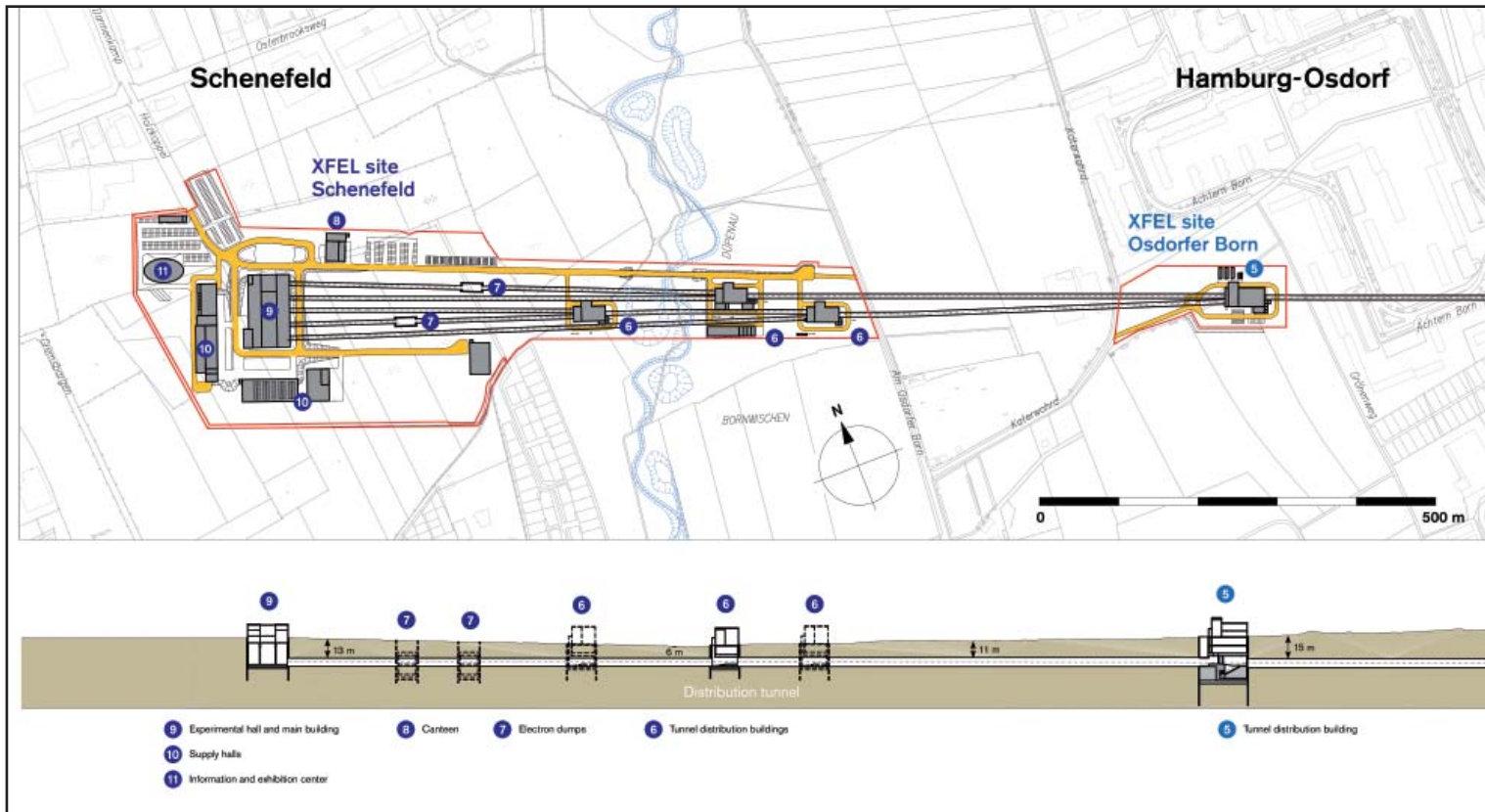


Figure 1 The 3.4-km-long European XFEL facility runs essentially underground and comprises three sites above ground. It will begin on the DESY campus in Hamburg-Bahrenfeld and will end south of the town of Schenefeld (Pinneberg district, Schleswig-Holstein). The lower part indicates the ground profile as well as the location of several buildings on the sites.

Figure 2

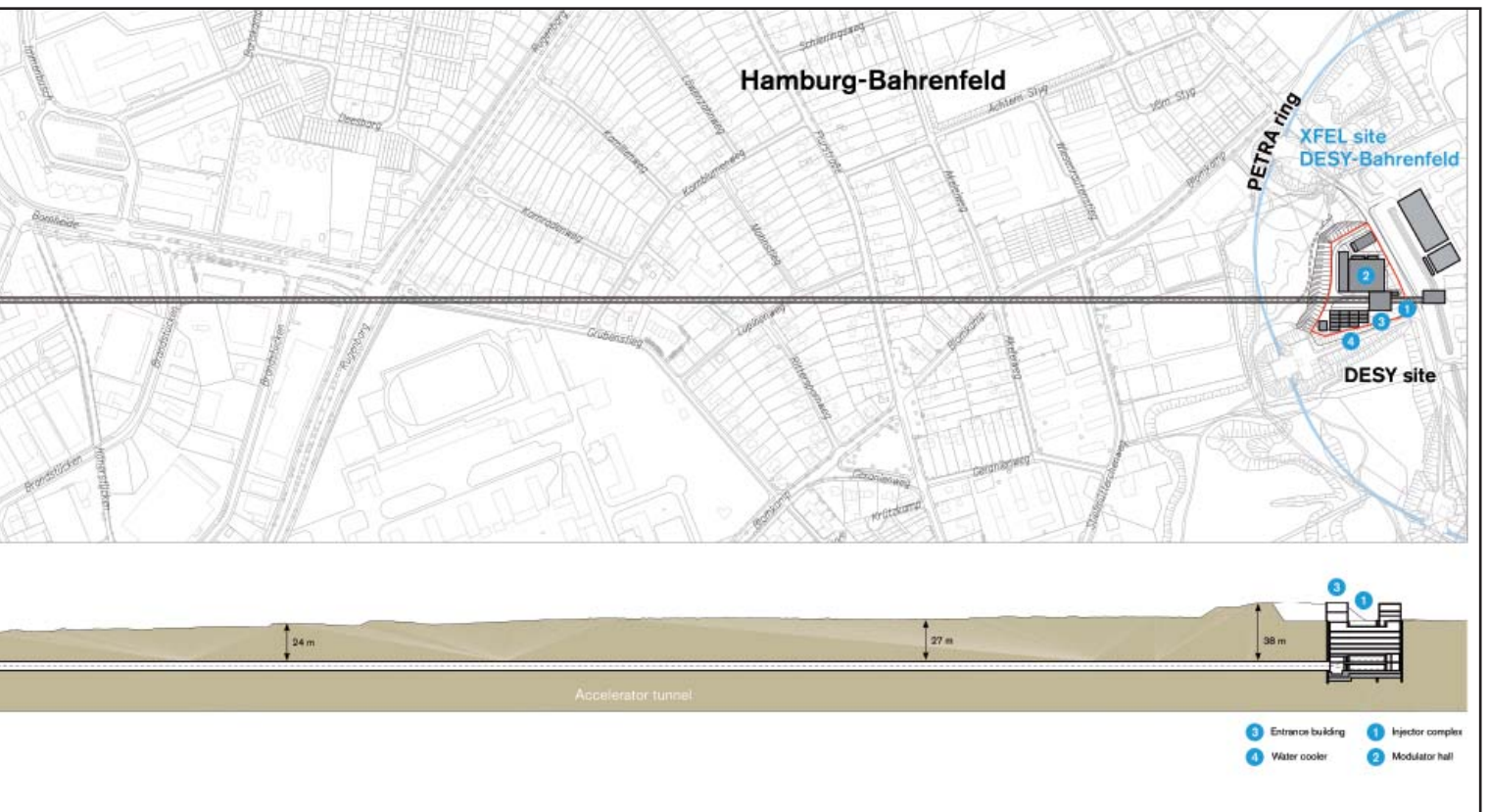
The new logo of the European XFEL: the three rectangles at the top represent the three stages of a free-electron laser user facility: (1) accelerating electrons, (2) generating bright flashes in undulators, and (3) using the flashes for science.



ments of fourteen nations have agreed to commit funding: China, Denmark, France, Germany, Greece, Hungary, Italy, Poland, Russia, Slovakia, Spain, Sweden, Switzerland and United Kingdom (in alphabetical order). The countries will determine shareholders of the to-be-founded European XFEL company being in charge of building, commissioning and operating the European XFEL facility. The shareholders will be institutes, science organizations and, in some case, the states themselves. DESY will become the German shareholder for the European XFEL GmbH. The shares will be distributed according to the relative contributions to the construction project with Germany and Russia being the largest contracting parties. At the meeting of the International Steering Committee on 22 September 2008, all delegations agreed on the formulations of the founding documents for the European XFEL GmbH.

These are the convention, regulating the relation between the participating countries, and the articles of association, regulating the operation of the European XFEL GmbH. After legal check and translation from English into six other languages, signing of the documents by ministers is scheduled for early 2009. As a next step the European XFEL GmbH can be founded with its council and international advisory bodies for accelerator, X-ray science and administrative and funding related issues.

The preparation of the documents, administrative issues and initial work on technical aspects of the photon beam systems were performed by the European XFEL project team, based at DESY. Through a very successful recruitment campaign, initiated in fall 2007, around ten engineers and scientists of wide-spread nationality joined the project in 2008. In addition,



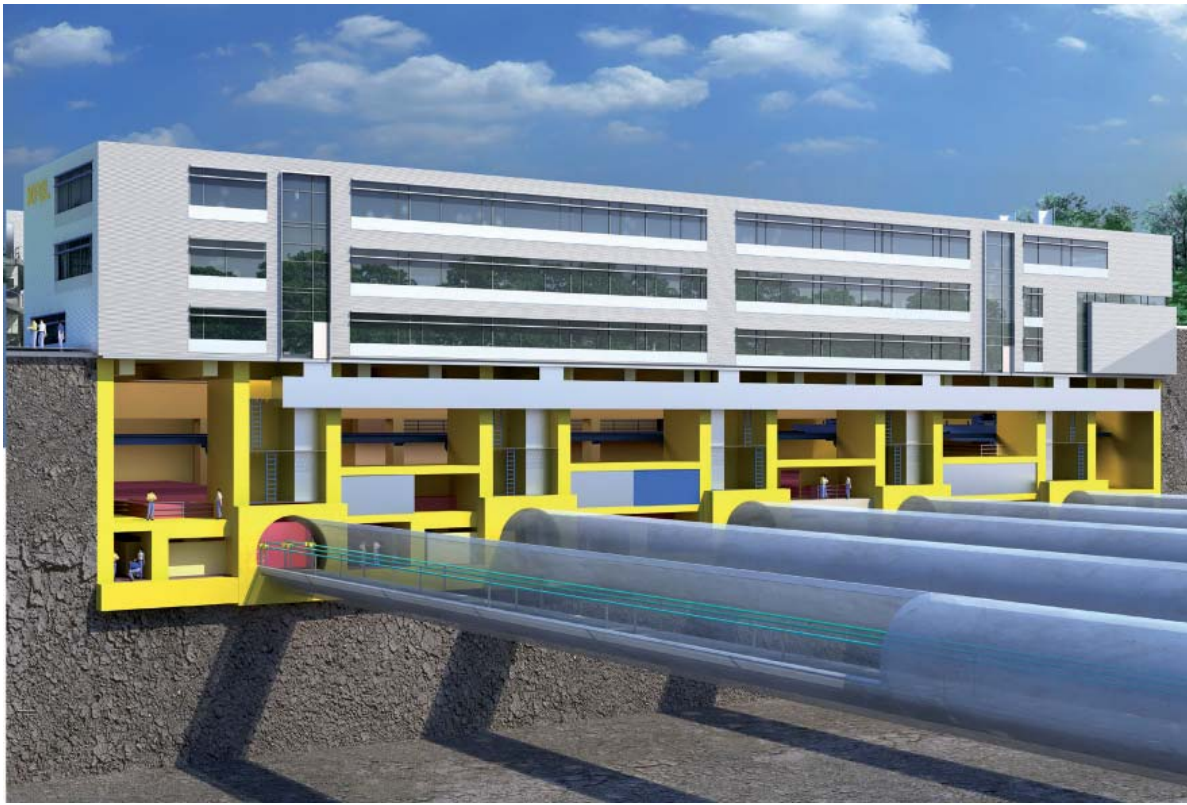


Figure 3

Model of the main building of the European XFEL on its Schenefeld site with the experiment hall (underground) and the office building including laboratories (above ground).

administrative staff, mostly coming from DESY, became members of the project. To face the necessity to build up staff for administrative and technical work, the Pre-XFEL grant, provided by the European Union for the preparation of large scale facilities projects in Europe, covers personnel costs and other items, e.g. renting office space.

Since on the future European XFEL campus in town of Schenefeld (next to Hamburg in Pinneberg district, Schleswig-Holstein) office space will not be available before 2013, it became necessary to find an interim accommodation. Two floors in an office building at Albert-Einstein-Ring 19 were rented, close to the DESY entrance at Luruper Chaussee. These offices provide space for up to 70 people and an extension is planned for 2009. Activities requiring laboratory and preparation space will continue to be carried out on the DESY campus, such as the assembly and measurement of the undulator segments and the testing and preparation of photon beam line and X-ray optics components.

In November 2008, the European XFEL got a new corporate design including the name, a logo, a new web site and templates for posters and presentations. In the last years, “XFEL” has become a generic term for X-ray sources based on free-electron lasers and electron linear accelerators. Therefore the planned XFEL facility was named “European XFEL”, and the research institution “European XFEL GmbH”. The newly designed logo, representing the three stages of an FEL user facility in a schematic way (Fig. 2), will help to increase the worldwide visibility of the European XFEL. The new website “www.xfel.eu” provides information on the facility, the project and the company.

Of major interest for the international partners are agreements on in-kind contributions to the project. These shall allow the partner countries to spend funds for personnel and construction through their administrations while participating in an international project that is not located in their own country. The interest of the European XFEL project in this far more complicated way of funding is the possibility to use experience and technical know-how of the partner institutes that otherwise might not be accessible. Proposals for in-kind contributions are evaluated by an In-Kind Contribution Review Committee in terms of appropriateness, technical feasibility and associated cost. Following recommendation by this committee, a contract is established defining the deliverables, milestones, timeline and the value of the contribution. The contributing partner has to receive funding for carrying out the committed work from its national funding agencies. The agreed value will be credited by the European XFEL GmbH to the respective country as part of its contribution, thereby following a timeline specified in the contract. The largest contribution in-kind will be the linear accelerator and its infrastructure.

After many years during which DESY has been leading the project, the European XFEL GmbH will be in charge after its foundation in 2009. Nevertheless, DESY will keep playing a special role which was defined in a collaboration agreement to be concluded with the European XFEL company. DESY is the largest partner and will host the project for the coming years. Furthermore, DESY’s contributions in the accelerator area, where many work packages are led and performed by the accelerator division of DESY, are of essential importance

to the European XFEL. DESY will lead and coordinate the European XFEL Accelerator Consortium that has been established to construct and commission the superconducting accelerator. The consortium integrates in-kind contributions by partner institutes from different countries. In the area of the photon beam systems specific contributions by DESY are planned. The development and construction of two-dimensional detectors and gas detectors for single-shot X-ray intensity and beam position diagnostics are most notable at present. Other contributions are expected to develop in the future.

The single largest budget item for the building of the European XFEL facility is the civil construction. In November 2008, the long-lasting and complex Europe-wide tendering procedure for the underground buildings (approx. 6 km tunnels with the associated shaft buildings and the 4500 m² underground experiment hall (Fig. 3)) was completed with the selection of two construction consortia, one for the injector complex and one for the linac tunnel and the distribution tunnels for the undulator and photon beamlines. On 12 December 2008, three contracts which sum up to a total amount of 240M€ were signed (Fig. 4). In parallel, preparatory work has already started: the access roads to the Schenefeld site were reinforced to carry heavy load trucks, the ground near the injector complex was cleared of trees and bushes, and the area on all three sites was surveyed. Initial major earth moving will commence in January 2009. The European XFEL is planned to operated as a user facility

similar to facilities like ESRF or PETRA III. To reach this goal a close connection to the future user community is necessary. The project therefore aims at stimulating the exchange and discussion with the users at the occasion of regular users' meetings and workshops focusing on scientific and instrumental aspects of specific experiment stations. The 2nd European XFEL Users' Meeting was held on 23-24 January 2008 and was attended by more than 200 people from 13 countries. Although there are still several years before start of operation, the long periods for development and procurement make it necessary to define the major requirements of the experiment stations soon. To start this refinement of parameters in fall 2008 the first two workshops for science and instrumentation of the Small Quantum Systems and the Single Particle and Biomolecule Imaging stations were held. Workshops for the other prioritized experiment stations will follow in 2009. The results from these workshops will provide valuable input for the development of a conceptual design for the FEL beam transport and the experiment stations. Experts from the user community shall be asked to participate in the review of the beamline and instruments design.

With major milestones achieved in 2008 the European XFEL is now ready for taking off. ●

Contact: Massimo Altarelli (European XFEL/DESY),
massimo.altarelli@xfel.eu or contact@xfel.eu, website: xfel.eu



Figure 4
In December 2008, the major contract for the underground civil construction works were signed at DESY. On the left: representatives of the two consortia (Züblin Aug. Prien and HochTief/Bilfinger Berger), on the right: representatives from DESY and the European XFEL Project Team.



New Technologies and Developments.

- **Beamline enhancements and photon diagnostics at FLASH** 82
- **Undulator development for the European XFEL** 85
- **Special X-ray monochromators for PETRA III** 86
- **High-power photon slits and shutters** 88
- **Generating brilliant beams** 90
- **Undulator demagnetization in LINAC based FELs** 92
- **Controlling experiments** 93
- **Advanced detection** 94

Beamline enhancements and photon diagnostics at FLASH.

A facility growing with user demands

Raman Spectrometer at beamline PG1

In 2008, the VUV-Raman spectrometer was completed after 4 years of design, manufacturing, and alignment tests by the University of Hamburg (group Rübhausen) at the PG 1 beamline in collaboration with DESY (Fig. 1). First successful experiments were performed in summer on excitons in cuprates. Recently, the alignment of the instrument was improved significantly to allow studies of low-energy quasi-particle excitations between 20 meV and 300 meV Raman shift with a resolution of about 4.4 meV of the Raman instrument at 80 eV incident photon energy.

At the same time, the performance of the PG beamlines was significantly improved to reach a resolution of greater 8000 and smaller foci at the experimental stations. Further improvements of resolution and efficiency of the Raman instrument and the PG beamlines are planned for 2009. The PG1 beamline will be complemented with installations enabling pump/probe experiments with the optical lasers.

Collaboration: University of Hamburg, DESY

Contact: Michael Rübhausen (Uni Hamburg),

ruebhausen@physnet.uni-hamburg.de

Natalia Guerassimova (DESY-HASYLAB), natalia.guerassimova@desy.de

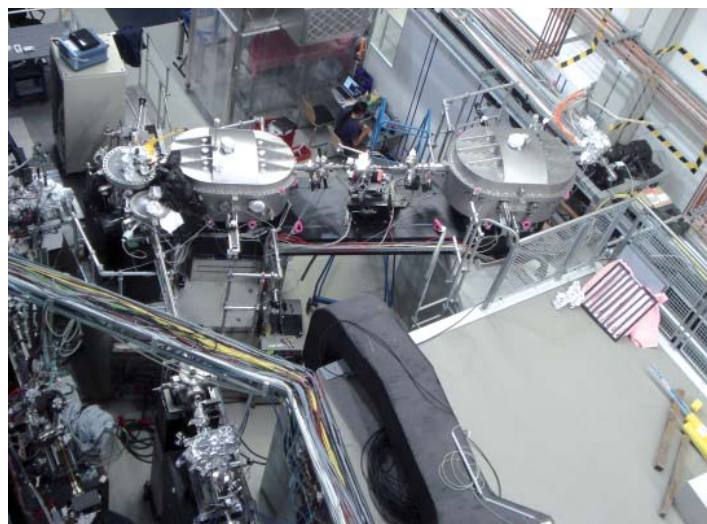


Figure 1

VUV-Raman spectrometer (monochromator/spectrograph, double instrument) for the investigation of low energy quasi-particle excitations using high resolution ($< 5\text{meV}$) and high stray-light rejection at the PG1 beamline.

THz beamline for THz-XUV pump-probe experiments

The new THz beamline transports Fourier-limited, ultra short, intense THz pulses generated by a purpose-built undulator into the experimental hall of FLASH and allows THz pump - XUV probe experiments (M. Gensch et al., *Infrared Phys. Technol.* 51, 423 (2008)). The unique properties include a natural synchronization to the XUV pulses due to the cascaded undulator design in the accelerator tunnel (Fig. 2, a and b), carrier envelope phase (CEP) stability of the THz pulses and pulse energies in the μJ regime that rival those of existing state-of-the-art THz FEL facilities. The construction of the beamline was completed in January 2008 and it is since under intensive commissioning to study beamline properties such as pulse duration, pulse energy or spectra for typical machine conditions and to develop appropriate photon diagnostic tools for the planned user facility. Figure 2c shows a first pulse duration measurement by NIR/THz cross-correlation. Already these preliminary measurements show that the beamline works up to theoretical prediction. A successful pilot THz pump - XUV probe experiment was carried out in collaboration between DESY and the University of Hamburg. The THz beamline will be available for FLASH users after the shutdown in 2010.

Collaboration: BESSY, DESY, DLR, FZ Dresden, University of Hamburg

Contact: Josef Feldhaus (DESY-HASYLAB), josef.feldhaus@desy.de

Michael Gensch (DESY-HASYLAB), michael.gensch@desy.de

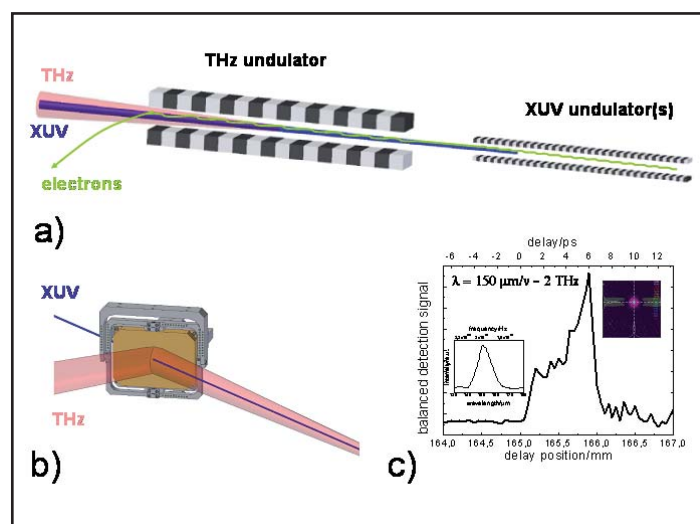


Figure 2

Cascaded undulator design in the FLASH tunnel (a), separation of THz and XUV beam at the first mirror in the THz beamline (b) and pulse duration measurement by NIR/THz cross-correlation (c).

New developments for the optical laser

The optical pump-probe laser system at FLASH (cf. HASYLAB Annual Report 2005, p.165) was upgraded with a second power amplifier – a Hydra-25 manufactured by Coherent Inc. (Fig. 3). This amplifier provides a several hundred times higher pulse energy than the initial optical parametric chirped pulse amplifier (OPCPA) albeit with a maximum repetition rate of only 10 Hz, as compared to 800 pulses at 5Hz = 4000 pulses per second for the OPCPA. The synchronisation of the optical laser pulses to the FLASH pulses is guaranteed by using the existing Ti: sapphire oscillator as the seed. The Hydra-25 relies on the chirped pulse amplification principle. The pulses are first amplified in a regenerative amplifier to a power level of 5 mJ and subsequently in a two-pass amplifier to 20 mJ. After the compressor a minimum pulse duration of 120 fs is available.

With pulse energies in the mJ range available, the bandwidth of feasible pump-probe experiments was tremendously broadened to e.g. highly nonlinear two-colour atomic and molecular physics experiments, solid state ablation, or plasma physics. Altogether, the number of shifts at FLASH using the optical pump-probe laser increased to more than 50 % over the last two years. To satisfy growing user demands, a development program has been started to build a laser system that will provide the FLASH bunch train pattern with more than 1 mJ per pulse and sub 10 fs pulse duration.

Contact: Stefan Düsterer (DESY-HASYLAB), stefan.duesterer@desy.de
Harald Redlin (DESY-HASYLAB), harald.redlin@desy.de



Figure 3
New Hydra-25 laser. The red line shows how the output beam of Hydra is coupled into the existing setup for beam control (delay line, attenuator, polarization rotation, safety shutter).

Wave-front sensors for XUV beamline alignment

Wave-front (WF) sensors were successfully used for fine alignment of FLASH beamlines and proved a valuable tool for observing the FEL beam quality as well as the performance of optical elements, such as metal filter foils or the gas attenuator. Beamline alignment was performed using an Imagine Optic WF sensor, while at the same time a very compact sensor developed by LLG was tested for future use by user groups. The Hartmann type sensors are largely independent of wavelength in the soft X-ray region and capable of measuring the wave-front of individual FEL pulses. In a Hartmann sensor, the incoming photon beam is divided into a large number of sub-rays in a pinhole array and monitored in intensity and position on a CCD camera; the incident wave-front is determined by comparison to a perfect spherical wave generated behind a pinhole. Ray tracing in upstream direction based on the measured wave-fronts is used to determine focal spot size and position. Figure 4 shows the beamline performance achieved for beamline BL2. The wave-front was optimized starting from $\lambda/1$ (RMS) at 27 nm and a focal spot size of 54 μm (FWHM) to $\lambda/9$ and a 30 μm spot size. Beamline BL1 was optimized also to $\lambda/9$ and 86 μm (FWHM) focal spot size.

Collaboration: DESY, Imagine Optic, Laser Laboratorium Göttingen (LLG)
Contact: Elke Plönjes (DESY-HASYLAB), elke.ploenjes-palm@desy.de
Kai Tiedtke (DESY-HASYLAB), kai.tiedtke@desy.de

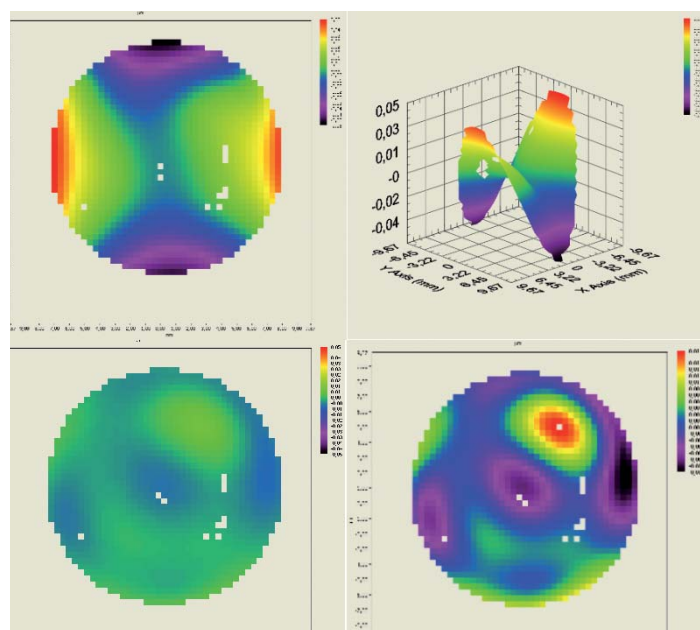


Figure 4
Top: BL 2 wave-front before alignment showing strong astigmatism (left: 2D, right: 3D); bottom: after alignment with only higher order aberrations remaining (left: same colour scale as top, right: colour scale optimized for improved WF).

Photon beam position monitor

The spatial and angular stability of the FEL radiation is crucial for the photon beam transport and focusing at the user experiment. This requires the use of beam position monitors which operate in parallel and in a non-destructive way. At FLASH, state-of-the-art photon beam position monitors have been successfully commissioned and implemented into the DOOCS control system during 2008. These detectors are part of the gas monitor detector system (GMD) integrated in the FEL beam-line as permanent devices.

The beam position monitor is schematically shown in Fig. 5. When an FEL pulse passes through the ionization chamber of the detector, the gas inside is ionized, and an electric field accelerates the ions upwards and the electrons downwards to split electrodes. The beam position is obtained from the normalized ratio of the electron and ion currents measured at the different electrodes. Two pairs of mutually perpendicularly oriented GMDs, 15 m apart, allow the determination of the vertical and horizontal position as well as the angle of the FEL photon beam.

Collaboration: DESY, PTB, IOFFE Institute

Contact: Kai Tiedtke (DESY-HASYLAB), kai.tiedtke@desy.de

Ulf Fini Jastrow (DESY-HASYLAB), ulf.jastrow@desy.de

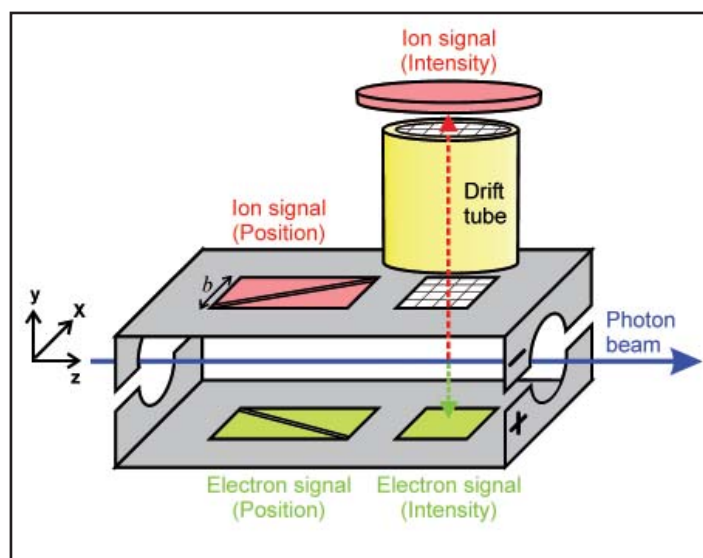


Figure 5

Schematic of the gas photon beam position monitor. The split electrodes on the left allow to detect the beam's center of mass.

Spectrometers

Knowledge of the precise photon energy of each individual FLASH pulse is essential for a variety of experiments, such as investigations of narrow atomic or molecular resonances or phase transitions. Also, online photon wavelength measurements could be used by the operators of the FEL machine to tune the FLASH beam. Currently, the photon energy is measured by redirecting the beam into a high resolution spectrometer and thus, it cannot be monitored simultaneously to the experiments. Two projects are developing spectrometers which provide real-time photon beam energy data. The online photo-ionization spectrometer (OPS), currently under development, is a gas-filled chamber that contains ion and electron time of flight (TOF) spectrometers. It will be used out of beam focus to ensure that the energies are read at intensities where only single-photon ionizations can occur. The second spectrometer (Fig. 6) is based on using the first diffraction order of a variable line spacing (VLS) grating inserted in place of a beamline mirror to determine the photon wavelength, while the main beam in zeroth order is reflected towards one of the experimental stations. Both spectrometers can be used parasitically during an experiment. ●

Collaboration: BESSY, DESY, PTB, University of Hamburg

Contact: Rolf Treusch (DESY-HASYLAB), rolf.treusch@desy.de

Kai Tiedtke (DESY-HASYLAB), kai.tiedtke@desy.de

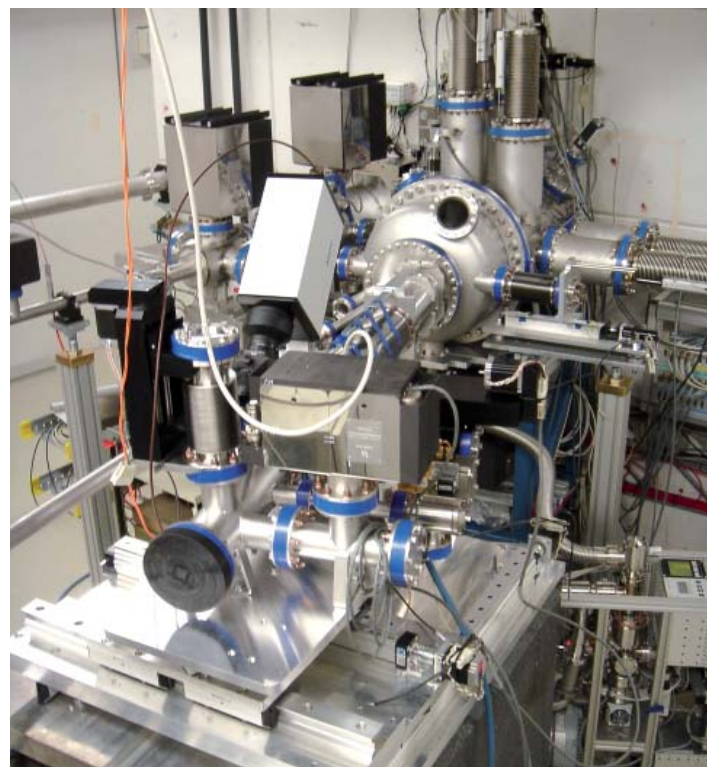


Figure 6

VLS spectrometer installed in the beamline.

Further information

K.Tiedtke et al., Gas detectors for x-ray lasers, *J. Appl. Phys.* 103, 094511 (2008).

Undulator development for the European XFEL.

A permanent magnet phase shifter

The European X-Ray Free Electron Laser (XFEL) will need very long segmented undulator systems [1]. They are made up of up to 42 undulator cells, each consisting of a 5m long undulator segment and a 1.1m long intersection unit. The radiation wavelength of these systems will be tunable via gap adjustment. In order to have proper phase matching between the radiation field and the micro-bunched electron beam, phase shifters are needed to delay the electron beam such that there is no change of the ponderomotive phase in different undulator segments.

A phase shifter suitable for the XFEL has to meet several requirements and boundary conditions:

- > For economic reasons only one standard device should be developed.
- > The worst case phase delay conditions are set by undulator SASE 3 when operated at 1.6nm, 17.5 GeV. Continuous tunability from 4 to 1.6nm requires a maximum delay of up to 720°.
- > The device must be neutral to the electron beam and cause no deflection within very stringent limits.
- > There must be no readjustments required once a device setting was changed since this would lead to very long tuning times for a complete system.
- > The total length is limited to 230mm.
- > The fringe field level must be low enough so that there is no interference with adjacent components such as undulator end plates or quadrupoles.

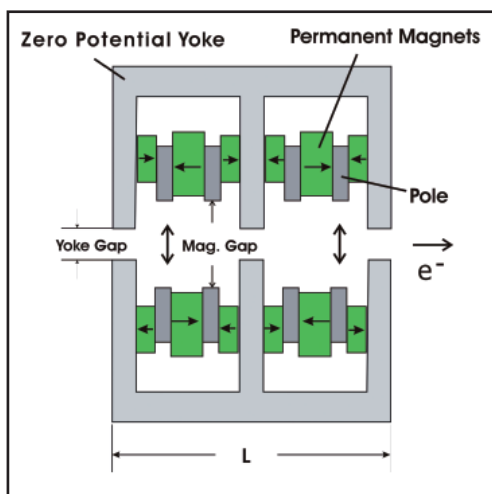


Figure 1
Magnetic principle of the phase shifter.

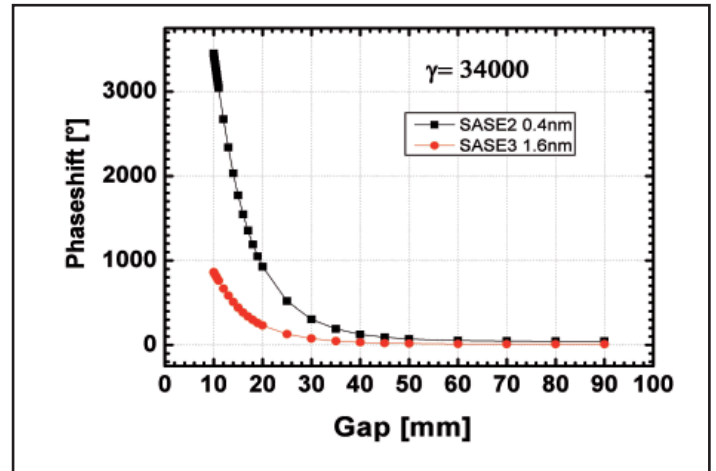


Figure 2

Total phase shift as a function of the gap. The red dotted curve shows that 820° at 1.6 nm can be reached.

Based on the above requirements a prototype was developed [2] which is shown in Fig. 1. The device is 230mm long. The magnetic active parts are encased inside two E-shaped zero potential soft iron yokes resulting in a low stray field level on the outside. All poles in this device have the same magnetic environment and thus behave identical. This supports very low total field integrals. In addition, the pole height can be tuned. For fine adjustments to minimize field errors, each pole can be shifted and tilted individually.

Figure 2 shows the dependence of the total phase delay as a function of the magnetic gap. For the SASE3 undulator case (1.6nm, red dots) a maximum of 820° is obtained. The phase delay increases for shorter wavelengths, as is the case for undulator SASE2 (black dots). The total field integral excursions were measured to be 0.003 Tmm (horizontal) and < 0.02 Tmm (vertical; resolution limited value). The fringe field level was below 0.1mT as measured 30mm outside the device. This prototype fulfills the requirements for use with the XFEL undulator systems as given above. However it was built without compromise and needs a profound design review before serial production. ●

Collaboration: DESY, Institute of High Energy Physics, Beijing, P.R. China
Contact: Joachim Pflüger (DESY-FS Undulator Systems), joachim.pflueger@desy.de

References

1. M. Altarelli et al., The European X-Ray Free-Electron Laser Technical Design Report, ISBN 3-935702-17

2. H.H. Lu, M.T. Wang, J. Zhuang, D. Wang, J. Pflüger, P. Neumann, M. Rueter, T. Vieltitz, Proceedings of FEL 2008, August 24-29, 2008 (Gyeongju, Korea)

Special X-ray monochromators for PETRA III.

Preservation of beam quality

The preservation of the exceptional beam quality provided by PETRA III undulators calls for ambitious technical solutions in the realization of the optical components in the beamline. Liquid nitrogen cooled X-ray monochromators with a novel Bragg angle drive mechanism and other challenging technical options were developed. The monochromator design also accounts for the “canted undulator” geometry, i.e. two beamlines with a narrow separating angle, which imposes additional constraints.

Direct drive monochromators

The high heat load X-ray monochromator concept is based on a central rotation axis and a fixed-exit beam. The Bragg axis is directly driven by an ex-vacuo 3-phase torque motor controlled by a high resolution incremental encoder system in-vacuo. The drive is connected via a ferrofluidic rotary feedthrough which also guides the liquid nitrogen tubing for the crystal cooling. There are no further couplings or gearboxes. This rigid drive train provides excellent stability, reproducibility, and resolution of the Bragg angle setting. So far, two prototypes were built by FMB Oxford. In a collaboration with the ESRF, one was installed at ID6 (ESRF) to test its high heat load behaviour and beam stability performance (Fig. 1). The other one remained at DESY to study the mechanical stability and to test the control system. Both these devices and further six systems will later be installed at PETRA III beamlines.

The prototype system revealed excellent stability of 0.026 arcsec (RMS) with a numerical resolution of 0.018 arcsec/step (Fig. 2), which is equivalent to 200000 encoder steps/degree. The read-out of the internal encoder was in agreement with an independent external measurement using a high-resolution autocollimator. Another special design feature is a piezo-driven z-axis of the second crystal, additional to the usual pitch and roll adjustments (both piezo-driven). Following a coarse alignment by stepper motors, this new degree of freedom allows a fine tuning of the vertical beam exit position while keeping the maximum of the rocking curve.

At PETRA III, the space available for the monochromator system depends on its position from the source and the type of the beamline, i.e. single or canted undulators. In the latter case, one of the undulator beams may pass through the other system requiring a jacket pipe surrounding the second beam pipe (Fig. 3).

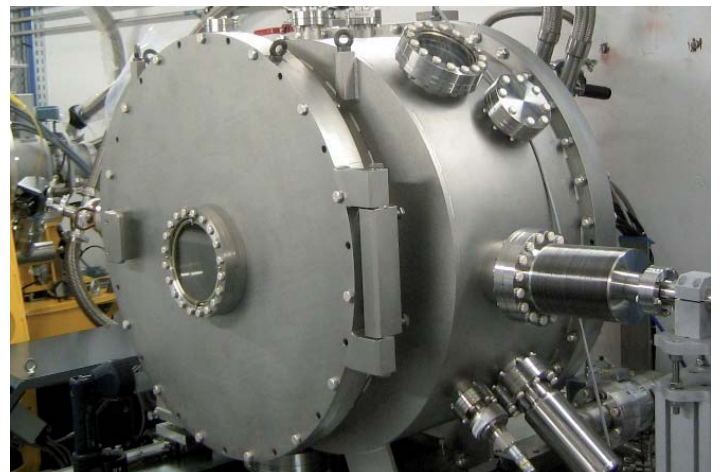


Figure 1

PETRA III monochromator installed for testing at ID6 (in collaboration with the ESRF).

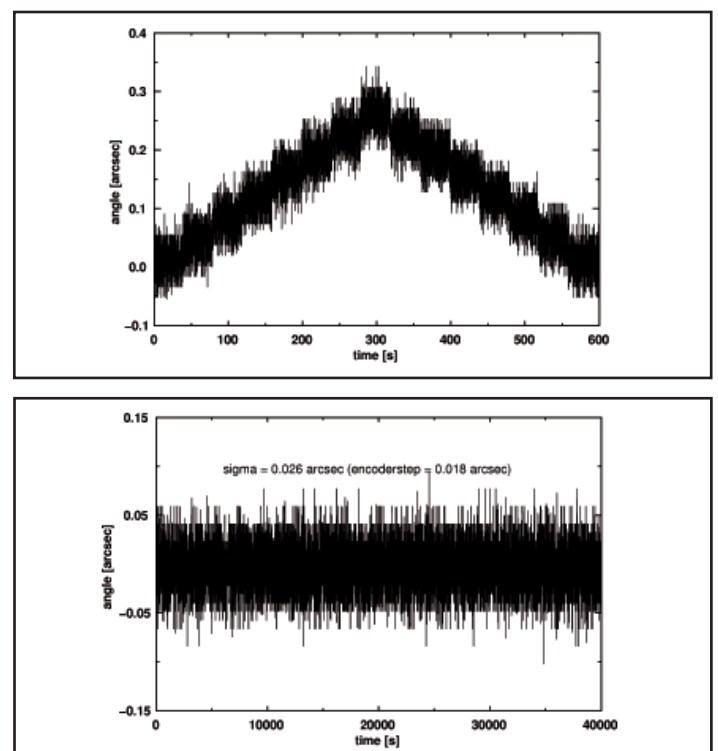


Figure 2

Measured step resolution of the directly driven Bragg angle axis. Top: servo encoder angle read-out vs. step rotation of the Bragg axis (two encoder steps each, equally spaced in time), bidirectional motion. Bottom: long term stability at fixed Bragg angle.

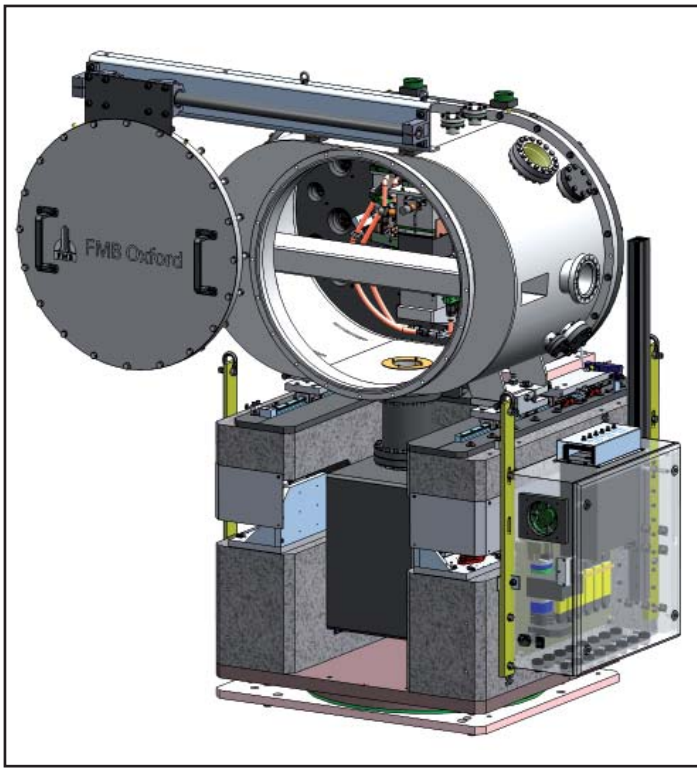


Figure 3

3D view of the PETRA III monochromator for a canted undulator beamline (courtesy of FMB Oxford). The rectangular jacket pipe allows the installation of the beam pipe and the operation of the second undulator beamline without breaking the vacuum of the monochromator and/or the second beamline.

Large Offset Monochromator

There are several concepts to arrange two canted undulator beamlines in order to provide maximum flexibility for each. One solution is to keep the angular separation of 5 mrad between the photon beams in the horizontal plane and separate the beam paths in the vertical plane. The most sophisticated system at PETRA III is a Large Offset Monochromator (LOM, Fig. 4) which vertically displaces the monochromatic beam by 1.25m resulting in a beam height of 2.65m at the experiment which resides on an elevated platform above the other beampath.

The large vacuum system consists of two rectangular vessels supported by a granite base. Inside each vessel, a crystal system is traveling along a high-precision linear rail to maintain the fixed beam exit. All degrees of freedom of the two crystal systems are controlled by stepper motors and multi-axes piezo-driven tables in order to maintain the optimum rocking curve and beam position under all operation conditions. Additionally, an integrated laser based alignment system will be used to stabilize the monochromatic beam independent of the X-ray beam monitors. ●

Contact: H. Schulte-Schrepping (DESY-FS Beamline Technology), horst.schulte-schrepping@desy.de

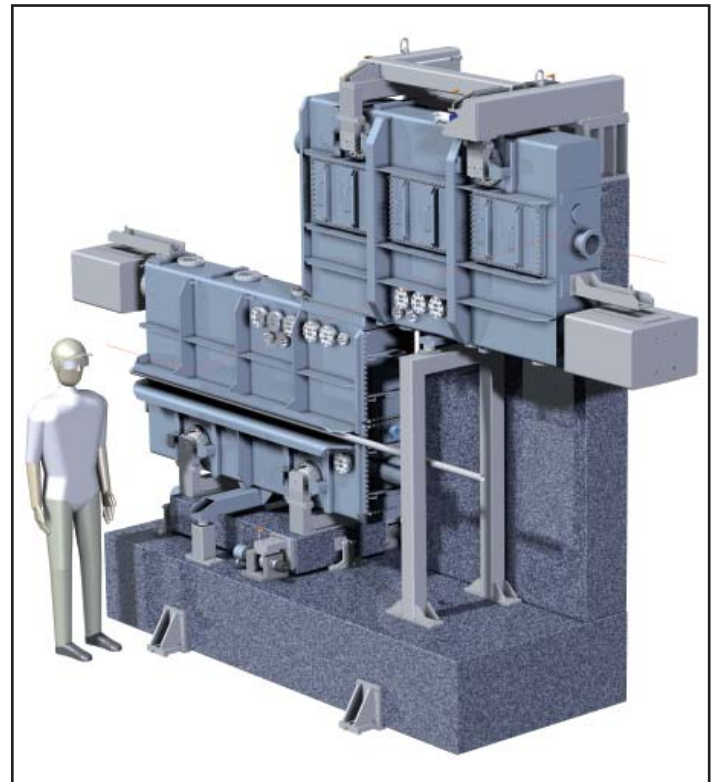


Figure 4

3D model of the Large Offset Monochromator (LOM) at PETRA III. The monochromatic beam enters from the left at 1.40m above ground and exits at 2.65m. Also shown is the beam pipe of the other canted undulator beamline.

High-power photon slits and shutters.

Developments for PETRA III frontends

The conversion of the PETRA storage ring into a brilliant hard X-ray light source poses challenges to the design of the beamline transport system. One of these challenges is to supply 14 beamlines with the extremely collimated undulator radiation while fulfilling the stringent personal safety requirements combined with easy controllability. In order to access beamlines and experiments while the machine is operating, the undulator beam and the Bremsstrahlung background have to be blocked inside the storage ring tunnel. This is achieved by a combination of a primary photon shutter (PS)

the primary beam power. The cooling channels are machined to wind in a spiral around the central copper block which is brazed into a stainless steel body. A tungsten disk behind the jaw serves to absorb most of the highly energetic X-rays thereby also reducing the background radiation at the experiment. The slit jaws are being adjusted by horizontal slides combined with two coupled wedge-driven lifting tables. The centre slide controls the slit width by driving a pneumatic cylinder, which is part of the coupled drive for the lifting tables and controls the “open” and “closed” state of the slit system. The two outer

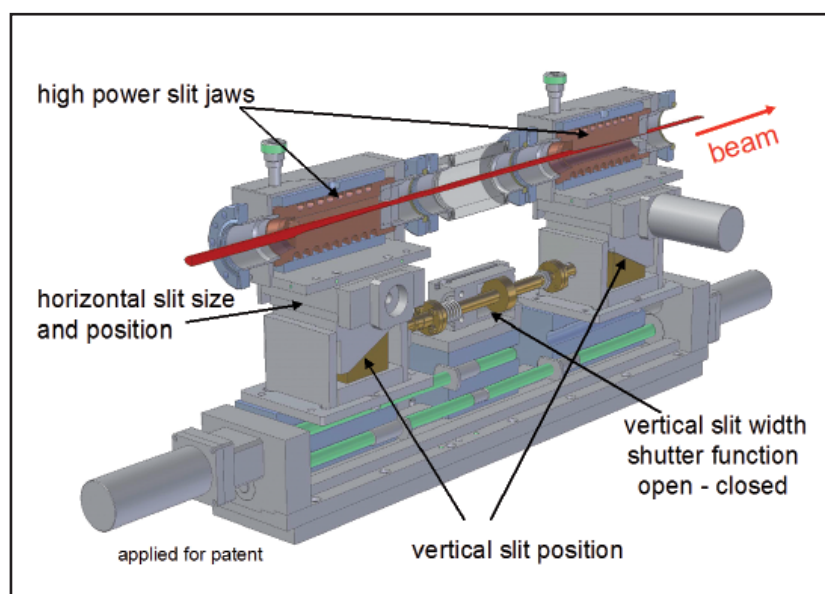


Figure 1
High power slit system and photon shutter for PETRA III undulator beamlines.

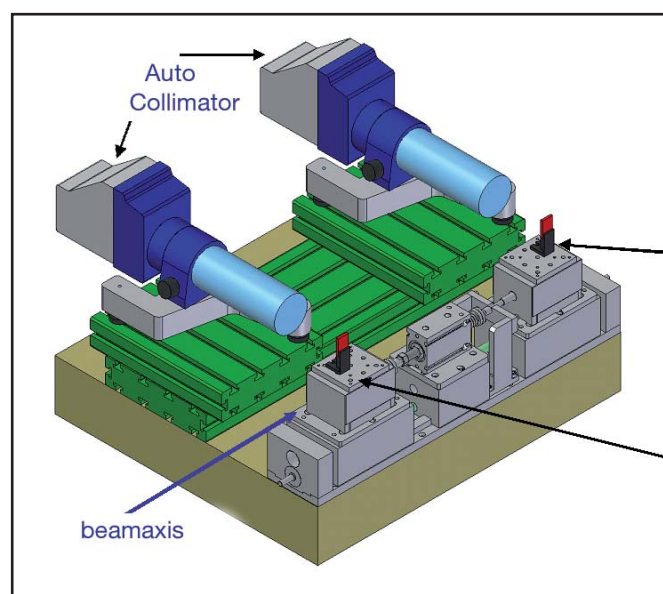


Figure 2
Measurement of the roll angle of the vertical slit jaw drives.

and a secondary beam-shutter (BS) which are both controlled by the personal safety interlock. The direct undulator beam with its high power density is stopped by the PS which is the main component of the machine protection system. A fail-safe operation of the PS is mandatory to avoid any damage of the BS, which is the critical component of the radiation safety system. In order to achieve this in an easy controllable way, a so-called „sacrificial absorber“ is inserted between PS and BS to detect a not fully closed PS.

The high power photon shutter (Fig. 1) is designed as a slit system which additionally acts as an absorber to block the direct undulator beam. The upper and lower jaws consist of an inclined water-cooled absorber - made out of GlidCop® - which accepts

slides are horizontally moved by a left-right hand spindle translated by the wedges into a vertical motion of both slits. Obviously, the precision of this combined vertical movement is critical regarding the roll angle around the beam axis. This quantity was measured independently for both jaws during travel using autocollimator systems (Fig. 2 right), proving that the stringent specifications are fulfilled. The additional shutter function of the device is achieved by the integrated pneumatic cylinder (see Fig. 1). The overlap of the slit jaws in the closed state (~1mm) is critical for the thermal protection of the downstream beamshutter. Any condition of non-fully overlapping slits has to be detected in a simple failsafe way. This requirement is realized using a sacrificial absorber in front of the BS which is

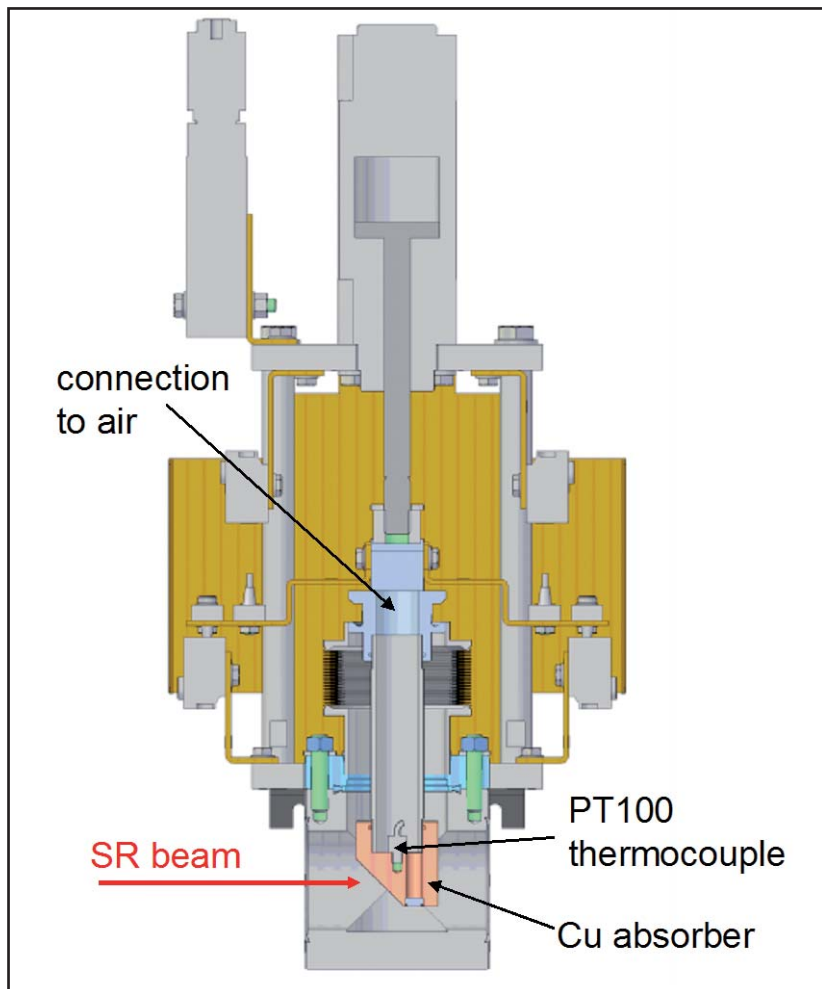
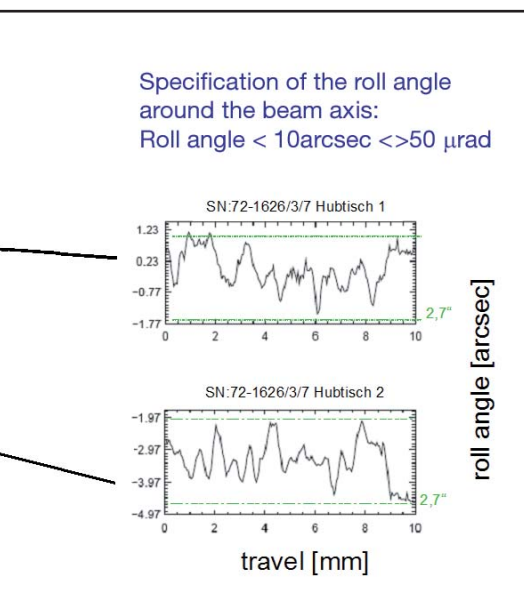


Figure 3
Cross section of the sacrificial absorber.

moved into the beam before the BS is permitted to close. A cross section of the sacrificial absorber is shown in Fig. 3. It consists of a Cu absorber brazed on a pipe connected to air. A bellows allows to move the sacrificial absorber into the beam. In a worst case scenario, the PS is not fully closed and the undulator beam would hit the copper block of the sacrificial absorber and ultimately burn a hole into it. This would cause venting of the beamline and consequently stop the beam operation before the BS is damaged. While this procedure is failsafe, it is of course not the desired scenario. In order to detect a non-closed PS before melting the sacrificial absorber, the absorber temperature is monitored by a thermocouple which will trigger an opening of the undulator in case of a

suspicious temperature increase. In order to precisely calibrate the time constants of the temperature rise, test experiments were carried out at the undulator beamline ID6 of the ESRF using a fast photon shutter for precise timing. Based on these data, it can be proven that there is sufficient time for the undulator to reach a powerless state before the temperature of the absorber becomes too high. ●

Contact: Ulrich Hahn (DESY-FS Beamline Technology),
ulrich.hahn@desy.de

Generating brilliant beams.

Undulators for PETRA III

PETRA III will have various undulators tailored to the specific needs of the experiments [1]. Ten out of the 14 undulators will be 2 m long planar devices with different period lengths (Fig. 1). The standard undulator (U29) is characterized by full energy tunability and a 1st harmonic position at 3.450 keV (29 mm period length, $K_{\max}=2.2$). Lower photon energies down to 2.4 keV are needed by certain X-ray spectroscopy techniques and will be served by the spectroscopy undulator (U32) having a larger period length. A short period device (U23) is optimized for hard X-ray scattering experiments and provides tunability above the 3rd harmonic. In the long straight section before the new octant, a longer version of U32 (5+5 m) with 12.5 mm minimum gap will be installed with the possibility to double the undulator length at a later stage.

This series of standard undulators is complemented by two specialized devices, one for the very hard X-ray regime, the other for XUV techniques. X-rays up to 300 keV as needed for the High Energy Materials Science Beamline will be provided by a 4 m long in-vacuum undulator (U19) having a period length of 19 mm. A minimum gap of 7 mm can be realized for the initial operation phase of the machine. This undulator will mainly be operated at high harmonics and is tunable above the 5th harmonic at 50 keV. The spectral characteristics are given in Figure 2. In collaboration with BESSY, an APPLEII undulator (UE65, 65.6 mm period length) is being built for the Variable Polarization XUV Beamline at PETRA III. In the circular mode, it will cover the energy range from 245 eV to 2.5 keV in the 1st harmonic and provide a high degree of polarization in the entire energy range [2].

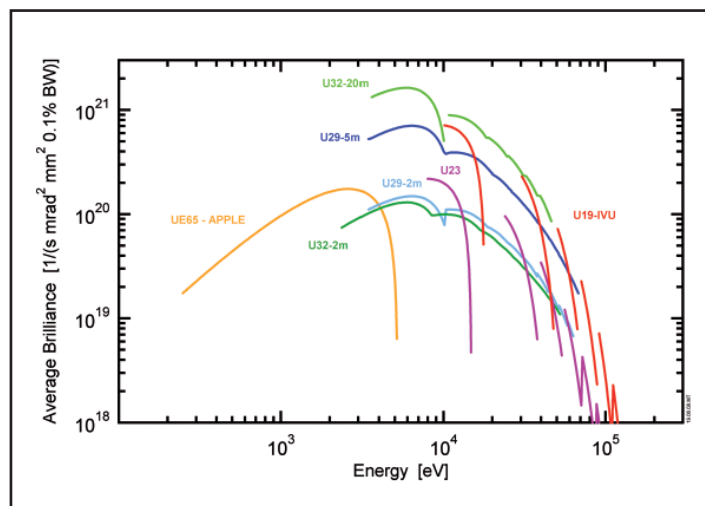


Figure 1
Spectral characteristics of PETRA III undulators.



Figure 2
A 2 m long undulator for PETRA III at the magnetic measurement bench.

Undulator pole alignment

The support frame of the 2 m long undulators is a progression of the common development of PETRA III and XFEL prototype undulators, and the mechanical design of the magnetic structure is an advancement of the well-proven concept used for the FLASH undulators. A new design feature, which allows very accurate fine-tuning of the magnetic field, is the possibility to tilt individual poles (up to 2 mrad), in addition to the height adjustment (up to 300 μm) (Fig. 3). For the tuning process, it is important to start with a well-defined initial configuration of the magnet structure. By means of an adjustment gauge with two micrometer dials per pole. The initial pole overhang and tilt are set to the nominal values with high accuracy (10 μm , 0.25 mrad) relative to the non-magnetic support structure.

The initial trajectory is scanned by a Hall-probe and residual errors are being assigned to the respective poles for which the necessary pole shift or tilt is calculated. For the vertical field component, an optimization of the local K-parameter is used. It is corrected in each half period of the undulator by shifting the pole vertically, thereby improving the horizontal trajectory as well as the phase shake (Fig. 4) reaching final values of only 1.2° (rms) for the phase shake and 10 Tmm² (rms) in the second field integral.

In a second step, the vertical trajectory is adjusted by pole tilting. The following adjustment comprises the correction of multipole components which are probed by wire scans to measure the

first and second field integrals. With the extended pole adjustment measures, multipoles can partly also be corrected by pole tuning rather than conventional shimming which is then later applied in addition.

Finally, the end poles of the undulator structure are trimmed to reduce the gap dependency of the first field integral. The residual field integral variations are in the order of 0.1 Tmm over the entire gap range and will be compensated by small air coils.

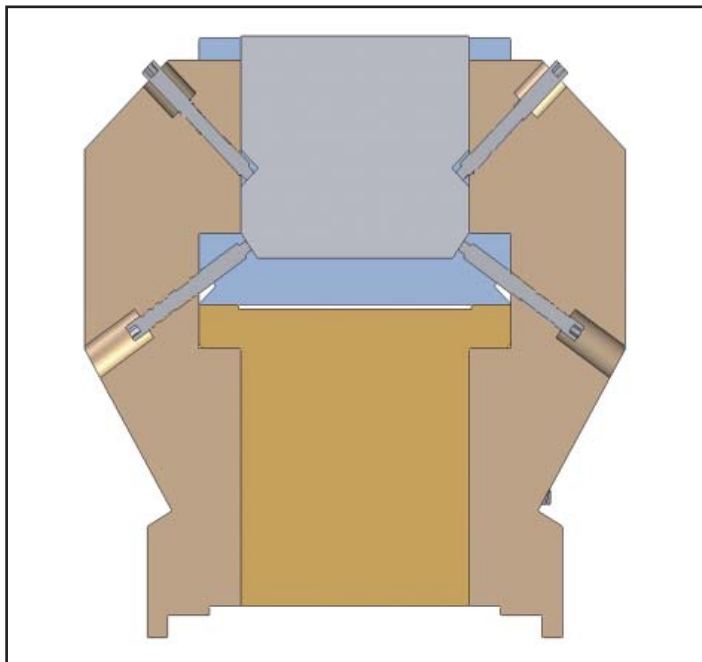


Figure 3
Schematic of the pole height and tilt adjustment by regulation screws, used for the magnetic fine tuning.

Control System

The undulator control system is based on off-the-shelf components commonly used for industrial automation. The use of the high performance real-time fieldbus EtherCAT makes it possible to implement both the numerical control (NC) and the programmable logic controller (PLC) as software tasks on a standard industrial PC instead of using expensive dedicated hardware. The gap drive consists of two independent servo axes for each magnet girder to allow for maximum flexibility, needed e.g. for tapering or beam height adjustment. Each axis is equipped with a multi-turn absolute rotary encoder to ensure an operational

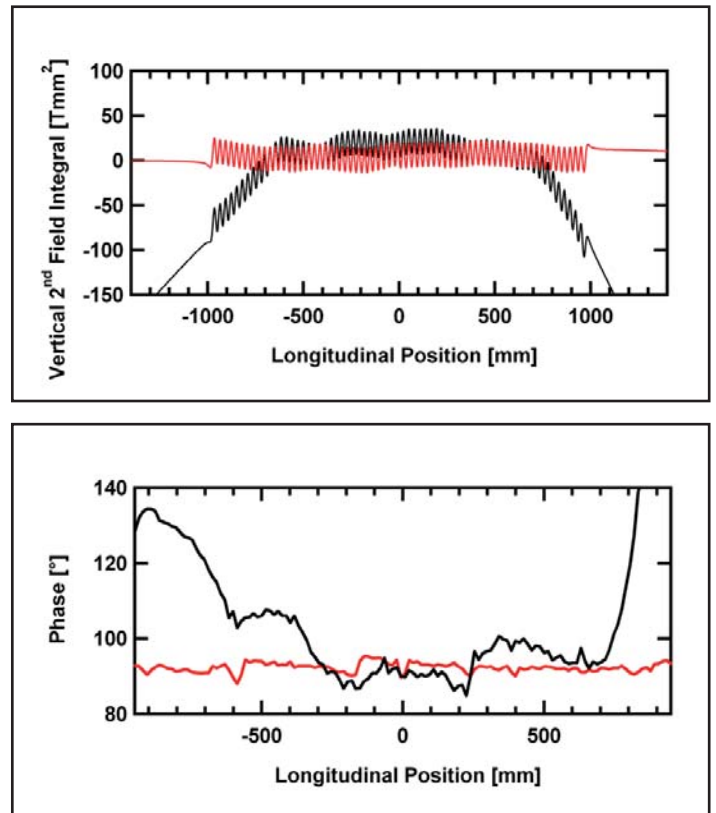


Figure 4
Vertical second field integral (top) and phase shake (bottom) after local K correction (red curves) compared to the initial state (black curves) of a 2 m undulator (U29) at 12 mm gap.

reliability even after electrical power loss. The four axes are synchronized electronically via the NC. The PLC monitors all mechanically relevant operating conditions like the tilt of girders or limit switches. It also controls peripheral components such as power supplies for corrector coils and provides interfaces for communication with the global and beam line control systems. ●

Contact: Markus Tischer (DESY FS Undulator Systems)
markus.tischer@desy.de

References

1. M. Barthelmess et al., "Status of the PETRA III Insertion devices", Proc. EPAC08, 2320 (2008).
2. J. Bahrtdt et al., "APPLE Undulator for PETRA III", Proc. EPAC08, 2219 (2008).

Undulator demagnetization in LINAC based FELs.

Long term experience at FLASH

In Linac based FELs the electron beam properties and the undulator performance are both crucial for the FEL process. The permanent magnets (PM) used in these undulators are usually made of NdFeB and it is well-known that this material is prone to radiation damage caused by energetic stray electrons hitting the vacuum chamber of the accelerator. While this is a highly relevant factor for the upcoming LINAC based light sources, little experience existed so far concerning the quantitative impact of this process. FLASH has been operating since a number of years and special measures were taken to both monitor and minimize the radiation dose on the undulator system providing valuable information for other facilities as well.

At FLASH, several measures were taken to minimize radiation damage: a collimator system in front of the undulator limits the phase space of the electron beam and a detection system along the undulator monitors the Bremsstrahlung and secondary particles generated by energetic electrons interacting with the walls of the vacuum chamber. Right from the beginning of the FEL operation in 2004, special procedures were established to monitor the radiation exposure and the evolution of PM degradation. These are basically twofold: firstly, a radiation damage threshold dose level for the undulator was determined. For this purpose, a dosimetry undulator (DU) was built and installed some meters before the main undulator system at a location with a considerably elevated radiation level. The DU is a short undulator (sketched in Fig.1) having three poles, one full (green) and two half poles (red, blue). It uses the same magnets and poles as the large system and can easily be mounted and dismantled for a off-line measurement of the magnetic field. Secondly, the radiation exposure of the FLASH undulator system and the DU was meticulously and continuously monitored. An array of 32 thermoluminescence (TLD) dosimeters, five for each of the six undulator segments plus two for the DU were placed close to the beam (about 1cm). They are being exchanged and evaluated in frequent intervals of 1-2 weeks. The DU intentionally receives a systematically higher dose than the main undulator system which allows a quantitative prediction of what will happen to the latter upon continued irradiation. The effect of the radiation exposure on the DU is shown in Fig. 1. It is seen that for 60kGy the central pole loses 3% of its strength (green curve) while the half poles (red and blue curves) suffer from smaller losses.

The average accumulated dose, i.e. the mean of the 30 readings of the TLD, is shown as a function of time in Fig. 2. Obviously, the slope of the radiation exposure was much steeper in the first two years after the beginning of operation. Also, a failure of a quadrupole resulted in significantly higher losses in April 2006.

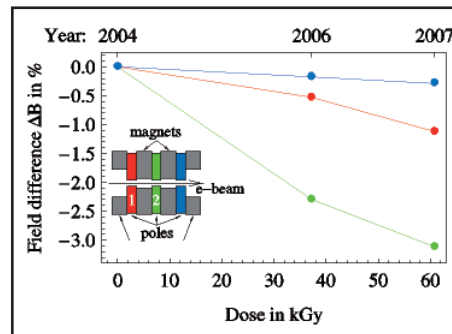


Figure 1
Relative peak field degradation of the three poles of the dosimetry undulator as a function of the measured dose.

Since then, only low dose rates of 300Gy/year or 6Gy/week are observed. This demonstrates the tremendous progress achieved using the collimator and the beam loss detection system. If the radiation damage profile along the undulator would be constant its effect would be to just weaken the K-parameter leading to a slight shift of the radiation wavelength. However, the profile varies and reflects the change in beam size. Using GENESIS 1.3 simulations [1] it was shown that a variation of the field as a result of irradiation of 0.4% is acceptable. If FLASH is operated at 6nm this effect would reduce the FEL power by less than 10%. About 8kGy are needed to produce this error (see Fig. 1, green curve). By extrapolating the total dose in Fig. 2 this would lead to about another 12 years of operation until a total dose of 8kGy corresponding to the 10% power reduction threshold is reached. ●

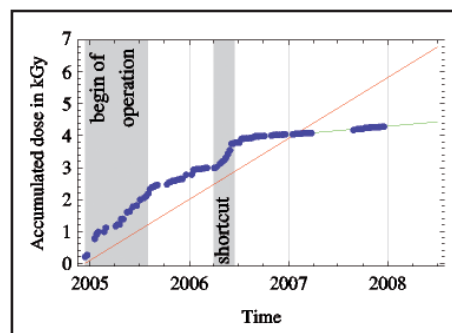


Figure 2
Accumulated dose in the FLASH undulator system.

Contact: J. Pflüger (DESY FS Undulator System),
joachim.pflueger@desy.de

References

1. J. Skupin, Y. Li, J. Pflüger, B. Faatz, T. Vielitz, "Proceedings of the EPAC", June 23-27, 2008 Genova, Italy, 2008.

Controlling experiments.

New online software for PETRA III

A new online system will be used to control experiments at PETRA III beamlines. It is a modular framework consisting of several software layers for hardware access, device abstraction, network connectivity, measurement procedures and user interfaces (Fig. 1). Various components of the system are being developed by international partners within the „TANGO collaboration“, which is presently constituted by ESRF, SOLEIL, ELETTRA, ALBA and DESY (<http://www.tango-controls.org>). So far, most of the experiments at HASYLAB beamlines are controlled by SPECTRA, monolithic software which was developed inhouse and continuously extended to cover all tasks necessary to efficiently control a variety of different instruments and beamlines. It has built-in interfaces to all relevant data busses, a concept for accessing device classes in a uniform way, a flexible graphics system for on-the-fly data display, procedures for various measurement techniques and an interface to the well-established Perl language interpreter for macro programming. The user may operate SPECTRA from the command line or use a graphical interface.

SPECTRA has basic networking capabilities which are adequate for applications at DORIS III. At PETRA III, however, beamlines are considerably longer and electronic devices are distributed over large distances requiring distributed control as well.

Therefore, a full-featured control system with sophisticated network connectivity is needed for the PETRA III experiments. Such a system also supports multi-client access which is increasingly asked for since it allows the beamline scientists to address their users' needs more efficiently. The multi-client connectivity can also be used to record and store relevant experiment parameters along with the actual data, like motor positions, pressure and temperature values, etc.

The new control system at PETRA III uses TANGO which already has the required networking functionality and an interface well suited for the intended purpose. It is platform independent, based on CORBA and uses properties, commands and attributes to exchange objects between servers and clients.

A server represents and controls a certain device and may depend on other servers. A typical example would be a monochromator server that is controlled by a single parameter, the photon energy, while itself uses other motor servers to control the mechanical movements of the device.

TANGO is an open source project which originated at the ESRF and is now being developed further by a collaboration of several synchrotron radiation facilities. A number of servers for a variety of devices have already been coded and are publicly available. TANGO is distributed with additional utility programs such as

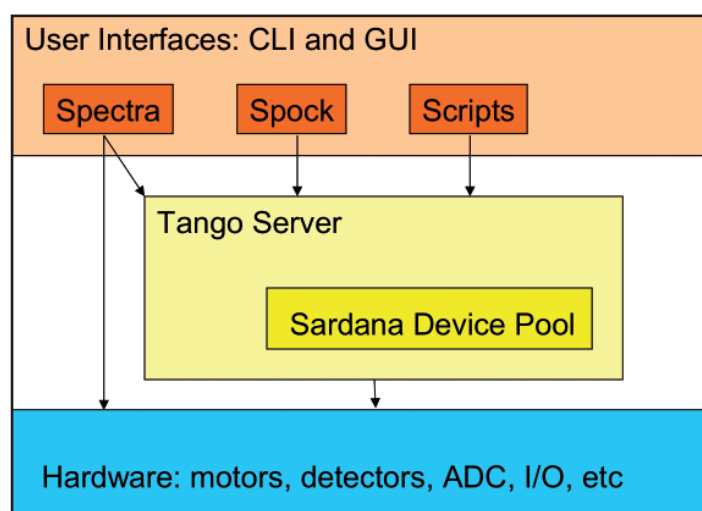


Figure 1

Schematic overview of the online system. TANGO is the central part that connects the user interfaces with the hardware.

a generic client (Jive), a server manager (Astor) and a program for code generation (Pogo). The amount of available software is constantly growing and the members of the TANGO collaboration meet twice a year to present new work, discuss future developments and exchange ideas and information. All collaborating facilities are strongly benefiting from these efforts to further extend the capabilities of the system. A recent new development is the SARDANA Device Pool, initiated at ALBA, which is an extension to the TANGO system implementing an additional layer of abstraction and enabling interesting additional applications. This activity is now also joint by ESRF and DESY. For the initial experiments at PETRA III, the SPECTRA software was made TANGO/SARDANA compatible. Servers for most devices are available and the TANGO system is being tested at several DORIS experiments. ●

Contact: Thorsten Kracht (DESY-FS Experiment Control),
thorsten.kracht@desy.de

Teresa Núñez Pardo de Vera (DESY-FS Experiment Control),
maria-teresa.nunez-pardo-de-vera@desy.de

Advanced detection.

Making the difference at old and new sources

Micro-electronics has revolutionized the field of X-ray detection by integrating full signal processing chains in each detecting element or pixel, thereby creating massively parallel detection schemes, which make much more efficient use of high photon intensities available at synchrotron sources. Such solid-state pixel detectors have already had a major impact at some beamlines at DORIS III, and is enabling new science at the Free-Electron Laser FLASH. This technology is also at the basis of the AGIPD detector under development for the European XFEL, which requires totally new detection concepts in order to profit optimally from the unique source properties. In order to handle the enormous data rates at the new photon sources dedicated, high energy physics like, data acquisition systems are developed. In many synchrotron experiments only a small fraction of the scattered or emitted photons are detected; either due to limited detector sizes, or long readout times, or low detection efficiencies. With the use of novel pixel detectors, like the Pilatus (www.dectris.com) or the Mythen (pilatus.web.psi.ch/mythen.htm) which are new generation 2D and 1D detectors, respectively, innovative experiments even at second generation synchrotron sources are possible. The detectors are position sensitive noise free single photon counting systems with short readout times and photo detection rates of 1MHz per pixel. This allows time resolved studies of processes with improved signal to noise ratios with short exposure times.

The Mythen has 1280 strips, 8mm strip length, 50 μ m pitch, 300 μ m thick sensors, 24 bit readout counter, and readout times down to 250 μ s. The PILATUS 100k has 487x195 pixels, 172 μ m square pixel size, 300 μ m thick sensors, 20 bit readout counters, and readout times down to 2.7ms.

The Mythen has been used at BW1 to examine the air/liquid interface of monolayers. Signals from such monolayers are intrinsically weak, but due to the noise free detection of the Mythen an exposure time of only 10s was sufficient to produce an analyzable dataset [1].

The Pilatus 100k has been used at BW4 where the 3ms delay between subsequent frames has been employed to record the spontaneous self assembly process of nanoparticles in fast drying drops in real time [2].

FLASH presents a totally different challenge for the detectors. With less than a 100 femto-second pulses, and wavelengths of 6 nano-meter or longer, photon counting hybrid pixel detectors are not an option. Certain detectors developed for astronomy are, however, very well suited for this energy range. We have started to use the pnCCD at diffraction beamlines at FLASH.

The pnCCD, successfully used in various satellite missions, is an integrating detector with very low noise, needed to distinguish individual photons. Figure 1 shows two of the three pnCCD modules integrated into the vacuum chamber at the experimental station. A few experiments of imaging of clusters have clearly indicated the large potential of these pnCCDs, and as a result two large 1k x 1k systems are under development, and will be operational by summer 2009. It is likely that these systems will find further use also at the new sources PETRA-III and the European XFEL.

The state-of-the-art detectors mentioned above, will provide for a much improved use of the new and existing photon sources,

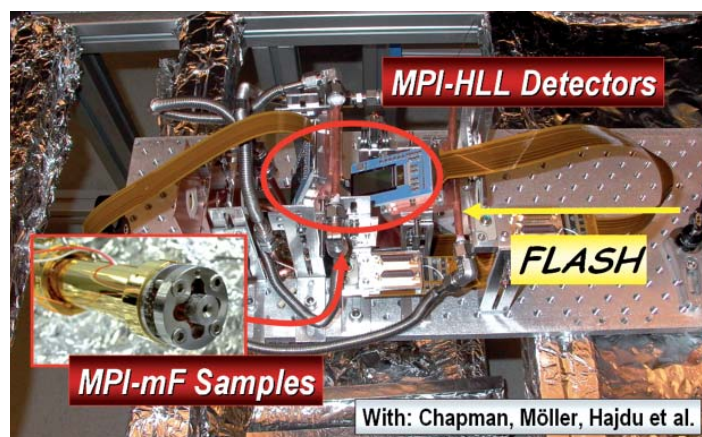


Figure 1

Picture of the pnCCDs at the experimental station at FLASH.

and thereby, surely, enable new science. However, in order to profit optimally from the European XFEL under construction in Hamburg, new detector schemes are needed. One of the challenges for the detectors for the European XFEL lies in the 5 MHz bunch repetition rate inside a bunch train, a feature that distinguishes the European XFEL from its competitors in the USA and Japan. In order to supply optimized detectors at the time of startup a number of development projects have been launched. One of these is the Adaptive Gain Integrating Pixel Detector (AGIPD) project led by DESY and involving the Paul Scherrer Institute, the University of Bonn and the University of Hamburg. AGIPD will handle the large dynamic range of the input signal, by dynamically (or adaptively) switching the gain per pixel. It will take images at 5 MHz repetition rates, and store them analogue on storage capacitors inside the pixels, see Figure 2. These storage capacitors are then read-out and digitized in the

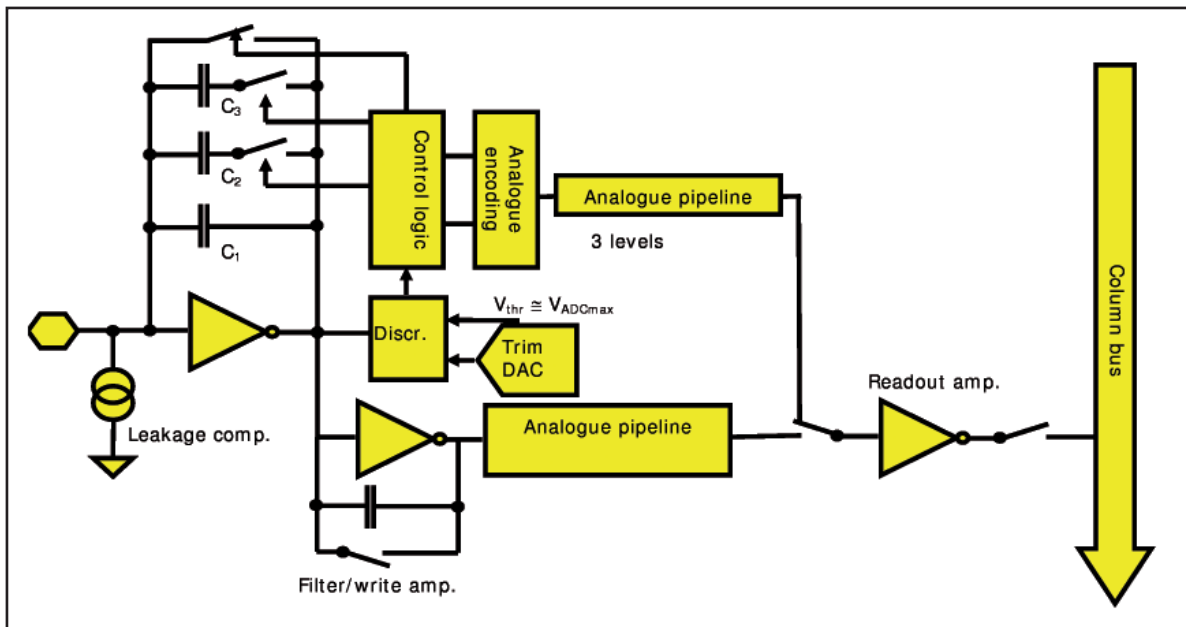


Figure 2
Principle of the
AGIPD detector.

100 msec between bunch trains. The noise and the leakage of the system will be small enough to allow for single photon sensitivity in the high gain regime, and be negligible compared to counting statistical uncertainties in the low gain regimes. In order to test the feasibility of the analogue storage cells, test structures have been fabricated in 0.13 micron CMOS, and electronically tested. The performance of the various transistors, the storage capacitors and the complete storage cells surpassed the requirements needed for the construction of the AGIPD system. The dynamic gain switching was successfully tested independently by PSI using a separate chip. These results give a large degree of confidence in the feasibility of the proposed system. A first 16x16 pixel prototype will be ready for testing by summer 2009.

These novel detectors, under construction for the European XFEL, will produce significantly larger data rates than currently generated at existing and being commissioned light sources, and by LHC experiments. The AGIPD detector Front End Electronics (FEE) ASIC stores up to 512 picture frames at 5MHz during the 600 μ s pulse train with a 10Hz repetition rate. The FEE ADC system digitizes the pixel charge in the storage pipeline producing 2MB of data per frame, which at the design rates results in 10GB/s of data. The challenge is to design and implement a DAQ architecture which can handle instantaneous rates of ~50GB/s when all detectors and beam lines are operated. The five-layer DAQ architecture proposed is shown in Figure 3. Key features are the train building/FEE layer, which build frame data into complete frame ordered trains, and the data cache file system. Data processing is planned for all layers post FEE and the development of data rejection processing algorithms, i.e. triggers, is essential for reducing bandwidth

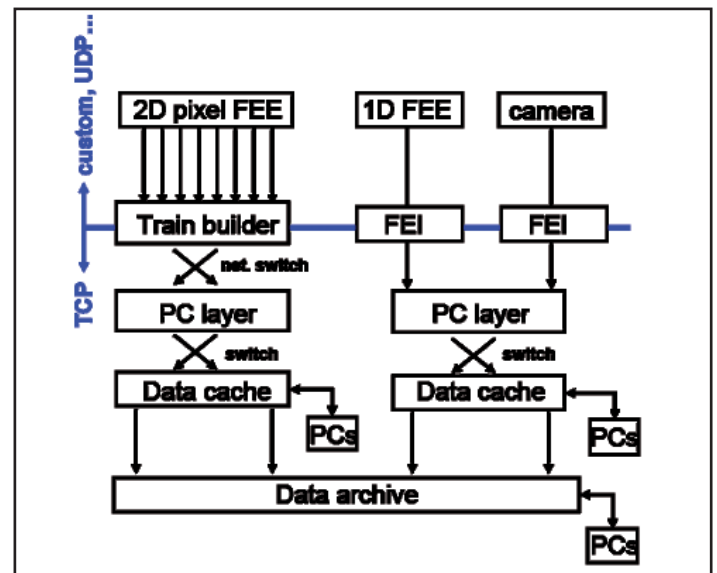


Figure 3
Conceptual layout of the DAQ for XFEL architecture.

and storage requirements. The use of a multi-layered architecture has the advantage that the size, processing capabilities and implementation technologies of all the layers can be tuned, scaled and even swapped according to the final requirements and capabilities. To overcome the increased needs of data management, access and processing GRID type solutions are being investigated. ●

Contact: H. Graafsma (DESY-FS Detector Systems),
heinz.graafsma@desy.de

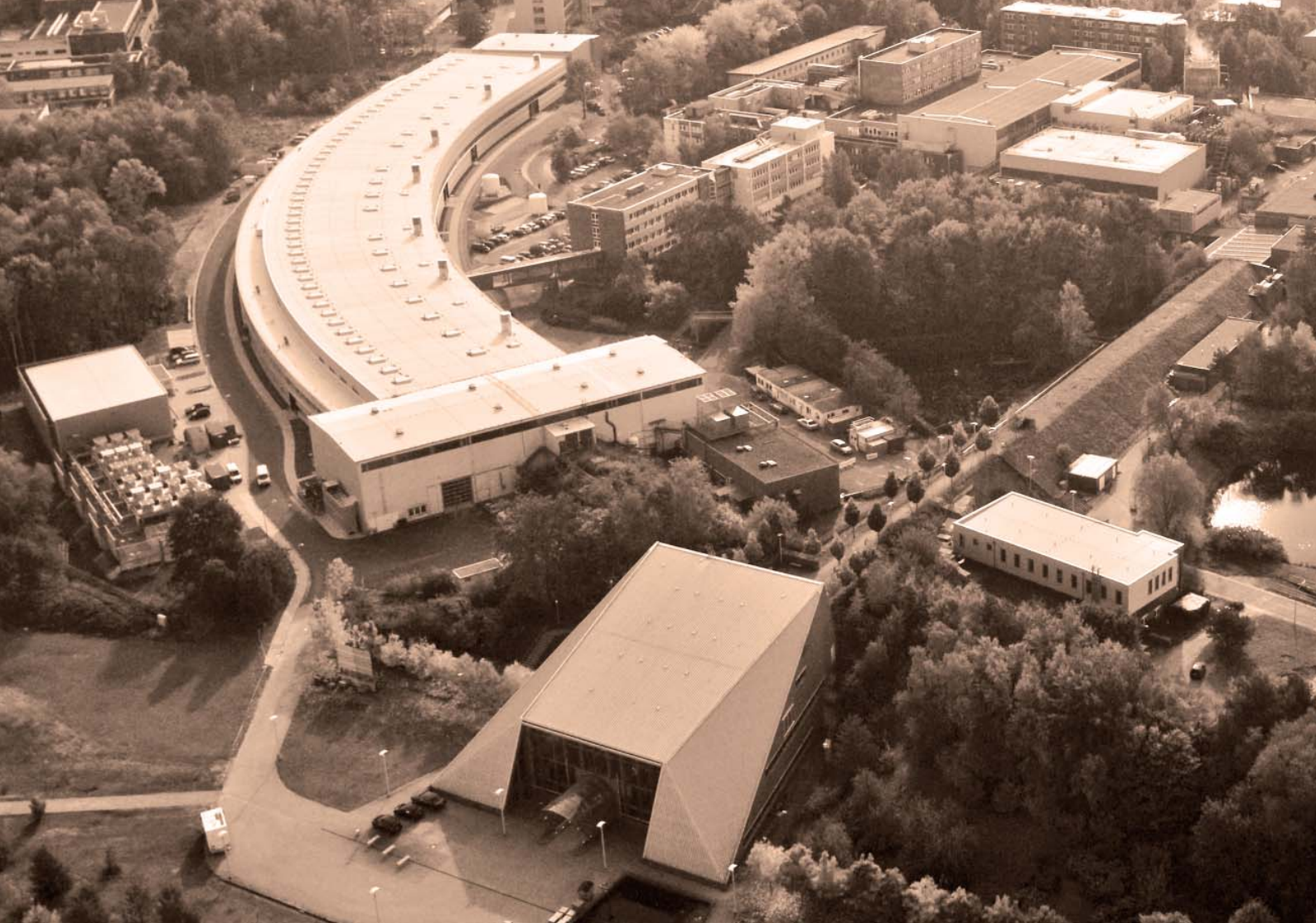
Authors

H. Graafsma¹, M. Lohmann¹, C. Youngman¹, R. Hartmann² and L. Strüder²

1. DESY; Notkestrasse 85; 22607 Hamburg
2. MPI-HLL, Otto-Hahn-Ring 6; 81739 München

References

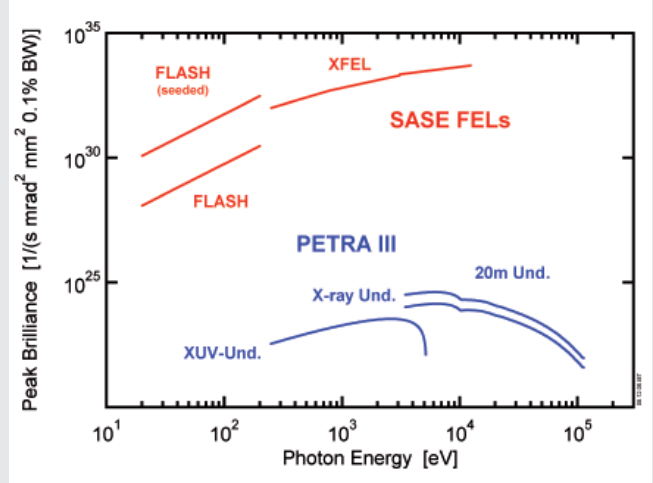
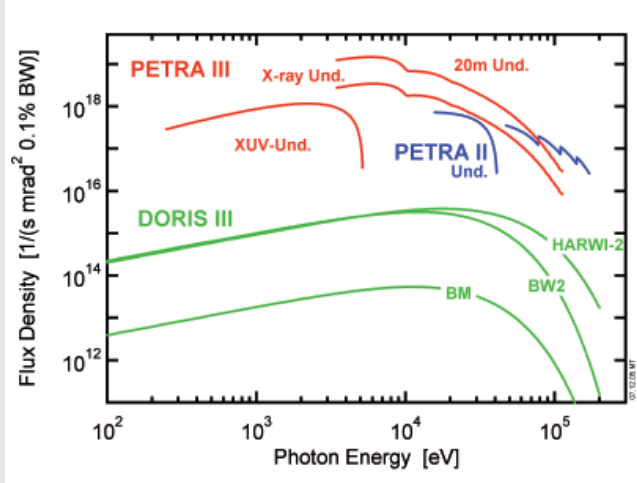
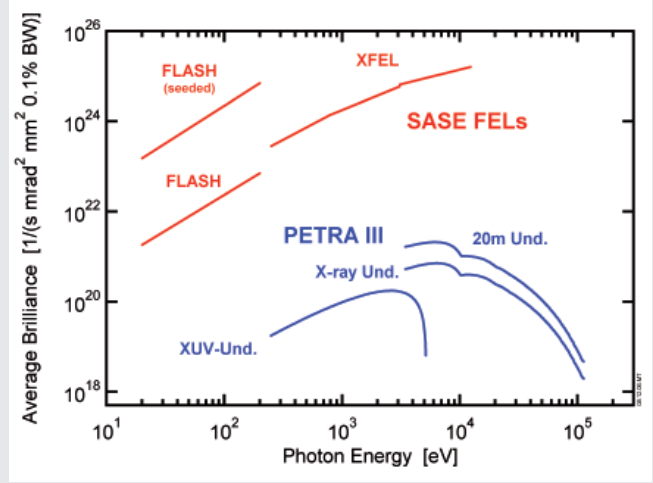
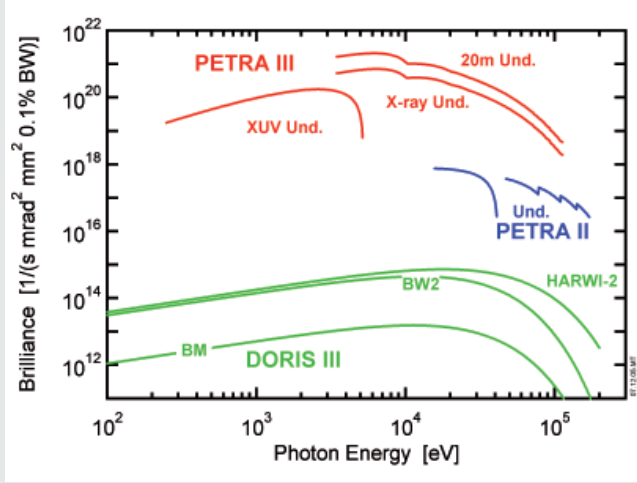
1. B. Struth et al. in preparation
2. P. Siffalovic et al., "Real-time tracking of superparamagnetic nanoparticle self assembly", Wiley InterScience, DOI:10.1002/sml.200800353, 2008.



Facts and Numbers.

>	Lightsource characteristics	98
>	DORIS III beamlines and parameters	99
>	FLASH beamlines and parameters	104
>	PETRA III beamlines and parameters	107
>	Committees 2008	110

Lightsource characteristics.

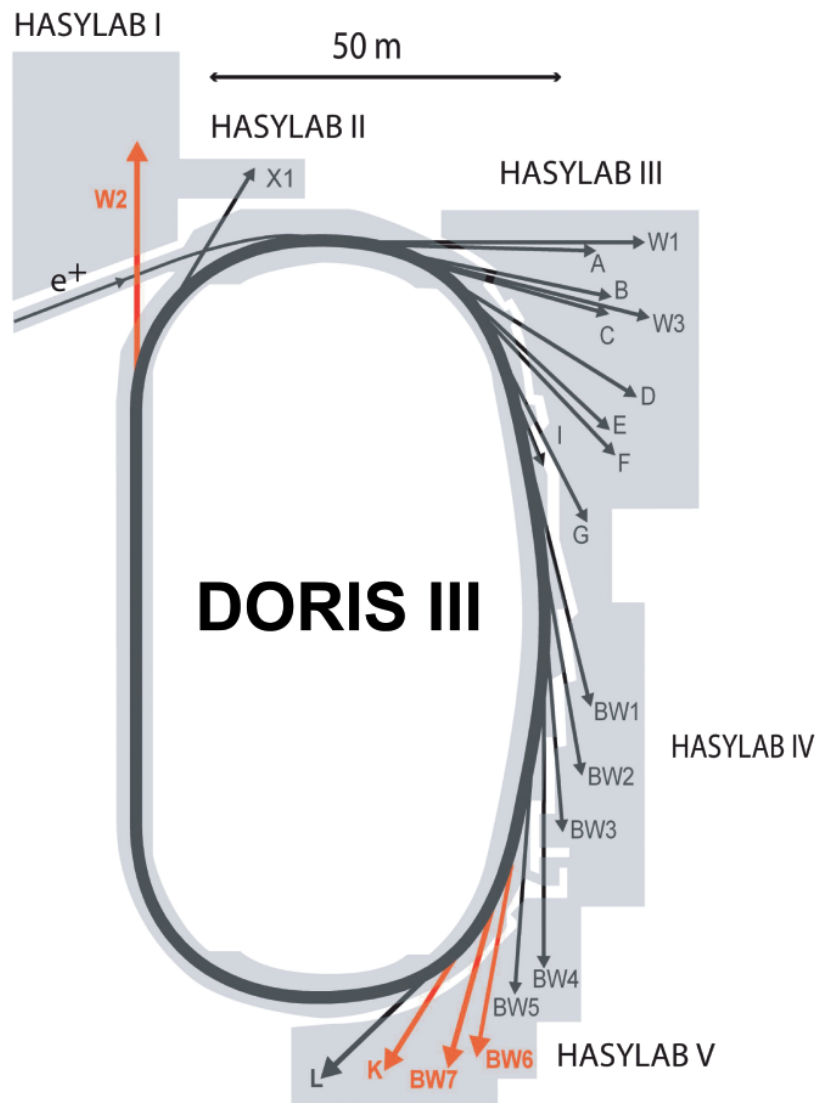


Storage ring sources

Free-electron laser sources
(in comparison with PETRA III)

DORIS III.

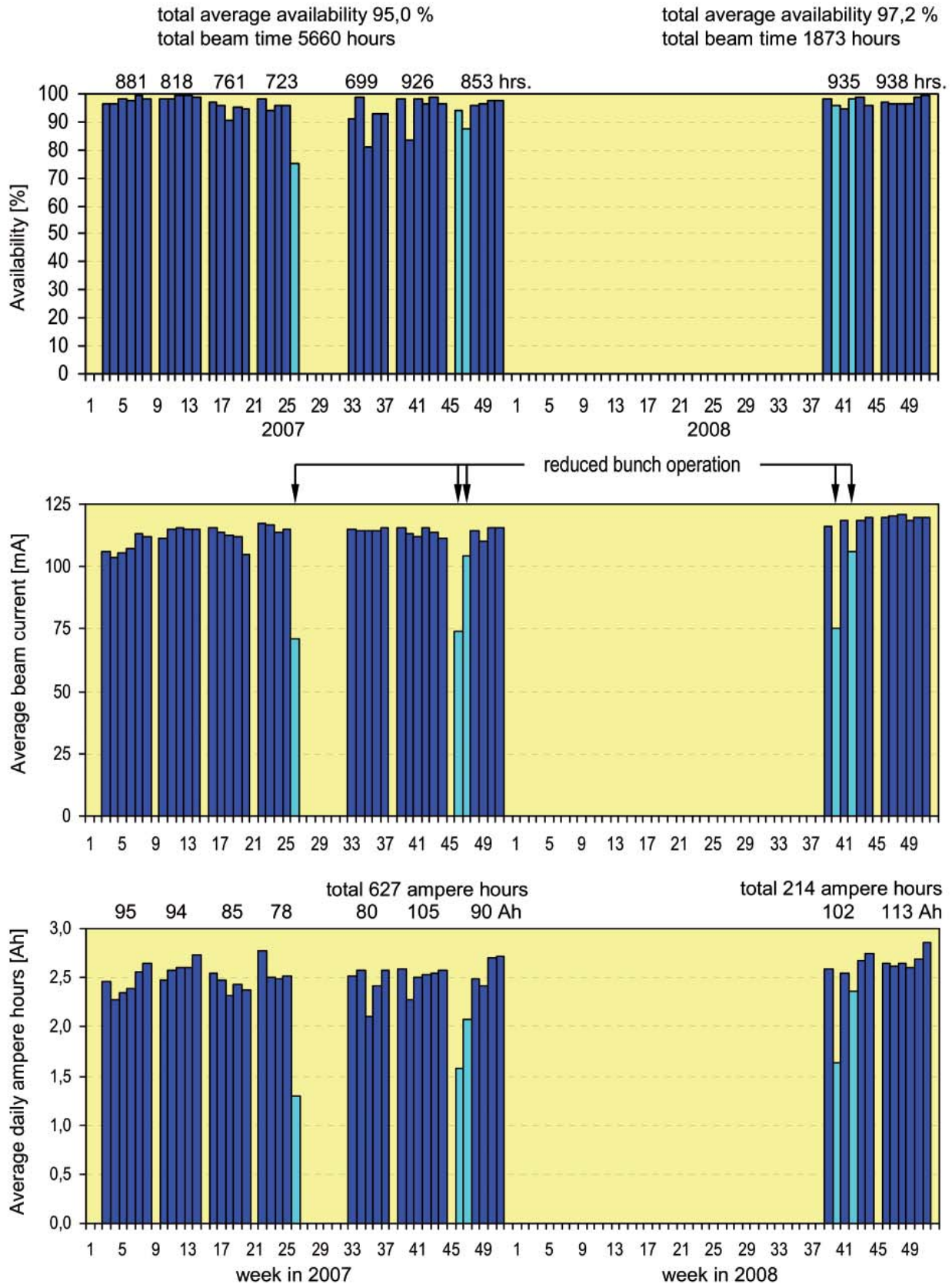
Beamlines and parameters



Machine parameters DORIS III (Present values)

Positron energy	4.45 GeV
Circumference of the storage ring	289.2 m
Number of buckets	482
Number of bunches	1 (for tests), 2, and 5
Bunch separation (minimum)	964 ns (for tests), 480 ns, and 192 ns
Positron beam current	140 mA (5 bunches)
Horizontal positron beam emittance	410 nmrad (rms)
Coupling factor	3%
Vertical positron beam emittance	12 nmrad (rms)
Positron beam energy spread	0.11% (rms)
Curvature radius of bending magnets	12.18 m
Magnetic field of bending magnets	1.218 T
Critical photon energy from bending magnets	16.0 keV

DORIS III beamtime statistics 2007 and 2008



Availability = Useable beam time for HASYLAB in % of scheduled beam time
Criterion: Beam current ≥ 40 mA; run duration ≥ 1 hour

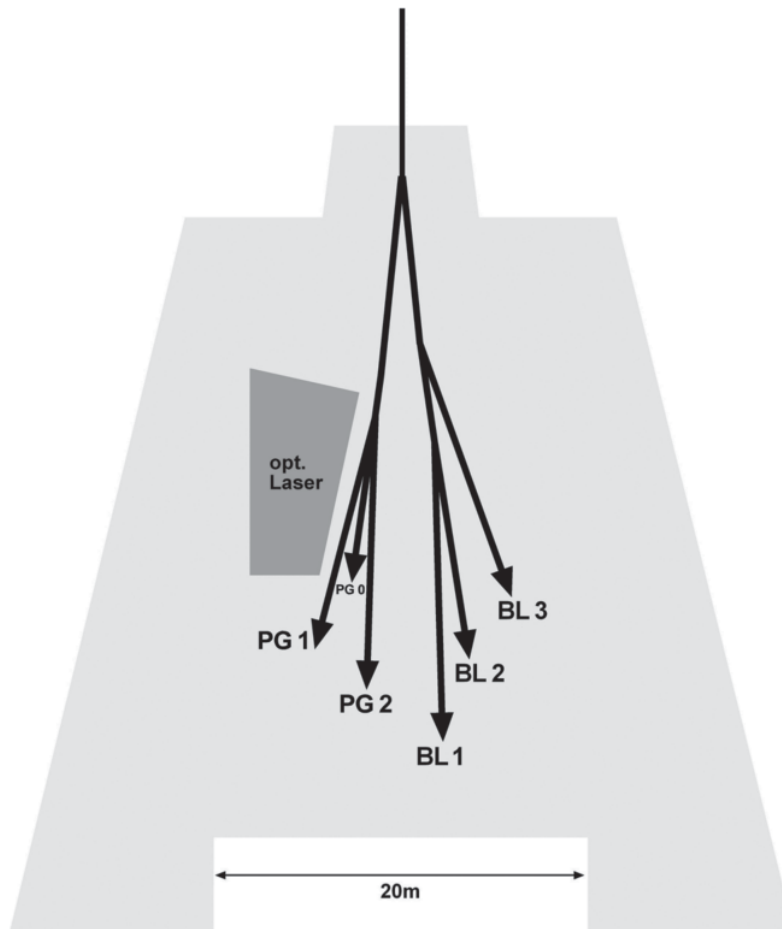
Year	2005	2006	2007	2008
Total integrated ampere hours	541	674	627	214

DORIS III beamlines and instruments

A1 X-ray absorption spectroscopy		
Bending magnet ($E_c = 16$ keV)		
Instrument for in-situ XAFS including fast energy scanning (refurbished, operational again spring 2009)	2.4 – 8 keV	DESY
A2 Small-angle X-ray scattering		
Bending magnet ($E_c = 16$ keV)		
Multi setup instrument for (simultaneous) small and wide angle scattering from soft matter samples	8 keV	DESY
B1 Anomalous small-angle X-ray scattering		
Bending magnet ($E_c = 16$ keV)		
Instrument for anomalous scattering (ASAXS)	5 – 35 keV	DESY
B2 X-ray powder diffraction		
Bending magnet ($E_c = 16$ keV)		
Heavy duty diffractometer including special setups for in-situ studies (refurbished, operational again spring 2009)	5 – 44 keV	DESY
BW1 X-ray diffraction / scattering		
4m X-ray undulator		
Horizontal diffractometer for liquid surface scattering	9.5 keV	DESY
UHV instrument for surface diffraction / standing waves including MBE sample preparation	2.4 – 12 keV	DESY U Bremen
Multi purpose heavy load 8-circle diffractometer	5 – 18 keV	DESY
Rheometer	9.9 keV	DESY
BW2 X-ray spectroscopy / diffraction / tomography		
4m X-ray wiggler ($E_c = 15.4$ keV)		
UHV instrument for hard X-ray photoelectron spectroscopy	2.4 – 10 keV	DESY
X-ray micro-tomography setup	6 – 24 keV	GKSS
Heavy load vertical diffractometer with CCD detector arm for grazing incidence diffraction	5 – 11 keV	DESY
BW3 Soft X-ray spectroscopy		
4m XUV (double) undulator		
High-resolution SX-700 plane grating monochromator, beam port for user supplied instruments	50 – 1500 eV	DESY
BW4 Ultra small-angle X-ray scattering		
2.7m X-ray wiggler ($E_c = 15.4$ keV)		
Flexible instrument for (ultra) small angle (grazing incidence) scattering experiments	6 – 14 keV	DESY
BW5 High-energy X-ray diffraction		
4m X-ray wiggler ($E_c = 26$ keV)		
Triple axis diffractometer in horizontal Laue scattering geometry including high magnetic field (10T) sample environment	60 – 250 keV	DESY
BW6 Macromolecular crystallography		
4m X-ray wiggler ($E_c = 15.4$ keV)		
End-station for protein crystallography, optimized for MAD or SAD	4 – 20 keV	MPG

BW7A Macromolecular crystallography		
4m X-ray wiggler ($E_c = 15.4$ keV)		
Crystallographic end-station with CCD detector, double multilayer optics, optimized for high-flux fast data collection	12.8 keV	EMBL
BW7B Macromolecular crystallography		
4m X-ray wiggler ($E_c = 15.4$ keV)		
Crystallographic end-station with CCD detector, new high-precision Phi spindle, EMBL Hamburg robotic sample changer (MARVIN)	14.7 keV	EMBL
C X-ray absorption spectroscopy / diffraction		
Bending magnet ($E_c = 16$ keV)		
Setup for high-energy XAFS in-situ studies including fast energy scanning	5 – 44 keV	DESY
Vertical diffractometer for grazing incidence X-ray diffraction	5 – 44 keV	DESY
D1 (X33) Small-angle X-ray scattering		
Bending magnet ($E_c = 16$ keV)		
Instrument optimized for automated solution scattering studies of biological macromolecules	8 keV	EMBL
D3 Chemical crystallography		
Bending magnet ($E_c = 16$ keV)		
4-circle diffractometer	7 – 35 keV	DESY
D4 Grazing incidence X-ray scattering		
Bending magnet ($E_c = 16$ keV)		
2-circle diffractometer, horizontal scattering plane	5 – 20 keV	DESY
E1 (Flipper2) Soft X-ray spectroscopy		
Bending magnet ($E_c = 16$ keV)		
UHV instrument for soft X-ray photoelectron spectroscopy	10 – 150 eV	U Hamburg
E2 X-ray reflectometry / grazing incidence diffraction		
Bending magnet ($E_c = 16$ keV)		
6-circle diffractometer for reflectometry & high-resolution diffraction	4 – 35 keV	DESY / RWTH Aachen
E4 X-ray absorption spectroscopy		
Bending magnet ($E_c = 16$ keV)		
Instrument for medium energy XAFS (will be closed down after start-up of instrument at A1)	2.8 – 10 keV	DESY
F1 Chemical crystallography		
Bending magnet ($E_c = 16$ keV)		
Kappa-diffractometer for low/high-temperature / high-pressure single-crystal diffraction	5 – 41 keV white beam	U Hamburg
F2 X-ray diffraction / VUV spectroscopy		
Bending magnet ($E_c = 16$ keV)		
Hutch1 MAX80 Multi-Anvil-X-ray apparatus for high pressure X-ray diffraction	5 – 80 keV white beam	GFZ
Hutch2 UHV instrument for angle-resolved UV photoelectron spectroscopy	5 – 41 eV	U Hamburg
F3 Energy dispersive scattering		
Bending magnet ($E_c = 16$ keV)		
Horizontal diffractometer with heavy load sample stage	white beam	DESY U Kiel

F4 X-ray test beam			
Bending magnet ($E_c = 16$ keV)			
Used for detector characterization			DESY
G3 Diffraction X-ray imaging			
Bending magnet ($E_c = 16$ keV)			
4-circle diffractometer for position resolved diffraction	5.4 – 26 keV		DESY
I (Superlumi) UV luminescence spectroscopy			
Bending magnet ($E_c = 16$ keV)			
Superlumi setup for luminescence analysis	3 – 40 eV		DESY
K1.1 (X11) Macromolecular crystallography			
Bending magnet ($E_c = 16$ keV)			
Crystallographic end-station with large surface area flat panel detector, cryoshutter, single horizontal axis of rotation	15.3 keV		EMBL
K1.2 (X12) Macromolecular crystallography			
Bending magnet ($E_c = 16$ keV)			
Crystallographic end-station with CCD and fluorescence detector, single axis of rotation, opt. for MAD and SAD	5.5 – 20 keV		EMBL
K1.3 (X13) Macromolecular crystallography			
Bending magnet ($E_c = 16$ keV)			
Crystallographic end-station with CCD detector, cryoshutter, micro-spectrophotometer, single horizontal axis of rotation, optimised for automated expert data collection	15.3 keV		EMBL
L X-ray micro probe			
Bending magnet ($E_c = 16$ keV)			
X-ray microprobe combining fluorescence analysis, absorption spectroscopy and diffraction	5 – 80 keV white beam		DESY
W1 X-ray spectroscopy / diffraction			
2m X-ray wiggler ($E_c = 8$ keV)			
High-resolution fluorescence in vacuo spectrometer	4 – 11.5 keV		DESY
Heavy load diffractometer for grazing incidence diffraction in vertical or horizontal scattering geometry	4 – 11.5 keV		DESY
W2 (HARWI II) High-energy X-ray engineering material science			
4m X-ray wiggler ($E_c = 26$ keV)			
Hutch1 Materials Science Diffraktometer (heavy load up to 600 kg)	60 – 250 keV 20 – 150 keV		GKSS
Micro-tomography setup (attenuation and phase contrast)	20 – 250 keV		GKSS
Diffraction-tomography "DITO" instrument	20 – 150 keV		TU Dresden TU Berlin
Hutch2 MAX200x Multi-Anvil X-ray apparatus for high pressure and temperature conditions	white beam		GFZ
W3 VUV spectroscopy			
Bending magnet ($E_c = 16$ keV)			
Angle-resolved photoelectron spectrometer with high energy resolution	8 – 32 eV		U Kiel
X1 X-ray absorption spectroscopy			
Bending magnet ($E_c = 16$ keV)			
Setup for high-energy fast-scanning XAFS for in-situ studies including chemistry lab	7 – 100 keV		DESY



Machine parameters FLASH (as achieved in 2008)

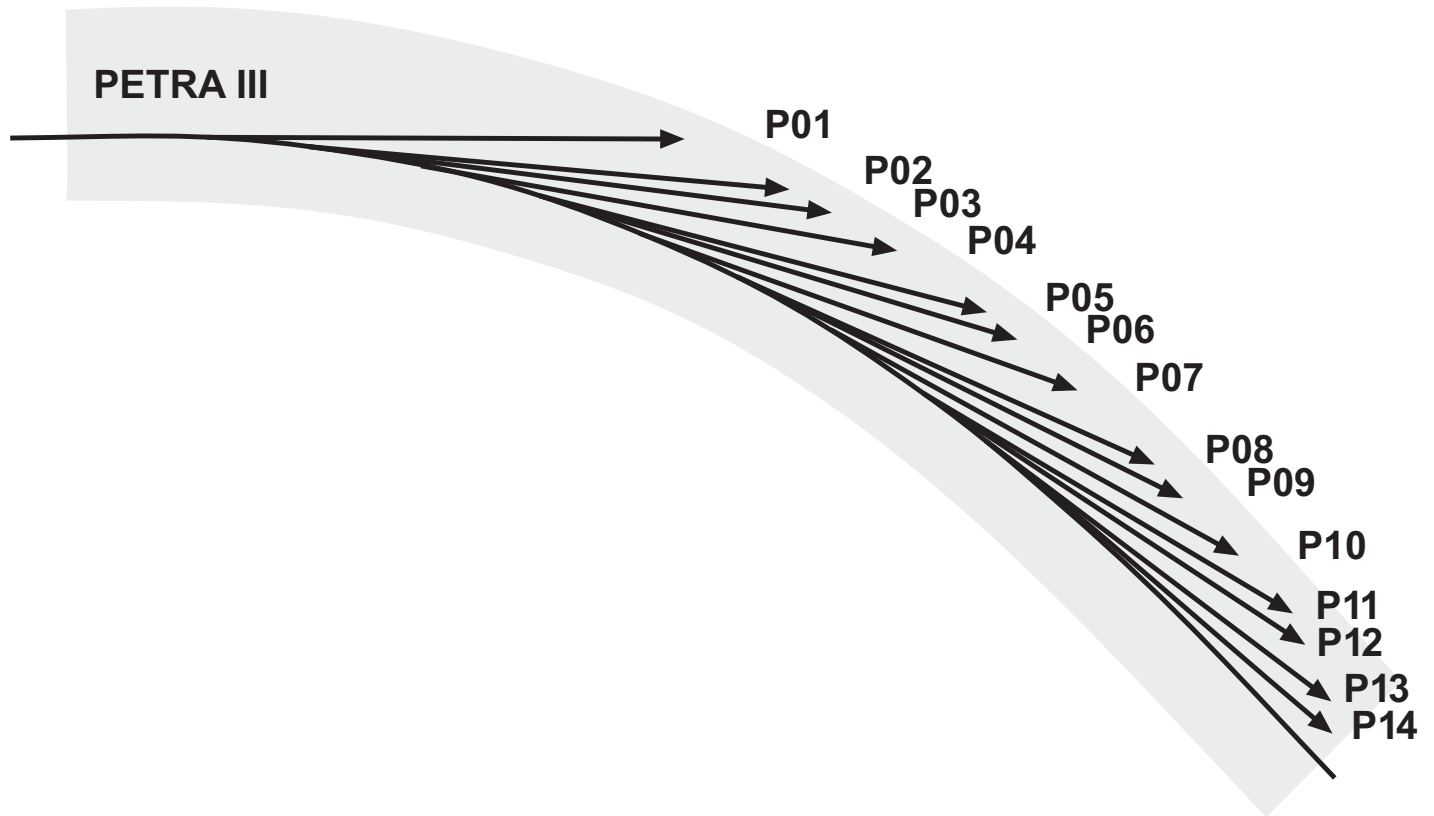
Electron energy (max.)	1.0 GeV
Length of the facility	315 m
Normalized emittance	2 mm mrad (rms)
Emittance	1 nm rad (rms)
Bunch charge	1 nC
Peak current	2 kA
Bunches per second (typ. and max.)	150 and 4000
Lasing parameters	
Photon energy (max.)	180 eV (fundamental)
Wavelength (min.)	6.9 nm (fundamental)
Pulse duration (FWHM)	10 - 50 fs
Peak power	1 - 5 GW
Bunch energy (average)	10 -100 μ J
Photons per bunch	10^{12} - 10^{13}
Average brilliance	10^{17} - 10^{19} photons/sec/mm ² /mrad ² /0.1%
Peak brilliance	10^{29} - 10^{30} photons/sec/mm ² /mrad ² /0.1%
Spectral bandwidth	1 % (FWHM)

FLASH beamlines and user instruments
(including instrumentation provided by university groups
and funded by the BMBF „Verbundforschung“)

BL1	
Focused FEL beam, 100µm spot size	DESY
Instrumentation for the preparation and electron and ion spectroscopy of mass-selected clusters	U Rostock
Magnetic X-ray diffraction imaging and holography	DESY HZB (BESSY)
Pump-probe setup for the study of transient response of melting/ablating solids	U Duisburg-Essen
Setup for resonant soft X-ray scattering	CFEL U Oxford
Experimental system for the spectroscopic study of molecular desorption from surfaces of solids	U Münster
Single-shot cross-correlator	U Hamburg
BL2	
Focused FEL beam, 20µm spot size	DESY
Instrumentation for two-colour pump probe experiments of atoms and molecules	DESY DCU Dublin LIXAM/CNRS Paris
Reaction microscope for the study of multiple ionization processes of atoms and molecules	MPI-K Heidelberg
Velocity map imaging spectrometer (electrons and ions) for atoms and molecules in strong fields	AMOLF Amsterdam
Setup for angle-resolved photoelectron spectroscopy (ARPES) of atoms and molecules	FHI Berlin
Station for spectroscopy of rare gas clusters and nanoparticles	TU Berlin
Single-shot single-particle (time-resolved) diffraction imaging of nanostructures and biological samples	CFEL LLNL Livermore U Uppsala
Setup for Thomson scattering spectroscopy to probe plasma dynamics in a liquid hydrogen jet	DESY LLNL Livermore U Oxford U Rostock
Instrumentation for measuring damage thresholds and optical properties of solid samples	ASCR Prague DESY IFPAS Warsaw LLNL Livermore
Setup for electron and ion spectroscopy to study multi-photon processes in gases	DESY PTB Berlin U Hamburg

BL3	
Unfocused FEL beam	DESY
Magneto-optical trap & reaction microscope to study ultra-cold plasmas	MPI-K Heidelberg
Setup with multilayer optics for sub-micron focusing to create and study plasmas and warm dense matter	U Belfast CFEL DESY U Oxford
System for angle-resolved photoelectron spectroscopy (ARPES) and ion spectroscopy of metal vapors	DESY U Hamburg
Microfocus setup for spectrometry of multi-photon processes in rare gases at extreme power densities	DESY PTB Berlin
XUV beam splitter with variable delay for photon diagnostics and time-resolved experiments	DESY HZB (BESSY) U Münster
Split multilayer-mirror & reaction microscope for time-resolved spectroscopy of small molecules	MPI-K Heidelberg
Microfocus setup for time-resolved imaging of rare gas clusters	TU Berlin
Experimental station for pump-probe experiments combining μ J-level, few-cycle THz and XUV FEL pulses	DESY U Hamburg
PG1	
Plane grating monochromator, microfocus (5 μ m spot size)	DESY, U Hamburg
High-resolution two-stage spectrometer for inelastic (Raman) scattering (permanent installation)	DESY U Hamburg
PG2	
Plane grating monochromator (50 μ m focus)	DESY, U Hamburg
Setup for resonant inelastic X-ray scattering (RIXS) and photoelectron spectroscopy of solids	U Hamburg
Electron beam ion trap (EBIT) for high-resolution spectroscopy of highly charged ions	MPI-K Heidelberg
Ion source and trap for spectroscopic studies of the photo-fragmentation of molecular ions and radicals (permanent installation)	U Aarhus MPI-K Heidelberg
System for angle-resolved photoelectron spectroscopy (ARPES) of solids and surfaces	U Kiel
Setup for the study of fs-dynamics of magnetic materials	U Hamburg HZB (BESSY)
XUV beamsplitter with variable delay for time resolved experiments	U Hamburg
Soft X-ray diffraction imaging system for magnetic materials and nanostructures	DESY U Hamburg U Heidelberg HZB (BESSY) FH Koblenz

Note: instruments are non-permanent installations unless noted otherwise



Machine parameters PETRA III (Design values)

Positron energy	6.0 GeV
Circumference of the storage ring	2304 m
Number of buckets	3840
Number of bunches	960 and 40
Bunch separation	8 ns and 192 ns
Positron beam current	100 mA (top-up mode possible)
Horizontal positron beam emittance	1 nmrad (rms)
Coupling factor	1%
Vertical positron beam emittance	0.01 nmrad (rms)
Positron beam energy spread	0.1% (rms)
Curvature radius of bending magnets	22.92 m (new part of the ring)
Magnetic field of bending magnets	0.873 T (new part of the ring)
Critical photon energy from bending magnets	20.9 keV (new part of the ring)

PETRA III beamlines and instruments under construction
(including instrumentation provided by university groups
and funded by the BMBF „Verbundforschung“)

P01 Inelastic and Nuclear Resonant Scattering			
10 m undulator (U32), high-β			
Hutch1 Nuclear resonant scattering setup Nuclear lighthouse effect spectrometer	6 – 40 keV	DESY	
Hutch2 Spectrometer for inelastic scattering with nanobeam	6 – 40 keV	DESY	
Hutch3 Nuclear resonant scattering with special sample environments: Extreme conditions and UHV	6 – 40 keV	DESY	
P02 Hard X-Ray Diffraction			
2 m undulator (U23), high-β			
Hutch1 Powder diffraction side station High-resolution powder diffractometer	60 keV	DESY TU Dresden	
Hutch2 Station for diffraction experiments under extreme conditions (high p, high T) Laser heating for the extreme conditions station	8 – 100 keV	DESY U Frankfurt	
P03 Micro- and Nanobeam Wide and Small Angle X-ray Scattering (MINAXS)			
2 m undulator (U29), high-β			
Hutch1 General Purpose μSAXS/WAXS station Setup for in-situ deposition experiments, AFM μGISAXS option with ellipsometer	8 – 23 keV	DESY TU München	
Hutch2 Setup for nanobeam Scanning-Experiments (SAXS/WAXS, GISAXS) Nanofocus endstation including in-situ deformation experiments	8 – 23 keV	DESY U Kiel	
P04 Variable Polarization Soft X-rays			
5 m APPLE undulator (UE65), high-β		DESY	
UHV-diffractometer for elastic and inelastic resonant XUV scattering	0.2 - 3.0 keV	U Köln	
Ultra-high resolution XUV photoelectron spectrometer for in-situ real-time investigation of dynamic processes in nano structures	0.2 - 3.0 keV	U Kiel U Würzburg	
PIPE: instrument for flexible two-beam experiments to investigate mass selected ions (atoms to nano particles) with photons	0.2 - 3.0 keV	U Giessen U Hamburg FU Berlin U Frankfurt	
Soft X-ray absorption spectrometer with variable polarization at 30 mK	0.2 - 3.0 keV	U Hamburg U München	
Nano focus apparatus for spatial and time resolving spectroscopy	0.2 - 3.0 keV	U Hamburg FH Koblenz	
P05 Imaging beamline			
2 m undulator (U29), low-β			
Hutch1 Micro tomography setup for absorption, phase enhanced and phase contrast tomography	5 – 50 keV	GKSS	
Hutch2 Nano tomography instrument combining hard X-ray microscopy and tomography	5 – 50 keV	GKSS	
P06 Hard X-ray Micro/Nano-Probe			
2 m undulator (U32), low-β			
Hutch1 Instrument for imaging at (sub-)micrometer spatial resolution applying X-ray fluorescence, X-ray absorption and X-ray diffraction techniques	2.4 - 100 keV	DESY	
Hutch2 Instrument for imaging by coherent X-ray diffraction and X-ray fluorescence with nanoscopic resolution	5 – 50 keV	DESY TU Dresden	

P07 High Energy Materials Science (HEMS)		
4 m in-vacuum undulator (U19), high- β		
Hutch1 Test facility	53 / 87 keV (fixed)	GKSS
Hutch2 Multi purpose diffractometer for bulk and interfaces	50 – 250 keV	DESY
Hutch3 Heavy-load (1t) diffractometer	50 – 250 keV	GKSS
Hutch4 3D-XRD strain and stress mapper Instrument for microtomography Instrument for high-resolution strain analysis	50 – 250 keV	GKSS GKSS TU Berlin
P08 High-resolution diffraction		
2 m undulator (U29), high- β		
Hutch1 High-resolution diffractometer X-ray diffractometer for liquid interfaces studies Extension for external sample environments and coherent scattering	5.4 – 30 keV	DESY U Kiel U Dortmund
P09 Resonant scattering / diffraction		
2 m undulator (U32), high- β		
Hutch1 High precision diffractometer for resonant scattering and diffraction	2.4 – 50 keV	DESY
Hutch2 Heavy load diffractometer for resonant scattering and diffraction, optional high magnetic fields	2.4 – 50 keV	DESY
Hutch3 High-resolution hard X-ray photoelectron spectroscopy instrument	2.4 – 15 keV	DESY U Mainz U Würzburg
P10 Coherence applications		
5 m undulator (U29), low- β		
Hutch1 Instrument for X-ray photon correlation spectroscopy and coherent diffraction imaging in SAXS geometry, rheology setup	4 – 25 keV	DESY
Hutch2 Instrument for X-ray photon correlation spectroscopy and coherent diffraction imaging at large angles X-ray waveguide setup Apparatus for lensless microscopy of biological cells Setup for XPCS with reference beams	4 – 25 keV	DESY U Göttingen U Dortmund
P11 Biological imaging / diffraction		
2 m undulator (U32), high- β		
Single-axis diffractometer for macromolecular crystallography	6 – 33 keV	HGF/ DESY MPG
Setup for imaging of biological systems	3 – 12 keV	
P12 Biological small-angle X-ray scattering		
2 m undulator (U29), high- β		
Instrument for biological SAXS on protein solutions and time resolved biomembrane related and soft matter research, tunable sample-detector distance	4 – 20 keV	EMBL GKSS
P13 Macro molecular crystallography I		
2 m undulator (U29), high- β		
Setup for highly collimated beams with variable focus size, in crystallo spectroscopies	4 – 17 keV	EMBL
P14 Macro molecular crystallography II		
2 m undulator (U29), high- β		
Protein micro-crystallography instrument	7 – 35 keV	EMBL

Note: for each undulator, high- β and low- β operation can be chosen freely

Committees 2008.

Photon Science Committee PSC

Peter Fratzl (Chair)	Max-Planck-Institute Potsdam, D
Anke Pyzalla (Vice Chair)	Max-Planck-Institute Düsseldorf, D (until Oct. 2008)
Don Bilderback	Cornell University, USA
Christian Bressler	EPFL Lausanne, CH
Rolf-Dieter Heuer	DESY Hamburg, D
Roland Horisberger	PSI Villigen, CH
Koen Janssens	University of Antwerp, B
Colin Norris	Diamond, CCLRC, UK
Vladimir V. Kvardakov	Kurchatov Institute Moscow, RUS
Paul Mourin	Synchrotron Soleil, F (until May 2008)
Jean-Pierre Samama	Synchrotron Soleil, F (since Oct. 2008)
Peter Siddons	NLSL Brookhaven, USA
Simone Techert	Max-Planck-Institute Göttingen, D
Joachim Ullrich	Max-Planck-Institute Heidelberg, D
Edgar Weckert	DESY Hamburg, D
Wilfried Wurth	University Hamburg, D
Jörg Zegenhagen	ESRF Grenoble, F

Project Review Panel PRP1: VUV- and Soft X-Ray - Spectroscopy

Wolfgang Drube (Secretary)	DESY Hamburg, D
Marco Kirm	University of Tartu, EE
Thomas Möller	TU Berlin, D

Project Review Panel PRP2: X-Ray - Hard Condensed Matter - Spectroscopy

Wolfgang Drube (Secretary)	DESY Hamburg, D
Johannes Hendrik Bitter	Utrecht University, NL
Michael Fröba	University Gießen, D
Wolfgang Grünert	University Bochum, D
Laszlo Vince	Ghent University, B

Project Review Panel PRP3: X-Ray - Hard Condensed Matter / Diffraction and Imaging

Hermann Franz (Secretary)	DESY Hamburg, D
Hans Boysen	University München, D
Bo Brummerstedt Iversen	Aarhus University, DK
Christan Kumpf	FZ Jülich, D
Bert Müller	University Basel, CH
Andreas Schreyer	GKSS Geesthacht, D

Project Review Panel PRP4: Soft X-Ray - FEL Experiments (FLASH)

Josef Feldhaus (Secretary)	DESY Hamburg, D
Massimo Altarelli	DESY/XFEL Hamburg, D
Marie-Emmanuelle Couprie	Synchrotron Soleil, F
Robert Donovan	University of Edinburgh, UK
Roger W. Falcone	LBL, USA
Gerard Meijer	FHI Berlin, D
Jan Michael Rost	Max-Planck-Institute Dresden, D
Christian Schroer	TU Dresden, D
Svante Svensson	Uppsala University, S
Dietrich von der Linde	University Duisburg-Essen, D
Edgar Weckert	DESY Hamburg, D
Wilfried Wurth	University Hamburg, D

Project Review Panel PRP5: X-Ray - Soft Condensed Matter / Scattering

Rainer Gehrke (Secretary)	DESY Hamburg, D
Tiberio Ezquerra	CSIC Madrid, E
Jochen S. Gutmann	University Mainz, D
Beate Klösgen	Univ. of Southern Denmark, DK
Oskar Paris	Max-Planck-Institute Potsdam, D

HUC – HASYLAB User Committee

Peter Müller-Buschbaum (Chair)	TU München, D
Jens Falta	University Bremen, D
Alexander Marx	MPG-ASMB Hamburg, D
Thomas Möller	TU Berlin, D

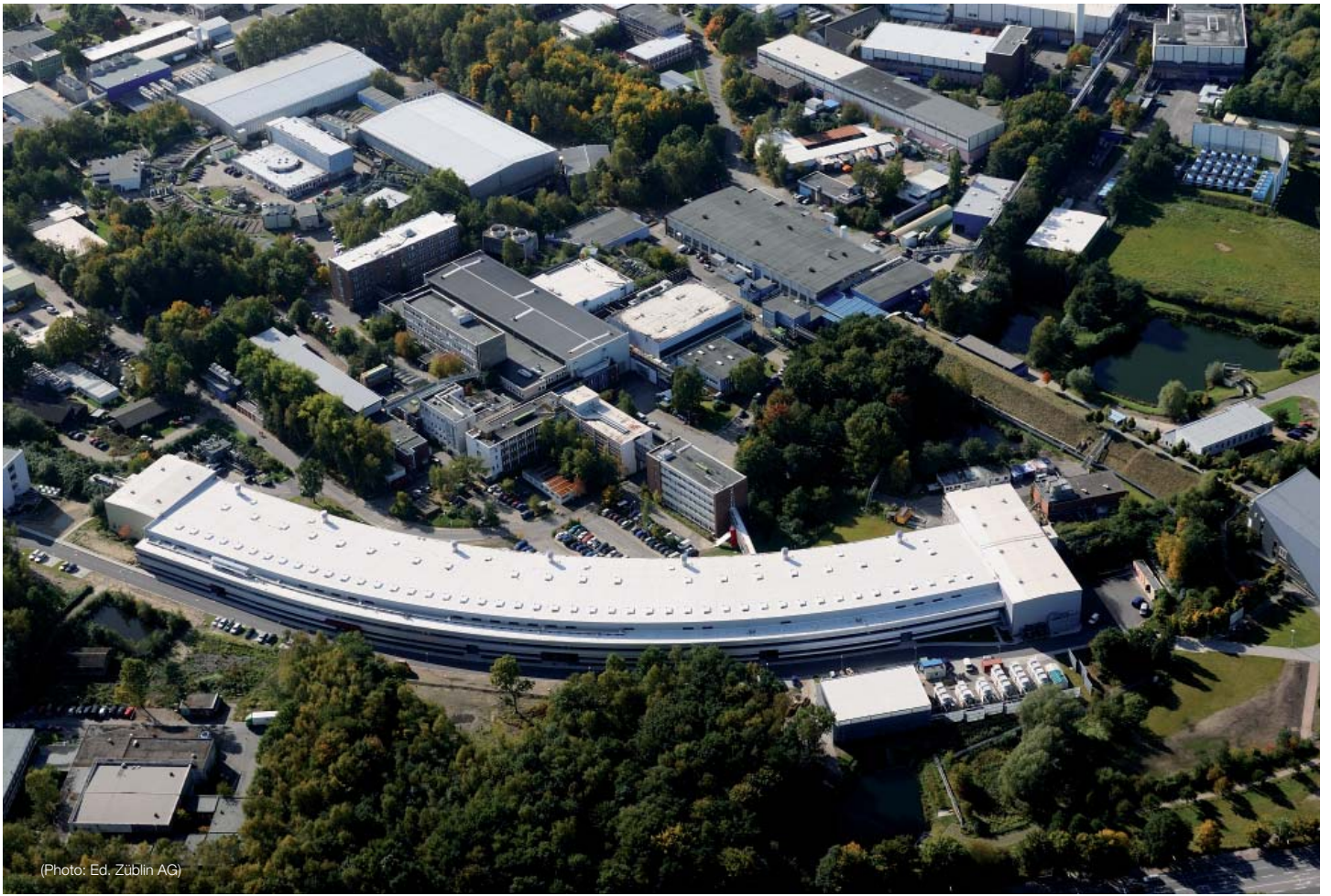


(Photo: Ed. Zublin AG)



Photographs and Graphics:

DESY

Eric Shambroom (areal photographs)

EMBL

Falcon Crest, aerial photographic enterprise

GFZ

GKSS

Max-Planck Unit for Structural Molecular Biology

University of Hamburg

Ed. Züblin AG

Figures of the Research Highlights were reproduced by permission from authors or journals.

Acknowledgement

We would like to thank all authors and everyone who helped in the creation of this annual report. ●

Imprint

Publishing and Contact:

Hamburger Synchrotronstrahlungslabor HASYLAB
at Deutsches Elektronen-Synchrotron DESY
A Research Centre of the Helmholtz Association
Notkestr. 85
D-22607 HAMBURG, Germany

Phone: +49 40 8998-2304

Fax: +49 40 8998-4475

E-mail: hasylab@desy.de

www.desy.de. and hasylab.desy.de

ISBN 978-3-935702-30-0

Realization:

Wolfgang Drube, Wiebke Laasch

Editing:

Wolfgang Caliebe, Wolfgang Drube, Rainer Gehrke,
Heinz Graafsma, Gerhard Grübel, Christian Gutt,
Wiebke Laasch, Wolfgang Morgenroth, Elke Plönjes-Palm,
Karen Rickers, Kai Tiedtke, Thomas Tschentscher, Edgar
Weckert, Susanne Weigert, Martin von Zimmermann

Layout: Britta Liebaug, Heike Becker

Printing: Heigener Europrint GmbH, Hamburg

Copy deadline: 31 December 2008

Reproduction including extracts is permitted subject to crediting the source.



Deutsches Elektronen-Synchrotron A Research Centre of the Helmholtz Association

With its 15 research centres and annual budget of approx 2.3 billion euros the Helmholtz Association is Germany's largest research institution. The 26500 employees produce top-rate scientific results in six research fields. The Helmholtz Association identifies and takes on

the grand challenges of society, science and the economy, in particular through the investigation of highly complex systems.

www.helmholtz.de